Studies on the host-pathogen interactions in *Theileria*-transformed leukocytes during host cell G2/M phase

Graduate School for Cellular and Biomedical Sciences

University of Bern

PhD Thesis

Submitted by

Conrad von Schubert

from Germany

Thesis advisor

Prof. Dr. Dirk. A.E. Dobbelaere

Division of Molecular Pathobiology

Vetsuisse Faculty of the University of Bern

Copyright notice

Abstract

The protozoan parasites *Theileria parva* and *T. annulata* are transmitted by ticks and cause lymphoproliferative disease in cattle in large areas of Africa, the Mediterranean, Middle East, Indian Subcontinent and central Asia. Whereas *Theileria* infection usually provokes only subclinical symptoms in its natural host, the buffalo, a high pathogenicity and mortality is observed in domestic animals. This results in significant economic loss and constitutes a prevailing problem for sustainable livestock production. As members of the phylum Apicomplexa, *Theileria* parasites have evolved the ability to invade and replicate within their host cells. After tick feeding, sporozoites invade lymphocytes or macrophages and immediately develop into a large syncytial schizont. Whereas many other members of the Apicomplexa remain in vacuoles throughout their intracellular stages, *Theileria* dwell freely in the cytoplasm and induce transformational processes in the host cell such as the activation of anti-apoptotic pathways, self-sufficiency regarding growth factors and continuous proliferation. Interestingly, parasite cell division is depending on host cell cytokinesis, which results in an equal distribution of the schizont over the forming daughter cells and thereby leads to a clonal expansion of parasitized leucocytes in the infected animal and the observed cancer-like aspects of the disease.

This thesis focuses on the intracellular schizont stage of the *Theileria* life cycle and delivers insight into the mechanism of equal parasite division during host cell mitosis and cytokinesis. The exploitation of host cell mitotic and cytokinetic mechanisms, while at the same time generating only minimal disturbance of these processes, are a main feature of the schizont‘s efficient expansion strategy within the host. It is shown that the parasite uses the mitotic spindle apparatus of the host cell to ensure its distribution over the two daughter cells. Polo-like kinase 1 (Plk1), an important regulator of host cell mitosis and cytokinesis, is recruited in a biphasic manner to the schizont surface. Plk1 accumulates at the parasite surface during G2 phase to disappear during prophase, most likely through the action of the Cdk1/cyclinB complex. At the onset of anaphase, Cdk1 activity abruptly ceases and Plk1 immediately re-associates with the parasite, lasting until telophase. During cell division, Plk1 activity is required for proper functioning of the central spindle, a structure that controls the specification of the cleavage plane and the initiation of cytokinesis. The *Theileria* schizont promotes the formation of host cell central spindles at its surface in a Plk1-dependent manner and invariably positions itself at the site of furrow ingression and cytokinesis, even when aberrant, precocious cytokinesis is induced. The described process allows an equal division of the parasite and constitutes an important feature in the parasite‘s propagation strategy resulting in clonal expansion of infected cells.

Furthermore, the initial characterization of the *Theileria* GPI-anchored surface protein gp34 is presented. When ectopically expressed, *T. parva* gp34 binds the host cell central spindle and midbody and induces cytokinetic defects. It is proposed that the protein constitutes one of the components involved in parasite cell division. Taken together, the presented work highlights the division of the *Theileria* schizont and demonstrates the parasite‘s dependency on host cell structures for equal distribution over daughter cells. It reflects the extensive host-pathogen interactions observed for this genus and provides an example of how *Theileria* co-opts conserved mammalian processes.

Table of contents

1. Introduction

The Apicomplexa

Apicomplexan parasites constitute a phylum of eukaryotic pathogens affecting humans and domestic animals. First described as early as 1674 by the Dutch scientist Antony van Leeuwenhoek, apicomplexans have always remained in focus of research, as they continued to threaten mankind by causing widespread disease. Prominent members such as *Plasmodium* or *Toxoplasma* are being studied closely in order to understand the mechanisms by which the pathogens harm their hosts, causing diseases such as Malaria or Toxoplasmosis. Besides a direct impact on human health by zoonotic Apicomplexa, other members of the phylum, e.g. *Theileria*, *Eimeria* or *Sarcocystis*, create severe economic losses by killing domestic animals or dramatically reducing their performance and thus impair sustainable livestock farming in large areas of the globe. Thus, apicomplexan parasites significantly contribute to poverty in rural areas of developing countries and pose a substantial hurdle for economic development in their endemic tropic and sub-tropic regions. In the past decade, concerted efforts led to the sequencing of whole genomes of selected pathogens and together with the ability to transfect and therefore manipulate parasites, scientists have boosted their knowledge on the underlying molecular mechanisms of disease. However, despite common mechanisms among the Apicomplexa, the families of parasites exhibit also fundamental differences in their biology and knowledge acquired for one parasite system might not apply to the other. This is reflected by the diversity of life cycles and hosts among the Apicomplexa and also the processes that lead to pathogenicity. In addition, not all parasites are equally amenable to scientific manipulation. Whereas *Toxoplasma* and *Plasmodium* are readily transfectable, this has not yet been achieved for parasites such as *Theileria*, requiring different methodological approaches for the work on these systems. The understanding of how each member of the Apicomplexa maintains infection is of importance and, despite all variations of apicomplexan life cycles, they all share a common theme which is the evasion of the immune system by the invasion of host cells and their manipulation for the pathogen‘s benefit.

A typical apicomplexan life cycle involves asexual reproduction in an intermediate host as well as sexual and asexual reproduction in a definitive host. In both types of hosts, infection involves an intracellular stage of the parasite. Thus, host cell invasion is a fundamental process which, in apicomplexans, evolved to a degree of stunning sophistication. When a suitable host cell is encountered by an invasive parasite, a non-replicative extracellular zoite, the invasion takes place within seconds with minimal disturbance of the invaded cell. Although the invasive stages of Apicomplexa do not possess flagella, cilia or pseudopods, most remain motile and host cell invasion has been shown to be driven by parasite motility [1, 2]. It is not surprising that the organelles required for host cell penetration dominate the apicomplexan morphology, resulting in markedly polarized invasive zoites. Three types of secretory organelles, the micronemes, rhoptries and dense granules, unload in timed succession and work in conjunction with the apical

complex located at the anterior end of the zoite, a structure formed of polar microtubules rings or rods which is found in most Apicomplexa. The proteins secreted by the zoite during invasion serve in adhesion to the host cell, its invasion as well as in the establishment and maintenance of a parasitophorous vacuole, the intracellular compartment that is occupied by the parasite throughout its intracellular stage. Other organelles include one or multiple nuclei, a mitochondrion, the Golgi complex as well as the apicoplast, a plastid derived from red algae which contains genes involved in lipid metabolism.

Invasive zoites clearly evolved to seek the shelter from the immune system in a host cell and consequently, they are quite similar across the phylum. However, intracellular stages differ to a great extent in size, architecture and the modes of asexual replication. The latter can be classified into endodyogeny, schizogony and endopolyogeny. In all three cases, replication and distribution of the genetic material occurs and ultimately leads to the formation of new invasive zoites that exit the host cell and invade other. Morphologically, the parasite is either longitudinally divided to form two intracellular daughters (endodyogeny), forms a syncytium which buds off zoites (schizogony), or generates a continuous pool of replicated genetic material that scaffolds the formation of new parasites in a budding process (endopolyogeny). Most Apicomplexa continuously cycle between invasion, intracellular replication and re-invasion of new cells within one host, thereby multiplying in the host organism and increasing the chance of transmission into another intermediate or the definitive host. A striking exception to this scenario poses the genus *Theileria*. Once successfully entered and developed into the intracellular stage, the parasite replicates its DNA and undergoes numerous rounds of karyogenesis without cell division, resulting in a large syncytial schizont. However, the budding of single-nucleated, haploid zoites does not occur immediately. Instead, the parasite remains in the schizont stage and undergoes cell division along with the host cell, resulting in a multiplication of the number of infected cells without the parasite ever leaving the shelter of the host cell. However, this variation in the theme is only efficient, if the host cell proliferates at a hight rate and does not react on the presence of the parasite by inducing an immune response and undergoing apoptosis. *Theileria* has thus evolved to control host cell processes such as proliferation and cell survival. The following section will introduce the parasite‘s life cycle and give an overview on the mechanisms of host-pathogen interaction applied by *Theileria* parasites.

Theileria **taking over control**

A *Theileria* life cycle follows the apicomplexan scheme with a definitive host, in this case ticks, that inject invasive zoites into large and small ruminants that constitute the intermediate hosts, in which exclusively asexual replication of the parasites occurs. The genus *Theileria* can be divided into the so-called „transforming“ and „non-transforming“ species. Transformation refers to the ability of the parasite, to maintain survival and induce the uncontrolled proliferation of infected leucocytes of the intermediate host. It is the unchecked proliferation of blood cells along with an metastatic potential that lead to the high pathogenicity of the transforming species, resulting in severe lymphoproliferative disease. Other *Theileria*

parasites target predominantly erythrocytes and only induce subclinical infections. Its is thus the transforming species that are in the focus of interest, not only by scientists. The two main transforming species are *Theileria annulata* and *T. parva*. *T. annulata* causes tropical theileriosis or Mediterranean coast fever of domestic buffalo and cattle and is transmitted by *Hyalomma* ticks. The parasite is widespread and can be found in Northern Africa, Southern Europe, the Middle East, the Indian Subcontinent and central Asia. Whereas, due to their co-evolution, the parasite only causes subtle reactions in its original host the water buffalo (*Bubalis bubalis*), cattle are severely affected. Similar observations were made for the original host of *T. parva*, the African buffalo (*Syncerus caffer*), which remains mostly asymptomatic during infection. Being transmitted by ticks as well (*Rhipicephalus appendiculatus*), *T. parva* can be found in the tick's endemic regions which are Central, East and Southern Africa. As observed for *T. annulata,* the parasite provokes East Coast Fever in evolutionarily unadjusted cattle.

Both species start their life cycle in cells of the salivary glands of infected ticks. Upon feeding of a tick, salivary glands mature and stimulate sporogony of the *Theileria* sporoblast. The resulting sporozoites are being injected into the intermediate host, where they are drained into local lymph nodes. Immediately, the small sporozoites attach to and enter leucocytes. In the case of *T. parva* T and B lymphocytes are targeted, whereas *T. annulata* enters cells of the monocyte/macrophage lineage and B cells. Entry differs from other apicomplexans, in that *Theileria* does not possess an apical complex or conoid and contains only two types of secretory organelles used in invasion, the rhoptries and dispersed microspheres. Lacking a clear polarization, sporozoites enter the cell in any orientation and the process does not seem to depend on parasite motility. Instead, parasite entry is mediated presumably by host cell endocytosis. The crucial parasite surface proteins required for entry are p67 in *T. parva* [3, 4] and the homologous SPAG-1 in *T. annulata* [5]. Host cell surface receptors that act as counterparts, on the other hand, remain largely unknown. An involvement of MHC class I receptors [6, 7] together with extensive proteolytic activity [8-10] have been ascribed to the entry process so far.

Once the sporozoite has been completely taken up by the host cell, another feature distinguishes *Theileria* from the other members of its phylum. Instead of modifying the endocytotic membrane that surrounds the parasite to form a parasitophorous vacuole, it escapes lysosomal destruction by immediate elimination of the surrounding plasma membrane. This process involves the discharge of rhoptries and microspheres and finally leads to a liberation of the sporozoite into the host cell cytoplasm, where it is no longer susceptible to host cell lytic processes. The liberated parasite then attaches to host cell microtubules, an interaction that is maintained throughout the intracellular stage. Soon after entry, the sporozoite undergoes multiple rounds of genomic replication as well as nuclear divisions without cytokinesis, resulting in a large syncytium referred to as the „macroschizont“ [11]. At this stage, the parasite starts to actively determine the fate of the host cell by extensive manipulation of the host's signaling activities (reviewed in [12]). The transformation process is characterized by a self-sufficiency for growth factors through autocrine cytokine signaling, continuous host cell proliferation, as well as increased cell migration and metastasis. The parasite replicates along with the highly proliferating host cell and neutralizes host cell defense mechanisms such as apoptosis or the triggering of a cytotoxic

immune response. Importantly, host cell transformation is fully dependent on the presence of the schizont and are thus believed to be of epigenetic nature. Elimination of the parasite with the drug Buparvaquone (BW720c) halts host cell proliferation and cells soon undergo apoptosis.

The parasite could interfere with host cell regulatory mechanisms of cell division and apoptosis by interference with the relevant signaling pathways or by directly influencing host cell transcription. Additionally, it is conceivable that cell cycle progression and apoptosis are controlled in an transcriptionally independent way by an action on host cell factors that regulate these processes. To date, a number of signaling pathways have been described to be altered in *Theileria* parasitized cells including the PI-3K-PKB, JNK, JAK-STAT or NF-κB pathways as well as Src kinase family members or casein kinase 2 (reviewed in [12]). Whereas PI-3K-PKB signaling, by the activation of transcription factors E2F and c-Myc, was clearly ascribed a role for *Theileria*-dependent cell proliferation [13, 14], there are indications that this may also apply for JNK and AP-1, ATF2-dependent transcription [15]. JNK signaling is also likely to be involved in the metastatic phenotype observed for parasitized cells, as AP-1 regulates the expression of metalloprotease-9 [16]. Together with c-Myc, the NF-κB transcription factor is required for the inhibition of apoptotic death and both are observed to be constitutively upregulated in infected cells. However, whereas NF-κB activation leads to the upregulation of anti-apoptotic proteins such as c-FLIP or cIAP1/2 [15, 17], c-Myc can downregulate the NF-κB-dependent expression of these genes and increase sensitivity to death receptor-induced apoptosis [18, 19]. It is not known, how the action of c-Myc is balanced in favor of cell survival in parasitized cells, but it was shown that downregulation of c-Myc in parasitized cells leads to an increased susceptibility to apoptotic cell death [20]. Also, the transcription factor can increase proliferation through the upregulation of cell cycle promoting genes or the downregulation of genes encoding cell cycle repressors and these events are presumably contributing to cell division in *Theileria*-infected cells. c-Myc upregulation, in turn, might involve transcription factors such as STAT3, which was found to be activated in parasitized cells by an GM-CSF autocrine loop and the JAK2/STAT3 pathway [20]. The mechanisms by which this and the other mentioned signaling pathways are subverted by the parasite are not known. The sole exception is the NF-κB pathway, which is assumed to be activated by proximity-induced activation of the IKK complex recruited to the schizont surface [21]. This is in line with the observation that no *Theileria*-encoded kinases or phosphatases, including cell-cycle regulators, are predicted to be secreted or membrane-associated [12]. As *Theileria*-parasitized cells show drastic changes in host cell protein phosphorylation [22, 23], other mechanisms must account for the manipulation of host cell signaling. The sequencing and annotation of *Theileria annulata* and *T. parva* genomes [24, 25] led to the identification of a number of enzymatic and non-enzymatic parasite proteins that are potentially involved in the host-pathogen interaction. Ranging from proteinases, over redox regulators involved in the regulation of signaling pathways, to DNA-binding proteins (reviewed in [12]), a number of parasite proteins are predicted to contain a signal peptide and to be surface-associated. Among secreted proteins are the *T. annulata* schizont AT hook (TashAT) DNA-binding proteins. Interestingly, expression of this protein family is linked to the transforming stage of the parasite and proteins, containing functional nuclear localization signals, were observed to translocate to the host cell

nucleus where they could influence host cell transcription [26]. Furthermore, an extensive family of subtelomere-encoded variable secreted proteins (SVSPs) has been identified in *T. annulata* and *T. parva*. As seen for the TashAT proteins, most members of the SVSP protein family contain signal peptides and nuclear localization signals. Endogenous proteins were observed to be secreted into the host cell cytoplasm from where they translocate to the nucleus and the functionality of the nuclear localization signals was confirmed for recombinantly expressed proteins [27].

The extent to which the transforming species *T. annulata* and *T. parva* control host cell processes is unique. It is conceivable that the pathogens target highly conserved host cell proteins and that the targeted processes are limited to the required minimum. The identification of these processes could finally lead to insight in the deregulation of cellular control mechanisms that are the foundation for other proliferative diseases such as cancer. On the other hand, advances in the field of cell biology help to understand and explain the severe pathology of *Theileria* infection, which is as diverse as the underlying molecular processes of disease. As a consequence of infection with transforming *Theileria* species, animals die from hyperemia, emphysema, pulmonary oedema and consequently respiratory failure [28]. Other important post mortem lesions are the extensive destruction of lymphoid tissues and liver, due to the hyperplasia of infected leucocytes and their dissemination into non-lymphoid tissue. As infection progresses and the number of parasitized leucocytes increases, anemia becomes an indicator for the parasite invasion of erythrocytes which constitutes the progression into the next life cycle phase, the piroplasmic stage. The process of parasite differentiation could be observed in vitro upon incubation of infected cells at 41°C and was reported to be a stochastic event [29-31]. During differentiation, schizont nuclear division continues without cell division leading to parasite enlargement and the formation of single-nucleated merozoites in a budding process referred to as merogony (also referred to as schizogony). At that time, host cell proliferation ceases and the relatively small merozoites are liberated as the host cell is destroyed by the parasites [31, 32]. Free merozoites then invade erythrocytes which are finally transmitted to feeding ticks, closing the parasite life cycle. Stages within the tick encompass gamogony and the formation of motile kinetes which migrate to the salivary glands during tick molting. Upon the next feeding of the tick, parasites again undergo sporogony and sporozoites are delivered to the intermediate host.

Synchronized division as key to success

Theileria schizont-infected cells are immortalized and can be easily cultivated in vitro. The transformation process leads to the clonal expansion of both the host cell and the parasite within. However, for this strategy to be efficient, the parasite needs to be delivered to both daughter cells upon each host cell division. Parasite and host cell division are synchronized and schizonts seem to be dependent on host cell cytokinetic processes, as parasite cell division never occurs on its own. It can be assumed than *Theileria* parasites have evolved to form multinucleated schizonts of comparably large size to increase the chance for equal distribution of genetic material as well as cell bulk during division. The process rarely

fails as schizont distribution is usually observed to be very equal and nearly all cells in culture contain a parasite. This high efficiency is most likely linked to the parasite‘s capability to bind to and align with host cell microtubules, especially with the mitotic apparatus during host cell division, and this interaction was used early on to explain the intracellular propagation of *Theileria* schizonts [33]. To date, however, the exact mechanism, by which *Theileria* schizonts are positioned during cell division remains unknown. Parasite delivery to both forming daughter cells is a crucial step in its life cycle and a prerequisite for clonal expansion and thus efficient replication of the intracellular stage. A high number of parasites, in turn, increases the likelihood of transmission onto feeding ticks in which the sexual stage with genetic recombination can take place. The work presented in this manuscript sheds light on the mechanism of schizont cell division and reports on a host cell kinase as well as a parasite surface protein likely to be involved in the process. The following section gives a short introduction to the processes of mitosis and cytokinesis and concludes with the aims of this study.

Mammalian cell division

The cell cycle is an ordered series of events that leads to a cell‘s duplication, including its genetic material and all organelles. Cell cycle steps are controlled by the concerted expression of regulatory proteins as well as post-translational processes such as protein phosphorylation and proteolysis. Together, they allow the dynamic modulation of enzymatic activity and a timed succession of events, required to complete the cell cycle. A typical somatic cell cycle starts with interphase, which allows cell growth and comprises the processes of DNA-replication during S phase, which is flanked by the two intermittent gap phases G1 and G2. Interphase is followed by cell division during mitosis and cytokinesis, collectively referred to as M phase (for a detailed review see [34]). During M phase, two identical sets of genetic material, complements of cytoplasm, and organelles such as the centrosomes, Golgi apparatus or mitochondria are distributed over the forming daughter cells. Whereas chromatids are separated during mitosis, the actual cell division, or cytokinesis, can only occur when this first process has taken place. With the onset of mitosis, most cells reduce their adhesion to allow a repositioning within the tissue after division and thus adopt a spherical shape. The early stages of mitosis (prophase and prometaphase) are characterized by nuclear envelope breakdown, chromatin compaction and the formation of a mitotic spindle involving highly dynamic microtubules (MTs) and the action of motor proteins and microtubule-associated proteins (MAPs). Although prometaphase MTs exhibit a high degree of self-organization and can form a bipolar spindle in the absence of MT-nucleating poles [35], the presence of such structures is required in somatic cells and is found in the centrosomes.

The single centrosome of a cell in G1 phase is duplicated during S phase forming a microtubule-organizing center (MTOC) which persists throughout S and G2 phase, allowing processes such as MT nucleation and MT-dependent vesicle transport. With the onset of mitosis, centrosomes move apart through the action of dynein and kinesin-related motor proteins such as Eg5 [36], and recruit maturation factors including γ-tubulin ring complexes which dramatically increase their MT-nucleating potential. At

the same time, the chromosome‘s centromeres allow the assembly of kinetochores, proteinacious complexes involved in the attachment of microtubule fibers that emanate from the spindle poles. Another important role for kinetochores is the recruitment of spindle assembly checkpoint (SAC) components that prevent mitotic progression until each chromosome is attached to the mitotic spindle in a bipolar (amphitelic) fashion (reviewed in [37]). The state of complete chromosome congression in the center of a mitotic cell is referred to as metaphase and at this stage the mitotic spindle consists of kinetochore fibers, overlapping interpolar MTs as well as astral MTs which emanate radially form the spindle poles. Whereas pole focusing of MTs is maintained by the motor protein dynein [38], the overlapping interpolar MTs are being cross-linked by the homotetrameric motor Eg5 [35]. Once the proper alignment of all chromosomes on the spindle apparatus is achieved in metaphase, the SAC is inactivated and allows the sudden transition into anaphase marked by the separation of sister-chromatids. Anaphase and the final stage of mitosis, telophase, involves a dramatic series of events. Kinetochore fibers shorten and deliver the chromatids to the spindle poles, while astral MTs elongate, become less dynamic and position the spindle through attachment to cortical sites. At the same time, overlapping interpolar MTs are being bundled and form the central spindle, a structure that is located in the spindle midzone and coordinates cytokinesis (reviewed in [39, 40]). The central spindle fulfills structural tasks by generating pushing forces that elongate the mitotic apparatus; however, its essential role lies in providing a signaling platform that conveys spatial information for the cleavage furrow which forms during late anaphase and telophase and physically divides the cell in the process of cytokinesis [41-43]. Central spindle formation and function involves MAPs, kinesin-related motors as well protein kinases and most proteins involved are highly conserved across a wide range of animal species. Among the most important components are the MAP protein regulator of cytokinesis 1 (PRC1), the chromosomal passenger complex (CPC), containing the mitotic kinase Aurora B, as well as the centralspindlin complex (reviewed in [39]). All complexes sequester in a narrow middle section of the central spindle through the action of the kinesin-related motor proteins, generating a zone of high signal intensity for cleavage furrow ingression. Furrowing depends on the formation of a contractile ring assembled from myosin II and actin filaments and this process is regulated by the spatially restricted sequestration and activation of the small GTPase RhoA (reviewed in [44, 45]). This is achieved through the action of the centralspindlin complex, which delivers the GDP-GTP exchange factor ECT2 to the central spindle [46]. The presence of a central spindle in between segregating chromatin masses thus coordinates the site of division with the position of the mitotic apparatus and ensures that the two sets of chromosomes are sequestered into the two forming daughter cells.

During telophase, the nuclear envelopes reform and chromatin starts to decondense while cleavage furrow ingression is being completed. MT dynamics decrease, eventually forming the longer and more stable asters seen in interphase. The central spindle becomes compacted through the forces exhibited by the contractile ring and forms the intracellular bridge. The middle section of the central spindle, harboring the cytokinesis regulatory proteins, now becomes the microscopically dense midbody. The physical separation of the two daughter cells is called abscission and occurs at either side of the

midbody during late telophase (reviewed in [40, 47]). The process involves the former central spindle MTs, trapped in the cytoplasmic bridge between cells, which deliver membrane vesicles to the site of abscission. Vesicles are believed to originate form the Golgi or to be generated by endocytosis and their fusion at the abscission site involves SNAREs, the large exocyst-tethering complex and Rab GTPase activity during early membrane delivery, as well as the ESCRT complex during abscission (reviewed in [40].

Mitotic kinases

The most critical step during M phase is the irreversible separation of sister chromatids by the mitotic apparatus and thus the metaphase-to-anaphase transition. A lack of bipolar (amphitelic) attachment or the nondisjunction of a chromosome leads to aneuploidy, the cause of genetic disorders and a feature of cancer cells [48]. The regulation of this critical cell cycle transition is governed by a mechanism that involves the rapid inactivation of cyclin-dependent kinase 1 (Cdk1).

Cdk‘s are the major cell cycle regulators and constitute a family of highly conserved serine/ threonine (Ser/Thr) kinases (reviewed in [34]). Cdk1 activity requires the association with cyclins and the Cdk1/cyclin complex is further regulated by its phosphorylation state, involving the concerted action of the cdk-activating kinase (CAK), the inhibitory kinases Wee1 and Myt1, as well as the activating Cdc25 phosphatases. Furthermore, the M phase regulator Polo-like kinase 1 has been assigned a role in Cdk1 activation (reviewed in [49]). Inhibitory phosphorylation of Cdk1/cyclin complexes occurs by the activation of cell cycle checkpoints that detect the presence of unreplicated or damaged DNA. The most interesting aspect of Cdk1 function is that Cdk1 activity drives a cell into mitosis and governs most processes until metaphase, whereas at the same time it prevents anaphase and telophase through inhibitory phosphorylation of their regulators (reviewed in [34]). Upon entry into mitosis, Cdk1 phosphorylates a wide range of substrates including nuclear lamins, kinesin-related motor proteins such as Eg5, MAP‘s, condensins and Golgi matrix proteins, and these phosphorylations are required for nuclear envelope breakdown, centrosome separation, spindle assembly, chromosome condensation and Golgi fragmentation, respectively. To prevent the reversal of these processes until a cell passes metaphase, Cdk1 activity is maintained at a high level by the action of the Cdc25C phosphatase, which counteracts the inhibitory phosphorylations on Cdk1 [50]. Once a cell reaches metaphase, the spindle assembly checkpoint is turned off resulting in the release of Cdc20, an activator of the anaphase-promoting complex (APC), which acts as a ubiquitin ligase, tagging proteins for proteasomal degradation (reviewed in [51]). The timed activation of the APC/Cdc20 complex results in the degradation of both Cdc25C [52] as well as cyclinB and thereby abruptly shuts down Cdk1 activity. Phosphatases such as Cdc14, PP1 and PP2A seem counteract Cdk1-dependent phosphorylation at the onset of anaphase and to promote the late mitotic stages (reviewed in [53]). This results in the inactivation of early mitotic Cdk1 substrates and at the same time removes the inhibitory impact of Cdk1 on anaphase processes. Regulators of anaphase and telophase that are known to be inhibited by Cdk1 phosphorylation are the central spindle

components PRC-1, ECT2 as well as the centralspindlin subunit MKlp1 (reviewed in [40]). Thus, the transition from metaphase to anaphase is mainly driven by the inactivation of the Cdk1/cyclinB1 complex and, due to the proteolysis of components required for Cdk1 activity, this transition is irreversible.

The regulatory processes of M phase underlie intricate spatiotemporal control. The recruitment of a kinase usually indicates its requirement at the sub-cellular structure. For example, during G2/M transition, the Ser/Thr kinases Aurora A, Nek2 and Cdk1 are targeted to the centrosomes and are involved in the entry into mitosis, centrosome separation or centrosome maturation [54, 55]. Aurora B also locates to the chromosome arms, where it phosphorylates histone H3 for chromosome condensation and triggers the release of cohesin from chromosome arms during prophase and prometaphase. The SAC kinases Aurora B, Bub1 or BubR1 localize to the kinetochores where they maintain checkpoint activity until metaphase [37]. With the onset of anaphase, spatial restriction of kinase activity is accomplished by the action of kinesin-related motors which, timed by the inactivation of Cdk1, deliver components to the MT overlap zone of the central spindle.

Besides Cdk1, the Ser/Thr kinase Polo-like kinase 1 (Plk1) is one of the most important regulators of mitosis [49, 56, 57]. Discovered in *Drosophila melanogaster*, the polo gene was found to encode a kinase required for mitosis and meiosis which is highly conserved across species. Ranging from one gene in yeasts, over a minimum of two in metazoans, and up to four genes in mammals (Plk1-4), Plk‘s constitute an important kinase family that regulates a variety of cellular processes (reviewed in [57]). Whereas actions of Plk1 in cell division are well understood, the roles of the other mammalian Plk‘s are just emerging. It has been shown that Plk3 is required for the G1/S transition by activation of the Cdk2-directed phosphatase Cdc25A and by inducing the expression of cyclin E which, in conjunction with Cdk2, triggers DNA replication [58, 59]. In addition, Plk3 is activated in response to DNA damage and mitotic stress and leads to cell cycle arrest and apoptosis involving p53 [59, 60]. There are indications that Plk2 might also be involved in S phase checkpoint functioning [61] as well as in the response to hypoxic stress and tumor growth [62]. Plk4 is known to be one of the major regulators of centriole duplication (reviewed in [63]), but first studies demonstrate also its relevance for cell cycle control and identify it as a binding partner for p53 [64]. The evolutionary emergence of Plk2-4 seems to be the consequence of more complex regulatory mechanisms of mammalian cell proliferation.

Close Plk1 orthologs are found in a wide range of species such as yeast (Cdc5, Plo1), frog (Plx1) or mammals with relatively similar functions in cell cycle control. Furthermore, Plk1 is upregulated in many human tumors, which points towards an oncogenic role of Plk1 (reviewed in [65]). As in the other Plk‘s, Plk1 contains an amino-terminal Ser/Thr kinase domain as well as a carboxy-terminal substrate binding domain, the Polo-box domain (PBD). The latter contains the so-called polo boxes, which are required for the binding of phosphorylated motifs in target proteins [66]. ‚Priming‘ of these motifs by phosphorylation has been shown to be mediated by either Cdk1 or Plk1 itself (recently reviewed in [67]). This binding mechanism of the substrate binding domain is interesting as it efficiently allows the enzymatic activity to be directed to discrete sub-cellular sites in a timed manner. Indeed, various tasks of

Plk1 during the cell cycle, ranging from the regulation of mitotic entry to the control of cytokinesis, are reflected by its dynamic sub-cellular localization (recently reviewed in [68, 69]). In addition, human Plk1 activity is triggered through Thr210 phosphorylation, a residue that is located in the kinase domain. The sole activating kinase that has been identified to date is the mitotic kinase Aurora A which, in conjunction with the activator BORA, phosphorylates Plk1 at mitotic entry [70, 71]. Another regulatory mechanisms is the APC/Cdh1-dependent ubiquitylation and subsequent proteasomal degradation of Plk1 during mitotic exit [72], a process shared by a number of M phase regulators. Plk1 is involved in the regulation of the G2/M transition [73, 74], and APC-dependent proteolysis of Plk1 is observed upon DNA damage preventing mitotic entry [75]. As Plk1 levels increase after DNA repair, Aurora A-mediated activation of Plk1 occurs [71]. In turn, Plk1 antagonizes the DNA damage response in a feedback loop, allowing mitotic entry. For entry, Plk1 activates Cdc25C phosphatase and inhibits Wee1 and Myt1 kinases resulting in Cdk1 activation and the beginning of mitosis (reviewed in [49]). During that time, Plk1 is observed at the centrosomes and centromeres, where it mediates centrosome maturation and microtubule nucleation as well as kinetochore-MT attachment and SAC function, respectively. Recruitment to kinetochores or centrosomes at mitotic entry involves Plk1 self-priming, for example on the kinetochore protein PBIP1 [76], or Cdk1 as a priming kinase (reviewed in [67]). Later mitotic tasks of Plk1 are the activation of the APC, resolution of chromosome arms, and spindle maintenance. With the onset of anaphase, Cdk1 activity ceases and with it Cdk1-dependent priming of Plk1 targets. Consequently, phospho-dependent interactions with binding partners during late M phase require Plk1 kinase activity (recently reviewed in [67]). It is noteworthy that Plk1 binding to its late target PRC-1 is inhibited by Cdk1-dependent phosphorylation of this protein and that an interaction thus requires Cdk1 shut-down [77]. During the late mitotic stages, Plk1 is involved in the regulation of spindle elongation as well as furrowing and cytokinetic abscission. These processes are linked to the formation and proper function of central spindles, and, accordingly, Plk1 is found at the central spindles and midbody during anaphase and telophase. The multitude of tasks of Plk1 during M phase clearly requires refined spatiotemporal control. This may explain why the overexpression or mis-localization of Plk1 results in defects that are also seen upon knock-down or chemical inhibition of Plk1 [78-80]. In summary, Plk1 constitutes a key player of M phase that can be considered at least as important as Cdk1.

The aim of this thesis has been the investigation of host-pathogen interactions of the transforming parasite *Theileria* during host cell division. The foundation and starting point of the presented work was the observation by Gongda Xue that host cell Plk1 is recruited to the parasite surface. However, the relevance of this recruitment for the parasite, its temporal pattern during cell cycle or the mode of Plk1 interaction with the parasite surface were unknown. Furthermore, at that time, a parasite protein termed gp34, has been identified in *T. parva* and *T. annulata* and was characterized as a glycosylphosphatidylinositol (GPI)-anchored ortholog expressed at the parasite surface during the schizont stage (results by Martina Peyer, Gongda Xue, Pascal Hermann). Interestingly, the protein was predicted to contain a Plk1 phosphorylation site as well as PBD binding sites and was thus considered a

potential interaction partner for Plk1 on the parasite surface. Apart from the characterization of Plk1 recruitment to the parasite, a short-term aim was to test if gp34 could be confirmed as an interaction partner of Plk1 in vitro as well as in vivo. The long-term goal was to identify the function of Plk1 binding to the parasite. The investigation was planned with respect to the parasite‘s alignment on the host cell mitotic spindle [33] as well as the described role of Plk1 in mitotic spindle formation, maintenance and central spindle function (reviewed in [49, 57, 68]).

2.1. The transforming parasite *Theileria* co-opts host cell mitotic and central spindles to persist in continuously dividing cells

Conrad von Schubert, Gongda Xue, Jacqueline Schmuckli-Maurer, Kerry L. Woods, Erich A. Nigg and Dirk A. E. Dobbelaere

PLoS Biology (2010) in press

This publication is based on the initial observation by Gongda Xue that host cell Plk1 is recruited to the surface of *T. annulata* and *T. parva* schizonts. I adopted this project at an early stage and started by characterizing the binding of Plk1 to the schizont surface. I found Plk1 to be bi-phasically recruited by the parasite, during late G2 phase and during anaphase. As dissociation of Plk1 from the schizont correlated with the period of Cdk1/cyclin B activity, I investigated the role of Cdk1 in counteracting Plk1 recruitment. Indeed, chemical inhibition of Cdk1 induced an immediate and strong recruitment of Plk1. Furthermore, I could demonstrate that both phases of Plk1 docking are independent of Plk1 catalytic activity. This finding is particularly important, as the interaction of Plk1 with its anaphase substrates is normally dependent on its kinase activity.

Chemical inhibition of Cdk1 in early mitosis induces cells to attempt immediate cell division, including cleavage furrow formation. The central spindle is a structure required for proper furrowing and cytokinesis and acts as a signaling platform for regulators of cell division, including Plk1. In Cdk1-inhibited cells, I observed a prominent formation of central spindles on the parasite surface, which coincided with Plk1 recruitment to the schizont. Assuming a functional correlation of these two events, I went on to demonstrate that Plk1 catalytic activity was required for the parasite-associated formation of the central spindle, whereas parasite-independent formation of the structure was unaffected.

The *Theileria* schizont appears to be divided by inclusion in the host cell cytokinetic process. The central spindle is involved in positioning the cleavage furrow precisely between divided sister chromatids, and by associating with this structure, the parasite could position itself for cell division. Indeed, cells that were chemically induced to divide prematurely, failed to distribute their chromatin properly over the forming daughter cells, however, the parasite was precisely positioned at the cleavage furrow in almost every cell. It has been proposed that anaphase astral microtubules, together with the central spindle, are the only structural constituents of the spindle apparatus required for furrow ingression. in this context, I could demonstrate that schizont positioning for cytokinesis is mediated by astral and central spindle microtubules. If either of the two structures is lost, positioning is impaired, whereas if an interaction with both structures is prevented, a distribution of the schizont over the daughter cells fails.

Figure contributions: all figures and supplementary data, except Figure 2A (Gongda Xue) and S6 (Jacqueline Schmuckli-Maurer); additional experiments requested in reviewing.

The transforming parasite *Theileria* co-opts host cell mitotic and central spindles to persist in continuously dividing cells

Conrad von Schubert[1], Gongda Xue[1,3], Jacqueline Schmuckli-Maurer[1], Kerry L. Woods[1], Erich A. Nigg[2,4] and Dirk A. E. Dobbelaere[1]

1 Molecular Pathobiology, DCR-VPH, Vetsuisse Faculty, University of Bern, Switzerland.

2 Max-Planck Institute for Biochemistry, Am Klopferspitz 18, D-82152 Martinsried, Germany

3 Present address: Friedrich Miescher Institute for Biomedical Research, Maulbeerstrasse 66, CH-4058 Basel, Switzerland

4 Present address: Biozentrum, University of Basel, Klingelbergstrasse 50/70, CH-4056 Basel, Switzerland

Abstract

The protozoan parasite *Theileria* inhabits the host cell cytoplasm and possesses the unique capacity to transform the cells it infects, inducing continuous proliferation and protection against apoptosis. The transforming schizont is a multinucleated syncytium that resides free in the host cell cytoplasm and is strictly intracellular. To maintain transformation, it is crucial that this syncytium is divided over the two daughter cells at each host cell cytokinesis.

This process was dissected using different cell cycle synchronization methods in combination with the targeted application of specific inhibitors. We found that *Theileria* schizonts associate with newly formed host cell microtubules that emanate from the spindle poles, positioning the parasite at the equatorial region of the mitotic cell where host cell chromosomes assemble during metaphase. During anaphase, the schizont interacts closely with host cell central spindles. As part of this process, the schizont recruits a host cell mitotic kinase, Polo-like kinase 1, and we established that parasite association with host cell central spindles requires Polo-like kinase 1 catalytic activity. Blocking the interaction between the schizont and astral or central spindle microtubules prevented parasite segregation between the daughter cells during cytokinesis.

Our findings provide a striking example of how an intracellular eukaryotic pathogen that evolved ways to induce the uncontrolled proliferation of the cells it infects, usurps the host cell mitotic machinery, including Polo-like kinase 1, one of the pivotal mitotic kinases, to ensure its own persistence and survival.

Introduction

The apicomplexan parasites *Theileria annulata* and *T. parva* are transmitted by ticks and cause severe lymphoproliferative disease in cattle in large areas of Africa, the Middle East and Asia. The pronounced pathology and high mortality are linked to the ability of *Theileria* to stimulate the uncontrolled proliferation of the cells it infects, inducing a phenotype typical of tumor cells. *T. parva* infects predominantly T- and B-lymphocytes, whereas *T. annulata* targets B-lymphocytes and macrophages/monocytes. *Theileria*-

transformed cells proliferate independently of antigenic stimulation or exogenous growth factors. Parasitized cells become resistant to apoptosis [1-3] and acquire the capacity to invade and multiply in non-lymphoid as well as lymphoid tissues (reviewed in [4-6]). In buffalo, the natural host of *Theileria*, and in domestic animals that survive infection, the parasite persists for years, resulting in a carrier state.

Theileria parasites differ from other Apicomplexan parasites, such as *Plasmodium* and *Toxoplasma,* in that they do not reside in a parasitophorous vacuole. Shortly after entry, the invading sporozoite dissolves the surrounding host cell membrane. Free in the cytosol, the sporozoite immediately associates with host cell microtubules (MTs) and differentiates into the schizont stage of the life cycle [7], a multinucleated syncytium that maintains the host cell in a transformed state.

Significant progress has been made understanding how this parasite manipulates its host. To achieve transformation, the parasite induces the activation of host cell signaling pathways that regulate cell proliferation and survival. This includes signaling pathways that regulate G1 to S transition, resulting in host cell DNA replication [6,8]. Transformation is entirely dependent on the presence of the parasite in the cytoplasm, however, and upon killing of the parasite by treatment with a specific theilericidal drug, cells lose the transformed phenotype, stop proliferating [9] and reacquire sensitivity to apoptosis.

Theileria-infected cells can be cultured indefinitely in vitro and in established cultures, more than 95% of the cells harbor the parasite. Parasite and host cell DNA replication is asynchronous, with the schizont predominantly undergoing DNA synthesis and nuclear division as the host cell enters mitosis [10]. Schizonts are strictly intracellular and, to maintain the host cell transformed phenotype, the organism must be passed on to both daughter cells each time the host cell goes through mitosis and cytokinesis (M phase). Viruses that transform their host cells have evolved mechanisms to guarantee their persistence in proliferating cells. In the case of retroviruses, this involves integration into the host cell genome (reviewed in [11]). DNA viruses such as Kaposi's sarcoma-associated herpesvirus, Epstein-Barr virus or papillomavirus, have evolved a conserved strategy to ensure genome segregation during mitotic cellular division that involves tethering episomal viral genomes to mitotic chromosomes using virus-encoded proteins (reviewed in [12]). How can *Theileria*, as a large and complex eukaryotic syncytium, persist in a continuously dividing host cell? Early microscopic observations have provided first clues for an involvement of the host cell mitotic apparatus [13]. However, the kinetics and molecular mechanism underlying the interaction between the schizont and its host cell during mitosis have not yet been investigated in detail.

The regulation of mitosis and cytokinesis involves a range of mitotic kinases, motor proteins and MT structures that undergo extensive reorganization to coordinate diverse functions such as chromosome segregation and cell division. In line with their multiple functions, regulatory proteins are subject to extensive spatio-temporal regulation, translocating between different structures where they fulfill specific functions. The mitotic spindle, which forms during early mitosis, consists of astral and interpolar MTs as well as kinetochore fibers that attach to condensed chromosomes. Cells are only allowed to exit mitosis when all chromosomes are correctly aligned on the mitotic spindle. At this point, Cdk1/cyclin B is inactivated and during the ensuing anaphase, kinetochore MTs shorten to deliver the sister chromatids

towards the poles. In the zone between the separating sets of sister chromatids (spindle midzone), a specialized structure, the central spindle, forms, consisting of bundles of antiparallel MTs with overlapping plus ends. By recruiting a specific set of regulatory proteins, including mitotic kinases such as Polo-like kinase 1 (Plk1) and Aurora B, as well as activators of the RhoA GTPase, the central spindle provides an important signaling platform that determines the plane of cleavage furrow formation and cytokinesis. For detailed information on central spindle assembly and cytokinesis, the reader is referred to recent reviews [14-16].

Plk1 has a broad range of functions during different stages of cell division and is subject to complex spatial and temporal control (reviewed in [17-19]). Plk1 is degraded at the end of M phase [72] and protein levels remain low during G1. Levels increase when cells enter S phase, accumulating strongly during G2. As the cell prepares for mitosis, Plk1 can be found localized to centrosomes and a first accumulation at centromeres can be observed. Upon progression through prometaphase and metaphase, Plk1 associates with spindle poles and kinetochores. The choice of Plk1 docking partners is regulated by Cdk1 [20] and upon Cdk1 inactivation at anaphase, Plk1 is released from kinetochores and recruited to the newly forming central spindle. Finally, during cytokinesis, Plk1 is found localized to the midbody. By phosphorylating different interacting partners, Plk1 contributes to a number of events linked to cytokinesis such as contractile ring formation and cleavage furrow ingression (see review by [17,21-23]). The application of RNAi-mediated Plk1 knock-down or Plk1 inhibition using dominant negative mutants proved highly valuable to dissect the early functions of Plk1 in mitosis. However, important new insights into the role of Plk1 during cytokinesis only became possible with the recent development of specific chemical tools that allow the rapid and complete inactivation of Plk1 at precise time-points during mitosis, and without interfering with earlier functions [24-27]. Armed with these new tools, we analyzed how the *Theileria* schizont interacts first with the mitotic spindle and subsequently with the central spindle during host cell M phase. We show that the parasite establishes a close interaction with both structures and found that its association with the central spindle depends on catalytically active Plk1. The latter associates with the schizont surface in a biphasic manner and recruitment is negatively regulated by host cell Cdk1.

Results

The *Theileria* schizont interacts with de novo synthesized astral and spindle midzone MTs.

To monitor the interaction of the schizont with de novo synthesized MTs, *T. annulata*-transformed cells were exposed to nocodazole, a drug that inhibits MT polymerization. After 16h of treatment, mitotic cells lacking MTs were arrested in prometaphase because of spindle checkpoint activation. Within minutes of nocodazole removal, new bundles of MTs formed that aligned closely with the parasite surface, stained with anti-TaSP1, a commonly used schizont surface marker [28] (Figure 1A). The appearance of multiple small microtubule asters early upon nocodazole release is most likely not due to parasite-induced MT nucleation as such asters could also be observed in uninfected bovine control cells (Figure S1A). At

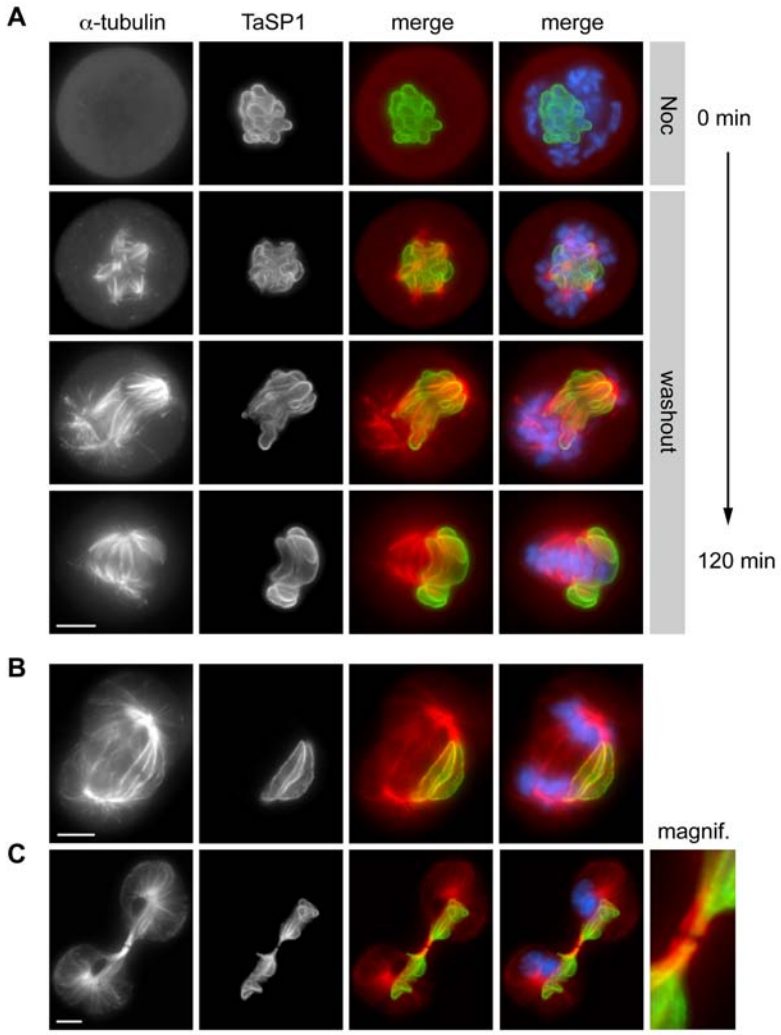

Figure 1. *Theileria* schizont interaction with mitotic and spindle midzone MTs. (A) *T. annulata*-transformed cells were arrested in prometaphase by treatment with nocodazole (Noc; top panels). Upon removal of nocodazole, MT polymerization was monitored by immunofluorescence microscopy (IFM) for up to 120 min. Cells were stained with antibodies directed against the schizont surface marker TaSP1 and α -tubulin; DNA was stained with DAPI; 'merge' represents an overlay of the three images. Noc, Nocodazole; 'washout' indicates removal of Nocodazole. (B, C) Unsynchronized *T. annulata*-transformed cells undergoing anaphase and telophase/cytokinesis. The panel labeled 'magnif' represents a magnification of the midbody region of the dividing cell shown in C. Scale bars represent 5 µm.

metaphase, the parasite was found oriented symmetrically towards both spindle poles, straddling the chromosomes assembled in the metaphase plate. At anaphase, spindle midzone MTs, located between the separating sister chromatids, were aligned longitudinally along large sections of the parasite as dense MT bundles (Figure 1B). As the cleavage furrow ingressed, central spindle MTs, including those associated with the parasite, became compacted and, during cytokinesis, both chromosome sets and the parasite were equally distributed between the two daughter cells (Figure 1C). TaC12 cells are of macrophage origin and in order to allow a morphological comparison, different stages of mitosis/ cytokinesis as observed in a bovine control cell line of macrophage origin (BoMac) or cells that no longer contain the parasite are presented in Fig S1B and C.

The accumulation of host cell MT bundles at the schizont surface does not require bipolar spindles as it could also be observed in cells treated with monastrol, a small-molecule inhibitor of the mitotic kinesin Eg5 that induces the formation of monopolar half-spindles [29] (Fig. S2). In monastrol-treated cells the parasite is less mobile compared to untreated cells, facilitating live imaging of MT interactions with the parasite surface. A kymograph analysis suggested that host cell astral MT bundles appear to be stably associated with the schizont surface (Fig. S2).

Biphasic cell-cycle dependent recruitment of host Plk1 to the schizont surface.

In previous work, we demonstrated that *T. parva* and *T. annulata* can aggregate the host cell kinases IKK1 and IKK2 at its surface, activating a signaling pathway that promotes survival of the transformed host cell [30]. Using immunofluorescence microscopy, we investigated whether this might also apply to mitotic kinases. In unsynchronized cultures of *T. annulata*-transformed cells, Plk1 was found to localize to the surface of the schizont in approximately 30% of cells. This was most striking in cells in G2 and also in cells undergoing anaphase (Figure 2A). Intriguingly, during prometaphase and metaphase, Plk1 was consistently absent from the schizont surface. The association of Plk1 with the parasite during different phases of the cell cycle is presented in Figure S3. Plk1 was not detectable in cells in G1. During G2, when Plk1 is abundantly expressed, prominent labeling of the schizont surface could be observed, coinciding with the time at which Plk1started to accumulate at host cell centromeres. Binding to the schizont was maintained until nuclear accumulation of cyclin B1 and nuclear envelope breakdown became apparent during prophase (data not shown). Once cells reached prometaphase and metaphase, Plk1 localized predominantly to the spindle poles and kinetochores, but was not associated with the schizont. With the onset of anaphase, Plk1 re-accumulated on the parasite surface. In cells progressing to telophase, Plk1 association with the parasite was largely restricted to the section of the schizont that is incorporated into the central spindle.

To analyze Plk1 recruitment to the parasite surface in more detail, we used different synchronization protocols. The different synchronization strategies used in this study are depicted schematically in Figure S4A. In a first set of experiments, *Theileria*-infected cells were synchronized in early S phase using a thymidine block. Cells were released from the arrest and Plk1 association with the schizont monitored by immunofluorescence microscopy as cells progressed towards G2 and M phase (Figure S5). The percentage of cells containing Plk1-binding schizonts increased progressively as they advanced through G2, and then decreased as they entered mitosis. Progression into M phase was monitored by immunoblot analysis of lysates, prepared at each time point, using antibodies specific for phospho-histone H3. Immunoblot analysis also showed that reduced association of Plk1 with the parasite as cells proceeded into mitosis was not due to declining Plk1 levels as these continued to increase during the course of the experiment. In cells synchronized in prometaphase by treatment with nocodazole, Plk1 could not be detected on the parasite (Figure 2B, left panels) confirming our observation made in unsynchronized cultures. The lack of Plk1 binding could not be attributed to the lack of microtubules as identical observations were made in cells synchronized in prometaphase by treatment with monastrol (Figure 2B, right panels) .

We next defined at which stage after metaphase the Plk1-parasite interaction was reinstated. By blocking the degradation of cyclin B using the proteasomal inhibitor MG132, inactivation of the Cdk1/cyclin B complex can be prevented, thus synchronizing cells in a metaphase-like state (see scheme Figure S4A) [26]. To follow progression through anaphase, telophase and exit from M phase, the degradation of cyclin B1 and securin, and the disappearance of the phospho-histone H3 epitope was monitored by immunoblot. Consistent with earlier observations, no parasite-associated Plk1 could be

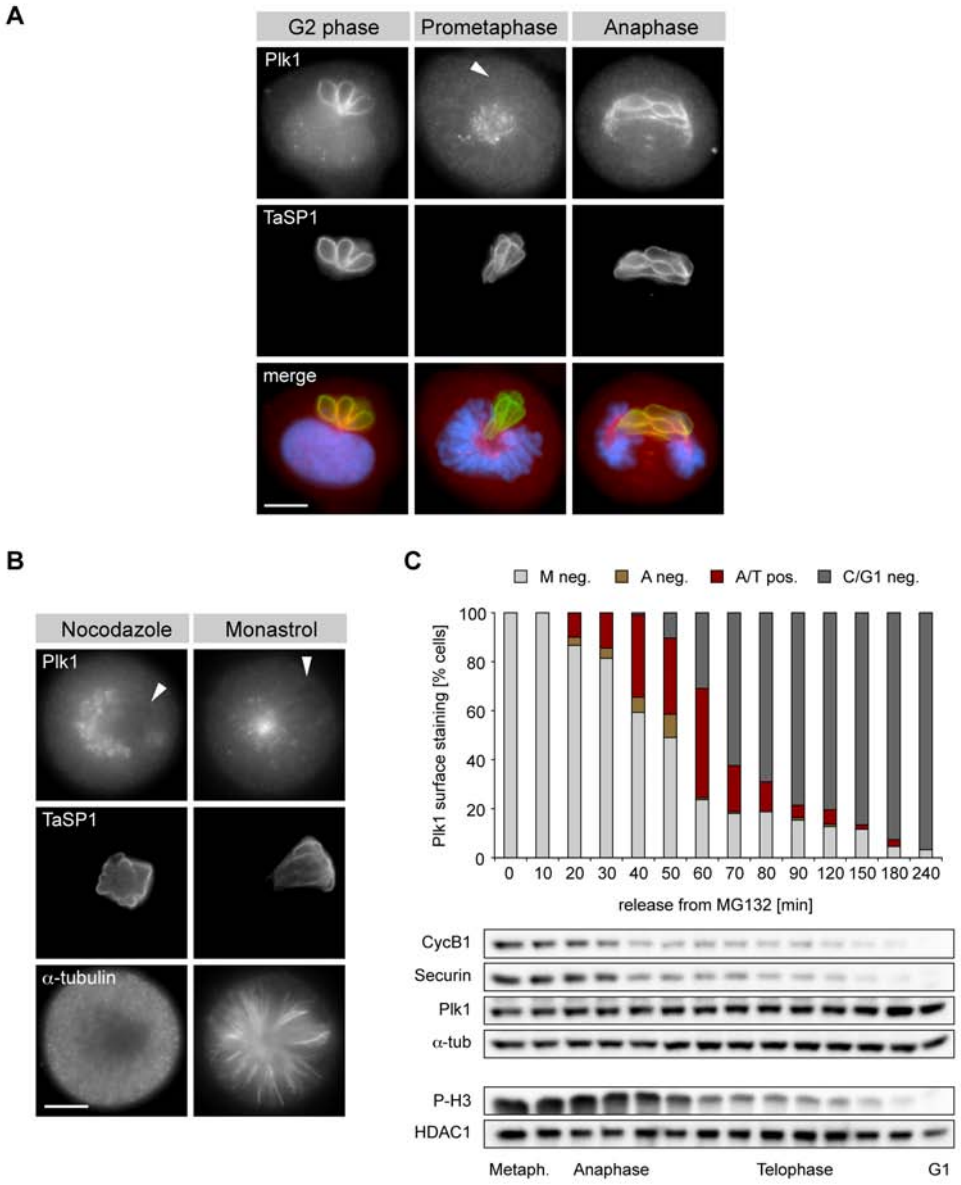

Figure 2. Biphasic recruitment of host Plk1 to the schizont surface. (A) *T. annulata*-transformed cells were stained with anti-Plk1, anti-TaSP1 and DAPI and analyzed by IFM. Cell cycle stages are indicated. Arrowhead indicates the position of the parasite. (B) Cells arrested in prometaphase by treatment with nocodazole (left panels) or monastrol (right panels) and analyzed by IFM using antibodies to Plk1, TaSP1 and α-tubulin. Arrowheads indicate the position of the parasite. C) Cells were released from MG132-mediated metaphase arrest and the percentage of cells containing parasites with surface-bound Plk1was determined by IFM (n≥100 cells/sample). M neg.: metaphase cells, parasite Plk1-negative; A neg.: anaphase cells, parasite Plk1-negative; A/T pos.: Ana- & Telophase cells, parasite Plk1-positive; C/G1 neg.: cells in cytokinesis or G1, parasite Plk1-negative. Progression through M phase was monitored by immunoblot analysis using antibodies as indicated. HDAC1 (histone deacetylase 1) and α-tubulin were used as loading controls. Scale bars represent 5 µm.

detected in metaphase-arrested cells (Figure 2C). Upon release from metaphase arrest, Plk1 associated with the parasite surface as soon as anaphase started. Binding was lost as cells completed cytokinesis and entered interphase/G1.

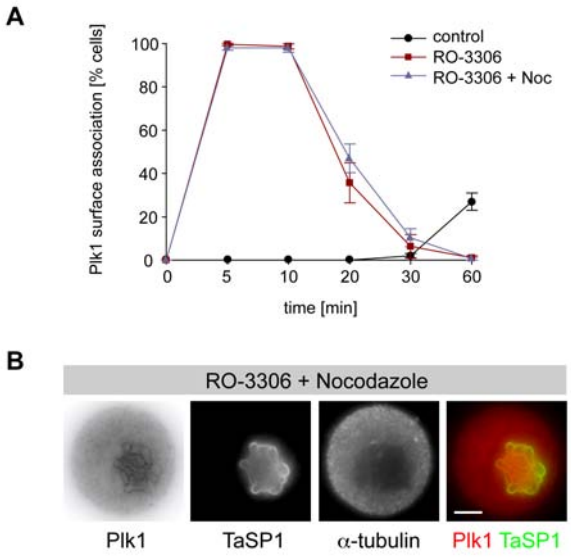

Figure 3. Cdk1 modulates Plk1 binding to the schizont surface. Cells arrested in prometaphase by nocodazole treatment were washed and immediately exposed to the Cdk1 inhibitor RO-3306 and Plk1 binding to the schizont surface was analyzed by IFM using antibodies to Plk1 (inverse gray/red), anti-TaSP1 (green) and anti-α-tubulin (B); DNA was stained with DAPI. (A) Time-course analysis showing the percentage of cells harboring parasites with surface-bound Plk1 following treatment with Cdk1 inhibitor in the presence (RO-3306 + Noc) or absence (RO-3306) of nocodazole. Control cells were released from nocodazole block in the presence of DMSO (control). Data represent the mean of three experiments (n=150 cells/sample), error bars indicate standard deviation (SD). (B) Cells treated with the Cdk1 inhibitor (RO-3306) in the presence of nocodazole (10 min). Scale bars represent 5 μm.

The capacity to induce transformation of the mammalian host cell is restricted to the schizont stage of *Theileria* and host cell proliferation ceases when the schizont differentiates to the next life cycle stage in a process called merogony [31,32]. Figure S4B provides an overview of the mammalian stages of the *Theileria* life cycle. Merogony can also be induced in vitro by exposure to heat shock [31] or treatment with chloramphenicol [33]. Merogony is an asynchronous stochastic process that occurs in individual cells over a period of 4 to 10 days. Upon induction, the number of cells harboring parasites expressing the differentiation marker Tamr1 gradually increased, reaching up to 45 %. This was accompanied by a pronounced reduction in the number of cells expressing Plk1, including cells containing the transforming schizont with Plk1 located to its surface (from typically 30% in normal cultures to <10%). The reduction in the number of cells expressing Plk1 likely reflects cell cycle arrest in G1 or G0. As parasites proceeded into merogony, they lost the capacity to bind Plk1 (Figure S6). In 13% of the cells, scattered, but weak, Plk1 binding to parasites in early stages of differentiation could still be observed (an example is shown in Fig. S6, middle row). No Plk1 binding could be detected when parasites had completed differentiation.

Taken together, these data show that host cell Plk1 interacts with the surface of the parasite in a biphasic manner, and that this is restricted to the transforming stage of the life cycle.

Plk1 binding to the schizont surface is modulated by Cdk1 and does not require Plk1 catalytic activity.

The pattern of Plk1 binding to the schizont surface correlated inversely with the spectrum of Cdk1/cyclin B activity. While Cdk1-mediated phosphorylation can create docking sites for Plk1 [34,35], in other cases Cdk1 prevents binding. Plk1 can also 'self-prime', however, and the choice of Plk1 docking partners through the course of mitosis and cytokinesis is thus controlled by the activation state of Cdk1 and that of Plk1 itself [20,36,37].

Cdk1 activity is required to maintain the mitotic state. Unscheduled inactivation of Cdk1 during mitosis induces a cytokinesis-like process that takes place before chromosome alignment and proper chromatid segregation has occurred [38] (Figure S4A). As shown in Figure 2B, Plk1 is not associated with the schizont in *Theileria*-transformed cells synchronized in prometaphase. Blocking Cdk1 activity by treatment with the chemical inhibitor RO-3306, however, induced the immediate accumulation of Plk1 on the schizont surface (Figure 3A and B). This also occurred in the presence of nocodazole, indicating that Plk1 recruitment to the parasite surface does not require mitotic MTs. In both cases, the association induced by Cdk1 inhibition was transient and downregulated within 30 minutes.

As Plk1binding to substrates can result from self-priming [20,36], we investigated the requirement of Plk1 catalytic activity for Plk1 binding to the parasite surface in more detail. TaC12 cells synchronized in S-phase were released from thymidine block and cultured in the presence or absence of the specific Plk1 inhibitor BI-2536 [39,40] at concentrations from 100 nM up to 1 μM. In agreement with the described role of Plk1 in early mitosis [27,39-42], cells released from S-phase in the presence of BI-2536 accumulated in G2/M and underwent prometaphase-like mitotic arrest, whereas control cells progressed through mitosis into G1 (shown for BI-2536 at 100 nM; Figure 4A). Accumulation in prometaphase was also observed in unsynchronized TaC12 cultures (Figure S7A). In BI-2536 cells that were still in G2, Plk1 was readily detected at the parasite surface, and this was even more marked at higher doses of BI-2536 (Figure 4B). In agreement with our observations described above, Plk1 association with the parasite was strongly reduced in those cells that had arrested in 'prometaphase' (Figure 4C and D). When Cdk1 was inhibited in cells arrested in 'prometaphase', Plk1 immediately reaccumulated at the parasite surface; this also occurred when BI-2536 was added at concentrations as high as 1μM (Figure 4C and D). In the presence of BI-2536, Plk1 interaction with the parasite could still be detected in the majority of the cells after 30 minutes, whereas Plk1 was absent from the parasite in cells treated only with Cdk1 inhibitor at that time point (Figure 4C). Importantly, in the presence of BI-2536, the pronounced ectopic cleavage furrow formation observed upon Cdk1 inhibition was inhibited (Figure S7F), confirming the reported role for Plk1 in regulating furrow ingression [21,22,24-27] (see also below and Figure S12).

We also determined whether Plk1 recruitment to the parasite during normal anaphase required Plk1 activity. In the presence of BI-2536, cells released from metaphase arrest entered anaphase, but failed to undergo furrow ingression. In these cells, Plk1 was found associated with the parasite surface (Figure 4E).

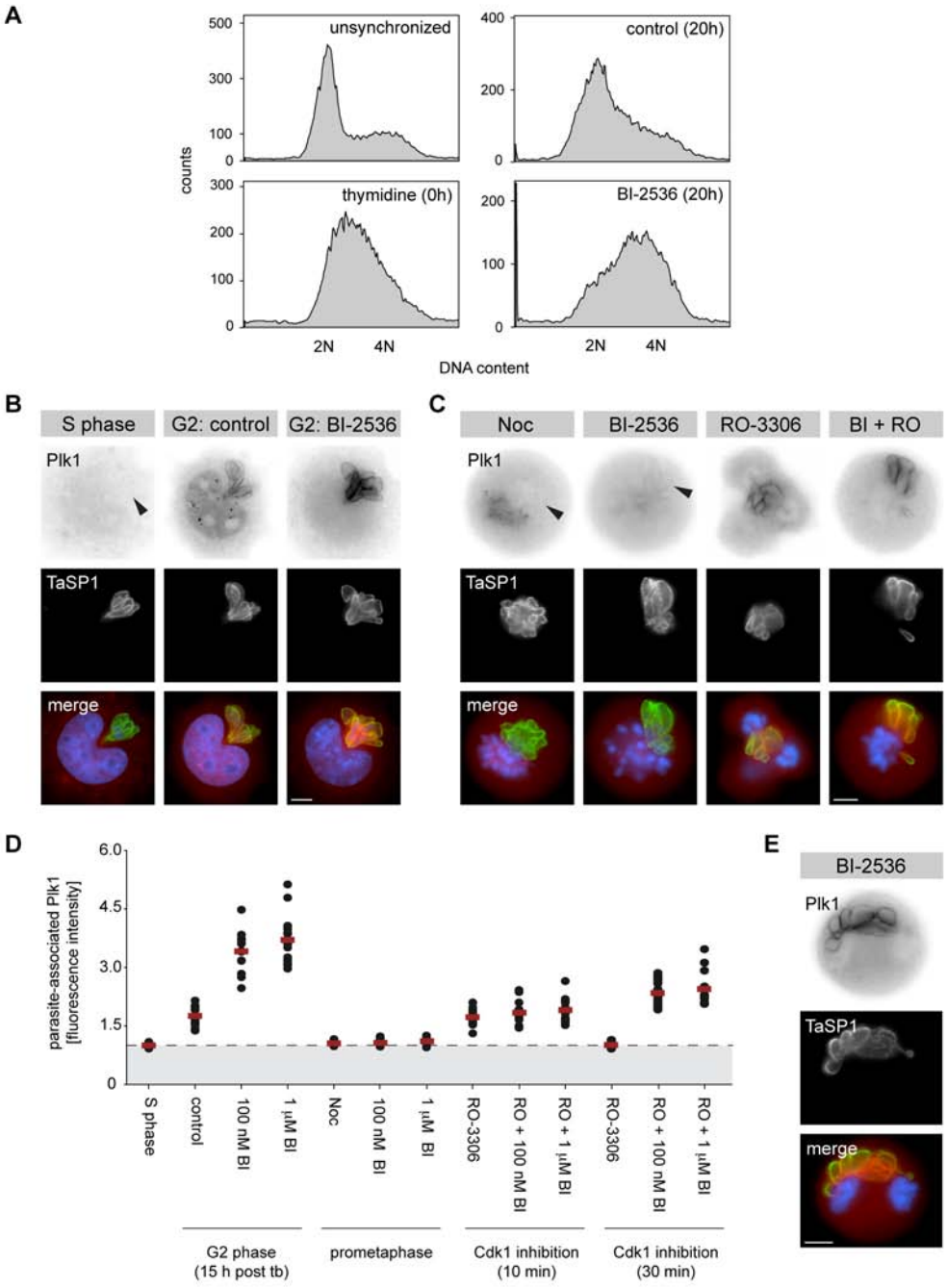

Figure 4. Plk1 binding to the parasite surface does not require Plk1 catalytic activity. (A) Unsynchronized or S phase-synchronized cultures of *T. annulata*-infected cells were analyzed by flow cytometry (left panels). Synchronized cultures (thymidine) were released for 20 h with either DMSO (control) or 100 nM BI-2536 (BI-2536). 2N, G1 phase; 4N, G2/M phase.(B) Representative micrographs of TaC12 cells in S phase arrest (S phase) or G2 phase cells that were released from S phase for 15 h in the presence of DMSO (control) or 1 µM BI-2536 (BI-2536). Arrowhead indicates the position of the parasite. Cells were stained for Plk1 and TaSP1 and analyzed by IFM; DNA was stained with DAPI. (C) S phase-synchronized TaC12 cells were released in the presence of nocodazole (Noc) or 1 µM BI-2536 (BI-2536) and prometaphase-arrested cells were harvested after 15 h. Nocodazole-blocked prometaphase cells were washed and released with Cdk1 inhibitor (RO-3306); cells that arrested in prometaphase by BI-2536 treatment were additionally treated with Cdk1 inhibitor (BI + RO). Cells were analyzed by IFM after 10 min incubation with Cdk1 inhibitor. Arrowheads indicate the position of the parasite. (D) The fluorescence intensity of Plk1 staining at the parasite surface and

in the host cell cytoplasm was measured at multiple locations in TaC12 cells; each dot represents the ratio of the average parasite surface and cytoplasmic Plk1 level of an individual cell. The following cells were analyzed: cells arrested in S phase by thymidine treatment (S phase), G2 phase cells released for 15 h from thymidine block in the presence of DMSO (control) or BI-2536 (100 nM BI, 1 µM BI), cells that arrested in prometaphase upon release from thymidine block in the presence of nocodazole (Noc) or BI-2536 (100 nM BI, 1 µM BI); nocodazole was removed by washing and arrested cells subsequently treated with Cdk1 inhibitor alone (RO-3306) or Cdk1 and PLK1 inhibitors (RO + 100 nM BI, RO + 1 µM BI), for 10 or 30 min. 15 cells were analyzed per sample and time point, horizontal red lines represent the average fluorescence intensity of each population; dashed line indicates a ratio of 1.0; tb, thymidine block. (E) Cells synchronously released from MG132-induced metaphase arrest were treated with 1 µM BI-2536, 15 min upon release, and analyzed by IFM. Scale bars represent 5 µm.

In further control experiments, BI-2536 was found to exert the same inhibitory effects in TaC12 cells as described in other systems; this included failure to maintain bipolar spindles (Figure S7B and C), cytokinetic failure (not shown) and the accumulation of binucleate cells (Figure S7D and E).

Although residual Plk1 activity can never be completely excluded, our findings indicate that Plk1 docking to the parasite surface can occur in the presence of Plk1 inhibitor concentrations that potently block several physiological functions of Plk1 in the cell. Together, these data indicate that Cdk1 negatively regulates Plk1 association with the schizont surface and that Plk1 binding does not appear to require catalytic activity.

Plk1 binds to the *Theileria* schizont via its Polo-box domain

To determine which region of Plk1 is responsible for binding to the schizont surface, different myc-tagged forms of Plk1 were transiently expressed in *T. annulata*-transformed cells. Immunofluorescence analysis showed that myc-tagged Plk1 localized to the parasite surface (Figure 5). When the N-terminal kinase domain (KDom) and the C-terminal Polo-box domain (PBD) were expressed separately, only the latter

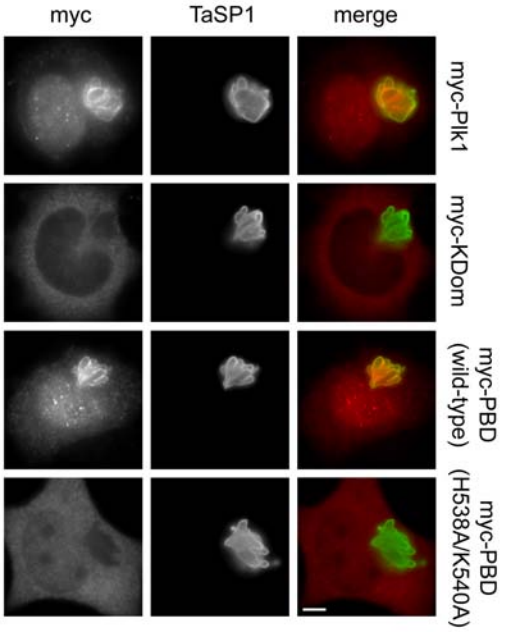

Figure 5. Plk1 binds to the *Theileria* schizont via its polo-box domain. *T. annulata*-infected cells were transfected with plasmids encoding myc-tagged versions of full-length Plk1 (myc-Plk1), Plk1 kinase domain (myc-KDom), Polo-box domain (myc-PBD, wild type) or H538A/K540A mutant PBD (myc-PBD H538A/K540A) and analyzed by IFM using anti-myc and anti-TaSP1 antibodies. Scale bar represents 5 µm.

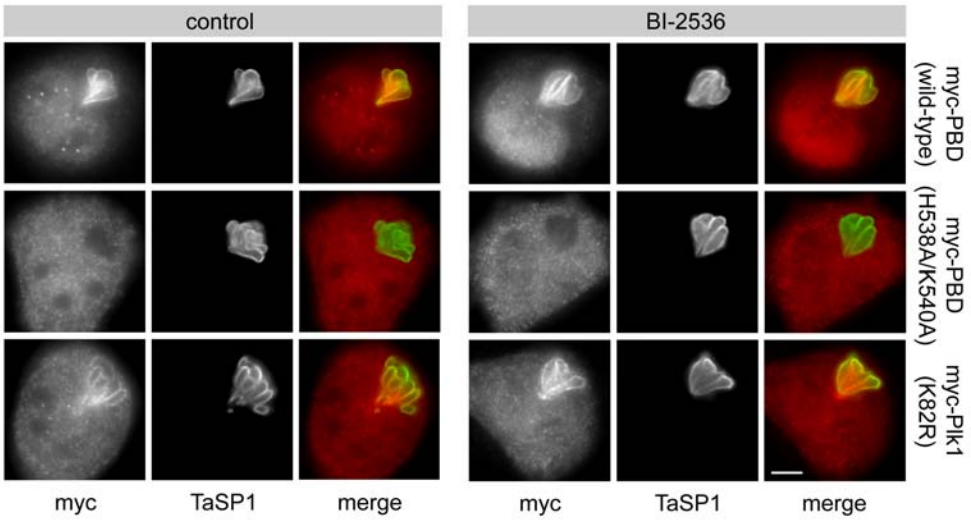

Figure 6. The binding of ectopically expressed Plk1 to the parasite surface does not require Plk1 catalytic activity. *T. annulata*-infected cells were transfected with plasmids encoding myc-tagged versions of Polo-box domain (myc-PBD, wild type), H538A/K540A mutant PBD (myc-PBD H538A/K540A) or catalytically inactive Plk1 (myc-Plk1 K82R) and cultured in the presence or absence of BI-2536 as indicated. Cells were analyzed by IFM using anti-myc and anti-TaSP1 antibodies. Scale bar represents 5 μm.

showed binding. H538 and K540 are important residues in the PBD that are required for phospho-ligand binding [35,43]. Mutation of these residues to alanine completely abrogated PBD binding to the parasite, indicating that a functional PBD with an intact phosphopeptide recognition domain is required for Plk1 interaction with the parasite. To exclude the potential participation of endogenous Plk1 in the creation of PBD docking sites on the parasite surface, cells transfected with PBD constructs were treated with BI-2536 (Figure 6). Inhibition of Plk1 activity did not interfere with myc-PBD, myc-PBD$^{H538A/K540A}$ or kinase dead full-length Plk1 (myc-Plk1^{K82R}) binding. This was also observed when doses as high as 1 μM were used (Figure S8), confirming that recruitment is, in all likelihood, independent of Plk1 activity.

The schizont recruits host cell central spindles to its surface in a Plk1-dependent manner.

Plk1 is closely involved in central spindle function and in helping to determine the site of contractile ring assembly and furrow ingression, ultimately resulting in cytokinesis (see reviews [14,15] and references therein). To test to what extent the schizont is linked to these processes, precocious anaphase and cytokinesis-like contractility were induced in prometaphase-arrested cells by Cdk1 inhibition. As cells proceeded to 'anaphase', de novo synthesized MTs assembled as central spindle-like structures at the schizont surface (Figure 7A). Even though normal sister chromatid separation did not take place, cells attempted cleavage (Figure S9). RhoA, the main regulator of actin dynamics, was found to accumulate at the cell cortex in a narrow zone in the immediate vicinity of the parasite (Figure7B). Interestingly, cleavage furrows occurred almost invariably at sites where MT bundles had assembled on the parasite surface (Figure 7C, Figure S9) and the position of host cell chromosomes had little or no influence on this

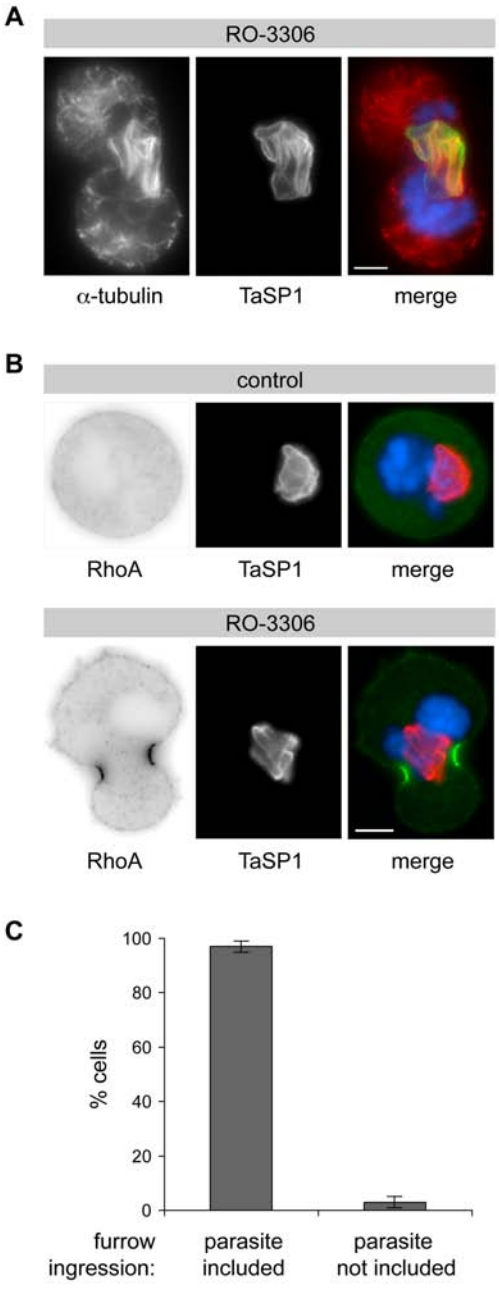

Figure 7. Upon induction of precocious cell division, cleavage furrows form in the immediate vicinity of the parasite. (A) *T. annulata*-transformed cells were synchronized in prometaphase by treatment with nocodazole. Upon nocodazole washout, precocious cell division was induced using RO-3306. After 20 min of treatment, newly formed microtubules were visualized by α-tubulin staining and the parasite is detected by anti-TaSP1. (B) RO-3306-induced RhoA accumulation and cleavage furrow formation are influenced by the position of the schizont. Cells synchronized in prometaphase as in (A) were treated for 20 min with either RO-3306 or solvent only (control) upon nocodazole washout. (C) The position of the parasite in cells undergoing cleavage furrow formation was monitored by IFM 30 min after RO-3306 induction shown in (A) and (B). Bars represent the percentage of cells in which the schizont was included in the cleavage furrow. Data represent the mean of three experiments with n=60 cells/sample, error bars indicate SD. Scale bars represent 5 µm, DNA was stained with DAPI.

process. These findings indicate that, by forming a foundation for Plk1-enrichment and MT polymerization the schizont may help focus MT-associated cytokinesis signals known to stimulate contractile ring assembly and furrow ingression.

Prompted by the findings above, we analyzed the central spindle-like structures associated with the parasite in more detail. In bona fide central spindles, anti-tubulin antibodies do not label the zone where antiparallel MT bundles overlap, most likely because of epitope masking caused by the accumulation of central spindle components such as PRC1, centralspindlin and the chromosomal passenger complex [15]. PRC1 is a major substrate of Plk1 that accumulates in the midzone during anaphase where it participates in central spindle MT bundling. Aurora B, a member of the chromosomal

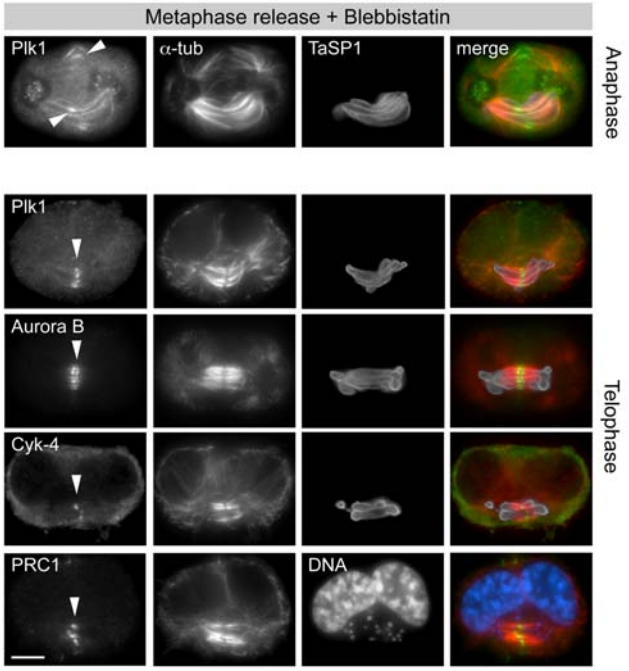

Figure 8. The schizont recruits host cell central spindles to its surface. Cells released for 80 min from MG132-induced metaphase arrest in the presence of the myosin II inhibitor blebbistatin (to prevent furrow ingression) were stained for central spindle proteins (arrowheads) as indicated; microtubules were stained using anti-α-tubulin; DNA was stained with DAPI. Scale bars represent 5 µm.

passenger complex, and Plk1 both translocate from kinetochores to the central spindle. There, Plk1 is recruited by PRC1 [20] and Mklp2 Neef, 2003 #2551], and contributes to anaphase spindle elongation and the regulation of cytokinesis [21,22,24-27]. To avoid potential side effects caused by nocodazole treatment and chemical inhibition of Cdk1, experiments were carried out using cells synchronized in metaphase by MG132, as these possess an intact mitotic spindle and undergo normal anaphase. In addition, to exclude the possibility that colocalization of the central spindle-like structures with the parasite surface merely occurred by apposition induced by furrow contraction, we made use of the myosin II inhibitor blebbistatin, which blocks contraction of the cleavage furrow without affecting mitosis or assembly of the contractile ring [44]. Upon removal of the MG132, cells progressed to anaphase and central spindle-like structures assembled on the parasite (Figure 8). The midzone components Plk1, Aurora B, PRC1 and Cyk-4/MgcRacGAP all localized to the centre of parasite-associated central spindle-like structures (arrowheads). Cyk-4/MgcRacGAP is a RhoGAP and member of the centralspindlin complex, which is required for central spindle assembly and also recruits the RhoGEF Ect2 to the central spindle (see review [15] and references therein; [21,22]). Similar observations were made with cells in which precocious anaphase was induced by Cdk1 inhibition (Figure S10). Together, our findings indicate that the central spindle-like structures assembling at the surface of the schizont resemble bona fide central spindles.

We next tested whether central spindle association with the parasite surface is dependent on Plk1 catalytic activity. In cells released from metaphase in the presence BI-2536, central spindle formation at the parasite surface was strongly reduced. Instead, central spindles formed in the centre of the cell, independent of the position of the parasite (Figure 9). Plk1 did not localize to the middle of the central spindles (Figure 9A, filled arrowheads) in BI-2536-treated cells but, as observed before, accumulated on

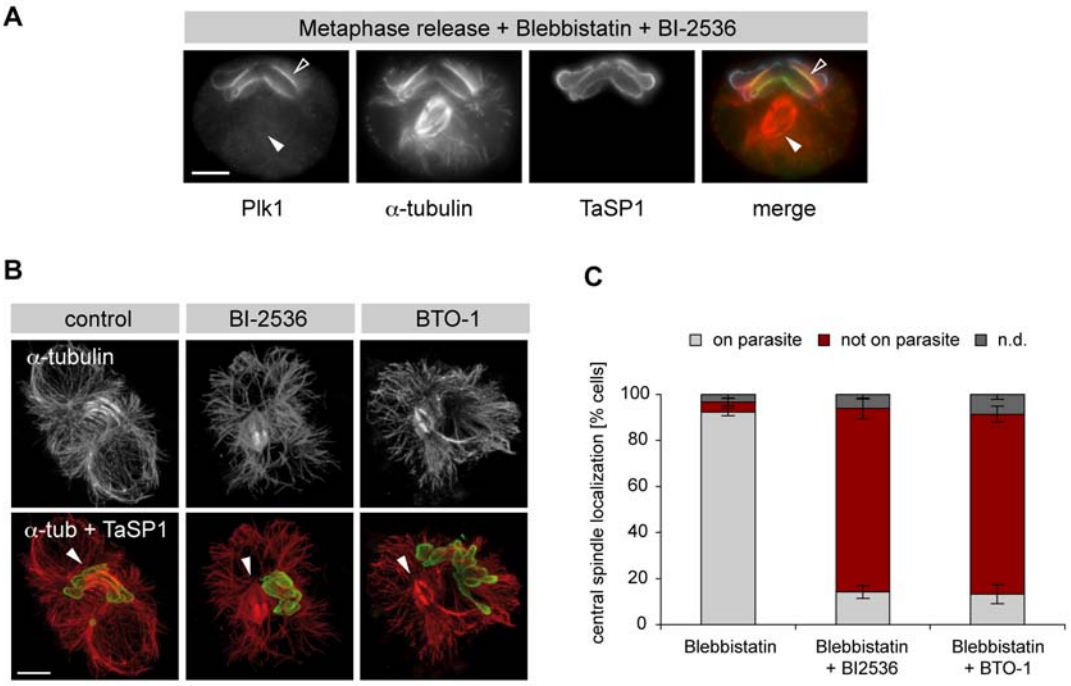

Figure 9. Recruitment of central spindles, but not astral MTs, to the parasite surface requires catalytically active Plk1. The effect of Plk1 inhibition on parasite-central spindle association was monitored by IFM in cells released (80 min) from MG132-induced metaphase arrest. (A) Cells were released from metaphase arrest in the presence of blebbistatin and BI-2536 and stained for Plk1, α-tubulin and TaSP1. Open arrowhead: parasite-associated Plk1; filled arrowheads: central spindles lacking Plk1. (B) Cells were released from metaphase arrest in the presence of blebbistatin only (control, left panels), blebbistatin and BI-2536 (BI-2536, middle panels) or blebbistatin and BTO-1 (BTO-1, right panels), and stained for α-tubulin and TaSP1. Whole cells are displayed by maximum intensity projection of confocal sections. Arrowheads indicate the position of the central spindle. (C) Cells were released from metaphase arrest in the presence of blebbistatin only, blebbistatin and BI-2536 or blebbistatin and BTO-1. Cells in anaphase and telophase were monitored by IFM for the central spindle association with the parasite based on staining of PRC1 and a parasite surface marker. Data represent the mean of 3 experiments ±SD with n=100 cells/sample; n.d. = not determined (includes all cells in anaphase or telophase that could not be classified). Scale bars represent 5 µm.

the parasite surface (Figure 9A, open arrowheads). Identical results were obtained using a second, structurally unrelated Plk1 inhibitor, BTO-1, indicating that the effects observed with BI-2536 are not off-target effects (Figure S11A). In Fig. 9B, whole cells are displayed by maximum intensity projection of confocal sections. Microtubule staining confirms that, when Plk1 was inhibited by BI-2536 or BTO-1, central spindle assembly was not linked to the location of the parasite in the cytoplasm and central spindle MT bundles failed to associate with the parasite surface. To facilitate monitoring the effect of Plk1 inhibition on the relative position of parasite and central spindles in more detail, cells were stained with an antibody that recognizes PRC1, an intrinsic marker of central spindles (Figure S11B). Whereas central spindles located at the parasite surface could be observed in >90% of control cells, this was reduced to <20% in cells treated with BI-2536 or BTO-1 (Figure 9C), reflecting a marked decrease in the parasite's affinity for central spindles. Interestingly, BI-2536 did not prevent the interaction of the schizont with

mitotic spindle MTs emerging from the spindle poles, and such interactions could still be observed during anaphase. This indicates that Plk1 activity is only required for interaction with the central spindle.

Interaction with host cell astral and central spindles is required for schizont segregation during cytokinesis.

Although our observations so far are consistent with the hypothesis that schizont interaction with mitotic and central spindle microtubules is required for its distribution over the two daughter cells - and thus for parasite maintenance, they do not provide functional evidence to that extent. During late anaphase, the schizont can still be found associated to host cell MTs emanating from the spindle poles (see for instance Fig. 1B, 2A and 8,9) and, in contrast to schizont interaction with central spindle MTs, this process does not require Plk1 catalytic activity. We tested whether preventing the interaction of the schizont with MTs emanating from the spindle poles or with central spindle MTs interfered with schizont segregation during cytokinesis. Treatment with nocodazole after the onset of anaphase can result in the disassembly of astral MTs, whereas midzone MTs remain differentially stable [45-47]. This allowed us to separate the contribution of astral MTs in positioning the parasite from that of central spindle MTs.

T. annulata-transformed TaC12 cells were released from metaphase arrest for 60 minutes and then exposed for 20 minutes to nocodazole. This resulted in the disassembly of astral spindle MTs and the parasite was found in close association with the central spindle (Fig. 10A, control + noc). As described [46], in the absence of astral MTs, furrow ingression was often asymmetric as was also reflected by the predominantly unilateral accumulation of RhoA (Fig. 10B). Whereas parasite division between the forming daughter cells *per se* was not affected, the schizont was distributed less evenly than in control cells. This was monitored by measuring the distribution of parasite surface area on either side of the cleavage furrow (Fig. 10C).

When added during metaphase, BI-2536 (and other Plk1 inhibitors), potently block cleavage furrow ingression [22,24,26]. When Plk1 is inhibited as cells enter anaphase, however, central spindle formation and cleavage furrow ingression can occur, but cells fail to complete cytokinesis [27]. In TaC12 cells, these conditions are met when BI-2536 is added 15 min after release from MG-132-induced metaphase arrest (Figure S12). While BI-2536 treatment prevented the 'incorporation' of the parasite into the central spindle, distribution between the forming daughter cells occurred with the same efficiency as observed for control cells (Fig. 10A, BI-2636 and Fig. 10C). Importantly, however, in cells that did not contain astral spindle MTs, schizont segregation was severely impeded when parasite-central spindle interaction was blocked by BI-2536 treatment (BI-2536 + Noc) and in many cases, the schizont remained completely sequestered on one side of the cleavage furrow. These data strongly indicate that both astral and central spindle MTs help facilitate parasite distribution between the two daughter cells during cytokinesis.

Taken together, these findings underpin the notion that the interaction with host cell astral and central spindle MTs is essential for proper segregation over the two daughter cells.

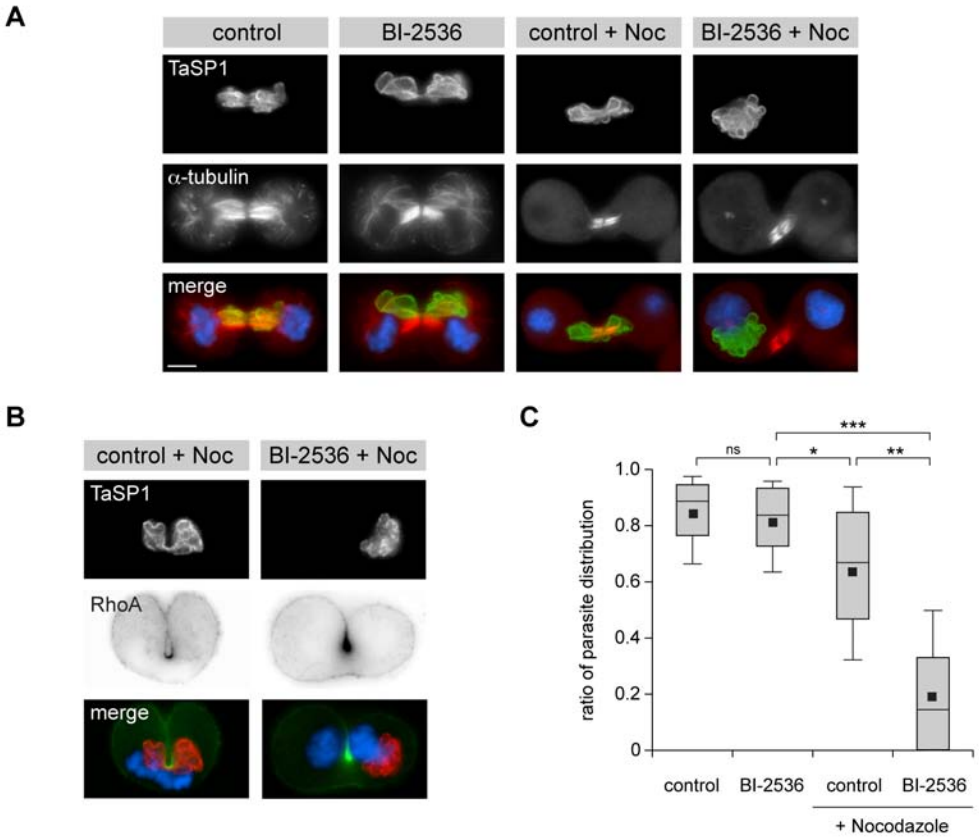

Figure 10. Interaction with host cell astral and central spindles is required for schizont segregation during cytokinesis. The respective role of astral and central spindles for parasite positioning was tested by nocodazole treatment of anaphase host cells and IFM analysis. Cells were released from metaphase arrest in the presence of control solvent DMSO (control) or BI-2536. After 60 min of release, cells were additionally subjected to 10 µM nocodazole over a period of 20 min. (A) Cells were stained for α-tubulin and TaSP1 to determine the position of the parasite relative to the central spindle and cleavage furrow. (B) Micrographs of cells displaying unilateral furrowing. Cells were treated as described in (A) but stained for RhoA and the parasite surface marker TaSP1. DNA was stained with DAPI; Scale bars represent 5 µm. (C) Cells were stained as in (A) and microscopic z-stacks of whole cells were generated. Two-dimensional projections were generated to measure the area occupied by the parasite on each side of the cleavage furrow. The ratio of both areas indicates the positioning with 1.0 representing an equal distribution over the two forming daughter cells. Data were obtained from 3 experiments with a total of 45 cells per condition. Significance was tested in a t-test (one-tailed, unpaired, unequal variance); ns = not significant; *, $p < 10^{-3}$; **, $p < 10^{-14}$; ***, $p < 10^{-30}$.

Discussion

Coevolving with their hosts, intracellular pathogens have developed a range of ways to use host cell MTs and their associated signaling pathways to their own advantage [48]. This ranges from microtubule-mediated viral transport in the cell [49,50] to microtubular network restructuring by parasites like *Toxoplasma,* which reside in a parasitophorous vacuole [51,52] or by inhabitants of the cytosol like *Trypanosoma cruzi* [53,54] and *Theileria*. Whereas *T. cruzi* utilizes host cell MTs to facilitate invasion and establishment of the parasite inside the cytosol [53,54], *Theileria* in addition evolved ways to usurp

structures involved in host cell mitosis and cytokinesis. Our findings reveal interesting differences in the strategies used by transforming viruses and *Theileria* to ensure persistence in continuously dividing cells. Thus, while viruses either integrate into the host cell genome or target mitotic chromosomes to guarantee long-term persistence [12], the transforming protozoan *Theileria,* rather than engaging chromosomes, evolved to single out the mitotic apparatus that mediates chromosome segregation and cytokinesis. How the parasite interacts with the host cell MTs or Plk1 during the different stages of the cell cycle is presently not known. TaSE, a protein reported to be secreted by the *T. annulata* schizont, was recently described to co-localize in a punctate manner with host cell MTs [55]. The pattern of schizont/MT interaction we observed, however, clearly differs from that of TaSE. TaSP1 was recently proposed to interact with MTs [56], but the functional relevance is not yet clear.

Considering the multiple levels in space and time at which individual regulator proteins participate in fine-tuning mitosis and cytokinesis, commonly used approaches such as RNA interference or the expression of dominant negative mutants, generally do not lend themselves well for studies on the later steps of M phase as they often inhibit important earlier events. This hurdle was eliminated by the recent development of specific small molecule inhibitors [25-27,44,57] and we exploited the new opportunities, created by these inhibitors, to investigate the interaction of *Theileria* with host mitotic structures during different stages of M phase.

Cdk1 regulates interaction of Plk1 with the schizont.

The biphasic pattern and the way in which Plk1 interacts with the parasite surface are intriguing. Plk1 binding to the parasite can first be observed during host cell G2 as the cell prepares for mitosis. During early mitosis, when Cdk1 becomes fully activated, Plk1 dissociates from the parasite surface to re-accumulate at the onset of anaphase, when Cdk1 is inactivated by the anaphase promoting complex/ cyclosome. The inverse correlation between Cdk1 activity and Plk1 interaction with the schizont, and the fact that pharmacological inhibition of Cdk1 induces rapid binding of Plk1 to the parasite clearly point towards Cdk1 as a negative regulator. This is reminiscent of Cdk1's known role as a spatio-temporal regulator of Plk1. Depending on the cell cycle stage, location and kinase substrate, Cdk1 can either create Plk1 binding sites or prevent Plk1 binding (reviewed in [17]). For instance, it has been shown that, in metaphase, Cdk1 prevents Plk1 binding to PRC1 by phosphorylating a site adjacent to the Plk1 docking site [20]; this block is lifted upon Cdk1 inactivation at anaphase. By analogy, it would be possible that Cdk1-mediated phosphorylation of the parasite surface prevents Plk1 from docking. Mammalian Plk1 lacks Cdk1 phosphorylation sites and a direct modification of Plk1 by Cdk1 can therefore be excluded. It is also conceivable, that Plk1 binding to the parasite involves one or more additional proteins, of host or parasite origin, forming a complex that can only bind in the absence of Cdk1 activity.

Transfection experiments revealed that Plk1 binds to the schizont through its PBD. Catalytically inactive Plk1and the PBD alone both bound to the parasite in cells treated with BI-2536, confirming that Plk1 itself is, in all likelihood, not the priming kinase. This is underpinned by the observation that, in the presence of either BI-2536 or BTO-1, increased - rather than reduced - Plk1 binding to the parasite could

be observed. This could also be observed with a third, unrelated Plk1 inhibitor. On the other hand, PBD mutants lacking H538/K540, required for electrostatic interactions with the negative charges of phospho-S/T groups, did not bind to the schizont surface, indicative of the involvement of a phosphate group in Plk1 docking. The fact that neither Plk1 nor Cdk1 appear to function as the priming kinase, points towards the involvement of another serine/threonine kinase. Although unusual, this is not without precedent; for instance, calmodulin-dependent kinase has been shown to create Plk1 binding sites in meiosis [58-60] Alternatively, it is conceivable that Plk1 binds to a moiety that mimics a Plk1 binding site, which is only accessible when Cdk1 is inactive. Plk1 binding to a substrate without priming phosphorylation has been observed in *Drosophila* for Polo binding to the MT-associated protein Map205; in this case the PBD was found to be required, but not sufficient, for interaction [61]. The nature of the schizont surface protein that provides a docking site for Plk1 is presently not known. Considering the complexity of the interactions between parasite and host cell during mitosis, the participation of several schizont proteins is plausible, and experiments are presently underway to address this topic.

Parasite-central spindle interactions

While many aspects of central spindle assembly are still enigmatic, a picture is emerging, indicating that central spindles show a high degree of self-organization (see review [15] and references therein). It has been shown that the combined presence of PRC1, centralspindlin and the chromosomal passenger complex suffices to induce the robust bundling of central spindle MTs. All three complexes required for self-organization can be detected in parasite-associated central spindles. The fact that central spindles can be detected at the parasite surface within a very short time after induction (within 10 to 20 minutes of Cdk1 inactivation) suggests that central spindles either assemble in situ or interact with the schizont immediately after they are formed. In cells in which furrow ingression was blocked by treatment with the myosin II inhibitor blebbistatin, newly formed central spindles were found almost invariably in association with the parasite surface. When Plk1 was inhibited, however, central spindles assembled independently of the position of the schizont. Parasite interaction with astral spindle MTs emanating from the spindle poles, on the other hand, was clearly not affected. Astral spindles have themselves been implicated in central spindle assembly (see reviews [15,62,63] and references therein). One plausible explanation could therefore also be that a subpopulation of MTs emanating from the spindle poles form stable interactions with the parasite surface where they subsequently self-organize into central spindles in a Plk1-dependent manner.

Whichever the mechanism, we propose that by interacting with astral MTs emerging from both spindle poles, the schizont is aligned strategically spanning across metaphase chromosomes arranged at the equator of the cell. This interaction in all likelihood also ensures that the parasite remains positioned correctly as the chromosome masses separate during anaphase, at which time a central section of the parasite interacts with midzone MTs that form the central spindle in preparation of the ensuing cytokinesis.

Cleavage furrow formation

MTs have been reported to be the main structural constituent of the spindle apparatus required for induction of cell cleavage [64]. The formation of a contractile ring required for cytokinesis depends on the focused localization of myosin II at the cortex of the cell and coordinated activation of the small GTPase RhoA. Astral MTs contribute by spatially coordinating cortical myosin recruitment generating a region of high contractility at the cell equator [65-67] and, together with central spindle MTs, they localize RhoA to the cell cortex [68]. The central spindle is thought to provide the platform for RhoA activation. Once recruited to PRC1, Plk1 acts to promote the localization of the RhoGEF, Ect2, to the central spindle by phosphorylating Cyk-4 (MgcRacGAP) which functions as Ect2 anchor and activator. This way, a signaling platform is created that triggers RhoA activation in a narrow zone overlaying the central spindle [68-70], regulating the onset of division [21,22]. In normally dividing *Theileria*-transformed cells, the parasite is almost always found symmetrically partitioned between the separating daughter cells with its middle section 'incorporated' into the central spindle and the midbody. Despite its size, the presence of the parasite does not appear to disturb cytokinesis. It is conceivable that by accumulating host cell central spindles at its surface, containing the signaling molecules required for RhoA activation, an uninterrupted interaction between the central spindle and cell cortex is guaranteed allowing flawless furrow ingression at the equator of the cell and unperturbed abscission.

Abscission, the final event in cytokinesis leading to two separate cells, involves vesicle transport and membrane fusion (reviewed in [14]). The centralspindlin complex, found first at the central spindle and subsequently at the midbody, not only regulates acto-myosin ring contraction but also vesicle transport to the cleavage furrow, required for abscission [71]. Our microscopic observations show that, during telophase, a short central section of the parasite is first trapped in the midbody as a narrow tube (see Figure 1C) and is subsequently included in the process of abscission. It is not known whether parasite-own structures provide specific cues in preparation of its abscission or whether such signals derive from the host cell. Whichever, once incorporated into the central spindle/midbody, the parasite does not affect host cell central spindle function or abscission and, from this point onwards, schizont cytokinesis appears to be a passive process that is largely controlled by the host cell. This is supported by the fact that, in the absence of host cell abscission, independent parasite division does not take place.

In summary, we propose a two-step model for the division of *Theileria* schizont between the separating daughter cells, involving first the mitotic spindle and subsequently the central spindle (Figure 11). As the host cell enters mitosis, the schizont binds newly forming MTs that emanate symmetrically from the spindle poles, allowing the schizont to position itself so that it spans the equatorial region of the mitotic cell where host cell chromosomes assemble during metaphase. This step is independent of Plk1 activity as it also takes place in the presence of potent Plk1 inhibitors. During anaphase, the schizont becomes closely associated with central spindles assembling in the midzone between the separating chromosomes. In contrast to the first step, this interaction requires catalytically active Plk1. By 'hijacking' the central spindle, an important spatial regulator of cleavage furrow formation, the schizont is

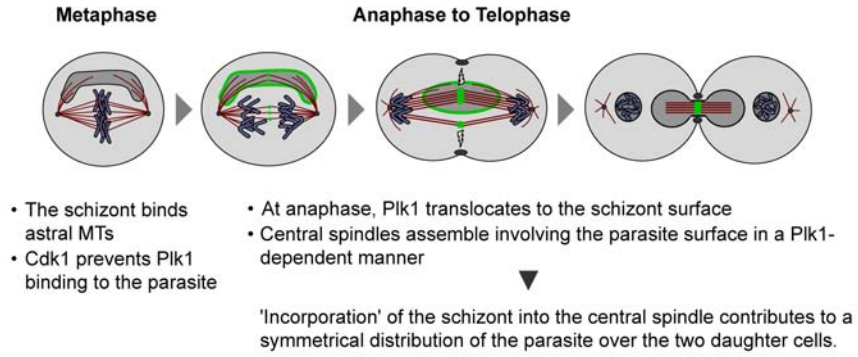

Figure 11. Schematic presentation of parasite interactions with astral and central spindle MTs during host M phase. Green depicts Plk1 binding to the parasite and central spindles.

strategically positioned to be included in the plane of cell division at each host cell cytokinesis, without disturbing the process.

Thus, while different transforming viruses either integrate into the host cell genome or target mitotic chromosomes to ensure persistence [12], the transforming protozoan *Theileria* evolved to single out the mitotic apparatus that mediates chromosome separation and cytokinesis. Considering the schizont is strictly intracellular [13] and its presence crucial for the constitutive activation of the signaling pathways that drive proliferation and protection against apoptosis (reviewed in [6,8]), we posit that this process is essential, not only for parasite persistence, but also for the exponential expansion of the parasite population.

In a more general context, there is mounting evidence from studies on protein-protein interactions that pathogens have evolved to target host proteins that function as hubs (those involved in many interactions) or bottlenecks (proteins central to many pathways) [72]. In earlier work we provided evidence that *Theileria* hijacks IKK, a central regulator of many NF-κB activation pathways [30]. By scavenging Plk1, a key regulator of mitosis, *Theileria* provides a second striking manifestation of this evolutionary process.

Materials and Methods

Cell culture and transfections

Theileria annulata (TaC12)-infected macrophages were cultured in Leibovitz 15 medium (Gibco) supplemented with 10% foetal calf serum (FCS, Amimed), 10 mM Hepes pH 7.2 (Merck), 2 mM L-glutamine (Gibco), 70 µM β-mercaptoethanol (Merck), and antibiotics (Lonza). The SV40-transformed cell line of *Theileria*-uninfected bovine macrophages (BoMac) was cultured in DMEM Glutamax medium (Gibco) supplemented with 10% FCS and antibiotics.

Plasmids encoding myc-tagged versions of human Plk1 (Figures 5, 6 and S8), including full-length wild-type Plk1, full-length kinase dead Plk1 (K82R), wild-type kinase domain (aa 1-330), wild-type PBD (aa 326-603), and mutant PBD (H538A/K540A), were previously described [43]. Cells were transfected using Lipofectamine 2000 (Invitrogen) following the manufacturer's recommendations. TaC12 cells stably expressing mRFP-α-tubulin (Figure S2) were transfected with the plasmid pmRFP-C1 (a kind gift by Daniel Gerlich, ETH Zürich) and selected using 2 mg/ml G418 (Alexis).

Synchronizations, drug treatments and western blotting

Stocks of the inhibitors BI-2536 (a kind gift by Boehringer Ingelheim, and partly purchased from Axon Medchem), BTO-1, blebbistatin (Sigma) MG132, monastrol and RO-3306 (Alexis) were prepared in DMSO. DMSO was added at the appropriate concentration to all control samples. Cells were washed in serum-supplemented medium when transferred to another medium. To test the binding of ectopically expressed versions of Plk1 in the presence of Plk1 inhibitor, cells were treated with 100 nM (Figure 6) or 1 μM BI-2536 (Figure S8) immediately after transfection and incubated for 8 h. For the microtubule re-polymerization assay (Figure 1A), cells were arrested in prometaphase by addition of 0.1 μg/ml nocodazole (Biotrend) for 16 h and harvested by shake-off followed by 30 min treatment with 3 μg/ml nocodazole. These cells were then released in drug-free medium for up to 120 min. For synchronous release from S arrest, cells were treated with 4 mM thymidine (Sigma) for 24 h and transferred into drug-free medium for up to 12 h (Figure S5). To demonstrate the absence of Plk1 from the parasite surface during early mitosis, cells were arrested in prometaphase by 16 h treatment with 0.1 μg/ml nocodazole or 100 μM monastrol and harvested by shake-off (Figure 2B). For the chemical induction of precocious cytokinesis, cells were arrested in prometaphase by 16 h treatment with 0.1 μg/ml nocodazole, harvested by shake-off, washed and then treated with medium lacking nocodazole but containing 10 μM RO-3306 for up to 60 min (Figure 3A, 7A-C, S9). Alternatively, prometaphase cells were kept in the presence of nocodazole and treated with RO-3306 plus 3 μg/ml nocodazole, with or without 100 nM BI-2536 (Figure 3A-C). To test the requirement of Plk1 catalytic activity for its binding to the parasite surface as well as the effect of Plk1 inhibition on ectopic furrowing (Figure 4B-D, S7F), cells were synchronized in S phase by thymidine block (see above), washed and immediately treated with 0.1 μg/ml nocodazole or BI-2536 (100 nM or 1 μM) for 15 h. Cells arrested in prometaphase were collected by shake-off and fixed or washed (nocodazole-blocked cells only) and treated with 10 μM RO-3306 or kept in the presence of BI-2536 and additionally subjected to 10 μM RO-3306 for 10-30 min.

To prevent cleavage furrow ingression, RO-3306-treatment was done in the presence of 100 μM blebbistatin (Figure S10). For synchronous release into anaphase, cells were arrested in prometaphase with 0.1 μg/ml nocodazole, harvested by shake-off, transferred into medium containing 20 μM MG132 for 2 h and finally released from metaphase arrest for 80 min in drug-free medium (Figure 2C) or medium containing 100 μM blebbistatin (Figure 8, 9A-C, S11A, B). For anaphase-specific inhibition of Plk1, these cells were additionally treated with 100 nM or 1 μM BI-2536 or 20 μM BTO-1 during washout (S12A), or 15 min after MG132 washout (Figure 4E, 9A-C, S7D and E, S11A and B, S12A-C). To investigate the role

of astral and central spindle microtubules for parasite positioning (Figure 10A-C), cells were released for from metaphase arrest as described above in the presence of 100 nM BI-2536 (added 15 min after MG132 washout) or inhibitor-free medium. After 60 min release the medium was supplemented with 10 µM nocodazole and cells were incubated for 20 min at 37°C. To test the effect of BI-2536 on spindle maintenance, metaphase-synchronized cells were additionally treated with 100 nM BI-2536 for 160 min (Figure S7B and C).

For the elimination of the parasite from TaC12 cells (Fig S1A and B), cultures were grown 4 days in the presence of 100 ng/ml of the theilericidal drug BW720c [73]. Cells were then subjected to a microtubule re-polymerization assay as described above. Chemical induction of merogony (Fig S6) was done as previously described [33]. Briefly, cells were cultivated in the presence or absence of 50 µM chloramphenicol (Sigma) for 10 days.

Synchronous entry into M phase (Figure S5) and progression from metaphase to anaphase (Figure 2C) were monitored by immunoblot analysis of protein extracts prepared in RIPA buffer (50 mM Tris-Hcl pH 7.5, 1 % NP-40, 0.25 % Na-deoxycholate, 150 mM NaCl, 1 mM EDTA, 1 mM PMSF, 1x Roche Complete protease inhibitor cocktail, 1 mM NaF, 1 mM Na_3VO_4). Primary antibodies were mouse monoclonal anti-cyclin B1 (clone GNS-11, Pharmingen), anti-Plk1 (clone 35-206, Calbiochem), anti-securin (clone DCS-280, MBL), anti-α-tubulin (clone DM1A, Sigma) as well as rabbit polyclonal anti-phospho-Ser10 histone H3 (Upstate) and anti-histone deacetylase 1 (Santa Cruz).

Immunofluorescence microscopy and time-lapse imaging

Interphase cells were grown on coverslips, cells harvested by mitotic shake-off were seeded on poly-L-lysine coated coverslips (Sigma). Samples were fixed with 4% paraformaldehyde in PBS for 10 min at room temperature (for Aurora B, c-myc, Plk1, TamR1, TaSP and α-tubulin staining), with methanol for 10 min at –20°C (for Cyk-4 and PRC1 staining) or with 10% trichloroacetic acid on ice for 15 min (for RhoA staining). Cells were subsequently permeabilized in 0.2% Triton X-100 (prepared in PBS) for 10 min at room temperature. Antibody incubations were done in PBS containing 10% heat-inactivated FCS, DNA was stained with DAPI (Molecular Probes) and cells were mounted using Glycergel (Dako). Widefield microscopy was done on a Nikon Eclipse 80i microscope equipped with a Retiga 2000R CCD camera (Qimaging) using 60x and 100x Plan Apo objectives (Nikon) and Openlab 5 software (Improvision). For confocal microscopy, a Leica TCS SP2 system was used, equipped with an acousto-optical beam splitter, a 63x Plan Apo objective (Leica) and Leica confocal software. Images were processed using Photoshop (Adobe) or Imaris (Bitplane) software. To measure the distribution of the parasite in dividing cells after nocodazole wash-in (Figure 10A-C), whole cells were stained for TaSP1/α-tubulin and recorded using z-stacks. Two-dimensional projections were generated and the parasite area on each side of the cleavage furrow was measured using Openlab software.

The following antibodies were used: mouse monoclonal anti-Aurora B (AIM-1, clone 6, BD Transduction Laboratories), anti-c-myc (clone 9E-10, Santa Cruz), anti-Plk1 (clone 35-206, Calbiochem), anti-Rho A (clone 26C4, Santa Cruz), anti-α-tubulin (clone DM1A, Sigma) and 1C12 which detects the *T. annulata*

schizont surface (kindly provided by Brian Shiels, University of Glasgow), as well as rabbit polyclonal anti-PRC1 (kindly provided by Francis Barr, University of Liverpool), anti-Tamr1 [74] (Brian Shiels, University of Glasgow), and the schizont surface marker anti-TaSP [28] (kindly provided by Jabbar Ahmed, Borstel Research Center); goat polyclonal anti-Cyk-4 (MgcRacGAP, Abcam) and rat monoclonal anti-α-tubulin (Abcam). Appropriate (isotype-specific) secondary antibodies conjugated with either Marina Blue, Alexa-Fluor 488, Alexa-Fluor 594 or Texas Red (Molecular Probes) were used.

To generate kymographs of TaC12 cells stably expressing mRFP-α-tubulin (Figure S2), cells were synchronized in prometaphase using monastrol (see above) and kept in the presence of the drug during time-lapse imaging. Fluorescence was recorded at 30 sec intervals over a period of 20 min and kymographs were generated from these data with a width of 5 pixels using NIS Elements imaging software (Nikon). Immediately after imaging, cells were fixed and stained (see above) to identify the position of the parasite in the previously recorded cells. To determine the percentage of cells displaying furrow ingression after release into anaphase in the presence of 100 nM BI-2536 (S12A), cells were synchronized and drug-treated as described above and observed by time-lapse imaging in 10 min intervals over a period of 4 h. Time-lapse imaging was done using a TE2000E-PFS microscope (Nikon) equipped with a Plan Fluor 20x, 60x objective (Nikon), Orca ER CCD camera (Hamamatsu) and incubation chamber (Life Imaging Services)

Flow cytometry

To test the effect of BI-2536 on cell cycle progression of TaC12 cells (Figure S7A), unsynchronized cultures were cultured in the presence of 100 nM BI-2536 or the equivalent volume of DMSO for 20 h. To monitor the effect of Plk1 inhibition on progression of M phase in TaC12 cells (Figure 4A), cultures were synchronized in S phase as described above and released for 20 h in the presence of 100 nM or 1 µM BI-2536. Cell suspensions were fixed in 80% ethanol at –20°C o/n followed by treatment with 200 µg/ml RNaseA in PBS at 37°C for 30 min. Finally, cells were stained in DAPI staining solution (100 mM Tris-HCl, pH 7.5, 150 mM NaCl, 1 mM $CaCl_2$, 0.5 mM $MgCl_2$, 0.1% NP-40, 3 µM DAPI) and cellular DNA content was measured using a BD LSR II and BD FACS Diva software (Becton-Dickinson).

Abbreviations

Cdk, cyclin-dependent kinase; DAPI, 4',6-diamidino-2-phenylindole; DMSO, dimethyl sulfoxide; HDAC1, histone deacetylase 1; KDom, kinase domain; MT, microtubule; Noc, nocodazole; PBD, polo-box domain; P-H3, phospho-S10 histone H3; Plk, Polo-like kinase; PRC1, protein regulator of cytokinesis 1; TamR1, *Theileria annulata* rhoptry protein 1; TaSP1, *Theileria annulata* surface protein 1; wt, wild type

References

1. Kuenzi P, Schneider P, Dobbelaere DA (2003) *Theileria parva*-transformed T cells show enhanced resistance to Fas/Fas ligand-induced apoptosis. J Immunol 171: 1224-1231.
2. Dessauge F, Lizundia R, Baumgartner M, Chaussepied M, Langsley G (2005) Taking the Myc is bad for Theileria. Trends Parasitol 21: 377-385.
3. Heussler V, Sturm A, Langsley G (2006) Regulation of host cell survival by intracellular *Plasmodium* and *Theileria* parasites. Parasitology 132 Suppl: S49-60.
4. Dobbelaere DA, Kuenzi P (2004) The strategies of the *Theileria* parasite: a new twist in host-pathogen interactions. Curr Opin Immunol 16: 524-530.
5 . Luder CG, Stanway RR, Chaussepied M, Langsley G, Heussler VT (2009) Intracellular survival of apicomplexan parasites and host cell modification. Int J Parasitol 39: 163-173.
6. Shiels B, Langsley G, Weir W, Pain A, McKellar S, et al. (2006) Alteration of host cell phenotype by *Theileria annulata* and *Theileria parva*: mining for manipulators in the parasite genomes. Int J Parasitol 36: 9-21.
7. Shaw MK (2003) Cell invasion by *Theileria* sporozoites. Trends Parasitol 19: 2-6.
8. Dobbelaere D, Baumgartner M (2009) Theileria. In: Schaible UE, Haas A, editors. Intracellular Niches of Microbes: A Pathogens Guide Through the Host Cell: Wiley-VCH. pp. 613 - 632.
9. Hudson AT, Randall AW, Fry M, Ginger CD, Hill B, et al. (1985) Novel anti-malarial hydroxynaphthoquinones with potent broad spectrum anti-protozoal activity. Parasitology 90: 45-55.
10. Irvin AD, Ocama JG, Spooner PR (1982) Cycle of bovine lymphoblastoid cells parasitised by *Theileria parva*. Res Vet Sci 33: 298-304.
11. Goff SP (2007) Host factors exploited by retroviruses. Nat Rev Microbiol 5: 253-263.
12. Feeney KM, Parish JL (2009) Targeting mitotic chromosomes: a conserved mechanism to ensure viral genome persistence. Proc Biol Sci 276: 1535-1544.
13. Hulliger L, Wilde KH, Brown CG, Turner L (1964) Mode of Multiplication of *Theileria* in Cultures of Bovine Lymphocytic Cells. Nature 203: 728-730.
14. Barr FA, Gruneberg U (2007) Cytokinesis: placing and making the final cut. Cell 131: 847-860.
15. Glotzer M (2009) The 3Ms of central spindle assembly: microtubules, motors and MAPs. Nat Rev Mol Cell Biol 10: 9-20.
16. Steigemann P, Gerlich DW (2009) Cytokinetic abscission: cellular dynamics at the midbody. Trends Cell Biol 19: 606-616.
17. Petronczki M, Lenart P, Peters JM (2008) Polo on the Rise-from Mitotic Entry to Cytokinesis with Plk1. Dev Cell 14: 646-659.
18. Taylor S, Peters JM (2008) Polo and Aurora kinases: lessons derived from chemical biology. Curr Opin Cell Biol 20: 77-84.
19. Archambault V, Glover DM (2009) Polo-like kinases: conservation and divergence in their functions and regulation. Nat Rev Mol Cell Biol 10: 265-275.
20. Neef R, Gruneberg U, Kopajtich R, Li X, Nigg EA, et al. (2007) Choice of Plk1 docking partners during mitosis and cytokinesis is controlled by the activation state of Cdk1. Nat Cell Biol 9: 436-444.
21. Burkard ME, Maciejowski J, Rodriguez-Bravo V, Repka M, Lowery DM, et al. (2009) Plk1 self-organization and priming phosphorylation of HsCYK-4 at the spindle midzone regulate the onset of division in human cells. PLoS Biol 7: e1000111.
22. Wolfe BA, Takaki T, Petronczki M, Glotzer M (2009) Polo-like kinase 1 directs assembly of the HsCyk-4 RhoGAP/Ect2 RhoGEF complex to initiate cleavage furrow formation. PLoS Biol 7: e1000110.
23. Atilla-Gokcumen GE, Castoreno AB, Sasse S, Eggert US (2010) Making the cut: the chemical biology of cytokinesis. ACS Chem Biol 5: 79-90.
24. Brennan IM, Peters U, Kapoor TM, Straight AF (2007) Polo-like kinase controls vertebrate spindle elongation and cytokinesis. PLoS ONE 2: e409.
25. Burkard ME, Randall CL, Larochelle S, Zhang C, Shokat KM, et al. (2007) Chemical genetics reveals the requirement for Polo-like kinase 1 activity in positioning RhoA and triggering cytokinesis in human cells. Proc Natl Acad Sci U S A 104: 4383-4388.
26. Petronczki M, Glotzer M, Kraut N, Peters JM (2007) Polo-like kinase 1 triggers the initiation of cytokinesis in human cells by promoting recruitment of the RhoGEF Ect2 to the central spindle. Dev Cell 12: 713-725.
27. Santamaria A, Neef R, Eberspacher U, Eis K, Husemann M, et al. (2007) Use of the novel Plk1 inhibitor ZK-thiazolidinone to elucidate functions of Plk1 in early and late stages of mitosis. Mol Biol Cell 18: 4024-4036.
28. Schnittger L, Katzer F, Biermann R, Shayan P, Boguslawski K, et al. (2002) Characterization of a polymorphic *Theileria annulata* surface protein (TaSP) closely related to PIM of *Theileria parva*: implications for use in diagnostic tests and subunit vaccines. Mol Biochem Parasitol 120: 247-256.
29. Mayer TU, Kapoor TM, Haggarty SJ, King RW, Schreiber SL, et al. (1999) Small molecule inhibitor of mitotic spindle bipolarity identified in a phenotype-based screen. Science 286: 971-974.
30. Heussler VT, Rottenberg S, Schwab R, Kuenzi P, Fernandez PC, et al. (2002) Hijacking of host cell IKK signalosomes by the transforming parasite *Theileria*. Science 298: 1033-1036.
31. Shiels B, Kinnaird J, McKellar S, Dickson J, Miled LB, et al. (1992) Disruption of synchrony between parasite growth and host cell division is a determinant of differentiation to the merozoite in *Theileria annulata*. J Cell Sci 101: 99-107.
32. Hulliger L, Brown CG, Wilde JK (1966) Transition of developmental stages of *Theileria parva* in vitro at high temperature. Nature 211: 328-329.
33. Schmuckli-Maurer J, Shiels B, Dobbelaere DA (2008) Stochastic induction of *Theileria annulata* merogony in vitro by chloramphenicol. Int J Parasitol 38: 1705-1715.

34. Elia AE, Cantley LC, Yaffe MB (2003) Proteomic screen finds pSer/pThr-binding domain localizing Plk1 to mitotic substrates. Science 299: 1228-1231.
35. Elia AE, Rellos P, Haire LF, Chao JW, Ivins FJ, et al. (2003) The molecular basis for phosphodependent substrate targeting and regulation of Plks by the Polo-box domain. Cell 115: 83-95.
36. Neef R, Preisinger C, Sutcliffe J, Kopajtich R, Nigg EA, et al. (2003) Phosphorylation of mitotic kinesin-like protein 2 by polo-like kinase 1 is required for cytokinesis. J Cell Biol 162: 863-875.
37. Kang YH, Park JE, Yu LR, Soung NK, Yun SM, et al. (2006) Self-regulated Plk1 recruitment to kinetochores by the Plk1-PBIP1 interaction is critical for proper chromosome segregation. Mol Cell 24: 409-422.
38. Vassilev LT, Tovar C, Chen S, Knezevic D, Zhao X, et al. (2006) Selective small-molecule inhibitor reveals critical mitotic functions of human CDK1. Proc Natl Acad Sci USA 103: 10660-10665.
39. Lenart P, Petronczki M, Steegmaier M, Di Fiore B, Lipp JJ, et al. (2007) The small-molecule inhibitor BI 2536 reveals novel insights into mitotic roles of polo-like kinase 1. Curr Biol 17: 304-315.
40. Steegmaier M, Hoffmann M, Baum A, Lenart P, Petronczki M, et al. (2007) BI 2536, a potent and selective inhibitor of polo-like kinase 1, inhibits tumor growth in vivo. Curr Biol 17: 316-322.
41. Barr FA, Sillje HH, Nigg EA (2004) Polo-like kinases and the orchestration of cell division. Nat Rev Mol Cell Biol 5: 429-440.
42. van de Weerdt BC, Medema RH (2006) Polo-like kinases: a team in control of the division. Cell Cycle 5: 853-864.
43. Hanisch A, Wehner A, Nigg EA, Sillje HH (2006) Different Plk1 functions show distinct dependencies on Polo-Box domain-mediated targeting. Mol Biol Cell 17: 448-459.
44. Straight AF, Cheung A, Limouze J, Chen I, Westwood NJ, et al. (2003) Dissecting temporal and spatial control of cytokinesis with a myosin II Inhibitor. Science 299: 1743-1747.
45. O'Connell CB, Wang YL (2000) Mammalian spindle orientation and position respond to changes in cell shape in a dynein-dependent fashion. Mol Biol Cell 11: 1765-1774.
46. Murata-Hori M, Wang YL (2002) Both midzone and astral microtubules are involved in the delivery of cytokinesis signals: insights from the mobility of aurora B. J Cell Biol 159: 45-53.
47. Murthy K, Wadsworth P (2008) Dual role for microtubules in regulating cortical contractility during cytokinesis. J Cell Sci 121: 2350-2359.
48. Munter S, Way M, Frischknecht F (2006) Signaling during pathogen infection. Sci STKE 2006: re5.
49. Radtke K, Dohner K, Sodeik B (2006) Viral interactions with the cytoskeleton: a hitchhiker's guide to the cell. Cell Microbiol 8: 387-400.
50. Greber UF, Way M (2006) A superhighway to virus infection. Cell 124: 741-754.
51. Walker ME, Hjort EE, Smith SS, Tripathi A, Hornick JE, et al. (2008) *Toxoplasma gondii* actively remodels the microtubule network in host cells. Microbes Infect 10: 1440-1449.
52. Coppens I, Dunn JD, Romano JD, Pypaert M, Zhang H, et al. (2006) *Toxoplasma gondii* sequesters lysosomes from mammalian hosts in the vacuolar space. Cell 125: 261-274.
53. Tyler KM, Luxton GW, Applewhite DA, Murphy SC, Engman DM (2005) Responsive microtubule dynamics promote cell invasion by *Trypanosoma cruzi*. Cell Microbiol 7: 1579-1591.
54. Rodriguez A, Samoff E, Rioult MG, Chung A, Andrews NW (1996) Host cell invasion by trypanosomes requires lysosomes and microtubule/kinesin-mediated transport. J Cell Biol 134: 349-362.
55. Schneider I, Haller D, Kullmann B, Beyer D, Ahmed JS, et al. (2007) Identification, molecular characterization and subcellular localization of a *Theileria annulata* parasite protein secreted into the host cell cytoplasm. Parasitol Res 101: 1471-1482.
56. Seitzer U, Gerber S, Beyer D, Dobschanski J, Kullmann B, et al. (2010) Schizonts of Theileria annulata interact with the microtubuli network of their host cell via the membrane protein TaSP. Parasitol Res 106: 1085-1102.
57. Johnson EF, Stewart KD, Woods KW, Giranda VL, Luo Y (2007) Pharmacological and functional comparison of the polo-like kinase family: insight into inhibitor and substrate specificity. Biochemistry 46: 9551-9563.
58. Hansen DV, Tung JJ, Jackson PK (2006) CaMKII and polo-like kinase 1 sequentially phosphorylate the cytostatic factor Emi2/XErp1 to trigger its destruction and meiotic exit. Proc Natl Acad Sci U S A 103: 608-613.
59. Rauh NR, Schmidt A, Bormann J, Nigg EA, Mayer TU (2005) Calcium triggers exit from meiosis II by targeting the APC/C inhibitor XErp1 for degradation. Nature 437: 1048-1052.
60. Liu J, Maller JL (2005) Calcium elevation at fertilization coordinates phosphorylation of XErp1/Emi2 by Plx1 and CaMK II to release metaphase arrest by cytostatic factor. Curr Biol 15: 1458-1468.
61. Archambault V, D'Avino PP, Deery MJ, Lilley KS, Glover DM (2008) Sequestration of Polo kinase to microtubules by phosphopriming-independent binding to Map205 is relieved by phosphorylation at a CDK site in mitosis. Genes Dev 22: 2707-2720.
62. D'Avino PP, Savoian MS, Glover DM (2005) Cleavage furrow formation and ingression during animal cytokinesis: a microtubule legacy. J Cell Sci 118: 1549-1558.
63. Eggert US, Mitchison TJ, Field CM (2006) Animal cytokinesis: from parts list to mechanisms. Annu Rev Biochem 75: 543-566.
64. Alsop GB, Zhang D (2003) Microtubules are the only structural constituent of the spindle apparatus required for induction of cell cleavage. J Cell Biol 162: 383-390.
65. Dechant R, Glotzer M (2003) Centrosome separation and central spindle assembly act in redundant pathways that regulate microtubule density and trigger cleavage furrow formation. Dev Cell 4: 333-344.

66. Glotzer M (2004) Cleavage furrow positioning. J Cell Biol 164: 347-351.
67. Werner M, Munro E, Glotzer M (2007) Astral signals spatially bias cortical myosin recruitment to break symmetry and promote cytokinesis. Curr Biol 17: 1286-1297.
68. Nishimura Y, Yonemura S (2006) Centralspindlin regulates ECT2 and RhoA accumulation at the equatorial cortex during cytokinesis. J Cell Sci 119: 104-114.
69. Kamijo K, Ohara N, Abe M, Uchimura T, Hosoya H, et al. (2006) Dissecting the role of Rho-mediated signaling in contractile ring formation. Mol Biol Cell 17: 43-55.
70. Yuce O, Piekny A, Glotzer M (2005) An ECT2-centralspindlin complex regulates the localization and function of RhoA. J Cell Biol 170: 571-582.
71. Simon GC, Schonteich E, Wu CC, Piekny A, Ekiert D, et al. (2008) Sequential Cyk-4 binding to ECT2 and FIP3 regulates cleavage furrow ingression and abscission during cytokinesis. EMBO J 27: 1791-1803.
72. Dyer MD, Murali TM, Sobral BW (2008) The landscape of human proteins interacting with viruses and other pathogens. PLoS Pathog 4: e32.
73. McHardy N (1978) In vitro studies on the action of menoctone and other compounds on *Theileria parva* and *T. annulata*. Ann Trop Med Parasitol 72: 501-511.
74. Shiels BR, d Oliveira C, McKellar S, Ben Miled L, Kawazu S, et al. (1995) Selection of diversity at putative glycosylation sites in the immunodominant merozoite/piroplasm surface antigen of *Theileria* parasites. Mol Biochem Parasitol 72: 149-162.

Acknowledgments

The authors would like to thank Francis Barr (University of Liverpool) for anti-PRC1 and stimulating discussions. Jabbar Ahmed (Research Center Borstel) is thanked for providing anti-TaSP1, Brian Shiels (University of Glasgow) for 1C12 and Daniel Gerlich (ETH Zürich) for pmRFP-C1. Isabel Roditi is thanked for critically reading the manuscript. Boehringer Ingelheim is thanked for kindly providing BI-2536. The reviewers are thanked for their constructive input. Our sincere thanks go to Andy Tait, Volker Heussler and Christine Clayton for expert problem-solving.

Supporting Information

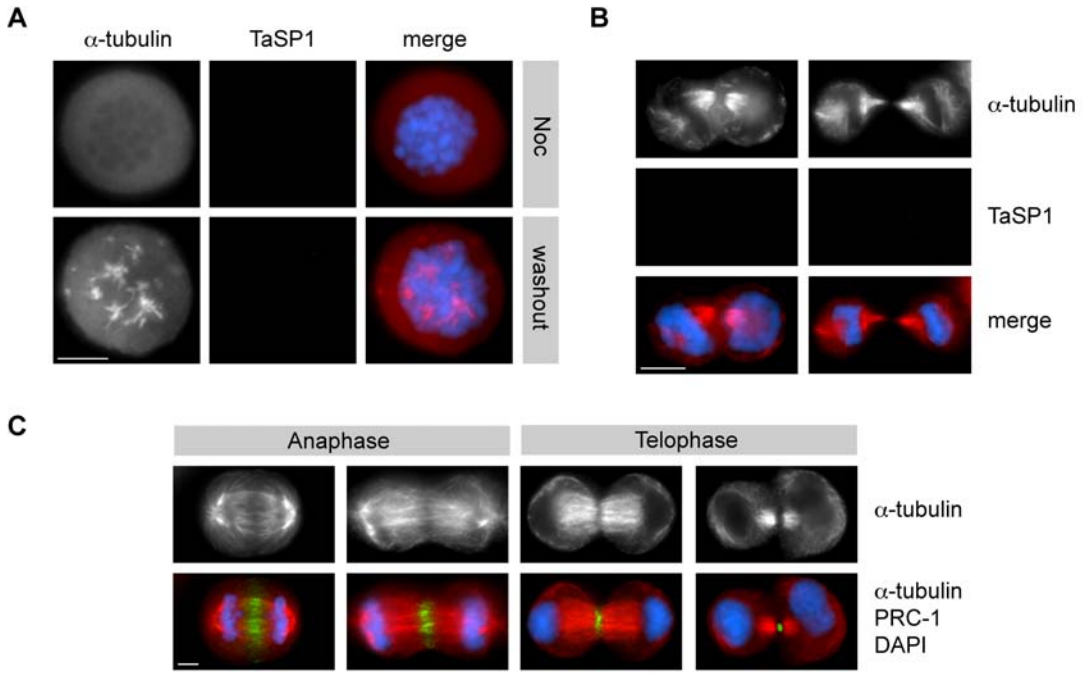

Figure S1. Microtubule repolymerization and spindle midzones in unparasitized macrophages. (A) Cells from which the parasite was eliminated by treatment with the theilericidal compound BW720c where subjected to a microtubule repolymerization assay. Samples were fixed and stained for α-tubulin and the parasite surface protein TaSP1. The absence of TaSP1 staining confirms that the parasite had been eliminated. (B) Central spindles in BW720c-treated cells stained as in A. (C) Spindle midzone, central spindle and midbody formation in transformed bovine macrophages (BoMac) stained with anti-PRC1 and anti-α-tubulin. DNA was stained with DAPI; scale bars represent 5 µm.

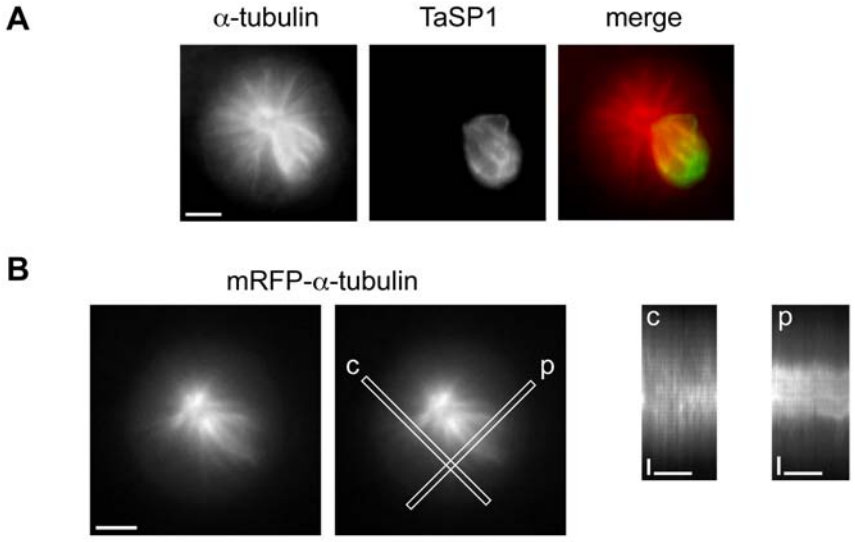

Figure S2. Mitotic microtubules are stably associated with the parasite surface. (A) IFM micrograph of the monastrol-treated cell observed by time-lapse imaging shown in B. The cell was fixed and stained with anti-α-tubulin and anti-TaSP1 immediately after live imaging. Scale bar represents 5 µm. (B) *T. annulata*-transformed TaC12 cells stably expressing mRFP-α-tubulin were synchronized in prometaphase by monastrol treatment and observed by time-lapse imaging in the presence of the drug. The two left panels show the same frame of an image sequence recorded in 30 sec intervals over 20 min. Data from 40 frames were used to generate kymographs. White rectangles show the regions chosen for the kymographs; p indicates the source used for the kymograph of microtubules associated with the parasite surface and c that for free microtubules. Results for c and p are shown in the righthand panels. Data are representative for 12 cells observed under identical conditions. Vertical bars represent 2 µm, horizontal bars represent 10 min.

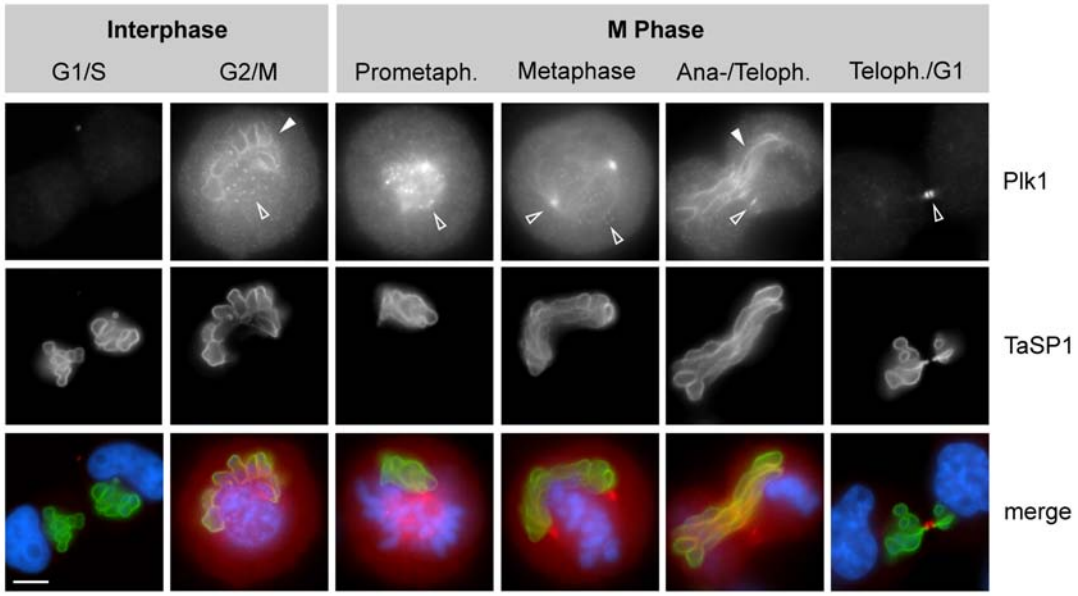

Figure S3. Plk1 association with the surface of the *T. annulata* schizont during different stages of the cell cycle. Plk1 recruitment to the parasite surface was analysed by immunofluorescence microscopy using anti-Plk1 (green) and anti-TaSP1 (red), DNA was stained with DAPI. Closed arrowheads point at Plk1 binding to the schizont. Plk1 can also be detected on host cell structures (open arrows) including centromeres/kinetochores, spindle poles, central spindles (ana- and telophase) and midbody (cytokinesis). Scale bar represents 5 µm.

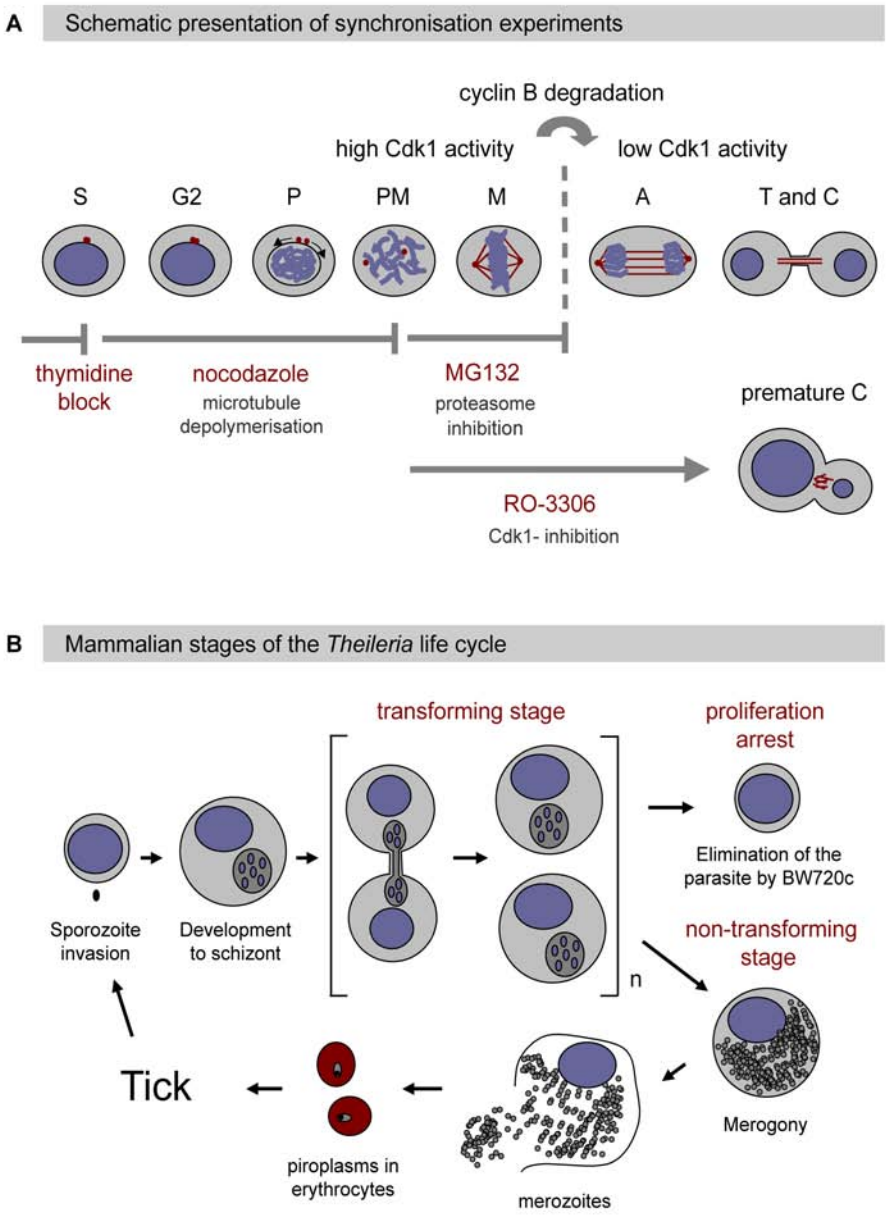

Figure S4. Schematic representation of synchronization experiments (A) and mammalian stages of the *Theileria* life cycle (B). S, synthesis phase; G2, gap 2 phase; P, prophase; PM, prometaphase; M, metaphase; A, anaphase; T, telophase; C, cytokinesis; Cdk1, cyclin-dependent kinase 1.

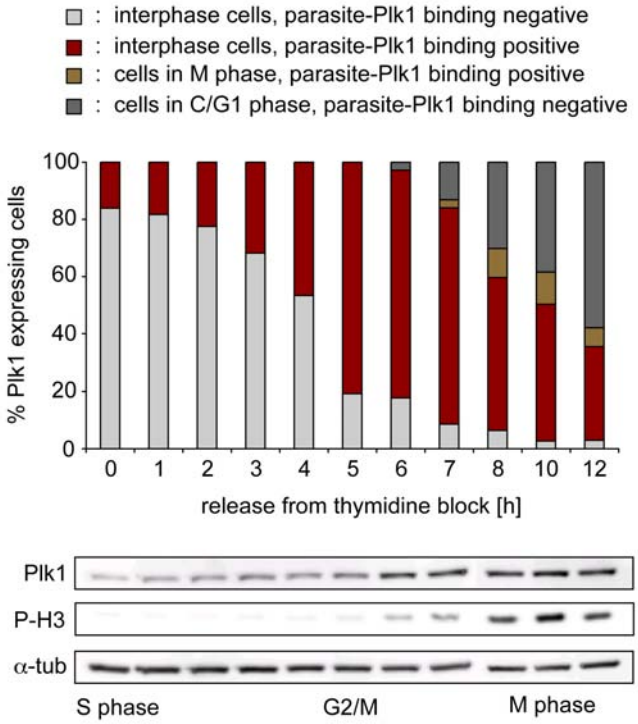

Figure S5. Monitoring Plk1 binding to the schizont in cells released from S phase arrest. *T. annulata*-transformed cells were synchronised in early S phase by thymidine block. At the indicated times after release, cells were examined by IFM for Plk1 binding to the parasite surface and lysates were prepared for immunoblot analysis. Data are presented as the percentage of cells containing parasites with surface-bound Plk1 in different cell cycle stages as indicated (n=200 cells/sample). Immunoblot: anti-Plk1 was used to follow the increase in Plk1 expression; anti-phospho-Histone H3 (P-H3) was used to monitor entry into M phase; α-tubulin (α-tub) was monitored as a loading control for both, supernatant and pellet of each lysate. Samples of time points 0-7 h and 8-12 h were run on separate gels.

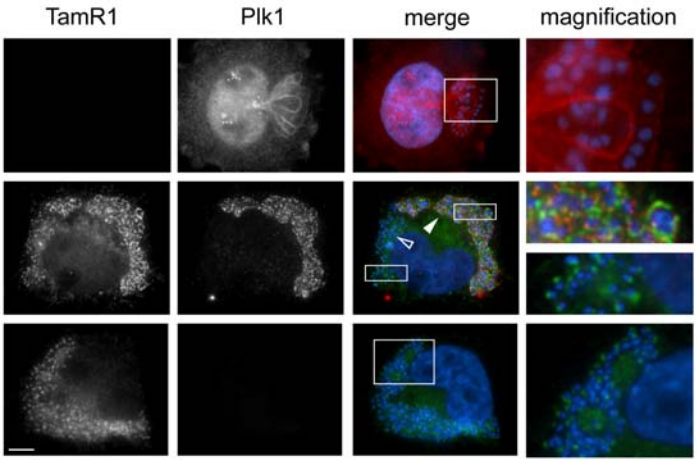

Figure S6. Plk1 binding to the parasite surface is downregulated during merogony. Top panels: *T. annulata*-transformed TaC12 cell in late G2 harbouring a schizont with Plk1 bound to its surface. The transforming schizont does not express TamR1, a marker for merogony; parasite and host cell nuclei were stained with DAPI. Middle panels: TaC12 cell containing schizonts in two stages of differentiation: partial merogony (closed arrow) and advanced merogony (open arrow); cells were stained for expression of TamR1 and Plk1. Squared areas are shown at higher magnification. Bottom Panels: TaC12 cell containing a parasite in an advanced stage of merogony. Scale bar represents 5 μm

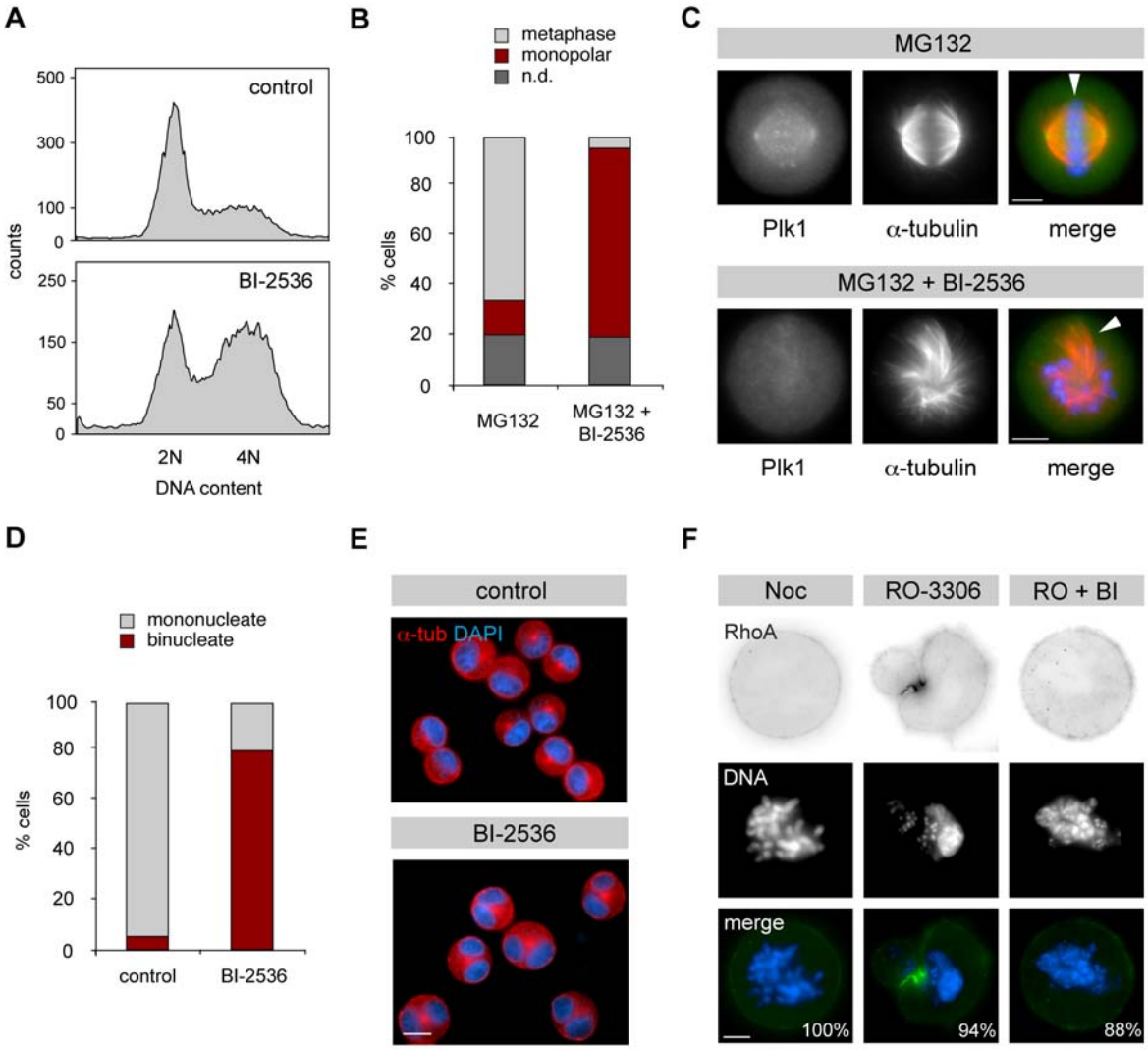

Figure S7 Effects of BI-2536 treatment on M phase progression in *T. annulata*-transformed cells. (A) Unsynchronized TaC12 cells (upper panel) or TaC12 cells cultured for 20 h in the presence of 100 nM BI-2536 (lower panel) were analyzed by flow cytometry. 2N, G1 phase; 4N, G2/M phase. (B) Metaphase synchronized TaC12 cells were either kept in the presence of proteasomal inhibitor (MG132) or additionally treated with 100 nM BI-2536 (MG132 + BI-2536). Cells were harvested after 160 min and bi-/monopolar spindles were quantified by IFM; n.d. indicates cells that could not be classified; data represent 250 cells/sample. (C) Micrographs show representative *T. annulata*-infected cells with bipolar metaphase plate (MG132) or collapsed monopolar spindle (MG132 + BI-2536) that were quantified in (B). Cells were stained for Plk1 and TaSP1 and analyzed by IFM. DNA was stained with DAPI; arrow head indicates the position of the parasite; scale bar represents 5 µm. (D) Metaphase-synchronized TaC12 cells synchronously released into anaphase and treated with DMSO (control) or 100 nM BI-2536 (BI-2536) at 15 min of release. Cells were analyzed after 4 h by IFM and the abundance of mononucleate and binucleate cells was determined for both samples; data represent 250 cells/sample. (E) Micrographs showing cells quantified in (D). Scale bar represents 10 µm. (F) S phase-synchronized TaC12 cells were released in the presence of nocodazole or 100 nM BI-2536 for 15 h and cells arrested in prometaphase were harvested from both cultures. Nocodazole-blocked prometaphase cells were either kept in the presence of the drug (Noc) or washed and treated with Cdk1 inhibitor for 30 min (RO-3306). Prometaphase cells obtained upon BI-2536-treatment were kept in the presence of 100 nM BI-2536 and additionally treated with Cdk1 inhibitor for 30 min (RO + BI). Cells were stained for RhoA and the occurrence of ectopic furrow ingression quantified (100 cells/sample) by IFM; DNA was stained with DAPI; scale bar represents 5 µm.

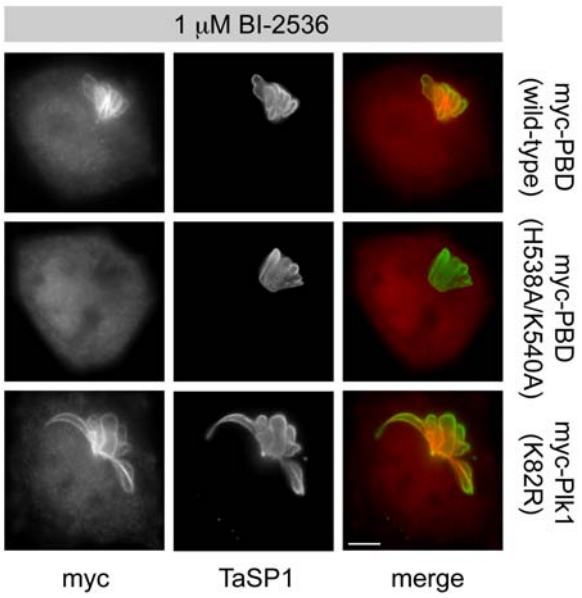

Figure S8. Ectopically expressed Plk1 PBD and catalytically inactive Plk1 can associate with the parasite surface in the presence of high doses of the Plk1 inhibitor BI-2536. *T. annulata*-infected cells were transfected with plasmids encoding myc-tagged versions of Polo-box domain (myc-PBD, wild type), H538A/K540A mutant PBD (myc-PBD H538A/K540A) or catalytically inactive Plk1 (myc-Plk1 K82R) and cultured in the presence or absence of BI-2536 at a concentration of 1 μM. Cells were analyzed by IFM using anti-myc and anti-TaSP1 antibodies. Scale bar represents 5 μm.

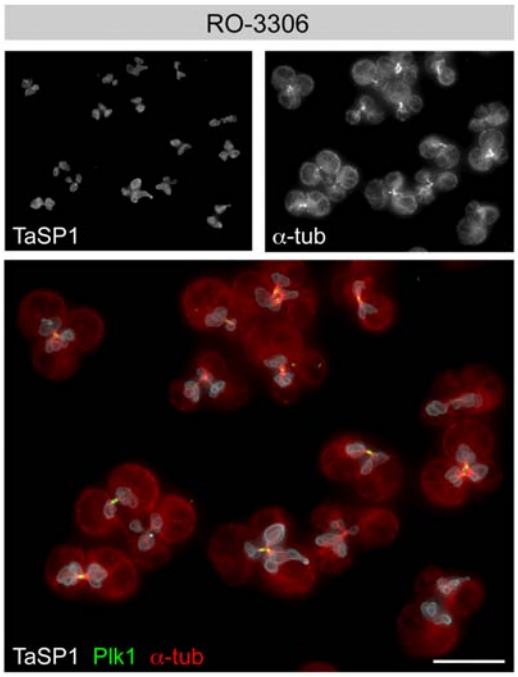

Figure S9. Cleavage furrow ingression occurs at sites where parasite-associated central spindle MTs assemble. *T. annulata*-transformed cells were synchronised in prometaphase, washed and precocious anaphase and premature cytokinesis were induced by immediately blocking Cdk1 activity using the specific inhibitor RO-3306 (30 min). The formation of central spindles was monitored using anti-α-tubulin and anti-Plk1. The parasite was visualised using anti-TaSP1. Scale bar represents 20 μm.

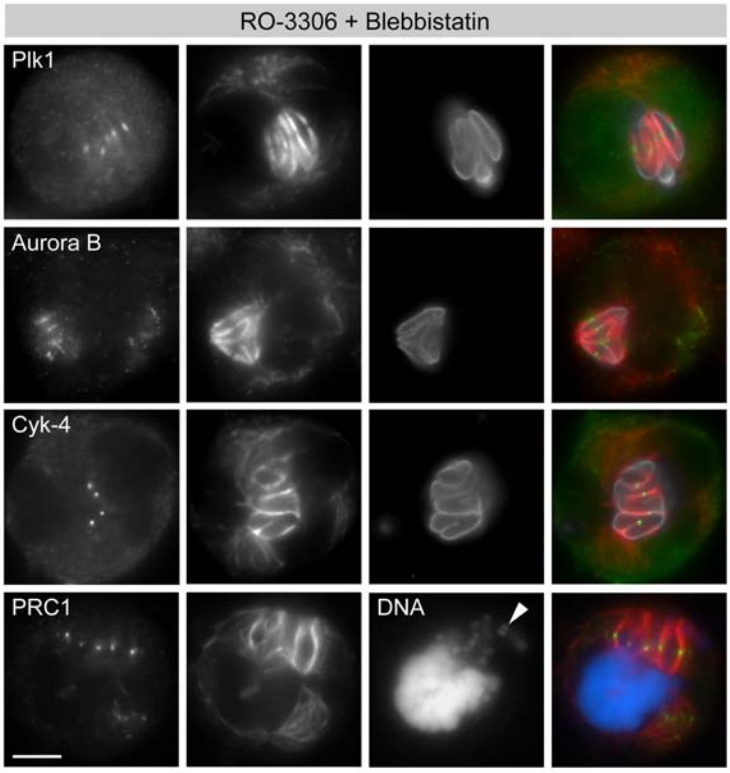

Figure S10. The *Theileria* schizont recruits central spindles to its surface. *T. annulata*-transformed cells were synchronised in prometaphase and precocious anaphase induced by blocking Cdk1 using the inhibitor RO-3306. Cleavage furrow contraction was prevented by treatment with the myosin II inhibitor blebbistatin. Parasite-associated central spindles were analysed for the presence of central spindle-specific proteins such as Plk1, Aurora B, Cyk-4 and PRC1 as indicated. MTs were visualised using anti-α-tubulin, the schizont was stained using anti-TaSP1; in the lower panels, DNA was stained with DAPI. Arrowhead indicates the position of the parasite. Scale bar represents 5 μm.

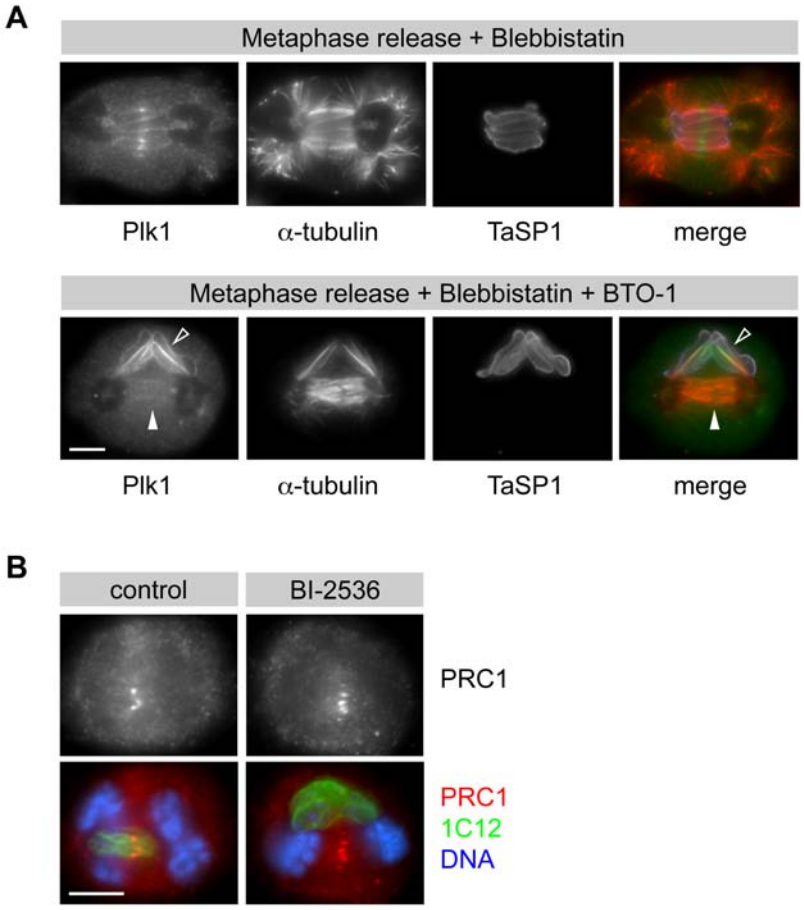

Figure S11. Recruitment of central spindle, but not astral, MTs to the parasite surface requires catalytically active Plk1.

(A) *T. annulata*-transformed TaC12 cells were released for 80 min from metaphase arrest in the presence of the Plk1 inhibitor BTO-1 or control solvent. Cleavage furrow contraction was blocked by treatment with the myosin II inhibitor blebbistatin. Anti-α-tubulin was used to identify central spindles and parasite-associated MTs emanating from the spindle poles. Open arrowheads point at Plk1 binding to the schizont surface; closed arrowheads indicate central spindles lacking Plk1 in the central section.

(B) Representative micrographs of IFM stainings that were used to quantitate the association of the parasite with central spindles in

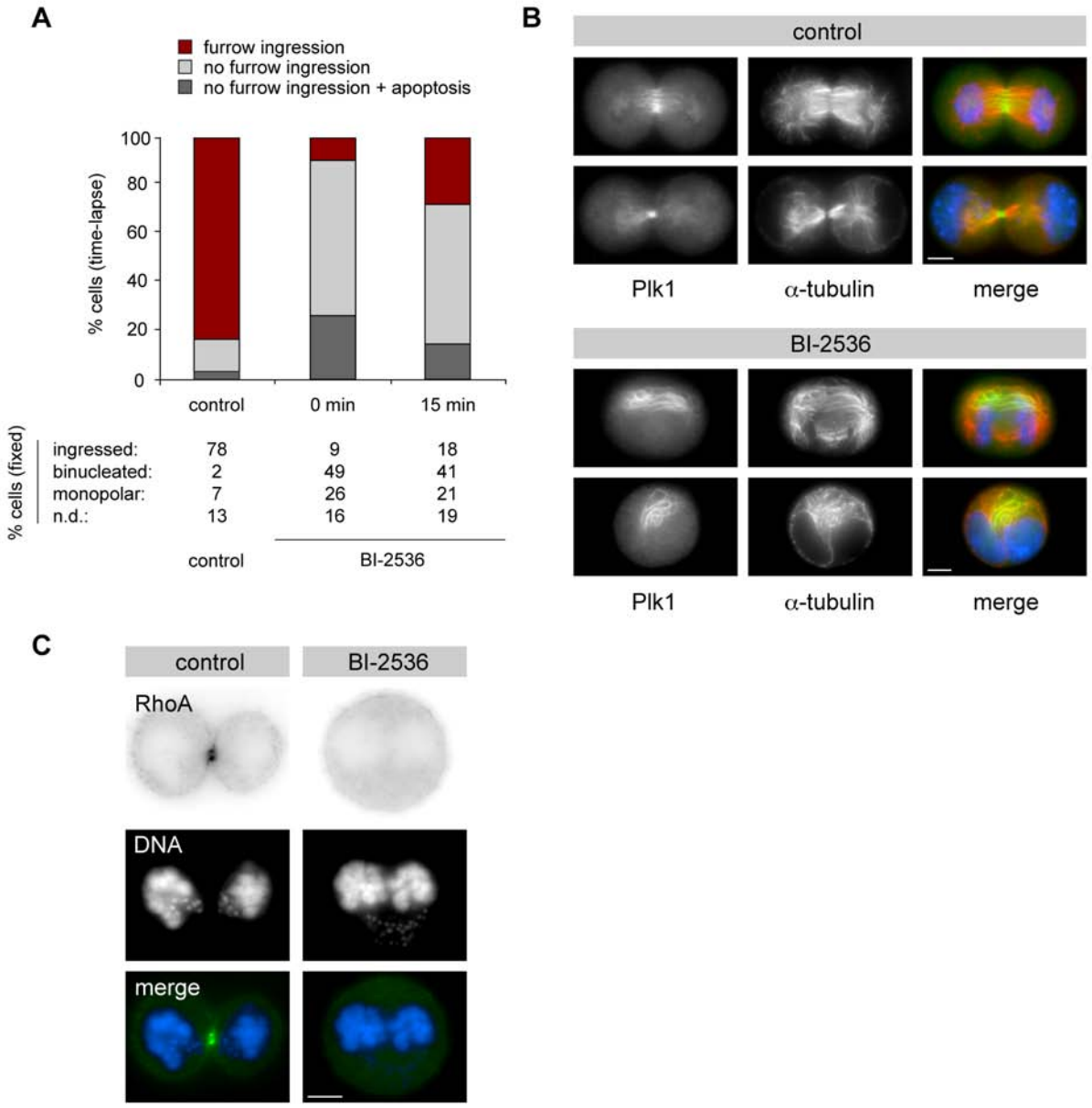

Figure S12. Effects of BI-2536 on furrow ingression in TaC12 cells. (A) *T. annulata*-infected cells were synchronized in metaphase using the proteasomal inhibitor MG132 and synchronously released into anaphase. Cells were treated with DMSO (control) or 100 nM BI-2536 (0 min) during MG132 washout; alternatively, cells were first exposed to100 nM BI-253, 15 min after MG132 washout (15 min). The histogram shows the abundance of furrow ingression in cells monitored by time-lapse imaging over a period of 4 h after MG132 washout. Additionally, cells were harvested at 80 min after MG132 washout, fixed and analyzed by IFM (lower panel). Data are presented as the percentage of cells showing cleavage furrow ingression (ingressed), cells that lacked any furrow ingression (binucleation) or cells showing collapsed monoplar spindles (monopolar); n.d. denotes cells that could not be classified; data represent 200 cells/sample (time-lapse) or 300 cells/sample (fixed). (B) Micrographs of cells in anaphase or telophae obtained in (A) that were released in the presence of DMSO (control) or 100 nM BI-2536. Cells were stained for Plk1 as well as α-tubulin, and analyzed by IFM; DNA was stained with DAPI. (C) Micrographs of representative cells obtained in (A). Cells were stained for RhoA and analyzed by IFM; DNA was stained with DAPI. Scale bars represent 5 µm.

2.2. Characterisation of gp34, a GPI-anchored protein expressed by schizonts of *Theileria parva* and *T. annulata*

Gondga Xue*, Conrad von Schubert*, Pascal Hermann, Martina Peyer, Regina Maushagen, Jacqueline Schmuckli-Maurer, Peter Bütikofer, Gordon Langsley, Dirk A.E. Dobbelaere

* shared first-authorship

Molecular & Biochemical Parasitology (2010) vol. 172 pp. 113-120

Theileria parva and *T. annulata* gp34 were identified and isolated by Martina Peyer. Antibodies against the two orthologs were generated by Martina Peyer and Pascal Hermann. Gongda Xue generated initial mammalian expression constructs and characterized Tp-gp34 to be GPI-anchored and expressed at the surface of *Theileria* schizonts. My contribution to this project started with the investigation of the subcellular localization of cytoplasmically expressed, unanchored gp34. I could demonstrate that ectopically expressed and endogenous Tp-gp34, but not Ta-gp34, was recruited to the midbody of dividing cells. As Tp-gp34 possesses putative Plk1 binding sites as well as a predicted phosphorylation site, I generated truncation mutants and mutants of the Plk1 motifs together with Pascal Hermann and Regina Maushagen. I could show that truncation of Tp-gp34 or elimination of the Plk1 phosphorylation site abrogated recruitment of Tp-gp34 to the midbody. Gongda Xue observed that, upon overexpression of wild-type gp34, a fraction of transfected cells became binucleate. Because the Plk1 phosphorylation site was required for Tp-gp34 midbody recruitment, I tested if elimination of all Plk1 motifs affected the binucleation phenotype of Tp-gp34 overexpression. Interestingly, the effect seemed independent of Tp-gp34 recruitment to the midbody, as elimination of the Plk1 phosphorylation site did not lower the extent of binucleation.

Theileria schizonts depend on host cell division for their cytokinesis and it was proposed that gp34 might contribute to the synchronous division of both host cell and parasite.

Figure contributions: all figures and supplementary data, except Figure 2B-F; all reviewer requests. Quantifications shown in Figure 5B were performed with Gongda Xue and Pascal Hermann. S127A/T128A mutagenesis of Tp-gp34 was performed by Pascal Hermann; S69A/S70A and Δ119-122 mutants were generated by Regina Maushagen under my supervision.

Molecular & Biochemical Parasitology 172 (2010) 113–120

Contents lists available at ScienceDirect

Molecular & Biochemical Parasitology

Characterisation of gp34, a GPI-anchored protein expressed by schizonts of *Theileria parva* and *T. annulata*

Gondga Xue[a,1,2], Conrad von Schubert[a,1], Pascal Hermann[a], Martina Peyer[a], Regina Maushagen[a,3], Jacqueline Schmuckli-Maurer[a], Peter Bütikofer[b], Gordon Langsley[c], Dirk A.E. Dobbelaere[a,*]

[a] *Division of Molecular Pathobiology, DCR-VPH, Vetsuisse Faculty, University of Bern, CH-3013 Bern, Switzerland*
[b] *Institute of Biochemistry & Molecular Medicine, Medical Faculty, University of Bern, CH-3012 Bern, Switzerland*
[c] *Laboratory of Comparative Cell Biology of Apicomplexan Parasites, Département de Maladie Infectieuse, Institut Cochin, 75014 Paris, France*

ARTICLE INFO

Article history:
Received 21 December 2009
Received in revised form 29 March 2010
Accepted 31 March 2010
Available online 8 April 2010

Keywords:
Apicomplexa
Transformation
Mitosis
Cytokinesis
Intracellular parasite
Surface protein

ABSTRACT

Using bioinformatics tools, we searched the predicted *Theileria annulata* and *T. parva* proteomes for putative schizont surface proteins. This led to the identification of gp34, a GPI-anchored protein that is stage-specifically expressed by schizonts of both *Theileria* species and is downregulated upon induction of merogony. Transfection experiments in HeLa cells showed that the gp34 signal peptide and GPI anchor signal are also functional in higher eukaryotes. Epitope-tagged Tp-gp34, but not Ta-gp34, expressed in the cytosol of COS-7 cells was found to localise to the central spindle and midbody. Overexpression of Tp-gp34 and Ta-gp34 induced cytokinetic defects and resulted in accumulation of binucleated cells. These findings suggest that gp34 could contribute to important parasite–host interactions during host cell division.

1. Introduction

The protozoan parasites *Theileria parva* and *T. annulata* are transmitted by ticks and cause severe lymphoproliferative diseases in cattle in large regions of Africa and Asia. Much of the pathology can be attributed to the fact that the intracellular schizont stages of these parasites are capable of transforming the leukocytes they infect, resulting in a rapid clonal expansion of the parasitized cell population. The schizont is strictly intracellular and differs from several other apicomplexan parasites such as *Plasmodium*, *Toxoplasma* or *Eimeria*, in that it is not enclosed in a parasitophorous vacuole [1]. Positioned in the cytosol, the schizont orchestrates the activation of an array of signalling pathways that promote host cell proliferation and protection against apoptosis (reviewed in [2,3]). Phenotypic analyses of *Theileria*-transformed cell lines also point towards interference with regulators of pro-inflammatory responses, which, in turn, are thought to contribute to the development of disease [4]. The interactions between the parasite and the host are complex, involving a range of different proteins, most of which are unknown. Members of the *T. annulata* TashAT family [5] and SuAT [6] have been reported to be released into the host cell cytosol and translocate to the nucleus, where they are hypothesized to interfere with host cell transcription. Another protein, called TaSE, was also reported to be secreted by the parasite and interact with host cell microtubules in a punctate manner [7]. Little is known about the repertoire of schizont surface proteins potentially involved in parasite–host cell interactions. Both *T. parva* and *T. annulata* express an immunodominant surface protein, designated polymorph immunodominant molecule (PIM) [8], or *T. annulata* surface protein (TaSP) [9], respectively. PIM is the major schizont antigen recognized by the sera of infected animals [10]. The protein shows unusual characteristics including extensive, variable QP-rich domains and its function is still unknown [11] although an interaction with microtubules has recently also been proposed [12]. Furthermore, it has been reported that antibodies raised against 11E, a secretory type glutaredoxin homologue also stain the schizont surface [13]. The availability of annotated *T. parva* and *T. annulata* genomes [14,15] opened up new opportunities to search for proteins predicted to be expressed on the schizont surface.

Abbreviations: GPI, Glycosylphosphatidylinositol; Plk1, Polo-like kinase1; PBD, polobox domain.

* Corresponding author. Tel.: +41 31 631 2625; fax: +41 31 631 2658.
E-mail address: dirk.dobbelaere@mopa.unibe.ch (D.A.E. Dobbelaere).

[1] These authors contributed equally to this work.

[2] Present address: Protein Kinase Lab, Friedrich Miescher Institute, CH-4058 Basel, Switzerland.

[3] Present address: Department of Otorhinolaryngology, University of Luebeck, D-23538 Luebeck, Germany.

0166-6851/$ – see front matter © 2010 Elsevier B.V. All rights reserved.
doi:10.1016/j.molbiopara.2010.03.018

Using bioinformatics, we searched the *T. annulata* and *T. parva* annotated proteomes [14,15] for schizont proteins predicted to contain an N-terminal signal peptide and a C-terminal GPI anchor signal. In this work, we characterise a GPI-anchored protein, called gp34, which is conserved in both *T. parva* and *T. annulata* and expressed on the surface of the transforming schizont.

2. Materials and methods

2.1. Isolation of gp34, generation of expression constructs and antibodies

To identify potential GPI-anchored proteins expressed on the schizont surface, a Complex/Boolean query of *T. annulata* geneDB (http://old.genedb.org/genedb/annulata) was carried out using the search parameters: 'Proteins containing a predicted GPI-anchor' and 'Proteins containing a predicted signal peptide'; only genes that were represented in the schizont EST library were further selected and those encoding proteins containing multiple membrane-spanning domains were not considered.

Coding regions of TA06510 and TP01_0939 were amplified by PCR from cDNA obtained from *T. annulata* (TaC12)-infected macrophages [16] and *T. parva* (Muguga)-infected T lymphocytes (TpM (D409)T4) [17]. Primers used for the isolation of the coding sequence excluding the regions encoding the signal peptide and GPI anchor signal were 5′-TGCGAATTCCAAAGCTTATTGAGGAGGATCTACG-3′, 5′-TGCCTCGAGAGTAACGAAACTTGATAATC-3′ for TA06510 and 5′-TGCAGATCTAAGCTTTCCTCGGGGAAGTCGGC-3′, 5′-TGCCTCGAGTCATCATAATCTGAAGGGGATTC-3′ for TP01_0939. PCR products were cloned into pGEX-6P vectors (GE Healthcare; digested with *Eco*RI–*Xho*I for TA06510 and *Bam*HI–*Xho*I for TP01_0939) using restriction sites introduced with the primers (*Eco*RI–*Xho*I for TA06510; *Bgl*II–*Xho*I for TP01_0939) and recombinant proteins expressed in *E. coli* BL21 Star (Invitrogen). Recombinant gp34 was purified using glutathione sepharose beads (GE Healthcare) and separated from GST using PreScission Protease (GE Healthcare). The purified protein was supplemented with GERBU adjuvant 10 (GERBU Biochemicals) and used to immunize rats (for anti-Ta-gp34 production) and rabbits (for anti-Tp-gp34). Antibodies were subjected to antigen-specific affinity purification as described [18].

To express epitope-tagged gp34 on the surface of mammalian cells, a pmaxCloning (Amaxa) expression plasmid was generated as follows: the *T. parva* gp34 precursor protein, the full coding sequence of TP01_0939 including the signal peptide, the mature protein, and the GPI anchor signal was amplified by PCR using the overlapping forward primers 5′-TGCAGATCTCGCCACCATGAAGTATATTTTATTTATTTTAATTTCAAC-3′ and 5′-TAATTTCAACTTGCGTGGTTTCCTCGGGGCCCGCCATGAAG-3′ as well as the reverse primer 5′-TGCCTCGAGTCATCAAAAGTTCATGAGTAAGAAAGCG-3′. The sequence encoding T7-QPRD1 of *T. parva* PIM was amplified from T7-QP-rd-His [11] by PCR and inserted downstream of the sequence encoding the signal peptide. The QPRD1 domain is recognized by an anti-PIM monoclonal MAb5 [11].

For the expression of Tp-gp34 in the cytoplasm of mammalian cells, part of the TP01_0939 coding sequence (representing aa 15–285 and lacking the signal peptide and GPI signal sequence) was amplified using the primers 5′-TGCAGATCTAAGCTTTCCTCGGGGAAGTCGGC-3′, 5′-TGCCTCGAGTAATCTGAAGGGGATTC-3′ and inserted into the pmaxCloning vector using *Bgl*II and *Xho*I restriction sites. A sequence encoding the C-terminal V5 epitope tag was amplified from pcDNA3.1-V5/His (Invitrogen) with the primers 5′-TGCCTCGAGGTCGACATCGATGGTAAGCCTATC-3′ and 5′-TGCGAGCTCATCGATCGTAGAATCGAG-3′ and inserted 3′ of the TP01_0939 insert via *Xho*I and *Sac*I restriction sites. Likewise, for the cytoplasmic expression of an unanchored version of Ta-gp34 in mammalian cells, the coding sequence of TA06510 representing aa 21–290 was cloned into pmaxCloning encoding the V5 tag after excision of the TP01_0939 sequence (see above) in a *Bgl*II–*Xho*I digest. The insert was generated by PCR using primers 5′-TGCGGATCCATTGAGGAGGATCTACG-3′ and 5′-TGCCTCGAGAGTAACGAAACTTGATAATC-3′ and digested *Bam*HI–*Xho*I.

To generate an N-terminally EGFP-tagged version of Tp-gp34, the TP01_0939 coding sequence representing the mature protein was excised from pGEX-6P–TP01_0939 (see above) in a *Bgl*II–*Xho*I digest and inserted into pEGFP-C1 (Clontech).

Plasmids used as control for the binucleation assay were pmaxGFP (Amaxa) and TP03_0882-ΔSP in pmaxCloning vector.

To generate truncation mutants of Tp-gp34, the TP01_0939 coding sequence was partially amplified by PCR using the primers 5′-TGCAGATCTAAGCTTATGGGGAAGTCGGCTCTGGAGG-3′ and 5′-CCGCTCGAGGGA TTTAGTTACGCTCC-3′ for aa 17–139, 5′-TGCAGATCTATGCTGACGAAGCTGGATGAAAG-3′ and 5′-TGCCTCGAGTAATCTGAAGGGGATTC-3′ for aa 140–285, or 5′-TGCAGATCTATGTATAAGGAATTCTATGG-3′ and 5′-TGCCTCGAGTACCGGGAACTCATCTATCGC-3′ for aa 81–220. For aa 17–285, the coding sequence was amplified using primers 5′-TGCAGATCTAAGCTTATGGGGAAGTCGGCTCTGGAGG-3′ and 5′-TGCCTCGAGTAATCTGAAGGGGATTC-3′. PCR products were inserted into the pmaxCloning vector encoding a C-terminal V5 tag (see above) using *Bgl*II/*Bam*HI and *Xho*I restriction sites.

Mutations of the Plk1 motifs in Tp-gp34 were generated by a two-step PCR. Using the TP01_0939 coding sequence as template, flanking primers and complementary mutagenic primers were used to generate two partially overlapping amplicons that were fused in a second PCR. The flanking primers used were 5′-TGCAGATCTAAGCTTATGGGGAAGTCGGCTCTGGAGG-3′ and 5′-TGCCTCGAGTAATCTGAAGGGGATTC-3′. The mutagenic primers were 5′-GCTAGGTTCAAGGAAGCCGCCAAGAAACACGCCGCC-3′ for S69A + S70A, 5′-CATATAAATTTGATGAAAGCGCCCCACTGTTTAGAAG-3′ for D104A, 5′-GAATCTCACTGTGTTTAGGAAGGCCAGC-3′ for Δ119–122, and 5′-GGCCAGCGCTGCTTACTCTCGCTCCTTC-3′ for S127A + T128A. Products from the second PCR were inserted into the pmaxCloning vector encoding a C-terminal V5 tag (see above) using *Bgl*II/*Bam*HI and *Xho*I restriction sites.

2.2. Cell culture, transfections and drug treatments

Theileria annulata (TaC12) and *T. parva* (Muguga)-infected cells were cultured in Leibovitz 15 medium (Gibco) supplemented with 10% fetal calf serum (FCS, Amimed), 10 mM Hepes pH 7.2 (Merck), 2 mM L-glutamine (Gibco), 70 μM β-mercaptoethanol (Merck), and antibiotics (Lonza). SV40-transformed cell lines of *Theileria*-uninfected bovine macrophages (BoMac) and monkey COS-7 cells, as well as HeLa cells were cultured in DMEM medium (Gibco) supplemented with 10% FCS and antibiotics. Transfections were done using Lipofectamine 2000 (Invitrogen) or Amaxa Nucleofection Kit V (BoMac) and R (COS-7) following the manufacturer's instructions. For elimination of the parasite, cultures of *Theileria annulata*-infected TaC12 cells were cultivated in the presence of 50 ng/ml of the theilericidal drug BW720c (Pitman-Moore). To induce merogony, TaC12 cells were treated for 8 days with 50 M chloramphenicol (Sigma) [16].

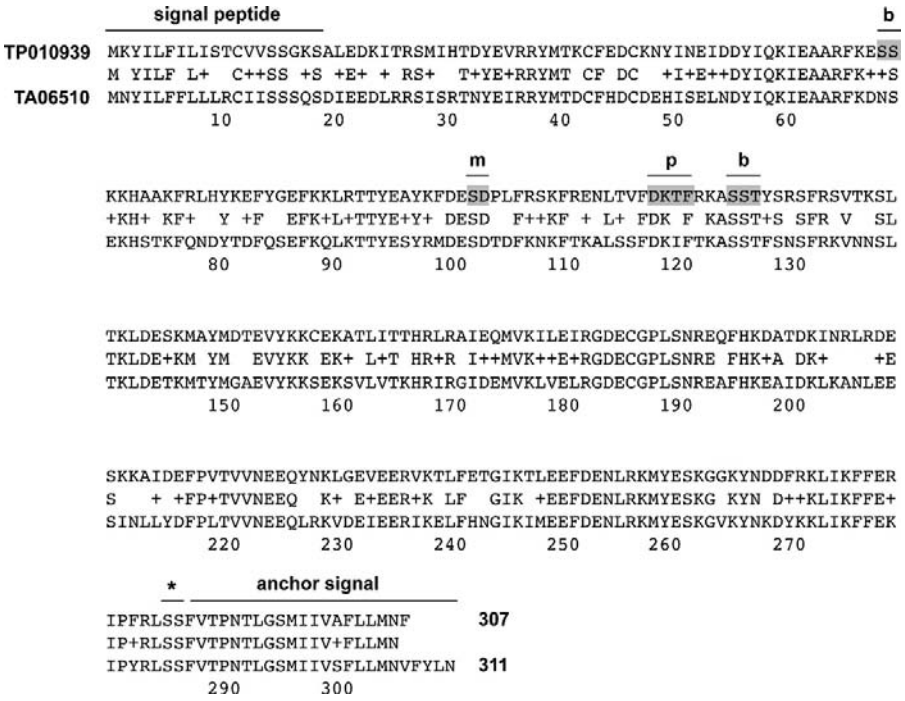

Fig. 1. Sequence comparison of *T. parva* and *T. annulata* gp34. Pairwise alignment of *T. parva* and *T. annulata* gp34. The predicted signal peptide (SignalP 2.0) and GPI-anchor attachment signal sequence (DGPI 2.04) of both proteins including the GPI-anchor attachment site (asterisk) are indicated. Predicted motifs of *T. parva* gp34 are indictated: b, putative Plk1 Polo Box Domain (PBD) binding site; m, potential mimicking site for phosphorylation-primed PBD binding; p, putative Plk1 phosphorylation site; relevant residues are shaded in gray. Sequence positions showing residue similarity are marked by a plus sign in pairwise alignment.

2.3. Microscopy and antibodies

Cells were grown on coverslips or poly-L-lysine coated coverslips (Sigma) and fixed with 4% paraformaldehyde in PBS for 10 min at room temperature or with methanol for 5 min at −20 °C. Cells were then permeabilized in 0.2% Triton X-100 prepared in PBS for 10 min at room temperature. Antibody incubations were done in PBS containing 10% FCS. DNA was stained with DAPI (Molecular Probes) and samples were mounted in Glycergel (Dako). Images were acquired on a Nikon Eclipse 80i fluorescence microscope equipped with a Retiga 2000R CCD camera (QImaging) using 40×, 60× and 100× Plan Apo objectives (Nikon) and Openlab 5 software (Improvision). Images were processed in Photoshop (Adobe).

Primary antibodies used in this study were: mouse monoclonal anti-Aurora B (AIM-1, clone 6, BD Transduction Laboratories), anti-cytochrome *C* (clone 7H8.2C12, BD PharMingen), IL-S40.2 (used in Fig. 2A), anti-PIM MAb5 (used in Fig. 2E and F; International Livestock Research Institute, Nairobi, Kenya), anti-α-tubulin (clone DM1A, Sigma), anti-V5 (Invitrogen), and 1C12 (detects *T. annulata* schizont surface; B. Shiels, University of Glasgow), as well as rabbit polyclonal anti-*T. parva* gp34, anti-TamR1 [19], and rat polyclonal anti-gp34. Appropriate secondary antibodies conjugated with fluorophores or horseradish peroxidase were used for IFM or western blot analysis, respectively.

To monitor cell division in COS-7 cells expressing EGFP-Tp-gp34, cells were transiently transfected (see above) and analysed by live imaging 4 h after transfection. Cells were recorded at 10 min intervals over 24 h at 37 °C and 5% CO_2 using a TE2000E-PFS microscope (Nikon) equipped with a Plan Fluor 20× objective (Nikon), Orca ER CCD camera (Hamamatsu) and incubation chamber (Life Imaging Services). Movies were compressed using Quicktime software (Apple).

2.4. Triton X-114 phase separation and PI-PLC treatment

For surface expression of gp34, HeLa cells were transfected with plasmid encoding the complete coding sequence of TP01_0939 and epitope tags (see above). Transfected cells were cultured at 32 °C for 20 h before harvesting for either immunofluorescence analysis or PI-PLC treatment. For the latter, cells were harvested by trypsinization, washed twice in PBS, and resuspended in 10 mM Tris pH 7.5 and 150 mM NaCl. To these samples, PI-PLC from *Bacillus cereus* (Sigma) was added to a final concentration of 5 mU/μl and incubated at 37 °C for 1 h. Washed cell pellet and supernatant were finally analyzed by western blot.

Triton X-114 (TX114) phase separation was performed as described in [20]. Briefly, *Theileria*-parasitized cells (TaC12, Muguga) were lyzed in Triton X-114 extraction buffer (20 mM Tris pH 7.4, 100 mM NaCl, 20 mM β-glycerophosphate, 20 mM NaF, 1 mM Na_3VO_4, 1 mM EDTA, 1× Roche protease inhibitor cocktail, 1% TX114) for 1 h with frequent mixing. After centrifugation, lysate supernatants were incubated 30 min at 37 °C for phase separation. Samples were centrifuged again and the detergent phase was re-extracted twice with TX114-free buffer. Proteins of the primary aqueous phase and the detergent phase were concentrated by acetone precipitation and subjected to western blot analysis.

3. Results and discussion

3.1. Identification and expression of gp34

A bioinformatics search of the predicted *T. parva* and *T. annulata* proteomes for GPI-anchored proteins expressed by the transforming schizont stage of both parasites yielded only few candidates. We focused on two hypothetical proteins XP_953835 (311 aa; TA06510)

and XP_766460 (307 aa; TP01_0939), which display 63% identity and 81% similarity to each other. An alignment of the two proteins including the indication of a number of relevant motifs is shown in Fig. 1. This level of inter-species homology is well below the average percentage protein identity of 83.7% [15]. It is also lower than that of the two adjacent predicted proteins (TP01_0938/TA06505 and TP01_0940/TA06515) suggesting that TA06510 and TP01_0939 might be either under immune selection or, alternatively, play a role in species-specific host cell adaptation [15,21]. The two genes contain no introns and appear to be unique to *Theileria*, as a general Blast search, including other closely related *Apicomplexa*, did not reveal any orthologues. Massively parallel serial sequencing of *T. parva* schizont RNA [22] revealed low numbers of Tp-gp34 transcript (106 transcripts per million), a level similar to *Theileria rab* genes [23]. Even though genes encoding schizont GPI-anchored membrane proteins were reported to have low d*N*/d*S* values similar to house-keeping genes [15], with a d*N*/d*S* ratio of 0.163, gp34-encoding genes deviate from this pattern, potentially reflecting a certain degree of diversification in their regulatory functions that occurred after speciation of *T. annulata* and *T. parva*, or exposure to the immune system.

The coding sequences were amplified by PCR and cloned into bacterial and mammalian expression vectors. Due to their apparent molecular mass in SDS-PAGE, the proteins were designated Ta-gp34 and Tp-gp34. Immunofluorescence microscopy (IFM) analysis using antibodies raised against both proteins confirmed that gp34 is expressed on the surface of *T. parva* and *T. annulata* schizonts (Fig. 2A). In both cases, a punctate staining pattern could be observed that differed from the smooth surface staining observed using anti-PIM or 1C12, a monoclonal antibody directed against another, uncharacterised, schizont surface protein [24]. Because of their flat shape, this pattern is best observed in *T. annulata*-transformed macrophages (Fig. 2A).

The capacity to transform parasitized cells is restricted to the schizont stage of *Theileria* and is lost when the schizont differentiates to the merozoite stage [25]. Using IFM, we investigated gp34 expression by parasites induced to undergo merogony by treatment with chloramphenicol [16]. The abundance of gp34 on the parasite surface correlated inversely with the expression level of the merozoite differentiation marker TamR1 and parasites showing high levels of TamR1 were negative for gp34 (Fig. 2B). Based on these observations we propose that expression of gp34 in the mammalian part of the parasite life cycle is restricted to the transforming schizont stage.

Western blot analysis of whole cell lysates prepared from *T. parva*-infected T cells (TpM(D409)T4) or *T. annulata*-infected macrophages (TaC12) (not shown) revealed proteins with an apparent molecular mass of 34 kDa (Fig. 2C). The protein was not found

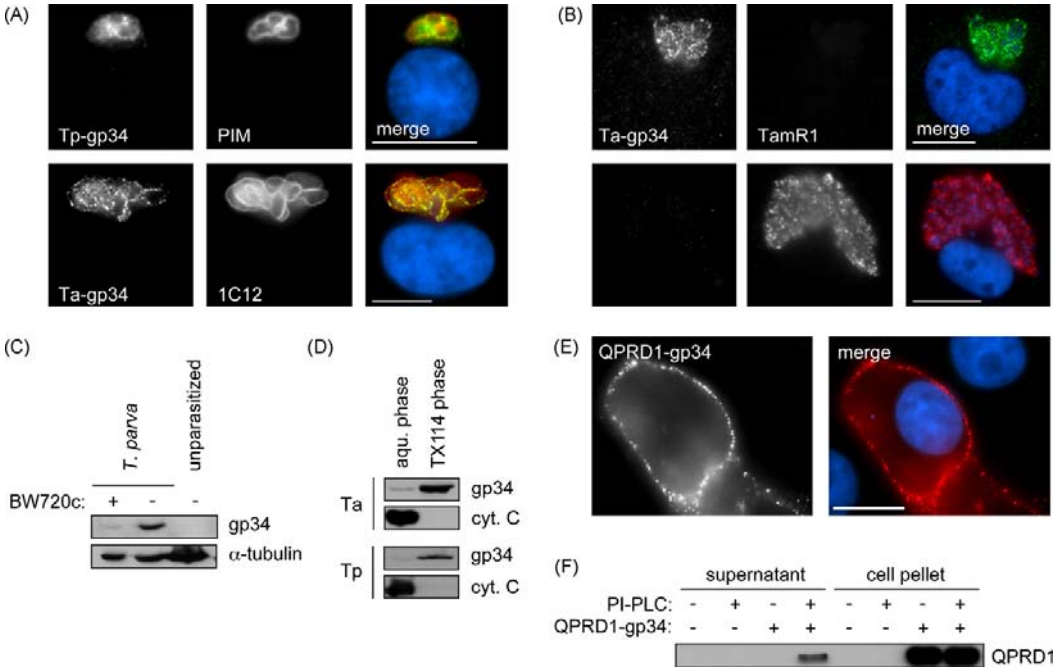

Fig. 2. Characterization of gp34 a GPI-anchored protein expressed specifically by *Theileria* schizonts. (A) gp34 is expressed at the surface of the schizont. Immunofluorescence microscopy of *T. parva*- and *T. annulata*-transformed cells was carried out using antibodies directed against Tp-gp34 and Ta-gp34; the mAbs anti-PIM and 1C12 were used as markers for the parasite surface; DNA was stained using DAPI (blue); 'merge' represents an overlay of the three images; the scale bar represents 10 μm. (B) gp34 expression is downregulated during merogony. To induce merogony, *T. annulata*-infected TaC12 cells were cultured for 8 days in the presence of 50 μM chloramphenicol. The upper panels show a gp34-expressing schizont that had not yet started differentiation and is negative for the differentiation marker TamR1. The parasite depicted in the lower panels expresses TamR1, but has ceased to express gp34; DNA was stained using DAPI (blue); scale bar represents 10 μm. (C) Western blot analysis using anti-Tp-gp34 of cell lysates prepared from *T. parva*-transformed T cells, T cells from which the parasite has been eliminated by treatment with the specific theilericidal drug BW720c for 4 days, or unparasitized BoMac cells; α-tubulin was used as loading control. (D) Western blot analyses using anti-gp34 antibodies of *T. parva*- and *T. annulata*-transformed leukcoytes subjected to Triton X-114 extraction and phase separation (aqueous phase and TX-114 phase). Blots were probed for cytochrome *C* to confirm differential extraction. (E) QPRD1-gp34 expression on the surface of HeLa cells transiently transfected with a plasmid encoding a Tp-gp34 fusion protein consisting of the Tp-gp34 N-terminal signal peptide, part of the PIM QP-rich domain (QPRD1) carrying a PIM-specific epitope, and the gp34 core protein plus the C-terminal GPI anchor attachment signal. Surface-expressed protein was detected by IFM using a mAb directed against QPRD1. The cell nucleus was stained with DAPI (blue); scale bar represents 20 μm. (F) Western blot analysis of QPRD1-gp34 released into the supernatant upon treatment of transiently transfected HeLa cells (see E) with phosphatidylinositol-specific phospholipase C (PI-PLC). Untransfected HeLa cells (–) were used as control; 'cell pellet' shows cell-associated QPRD1-gp34 in cultures of transfected (+) or untransfected (–) HeLa cells, exposed or not exposed to PI-PLC.

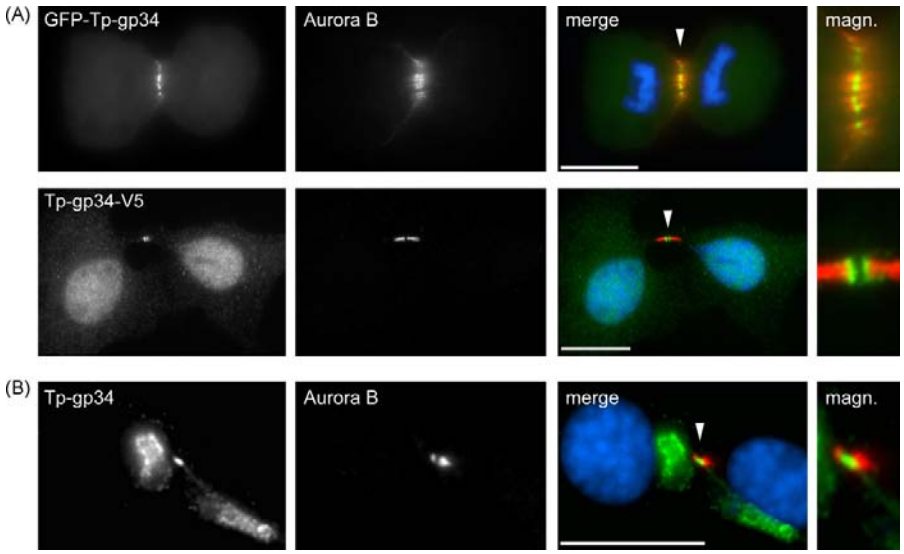

Fig. 3. Tp-gp34 interaction with the central spindle and midbody. (A) IFM of COS-7 cells transiently expressing V5- or GFP-tagged forms of Tp-gp34 (green); the signal peptide and GPI anchor attachment signal were removed to guarantee cytosolic expression. The central spindle (upper panels; cell in anaphase) and midbody (lower panels; cell finishing cytokinesis) were stained using anti-Aurora B (red). DNA was stained with DAPI (blue). In the lower panels, ectopically expressed gp-34 can be seen accumulating in the nucleus; magn. = magnified image of the central spindle and midbody; the scale bar represents 20 μm. (B) IFM analysis using anti-Tp-gp34 (green) showing a representative example of *T. parva*-transformed cells in the process of completing cytokinesis; the midbody is visualized using anti-Aurora B (red); the arrowhead points at Tp-gp34 accumulation at the midbody; magn. = magnified midbody; scale bar represents 10 μm.

in extracts prepared from an (unparasitized) BoMac cell line and gp34 could hardly be detected upon elimination of the parasite by treatment with the theilericidal drug BW720c, confirming its parasite origin. Typical of GPI-anchored proteins, upon extraction with Triton X-114, both Ta- and Tp-gp34 partitioned into the detergent phase, whereas the hydrophilic marker protein, cytochrome *C*, remained in the aqueous phase (Fig. 2D).

We next tested whether the gp34 signal peptide and GPI-anchor signal are also functional in higher eukaryotes. To facilitate detection, a fragment of the PIM QP-rich domain (QPRD1) that harbours an epitope detected by MAb5 [11] was inserted immediately downstream of the predicted gp34 signal peptide sequence. Transiently expressed in HeLa cells, QPRD1-gp34 could be detected at the plasma membrane (Fig. 2E), showing the punctate pattern that was also observed in schizonts (see Fig. 2A). To verify if ectopically expressed QPRD1-gp34 was indeed GPI-anchored, cells were harvested and incubated with phosphatidylinositol-specific phospholipase C, which releases GPI-anchored proteins from the plasma membrane, while cells remain viable [26]. Treatment with PI-PLC led to a release of gp34 into the culture supernatant (Fig. 2F), confirming the protein was GPI-anchored.

3.2. Expression and localisation of gp34 in mammalian cells

Due to the absence of a surrounding parasitophorous vacuole, gp34, expressed on the surface of the *Theileria* schizont, is optimally positioned to interact with host cell structures. To investigate if gp34 has the capacity to bind to specific host cell structures, we transiently expressed Tp-gp34 or Ta-gp34 (shown for Tp-gp34) as soluble V5- or GFP-tagged proteins in COS-7 cells. To ensure expression in the cytosol, the constructs were designed to lack signal peptide and GPI anchor attachment signal sequences. In interphase cells, tagged Tp-gp34 and Ta-gp34 were routinely found in both the cytosol and the nucleus of transfected cells. The reason why ectopically expressed gp34 is also found in the nucleus is not clear, as the protein does not possess any obvious nuclear localisation signals. One possibility is that gp34, when expressed in the cytoplasm as a soluble protein, enters the nucleus by the (potentially fortuitous) interaction with a host cell protein that accumulates in the nucleus. Whichever, immunofluorescence analysis shows that parasite-expressed gp34 is normally tethered to the schizont surface and we presently have no microscopic evidence for nuclear translocation of gp34 in *Theileria*-transformed cells. The relevance of nuclear translocation observed for ectopically expressed gp34 must therefore be interpreted with caution.

In COS-7 cells that had completed mitosis, GFP-Tp-gp34 and Tp-gp34-V5 were both found to localize to the central spindle and midbody (Fig. 3A). Central spindles are formed in the spindle midzone during sister chromatid separation and are compacted during the final stages of cell division to form the midbody that resides in the cytoplasmic bridge between the dividing daughter cells. Intriguingly, in contrast to Tp-gp34, V5- or GFP-tagged Ta-gp34 failed to interact with these structures (not shown). Similar observations were made when *Theileria*-transformed cells were stained for endogenous gp34. In dividing *T. parva*-infected T cells, gp34 was often found concentrated at the midbody (Fig. 3B), whereas no such accumulation could be observed in dividing *T. annulata*-infected macrophages (not shown). Midbody staining was not due to spurious cross-reactivity, as, in control experiments using unparasitized BoMac cells, anti-Tp-gp34 did not label midbodies (not shown).

Thus, despite the fact that Ta-gp34 and Tp-gp34 show many similarities, they also show some differences in their capacity to interact with host cell structures. The exact reason for this discrepancy is not yet known and may be based on differences between the two proteins in specific binding- or phosphorylation-motifs required for interaction with central spindle- or midbody-specific components.

3.3. Truncation/mutation analysis of Tp-gp34 expressed in mammalian cells

Next we carried out a more detailed analysis of Tp-gp34 to identify domains or motifs required for central spindle and midbody

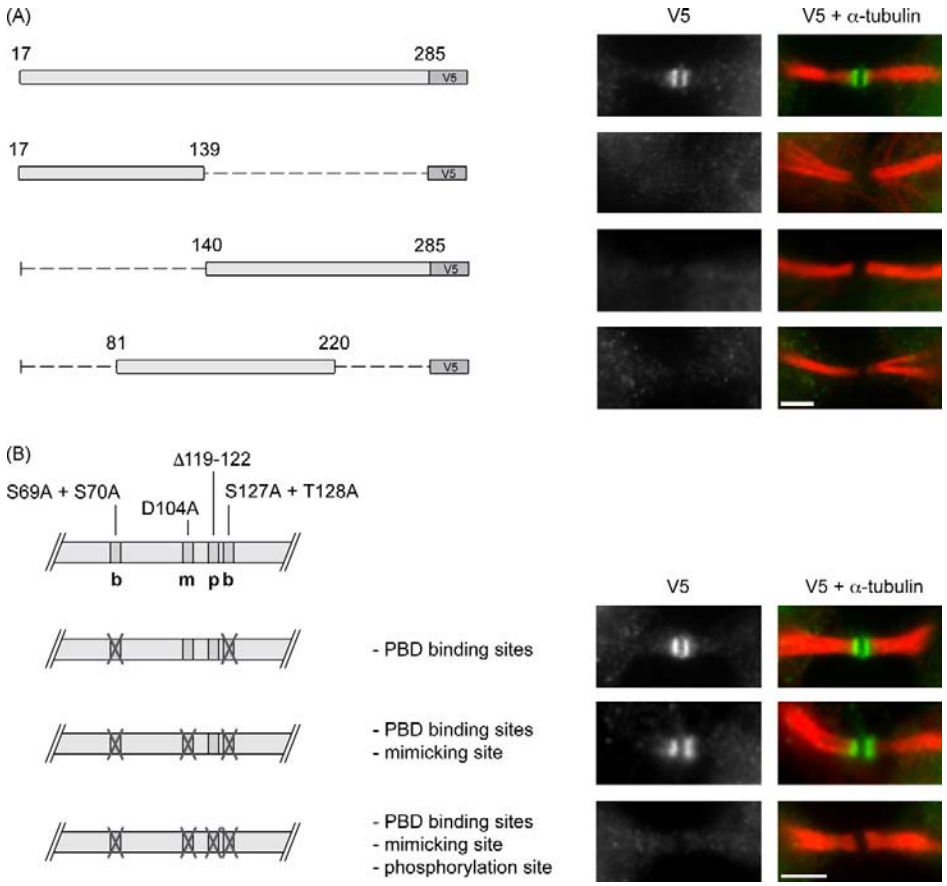

Fig. 4. Truncation/mutation analysis of Tp-gp34 localisation to central spindle/midbody in COS-7 cells (A). COS-7 cells were transfected with plasmid constructs encoding full-length V5-tagged Tp-gp34 (excluding the signal peptide and GPI-anchor attachment signal) or truncation mutants spanning the N-terminal half (aa 17–139), the C-terminal half (aa 140–285) or the central region (aa 81–220) of Tp-gp34. Cells were stained for α-tubulin (red) to identify the midbody and V5 (green) for Tp-gp34 expression. Representative examples of midbody localisation are shown on the right. (B) The top panel shows a scheme of potential Plk1-interaction motifs in Tp-gp34 including the PBD binding sites (b), a mimicking site for PBD binding (m) and a Plk1 phosphorylation site (p); the corresponding aa substitutions and eliminations are indicated. COS-7 cells were transfected with plasmid constructs encoding mutagenized versions of full-length V5-tagged Tp-gp34 (aa 17–285) as indicated. Cells were stained and analysed as described for (A); scale bars represent 3 μm.

localisation. A range of different constructs, tagged C-terminally with a V5 epitope, were expressed in COS-7 cells and localisation monitored by IFM. Results presented in Fig. 4 shown that neither the N-terminal nor the C-terminal half of Tp-gp34 was capable of associating with the central spindle/midbody and the same applied to a construct spanning the middle region of the protein (aa 81–220). These data indicate that expression of a full-length Tp-gp34 is required to guarantee localisation to the central spindle/midbody in transfected COS-7 cells. Plk1 binding and phosphorylation have been shown to play an important role in targeting proteins to the central spindle/midbody [27]. We therefore tested a number of candidate motifs in Tp-gp34 that could potentially participate in this process. These included two putative Plk1 binding sites [28], a putative Plk1 phosphorylation site [29], as well as a site that could potentially mimic a PBD binding site (see Fig. 4B). An analysis involving the progressive elimination of these sites clearly showed that the phosphorylation site (aa 119–122, DKTF) was essential for targeting Tp-gp34 to the central spindle/midbody as perturbation of this site completely abrogated central spindle/midbody localisation. The absence of this phosphorylation site in Ta-gp34 (DKIF rather than DKTF) could help explain why Ta-gp34 fails tot localise to these structures when expressed in COS-7 cells. Thus, the interaction of Tp-gp34 with the central spindle/midbody in COS-7 cells is dependent on the protein being full-length (without predicted signal peptide and GPI anchor signal) and the presence of a putative Plk1 phosphorylation site. While interesting in its own right, it remains to be demonstrated that this site is indeed phosphorylated and also the biological significance of this localisation must be interpreted with care, in particular as Ta-gp34 does not show these characteristics in COS-7 cells.

3.4. Overexpresssion of gp34 induces binucleation in mammalian cells

While examining cultures of cells transiently expressing gp34, we frequently observed binucleate cells or cells containing abnormal nuclear morphology indicative of a potential interference with mitosis/cytokinesis (Fig. 5A). To analyse this observation in more detail, V5-tagged Ta-gp34 or Tp-gp34 were transiently overexpressed in the cytosol of *T. annulata*-transformed TaC12 cells or BoMac cells. Mitosis and cytokinesis of transfected, V5-positive, cells were closely monitored by IFM and the number of V5-positive cells containing more than one nucleus was recorded. Overexpression of gp34 from either species did not affect mitotic events such as spindle formation, spindle maintenance or the formation of a

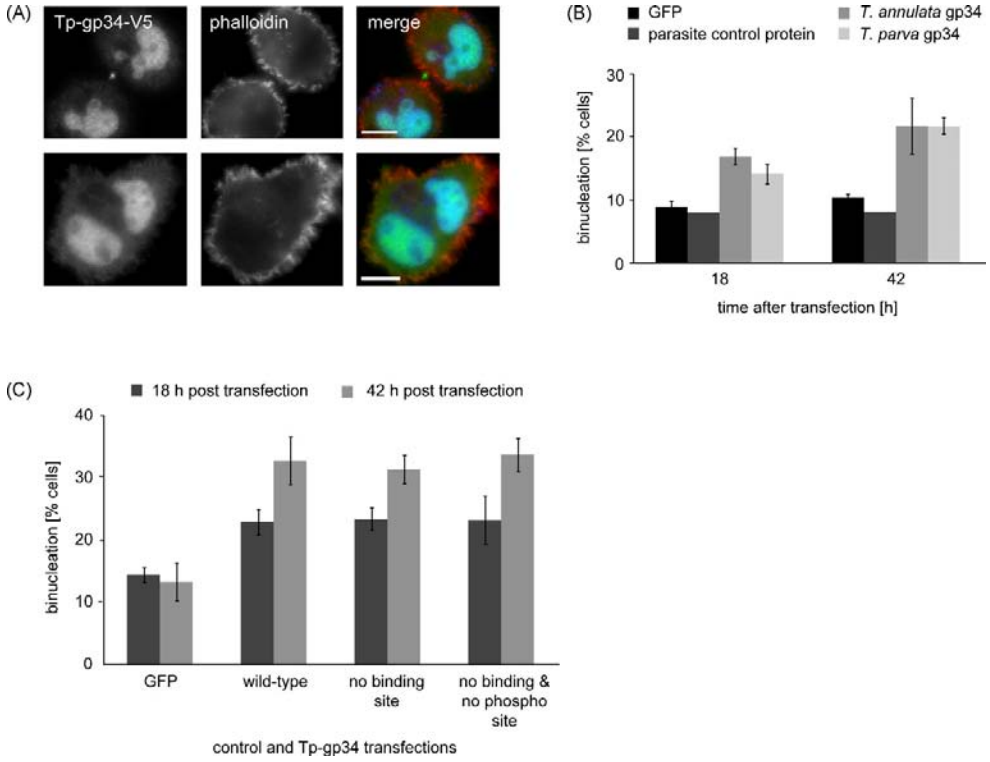

Fig. 5. Overexpression of gp34-V5 induces cytokinetic defects. (A) Overexpression of Tp-gp34 in TaC12 cells provokes binucleation (lower panels), or nuclear abnormalities (upper panels) in dividing cells; nuclear accumulation of Tp-gp34-V5 and midbody staining is prominent; cell boundaries were visualized by phalloidin staining (red); DNA was stained with DAPI (blue); scale bars represent 10 μm. (B) At 18 or 42 h after transfection, the number of binucleated cells was monitored in BoMac cells overexpressing either GFP, a parasite control protein or gp34 from either species. Data represent the mean of four experiments with $n = 40–300$ cells/sample; error bars indicate standard deviations. (C) To test if the putative Plk1 motifs described in Figs. 1 and 4 are important for inducing binucleation, BoMac cells were transfected with constructs encoding wild-type Tp-gp34 (aa 17–285), a mutant form lacking all possible PBD binding sites, or a form of Tp-gp34 lacking all binding sites as well as the Plk1 phosphorylation site. Transfected cells were analyzed by IFM after 18 and 42 h and quantified for binucleation. GFP expression was used as negative control. Data represent the mean of three repetitions from two experiments with $n = 100–200$ cells/sample; error bars indicate standard deviations.

metaphase plate. The process of cytokinesis, however, appeared to be disturbed, resulting in a significant increase in the number of binucleate BoMac cells (Fig. 5B). Similar effects could be observed in transiently transfected *T. annulata*-transformed TaC12 cells (data not shown). In this case, a 3-fold increase (from 8 to 25%) in the number of binucleate cells was observed over a period of 36 h.

We also tested Tp-gp34 mutants that lacked putative PBD binding sites, as well as a mutant in which both the PBD binding sites and the putative Plk1 phosphorylation site were disrupted. Interestingly, also in the latter case the number of binucleate cells increased significantly in gp34-expresssing cells compared to control cells.

We further used live video imaging to monitor cell division in BoMac cells expressing GFP-labelled gp34. Live imaging revealed an interference with furrow ingression and/or progression to full abscission. In a number of cases, cells entered mitosis, progressed to metaphase, but no obvious anaphase and furrow ingression could be observed (movie S1). In other cells, ingression started but was subsequently interrupted and furrow regression and the formation of binuclear cells could be observed (movie S2).

Thus, whereas gp34 overexpression in mammalian cells can clearly interfere with cytokinesis/abscission, a link between these findings and the localisation of gp34 to the central spindle/midbody observed in transfected COS-7 cells is not obvious, in particular as Ta-gp34, while perfectly capable of affecting cytokinesis, does not localise to these structures. The reason for this discrepancy is not yet known. Cytokinesis is a highly intricate process, subjected to multiple layers of regulation and involving the precise spatio-temporal activation of key regulator proteins [27]. Exactly where ectopically expressed gp34 interferes with this process remains to be elucidated.

4. Concluding remark

GPI-anchored proteins are usually expressed on the surface of cells, where they interact with the extracellular environment. Expressed on the surface of the *Theileria* schizont, gp34 is special in that it faces directly into the cytosol of another eukaryotic cell. The function of gp34 is not yet understood. The fact that no orthologues of gp34 were found in any other organism supports the concept that gp34 has a unique function in the biology of *Theileria*. To maintain the transformed state, the schizont must be partitioned over the two daughter cells at each host cell division. This process is important for parasite persistence. Whether gp34 participates in this process has not yet been established, but some of our findings indirectly suggest that gp34 could be involved. In particular the striking interference with cytokinesis/abscission by ectopically expressed gp34 could reflect the capacity of parasite-expressed gp34 to interact with key regulators of host cell cytokinesis. The physiological relevance of these observations, however, still needs to be confirmed. Experiments are presently underway to identify

gp34-interacting partners of host cell origin. This, in turn might help elucidate the intricate interplay between the schizont and the host cell during mitosis.

Acknowledgements

This work was funded by the Swiss National Science Foundation (Nr 3100A0-116653), The Wellcome Animal Health Initiative (GR075820MA) and the Integrated Consortium on Ticks and Tick-borne Diseases ICTTD (Nr 510561). Stephan Grimm is thanked for excellent technical help, ILRI for anti-PIM antibodies and Brian Shiels for 1C12.

Appendix A. Supplementary data

Supplementary data associated with this article can be found, in the online version, at doi:10.1016/j.molbiopara.2010.03.018.

References

[1] Shaw MK. Cell invasion by *Theileria* sporozoites. Trends Parasitol 2003;19:2–6.
[2] Luder CG, Stanway RR, Chaussepied M, et al. Intracellular survival of apicomplexan parasites and host cell modification. Int J Parasitol 2009;39:163–73.
[3] Dobbelaere D, Baumgartner M. Theileria. In: Schaible UE, Haas A, editors. Intracellular niches of microbes: a pathogens guide through the host cell. Wiley–VCH; 2009. p. 613–32.
[4] Morrison WI. Progress towards understanding the immunobiology of *Theileria* parasites. Parasitology 2009;136:1415–26.
[5] Swan DG, Phillips K, Tait A, et al. Evidence for localisation of a *Theileria* parasite AT hook DNA-binding protein to the nucleus of immortalised bovine host cells. Mol Biochem Parasitol 1999;101:117–29.
[6] Shiels BR, McKellar S, Katzer F, et al. A *Theileria annulata* DNA binding protein localized to the host cell nucleus alters the phenotype of a bovine macrophage cell line. Eukaryot Cell 2004;3:495–505.
[7] Schneider I, Haller D, Kullmann B, et al. Identification, molecular characterization and subcellular localization of a *Theileria annulata* parasite protein secreted into the host cell cytoplasm. Parasitol Res 2007;101:1471–82.
[8] Baylis HA, Allsopp BA, Hall R, et al. Characterisation of a glutamine- and proline-rich protein (QP protein) from *Theileria parva*. Mol Biochem Parasitol 1993;61:171–8.
[9] Schnittger L, Katzer F, Biermann R, et al. Characterization of a polymorphic *Theileria annulata* surface protein (TaSP) closely related to PIM of *Theileria parva*: implications for use in diagnostic tests and subunit vaccines. Mol Biochem Parasitol 2002;120:247–56.
[10] Toye PG, Goddeeris BM, Iams K, et al. Characterization of a polymorphic immunodominant molecule in sporozoites and schizonts of *Theileria parva*. Parasite Immunol 1991;13:49–62.
[11] Casanova CL, Xue G, Taracha EL, et al. Post-translational signal peptide cleavage controls differential epitope recognition in the QP-rich domain of recombinant *Theileria parva* PIM. Mol Biochem Parasitol 2006;149:144–54.
[12] Seitzer U, Gerber S, Beyer D, et al. Schizonts of *Theileria annulata* interact with the microtubuli network of their host cell via the membrane protein TaSP. Parasitol Res 2010;106:1085–102.
[13] Ebel T, Middleton JF, Frisch A, et al. Characterization of a secretory type *Theileria parva* glutaredoxin homologue identified by novel screening procedure. J Biol Chem 1997;272:3042–8.
[14] Gardner MJ, Bishop R, Shah T, et al. Genome sequence of *Theileria parva*, a bovine pathogen that transforms lymphocytes. Science 2005;309:134–7.
[15] Pain A, Renauld H, Berriman M, et al. Genome of the host-cell transforming parasite *Theileria annulata* compared with *T. parva*. Science 2005;309:131–3.
[16] Schmuckli-Maurer J, Shiels B, Dobbelaere DA. Stochastic induction of *Theileria annulata* merogony in vitro by chloramphenicol. Int J Parasitol 2008;38:1705–15.
[17] Dobbelaere DA, Prospero TD, Roditi IJ, et al. Expression of Tac antigen component of bovine interleukin-2 receptor in different leukocyte populations infected with *Theileria parva* or *Theileria annulata*. Infect Immun 1990;58:3847–55.
[18] Hemphill A. Subcellular localization and functional characterization of Nc-p43, a major *Neospora caninum* tachyzoite surface protein. Infect Immun 1996;64:4279–87.
[19] Shiels BR, d Oliveira C, McKellar S, et al. Selection of diversity at putative glycosylation sites in the immunodominant merozoite/piroplasm surface antigen of *Theileria* parasites. Mol Biochem Parasitol 1995;72:149–62.
[20] Bordier C. Phase separation of integral membrane proteins in Triton X-114 solution. J Biol Chem 1981;256:1604–7.
[21] Weir W, Sunter J, Chaussepied M, et al. Highly syntenic and yet divergent: a tale of two *Theilerias*. Infect Genet Evol 2009;9:453–61.
[22] Bishop R, Shah T, Pelle R, et al. Analysis of the transcriptome of the protozoan *Theileria parva* using MPSS reveals that the majority of genes are transcriptionally active in the schizont stage. Nucleic Acids Res 2005;33:5503–11.
[23] Langsley G, van Noort V, Carret C, et al. Comparative genomics of the Rab protein family in Apicomplexan parasites. Microbes Infect 2008;10:462–70.
[24] Shiels BR, McDougall C, Tait A, et al. Identification of infection-associated antigens in *Theileria annulata* transformed cells. Parasite Immunol 1986;8:69–77.
[25] Glascodine J, Tetley L, Tait A, et al. Developmental expression of a *Theileria annulata* merozoite surface antigen. Mol Biochem Parasitol 1990;40:105–12.
[26] Paulick MG, Bertozzi CR. The glycosylphosphatidylinositol anchor: a complex membrane-anchoring structure for proteins. Biochemistry 2008;47:6991–7000.
[27] Barr FA, Gruneberg U. Cytokinesis: placing and making the final cut. Cell 2007;131:847–60.
[28] Elia AE, Cantley LC, Yaffe MB. Proteomic screen finds pSer/pThr-binding domain localizing Plk1 to mitotic substrates. Science 2003;299:1228–31.
[29] Nakajima H, Toyoshima-Morimoto F, Taniguchi E, et al. Identification of a consensus motif for Plk (Polo-like kinase) phosphorylation reveals Myt1 as a Plk1 substrate. J Biol Chem 2003;278:25277–80.

3. Results and discussion

The *Theileria annulata* schizont dwells freely in the cytoplasm of its host cell, lacking a surrounding parasitophorous vacuole. The parasite‘s surface displays an affinity for host cell MTs which is seen during schizont establishment after invasion of the host cell [81-83] and, most impressively, as the parasite positions itself on the host cell mitotic spindle (Chapter 2.1., Figure 1). Throughout the cell cycle, the schizont is oriented towards the MT organizing centers (MTOCs), however, MT interactions during interphase are less prominent compared to M phase (Figure 1). This might reflect the 5 to 10-fold higher turnover of mitotic over interphase MTs, which, together with high growth rates, generates large populations of dynamic MTs (reviewed in [84]). Although the interaction of the mitotic spindle with the parasite *per se* has been described before [31, 33], the interaction dynamics of the parasite with M phase MTs, i.e. parasite positioning during mitotic spindle formation or the interaction with MT subpopulations during cytokinesis, have not been investigated before and are novel findings of this study. This work identifies the host cell mitotic Ser/Thr kinase Plk1 as one of the factors that ensure proper distribution of the *Theileria annulata* schizont during cell division (for detailed results, the reader is referred to Chapter 2.1.). The process involves the Plk1-dependent alignment of the host cell central spindle with the parasite surface. Whereas astral MTs ensure bipolar parasite positioning on the mitotic apparatus throughout M phase, the association with central spindle MTs precisely centers the parasite at the equatorial plane and might allow unperturbed furrow ingression and cytokinetic abscission by the host cell. The mechanism of parasite division during host cell cytokinesis presented in this study raises a number of questions: (i) how does the parasite align on the mitotic spindle during different stages of M phase (ii) what is the necessity for the parasite to associate with the central spindle, if astral MTs sufficiently position it during cell division (iiI) is there a mechanistic reason for the bi-phasic recruitment of Plk1 to the schizont, and (iv) how can inhibition of Plk1 kinase activity disrupt the interaction of the parasite and the central spindle, if Plk1 is not essential for central spindle formation? This chapter discusses these and other questions in the light of our current understanding of mammalian somatic cell division. It concludes with a proposal for a mechanism for *Theileria* schizont cell division that is characterized by the close interplay with tightly regulated events that control the host cell cycle.

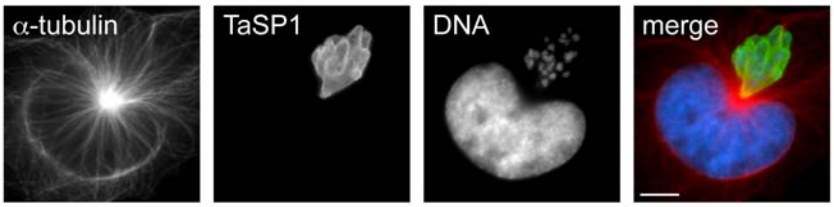

Figure 1. Positioning of the *Theileria annulata* schizont during host cell interphase. TaC12 cells were stained with antibodies raised against α-tubulin and the parasite surface protein TaSP1. DNA was stained with DAPI; ‚merge‘ denotes an overlay of all three channels; scale bar represents 5 µm.

Are centrosomes required for parasite positioning?

To understand the mechanism by which the parasite aligns on the mitotic spindle apparatus, one has to define which components of the mitotic spindle are required for this process and how an interaction with the parasite could be mediated. A prominent feature of the transforming *Theileria* species is their orientation towards the MTOC. During Interphase, the schizont adopts a pointed conformation and seems to be attached to, or closely associated with, the centrosome located near the nuclear membrane (Figure 1). During during M phase it is pointed to the spindle poles in a bi-polar fashion (Chapter 2.1., Figure 1). The observation that, in cells containing multipolar spindles, the parasite is pointed towards each pole also underpins the assumption that the parasite associates with centrosomes (not shown). These cells were synchronized for a prolonged time in S phase by treatment with the drug hydroxyurea (HU), which blocks replication but is permissive for the centrosome cycle. After about two rounds of centrosome replication, cells were released to enter M phase and parasite alignment on multipolar spindles was observed. However, closer observation showed that in many of these cells as well as in many untreated interphase and mitotic cells, the parasite often lacked direct contact with the centrosome.

Another observation that challenges requirement of centrosomes for parasite positioning was made in interphase cells treated with taxol. It has been reported that taxol treatment induces pronounced MT polymerization during interphase and that centrosomes lose their MT-organizing capacities [85]. In taxol-treated parasitized interphase cells, very long parallel MT bundles were observed that did not originate at the centrosomes but were still capable of aligning with the parasite, which adopted a stretched conformation parallel to the MT bundles (not shown).

The dispensability of centrosomes for parasite spindle positioning was also seen in cells that had immature centrosomes. During mitotic entry, centrosomes are the major sites for MT nucleation. The centrosome-dependent nucleation of MTs requires the recruitment of maturation factors, including the Y-tubulin ring-complex (Y-TuRC), which is believed to act as a priming scaffold for MT polymerization. Plk1 has been shown to directly [86] and indirectly [87] trigger recruitment of Y-TuRCs to the centrosomes. Furthermore, it is required for centrosome integrity by phosphorylation of the peri-centriolar matrix component Kizuna [88]. Downregulation of Plk1 catalytic activity prior to mitotic entry consequently results in the lack of Y-TuRC recruitment to the centrosomes and centrosome fragmentation [74, 88-90]. In these cells, acentrosomal spindles form that adopt an unfocused, rosette-like conformation and are believed to be formed of MTs that are nucleated at the chromosomes [74]. Thus, to test the requirement of centrosomes for parasite spindle alignment, parasitized cells were treated with the Plk1 inhibitor BI-2536 [91, 92] before entry into mitosis. Interestingly, in these cells the parasite was aligned on the acentrosomal spindles and, importantly, showed an pronounced orientation to the unfocused pole of the spindle (not shown). In parasitized prometaphase cells that were treated with nocodazole for complete MT depolymerization, removal of nocodazole allowed the polymerization of MTs originating from numerous nucleation centers that appeared to be largely nucleated at the host cell chromosomes (Chapter 2.1., Figure 1A). Observations in living cells show that MTs emanating from these asters

immediately and predominantly associate with the parasite surface (not shown) and that the parasite regains its positioning already at an early stage on the forming mitotic spindle. These early spindles show splayed poles, which could be provoked by the presence of the parasite, but indicate the presence of multiple asters distinct from the centrosomal asters. It was shown for kinetochore MT-fibers (K-fibers) that emanate from chromosomes, that they integrate into the forming spindle through a NUMA-dependent sliding of their distal ends on MTs to the centrosomes [93]. It is possible that a similar process applies to MT-asters associated with the parasite but not the centrosomes. It could be tested if these asters contain NUMA at their MT minus ends and if these asters would lack an association with the centrosomes.

Taken together, these observations support the notion that parasite positioning, rather than being dependent on centrosomes, is mediated by the action of MT-associated factors for its positioning. But which factors could be involved?

Pulling the parasite into position

There are two possibilities how the parasite gains its poleward orientation independently from centrosomes: (i) through the dynamics of the spindle MTs themselves, and (iii) through the action of cytoplasmic dynein 1. Even in a stable metaphase spindle, the complete MT lattice constantly moves towards the spindle poles in a process called ‚flux' [94, 95]. This phenomenon is explained by the continuous addition of tubulin subunits at the MT plus end and their removal at the minus end at the spindle pole. MT flux could therefore provide a driving force for the observed poleward movement of the schizont. With the recent identification of a candidate *Theileria annulata* surface molecule, reported to interact with host cell α-tubulin [96], it can be assumed that a static interaction of the parasite surface with fluxing MTs could already contribute to bipolar positioning of the schizont. The presence of poleward fluxing MTs at the parasite surface could be tested through the expression of photoactivatable fluorescent tubulin and the tracking of activated regions on the MTs. Depletion of the proteins MCAK and Kif2a completely eliminates poleward flux in human cells [97], and it would be worth investigating, if a lack of flux affects parasite positioning.

The association of cytoplasmic dynein with the parasite surface could also account for or contribute to parasite orientation on the mitotic spindle. This assumption could be tested by the overexpression or microinjection of p50 dynamitin [98], a subunit of the dynactin complex required for dynein motor activity [99], as well as by microscopic analysis of a potential parasite recruitment of cytoplasmic dynein. However, the question should be raised if a bulk recruitment of cytoplasmic dynein to the parasite surface would interfere with the native tasks of this motor protein complex. It can be assumed that a cytoplasmic depletion of dynein would negatively affect crucial events such as chromosome alignment during metaphase [100] and the poleward movement of chromatids during anaphase [101].

How to position a cleavage furrow

Bundled MTs are known to be the only structural component of the spindle apparatus required for cell division [102]. In somatic cells, essential positional cues for cleavage furrow formation are being generated on the interpolar MTs that form the central spindle [41-43]. Similar signals are believed to be also emitted in a radial manner by astral microtubules to the cell cortex [103-106], where contractile ring formation and contractility are induced. The process of furrow ingression depends on the persisting activity of the small GTPase RhoA in a narrow zone at the equatorial cortex [46, 107]. The positional cue that determines the zone of RhoA activity consists of the centralspindlin complex, containing the plus end-directed kinesin Mklp1 and the Rho GAP CYK-4, as well as the Rho GEF Ect2 [41, 46, 108, 109]. Active RhoA promotes recruitment of F-actin and myosin II to the cortex, F-actin polymerization, as well as myosin II activity (reviewed in [44, 45]). The current model of furrow initiation proposes a subpopulation of stable chromosome-associated astral MT bundles which extend into the equatorial plane and associate with the cell cortex through the action of the yet unidentified plus end-directed stabilization factors that originate from the centromeres [103]. The centralspindlin-Ect2 complex is then thought to be delivered to the cortex along these stable MTs in an Mklp1-dependent manner, thereby determining the region of contractile ring formation. Accordingly, in cells with mono-polar spindle, injected with dominant-negative Mad2 to inactivate the spindle checkpoint, furrowing occurs distal from the chromosome mass at sites were the stable astral MTs reach the cortex [103]. Similar results were obtained for cells in which astral MTs were stabilized by taxol treatment, and furrowing correlated with the presence of stable MT-cortex interactions [110]. This mechanism also offers an explanation of how actin-myosin II contractility could be restricted to the equatorial zone, as this region receives cytokinetic signals through stable MTs emanating from both poles thereby creating a local maximum of MT density and thus RhoA activity [107, 111]. Furthermore, it was proposed that RhoA itself could contribute to MT stability, thereby providing a positive feedback loop which favors delivery of RhoA regulators to the equatorial region [112].

However, the majority of astral microtubules is dynamic and appears to inhibit furrowing at the polar regions by an yet unidentified mechanism, as their elimination results in excessive cortical contractility when the cytokinetic phase is induced through inactivation of the spindle checkpoint [113-116]. How is this dual role for astral MTs explained? It is possible that the rapid turnover of centrosome-nucleated astral MTs prevents efficient delivery of centralspindlin-Ect2 complex to the polar cortex and thereby prevents RhoA activation at a level that induces furrowing [113, 116]. Alternatively, different populations of astral MTs might deliver distinct regulators of cytokinesis to the cortex [111, 116]. In *C. elegans*, γ-tubulin-nucleated MTs in early anaphase induce furrowing whereas γ-tubulin-independent MTs of late anaphase suppress it [116]. The interesting aspect is that furrowing can still appear in the absence of astral MTs, but without the precision of an intact spindle apparatus [102, 116, 117]. The primary furrow-inducing signal generated at the central spindles (centralspindlin-Ect2) must thus be diffusible and reach the cortex without transport on astral MTs. It thus appears that astral MTs spatially narrow and refine a gradient of furrow-inducing signal originating at the central spindle, and increase the efficiency of cell division.

However, apart from this likely role of astral MTs in fine tuning cytokinesis, there is now evidence that during the first few minutes of anaphase onset, astral MTs are in fact essential for the initiation of furrowing [116]. It was proposed that this period of time is required for the establishment of stable interactions of astral MT and the cortex and thus first efficient wave of centralspindlin-Ect2 delivery to the site of contractile ring formation. After this period, astral MTs are dispensable for cytokinesis and furrowing completes driven by the central spindle.

How to position a parasite at a cleavage furrow

In *Theileria*-infected cells, cleavage plane determination and furrowing might be severely affected by the presence of the large schizont, reaching 10-15 microns in length and about 5 microns in width during host cell anaphase. The sheer presence of such a large structure might disturb the delicate mechanisms of furrow induction described in the previous section. Furthermore, cytokinetic abscission would be believed impossible, as the cortex at the cleavage furrow has to stably associate with the central spindle to form the intercellular bridge (reviewed in [47]). Nevertheless, cultures of *Theileria*-infected cells grow at high rate and in general contain relatively few binucleate cells. Furthermore, timing and duration of cell division in parasitized cells are normal. This indicates that the process of host cell division is not, or only minimally, affected by the presence of the parasite. Interestingly, throughout M phase, the parasite stably binds bundles of astral MTs and thereby likely integrates into the spindle apparatus without disturbing the processes of cytokinesis. When monitored live in cells arrested in prometaphase by treatment with the drug monastrol, as expected, most free astral MTs are structurally and spatially dynamic. Astral MTs bound to the parasite surface, however, appear bundled and remain at the same length and exact same position throughout an observation time of 20 min (Chapter 2.1., Figure S2). Considering the reported average lifetime for astral MTs of about 1 min [103], this suggests that MTs are being stabilized on the parasite surface, or at least, that a bundling activity prolongs the net association time of MT bundles with the parasite.

During metaphase, a stable association with discrete astral MTs positions the parasite in a bipolar fashion (Chapter 2.1., Figure 1). With the onset of anaphase, MT stabilization and bundling on the parasite seem to increase, as the density of parasite-associated MTs was observed to grow markedly. Monitoring the effect of the parasite-MT interactions in normally dividing cells is difficult, as the cytokinetic phase (C phase), marked by furrow ingression, starts in anaphase. Inhibition of actin-myosin contractility by treatment with the myosin II inhibitor blebbistatin [118] allows the observation of anaphase MTs without the spatial constrains of the cleavage furrow. In *Theileria*-infected cells entering anaphase in the presence of blebbistatin, parasite-associated MTs extend towards and often associate with the cell cortex (Figure 2A, upper and lower panels, respectively). This observation is particularly interesting, considering the role of astral MTs during early anaphase for delivering centralspindlin-Ect2 to the cortex. Also, it appears that a fraction of the MTs linking the cortex with the parasite surface originates from cortical

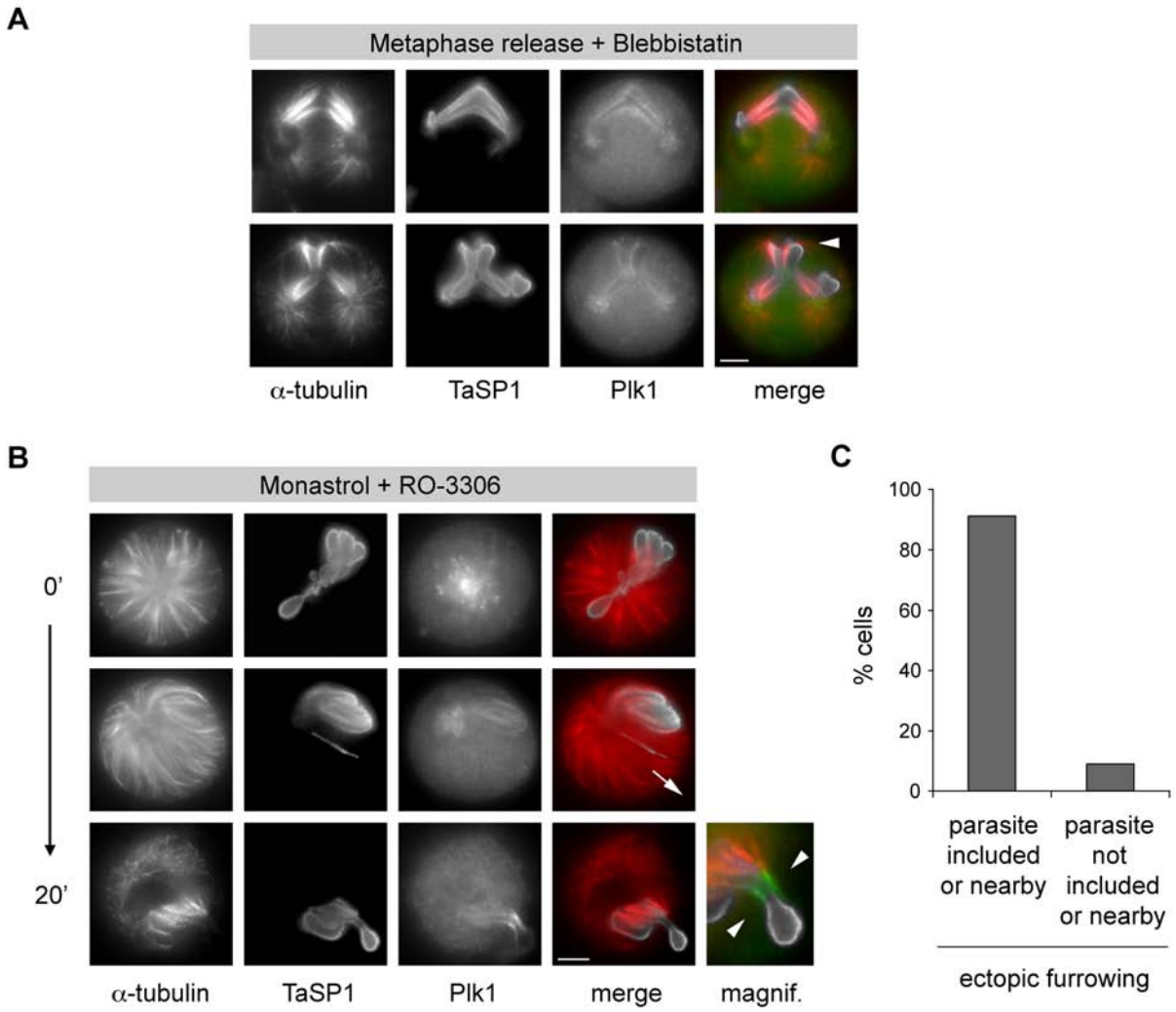

Figure 2. Cytokinetic phase MTs are stably associated with the parasite surface and position the schizont at the site of furrow ingression. (A) TaC12 cells were synchronized in prometaphase by treatment with 0.1 µg/ml nocodazole for 16 h, washed and released in the presence of 20 µM MG132 for 2h. Metaphase-synchronized cells were washed and released for 80 min with 100 µM of the myosin II inhibitor blebbistatin. Cells were fixed and stained with antibodies raised against α-tubulin, the parasite surface protein TaSP1 and Plk1; arrowhead indicates astral MTs that link the parasite surface with the host cell cortex. (B) TaC12 cells were synchronized in prometaphase by treatment with 100 µM Eg5 inhibitor monastrol for 16h. Cells were kept in the presence of the drug and were additionally treated with 10 µM Cdk1 inhibitor RO-3306 for up to 20 min. Cells were fixed and stained with antibodies raised against α-tubulin, TaSP1 and Plk1; arrow indicates the orientation of astral MTs away from the chromosome mass upon induction of premature cytokinesis; arrowheads indicate the ectopic cleavage furrowing. (C) The position of the parasite in cells undergoing RO-3306-induced furrowing was determined after 20 min treatment. Data are from one experiment with n=100 cells/sample. Scale bars represent 5 µm.

nucleation centers or parasite-associated nucleation centers that are located close to the cortex, and it remains to be tested whether these MT asters also recruit CYK-4 or Ect2.

Already in metaphase, the schizont is positioned adjacent to the cortex, spanning the metaphase plate of aligned chromosomes. During anaphase, maintaining its position, the parasite adopts an angled shape, possibly due to the polymerization and stabilization of astral MTs from both poles which might exert opposing forces on the parasite. It could be that this configuration is permissive or even favorable for the induction of furrow ingression, as the schizont surface might facilitate the delivery of a critical mass

of MTs to the cortex. It would thus be worth investigating, if furrowing preferentially starts at the region nearby the parasite. Additionally, the functionality of parasite-associated astral MTs in early stimulation of furrowing [116] could be tested in cells in which the essential central spindle component PRC1 is lacking. Knock-down of PRC1 results in the total absence of a central spindle but still allows transient furrowing, due to astral MTs that deliver cytokinetic signals, such as the chromosomal passenger complex, to the cortex [119]. It would be thus interesting to test, if, under these conditions, triggering of furrow ingression is impaired at the position of the parasite, or if its association with astral MTs allows uniform furrow ingression.

An alternative way to test if parasite-associated astral MTs participate in furrow induction is the chemical induction of furrowing in arrested cells that contain mono-polar spindles [103]. In monastrol-treated cells, the parasite is integrated in the centered, mono-polar spindle (Figure 2B, upper panels). Upon inhibition of Cdk1 with the specific drug RO-3306 [120], astral microtubules extend away from the chromosome mass and the parasite is repositioned accordingly (Figure 2B, middle panels). As cells proceed through chemically induced anaphase, MT dynamics decrease and most astral MTs disappear, except for the parasite-bound bundles, which now reach the cell cortex and appear to induce furrowing. Consequently, in about 90% of the cells, cleavage furrows form directly adjacent to the parasite (Figure 2C) and in many cases even include a small fraction of it (Figure 2B, lower panels). As seen for astral MTs of early anaphase as well as for central spindles, Plk1 accumulates at the plus end of the parasite-associated MTs. It can thus be postulated that the stabilization of astral MTs located at the parasite surface favors the delivery of cytokinetic factors to the cortex and thus, to a certain extent, directs furrowing to the parasite.

However, in anaphase cells, in which astral MTs were eliminated with nocodazole, the parasite was found to be still reasonably well positioned at the cleavage furrow (Chapter 2.1., Figure 10). After the initial induction of furrowing by stable astral MTs, their elimination is believed to be compensated by the nocodazole-resistant central spindle MTs which maintain furrow ingression [116]. Under these conditions, furrowing is likely to be maintained by the large fraction of central spindle MTs associated with the parasite surface. This could also rescue a slight malpositioning of the parasite due to the lack of astral MTs. If the association of central spindles as well as astral MTs with the parasite surface are both prevented by chemical inhibition of Plk1 and by nocodazole-treatment, respectively, proper positioning of the schizont at the cleavage furrow is lost. In this case, the constituents of the spindle apparatus that are required for cytokinesis are inaccessible for the parasite or completely lacking, and its positioning during cleavage furrow ingression fails.

Parasite and host cell division always occur at the same time, and parasite constriction and abscission seem to fully rely on the host cell, as they are never observed to occur independently. The schizont therefore depends on host cell cytokinesis to ensure its own division, and, since *Theileria* schizonts only replicate intracellularly, the parasite requires host cell M phase to complete with minimal disturbance. The consistent affinity of the parasite surface for MTs provides parasite positioning throughout the cell cycle. During M phase, the parasite associates with MTs involved in the spatio-temporal regulation of

cytokinesis and thereby passively integrates into the process of cell division. It therefore seems unlikely that the parasite interferes with or modulates mitotic regulatory processes, if an interaction with structural components of cell division allows its distribution over the forming daughter cells.

Taken together, the *Theileria annulata* schizont is able to adopt highly regulated cellular mechanisms that control cell division without disturbing the process itself. However, a number of open questions remain: (i) why is there a mechanistic difference in how the parasite binds astral and central spindle MTs (ii) what is the nature of these distinct MT interactions, and (iii) what is the relevance of the central spindle interaction for the process of cytokinetic abscission? Finally, it should also be addressed what the role of parasite-associated Plk1 is.

Stabilizing MTs

The building blocks of MTs are heterodimers of α- and β-tubulin. The dimers polymerize longitudinally to from protofilaments, of which 13 laterally associate to a cylindrical shape. MTs posses a directionality as their subunits always associate in a head-to-tail orientation, with the GTP-bound β-tubulin exposed at the faster polymerizing plus end. Hydrolysis of the β-tubulin-bound GTP shorty after addition of a dimer curls and destabilizes protofilaments. MT growth therefore requires the continued addition of fresh GTP-tubulin. The transition from MT growth to shrinkage is termed catastrophe, whereas the reverse process is called rescue. In a cell, MT stability is mainly determined by the following factors: MT nucleation and polymerization rates as well as MT end-stabilization and severing. To prevent protofilaments containing GDP-bound tubulin heterodimers from curling and depolymerizing, the cell uses plus- end and minus end-directed capping proteins or components that actively promote MT polymerization to stabilize MTs (reviewed in [84]). Collectively referred to as MT-associated proteins (MAPs), these components are expressed at relatively constant levels throughout cell cycle and their activity is regulated predominantly by phosphorylation (reviewed in [39, 121]). It is their concerted action that determines the net stability of MT in general, but also subpopulations of MT within a cell [122].

A very simple model explaining the interactions of the schizont with the spindle apparatus includes the interaction of the parasite surface with the minus end-directed motor dynein. It was shown for mammalian epithelial prophase cells that dynein-dynactin tethers prophase MTs to the nuclear envelope and thereby locally promotes their stabilization [98]. It is not known how dynein-dynactin exerts this effect and which additional motor proteins or MAPs contribute to it. However, this mechanism could also occur at the parasite surface. The assumption is appealing, since only one host cell component could provide the stabilizing effect on the parasite-associated MTs as well as the poleward orientation of the schizont.

It could also be that the parasite directly recruits MT stabilizing proteins such as the assembly promotor XMAP215/TOG (reviewed in [123]), the plus end binding protein EB1, or the nucleation factors TPX2 and Ɣ-tubulin. In *Xenopus* egg extracts, TPX2 is known to indirectly regulate MT nucleation at the chromosomes and spindle poles through its association with Ɣ-tubulin and Aurora A kinase (reviewed in [124]). Interestingly, a gradient of active TPX2 was shown to be established around *Xenopus*

chromosomes, established by the localized activity of a guanosine nucleotide exchange factor (GEF) and local accumulation of Ran-GTP. TPX2, cytoplasmically inactivated in a complex of α,β-importin, is liberated through the action of Ran-GTP at the chromosomes and promotes MT nucleation [125, 126]. As *Xenopus* egg do not posses centrosomes, this process might emerge from the requirement of alternative MT nucleation centers and might not apply to mammalian cells. However, localized Ran-GTP accumulation at mammalian kinetochores was described to be linked to K-fiber nucleation [127]. Maybe a similar gradient of Ran-GTP is generated at the parasite surface through the local activation of a GEF, promoting MT nucleation.

ϒ-tubulin, however, cannot be observed at the parasite surface by IFM. It would be expected that ϒ-tubulin recruitment results in increased MT nucleation at the parasite. This does not seem to be the case, as MT nucleation appears predominantly at the chromosomes soon after nocodazole washout in parasitized cells (Chapter 2.1., Figure 1, S1). Importantly, the number of MT asters forming in parasitized cells, does not differ from the number observed in cells in which the parasite was eliminated with the drug buparvaquone/BW720c (Chapter 2.1., Figure S1). The parasite surface is thus unlikely to promote ϒ-tubulin-dependent nucleation.

Interestingly, Plk1 is known to be required formation and maintenance of the mitotic spindle [74, 89, 128]. In *Xenopus*, Plx1 (Plk1) localizes to mitotic chromosomes where it is assumed to inactivate Stathmin/Op18. The protein Stathmin/Op18, an important factor of MT stability, is found in many species and follows a similar mechanism of localized activity. Stathmin/Op18 is known to actively reduce the MT polymerization rate [129], as it sequesters tubulin heterodimers into a stable complex and thereby makes them unavailable for polymerizing MTs. The inactivation of Stathmin/Op18 by chromosome-bound Plx1 creates a gradient of Stathmin/Op18 activity in the cytoplasm [122, 130, 131]. Consequently, MT stability increases around the chromosomes and locally supports spindle formation. In mammalian cells, the mechanisms, by which mammalian Plk1 maintains spindle integrity, are not understood. When Plk1 is chemically inhibited, some MTs, such as kinetochore-fibers, are destabilized, whereas others, including astral MTs, show excessive growth [128]. The elongating astral MTs, observed upon Plk1 inhibition, exert pushing forces when reaching the cell cortex, leading to spindle collapse. With the protein Centrobin/NIP2, a centrosomal MT-stabilizing factor has been described, which is regulated by Plk1 to promote spindle formation [132].

The MT stabilization factor XMAP215/TOG is known to counteract the catastrophe-promoting protein MCAK [123]. Together, these two proteins determine the balance between MT growth and shrinkage, as XMAP215/TOG-depleted cells possess shorter spindles. The major role of XMAP215/TOG, however, appears to lie in the maintenance of pole integrity and spindle bipolarity [133-135]. The plus end protein EB1, highly conserved among species, stabilizes MTs by increasing MT rescue and decreasing catastrophe rates (reviewed in [136]). Knock-down of *Xenopus* EB1 strongly reduces MT length [137]. It could be tested whether immunodepletion or knock-down of XMAP215/TOG or EB1 would affect the relative stability and abundance of MTs at the parasite surface. A lacking effect on this MT population would indicate a stabilization process independent from XMAP215/TOG or EB1.

In summary, it is possible that the schizont recruits MT stabilization factors such as XMAP215/TOG and EB1, or negatively regulates inhibitors of MT polymerization like Stathmin/Op18, promoting MT polymerization on its surface. It should be therefore tested, if such factors are recruited to the schizont surface. However, such a recruitment would have to be well equilibrated, as excessive MT sequestration to on the parasite could affect proper spindle formation and might lead to spindle collapse. Finally, it could be argued that a direct parasite-MT interaction could still permit the regulation of MT dynamics at the parasite independent of a specific interaction with a MAP. A high affinity for MTs could prevent the parasite from losing contact with the mitotic spindle, when MT dynamics are high during mitosis. But then, how does one explain the fact that parasite-bound astral MTs are very stable compared to free MTs (Chapter 2.1., Figure 1)? Also, why does the assembly of the mitotic spindle occur predominantly around the schizont (Chapter 2.1., Figure S2)?

Central vs. astral

The existence of a general mechanism for MT stabilization on the parasite surface, such as a dynein-dependent stabilization, would suffice to describe the parasite-MT interactions as such, but the association with distinct subsets of MTs would be arbitrary and simply depend on their spatial availability for the parasite. The data presented in this study, however, indicate a mechanistic difference in how the parasite associates with subpopulations of late M phase MTs. In anaphase cells, lacking Plk1 catalytic activity, the schizont is incapable of associating with the central spindle MTs whereas it readily binds astral MTs (Chapter 2.1., Figure 9, 10, S11). This finding raises the question how different classes of MTs emerge in a mitotic cell and which factors are involved that distinguish them?

MT functions vary throughout cell types or cell cycle stages and this variation is predominantly created by MAPs that associate with and alter the dynamics of MT subsets (see above, reviewed in [84]). But how do these factors specifically bind certain MTs and not others? One of the answers lies in the post-translational modifications (PTMs) of the α- and β-tubulin subunits of the tubulin heterodimer. Their functional roles are just beginning to be discovered, although a number of tubulin PTMs have been known for long, including phosphorylation, detyrosination, acetylation, glycylation, glutamylation and palmitoylation (reviewed in [138]). Some of these PTMs have been linked to MT populations of mitotic cells. Whereas astral MTs are mostly unmodified and thus tyrosinated, stable interpolar MTs are found to be detyrosinated, acetylated and polyglutaminated. Astral MT tyrosination is maintained by tubulin tyrosine ligase (TTL) and required for mitotic spindle orientation [139]. MT tyrosination is recognized by GAP-Gly domain-containing plus-end tracking proteins such as CLIP-170 and p150Glued/dynactin that promote cortical MT attachment [140-142]. Acetylation, on the other hand, is found on stable MTs. It occurs on Lys40 of α-tubulin, which resides on the luminal face of MTs and loss of acetylation does not have a phenotype in various species (reviewed in [143, 144]). Also, due to its luminal placement, acetylation is inaccessible for cytosolic factors.

It could be that parasite surface proteins, specifically recognizing tubulin PTMs, are mediating the parasite interaction with the different subsets of MTs in a cell. The subpopulations of dynamic interphase or mitotic astral MTs, for example, are largely lacking tubulin modifications. A hypothetical surface protein binding tyrosinated MTs would therefore account for interphase MT interactions and mitotic astral MT interactions with the parasite. Detyrosinated or polyglutaminated central spindle MTs, on the other hand, could be bound by a parasite factor specifically recognizing one of these modifications and this interaction could be triggered by Plk1 activity. It could also be assumed that Plk1 is involved in the regulation of tubulin modifications during M phase, although no such role has been reported up until now.

As tubulin PTMs provide specific docking sites for MAPs, they allow the formation of biochemically and functionally distinct groups of MTs. Apart from this feature, evidence is emerging that MT subpopulations are being determined by their nucleation point. For example, in *C. elegans*, two subsets of astral MTs have been identified, one triggering the assembly of a contractile ring in the equatorial region, the other suppressing furrowing at the polar regions [111]. The authors identified the former group of MTs to be nucleated in a Ɣ-tubulin-dependent manner at the centrosomes, whereas nucleation of the latter group of MTs was independent of Ɣ-tubulin but required the activity of Air-1/Aurora A. Since the different functions of these MT populations manifest themselves at the MT plus ends at the cortex, the authors propose that centrosomal Air-1/Aurora A might determine the loading of certain MAPs at MT minus ends. These factors would then be transported to the plus ends in a kinesin-dependent manner.

In mammalian cells, a similar principle was proposed, explaining the differential functions of astral MTs in triggering or inhibiting furrowing. Chromosome-bound MT are believed to be loaded with yet unidentified MAPs at centromeres, that are then delivered to the MT plus ends where they increase MT stability and trigger contractile ring formation [103]. Dynamic centrosome-nucleated astral MTs, on the other hand, are proposed to prevent furrowing outside the equatorial region. Taken together, these observations demonstrate that the loading of specific MAPs, which determine MT stability and function, account for the distinct characteristics of MT subsets.

Extending this thought to *Theileria*-parasitized cells, one could argue that a surface molecule, which would bind MAPs specific for a certain population of spindle MTs, could provide these factors to MTs on the parasite. In this model, the parasite would bypass the necessity for site-specific loading of these MAPs onto MTs. The stability and functionality of a certain group of MTs could therefore be induced by the increased delivery of the respective MAPs. For example, the parasite surface could provide its own or a scavenged protein specifically binding a factor required for central spindle formation, such as the antiparallel MT bundling protein PRC1 [119, 145]. This scenario implies that astral MTs from both poles, bound by the parasite surface, would associate with PRC1 and would consequently be bundled in an antiparallel fashion. Antiparallel MT bundling is the key of central spindle formation (reviewed in [39, 40]) and PRC1 was shown to recruit other crucial central spindle components such as the centralspindlin complex or the kinesins Mklp2 and KIF4 [146, 147]. Mklp2, in turn, recruits with Aurora B another essential factor [148]. Thus by promoting the interaction of PRC1 with antiparallel MTs, a cascade of central spindle formation could be triggered (reviewed in [40]).

However, no association of PRC1 with the parasite was observed, other than along with central spindles. It could be argued that a stable association of PRC1 with the parasite would only be possible in the presence of MTs. This would to prevent a bulk recruitment of PRC1 to the parasite which could affect parasite-independent central spindle formation. However, how can one explain the absence of parasite-associated central spindle, but not astral MTs, in Plk1-inhibited cells and why, in these cells, does the presence of overlapping astral MTs not allow a parasite-independent recruitment of PRC1? Plk1 activity is dispensable for central spindle formation (reviewed in [68]) and in the absence of Plk1 catalytic activity, central spindles form, lacking an association with the parasite. As Plk1 recruitment to the parasite surface in untreated cells coincides with the appearance of central spindle MTs at the surface, one could assume that local Plk1 activity promotes the parasite recruitment of factors such as PRC1 or influences the stability of plus end-overlapping midzone MTs. How PRC1 specifically stabilizes central spindle MTs has remained elusive, but recent findings link it to a family of MAPs, specific for overlapping MTs [149].

CLASPing the central spindle

PRC1 is brought to MT plus ends by the kinesin Kif4a where it bundles overlapping MTs. The bundling activity of PRC1 during is inhibited during early mitosis by Cdk1-dependent phosphorylation [41]. At the metaphase-anaphase transition, delivery of PRC1 to the midzone MTs is timed by the shutdown of Cdk1 activity and the phosphatase Cdc14 [150]. It has now been shown that, with the onset of anaphase, PRC1 associates with CLASP1/Orbit/Mast/Stu1p, an essential factor for central spindle stability [149].

CLASPs are evolutionarily conserved MT stabilizers that can be found at MT plus ends. CLASPs are believed to receive their plus end specificity through an interaction with plus end-tracking proteins (+TIPs) such as EB1 and CLIP-170 [151, 152]. The two mammalian CLASPs regulate MT stability throughout cell cycle. During interphase, CLASPs stabilize MTs in the vicinity of leading edge cortex [151, 152]. In a variety of species, including budding yeast, *C. elegans*, *Drosophila*, *Xenopus* and humans, CLASP1 and its orthologs were linked to mitotic spindle formation and mitotic progression [153-156]. With the onset of anaphase, CLASPs localize to the MT overlap region of the spindle midzone, but not to plus ends of astral MTs [157, 158]. This timing is explained by CLASP1 interaction with the central spindle marker PRC1 [149]. In frogs and flies, repression of CLASP during anaphase leads to depolymerization of midzone MTs [156]. Importantly, astral and peripheral midzone MTs are unaffected by CLASP repression and still capable of initiating cleavage furrows, which ultimately regress due to the lack of the central spindle [158].

The insight into the role of CLASPs as essential stabilizers of the central spindle is very interesting, as it could elegantly explain the observed specificity of the *Theileria* schizont for the host cell central spindle: during metaphase, the parasite associates with astral MTs through one of the mechanisms discussed above, including a direct MT binding, recognition of tyrosinated MTs, dynein-mediated MT interaction or recruitment of general MT stabilization factors, such as EB1 or XMAP215/TOG. This mechanism of astral MT binding could be maintained also throughout anaphase and telophase. With the onset of anaphase,

however, a parasite surface molecule specifically recognizing CLASP1, could recruit the protein to the parasite surface. The presence of CLASP1 and its interaction with PRC1 could then trigger the stabilization and bundling of parasite-associated MTs. It is conceivable that by binding and presenting CLASP1, the parasite could favor central spindle formation at its surface.

How does this model conform to the observed Plk1-dependency of central spindle binding of the *Theileria* schizont? Although CLASP1 isoforms are predicted to contain Plk1 phosphorylation sites, nothing is known on a potential interaction of these isoforms with the kinase. Furthermore, Plk1 is not required for central spindle formation as such, which makes its role as a CLASP1-regulating kinase unlikely. However, the role of Plk1 for anaphase spindle elongation [159] points towards an involvement in the modulation of spindle midzone MT dynamics. Nevertheless, it cannot be excluded that a Plk1-dependent phosphorylation of a parasite surface protein or CLASP1 itself is be required for stable CLASP1 binding to the parasite. In line with the typical spatial regulation of Plk1, this task would be carried out with the onset of Plk1 recruitment to the parasite during anaphase. Furthermore, it would have to be assumed that, upon Plk1 inhibition, the remaining astral MTs associated with the parasite are not permissive for bundling. Consequently, in the absence of Plk1 activity, the parasite would only be positioned in the spindle midzone by astral MTs and the central spindle would form separate from the parasite in the midzone.

Alternatively, a parasite surface protein could exist, which exerts a function similar to CLASP at the central spindle. A potential stabilizing effect on overlapping MTs could be triggered through phosphorylation by Plk1. Indeed, a vast number of parasite proteins, predicted to posses a signal peptide, contain putative Plk1 phosphorylation sites. The increased stability of overlapping MTs at the parasite surface, in turn, could promote the recruitment of central spindle factors.

Taken together, it can be said that the formation of central spindles on the parasite, in all likelihood, requires the recruitment of specific MAPs and motors. It could be that parasite-associated MTs lack the loading of these proteins, as it would occur in a normal spindle midzone, and are thus not involved in normal central spindle formation. Thus, a compensatory recruitment of central spindle MAPs, dependent on Plk1 activity, could induces the formation of functional central spindles, which carry all essential components (Chapter 2.1., Figure 8, S10). The phase of Plk1 recruitment to the parasite during M phase lasts from the onset of anaphase until telophase, when the cleavage furrow has maximally ingressed (Chapter 2.1., Figure 2, S3). This observation raises two questions: (i) does the formation of a central spindle at the parasite surface require persisting Plk1 activity, and (ii) are central spindles still bound to the parasite after the dissociation of Plk1 from the parasite surface? Clearly, dissociation of Plk1 from the schizont during telophase does not lead to a dissociation of the central spindle (Chapter 2.1., Figure 8, S10), pointing towards a stable association of parasite and central spindle at that time. However, when Plk1 is chemically inhibited at a time that allows furrow ingression, central spindles fail to associate with the parasite (Chapter 2.1., Figure 9, 10, S11). The fact that furrow ingression was initiated despite Plk1-inhibition indicates that inhibition occurred after onset of anaphase [89], allowing the induction of furrow ingression. The absence of central spindles from the schizont surface in these cells indicates that, at this

stage, parasite-associated central spindles are still in the process of formation and not jet fully stabilized. Again, this points towards a mechanistic difference in parasite-associated versus normal central spindle formation, as the stability of the latter is unaffected by Plk1 inhibition. It would thus be interesting to test, if inhibition of Plk1 at an even later time point also leads to the instability of parasite-bound central spindles.

Finally, the findings suggest that Plk1 in fact promotes the formation of central spindles on the parasite rather than just the association of a preformed structure and that central spindle MT binding is independent of Plk1 activity. Otherwise, it would be difficult to explain the dissociation of Plk1 but persistent stable association of central spindle MTs with the schizont during telophase, when furrow contraction is inhibited using the myosin II inhibitor blebbistatin.

The dynamic association of Plk1 with the parasite surface

Plk1 recruitment to the schizont surface starts in G2/M phase, at a time when Plk1 is observed on centromeres (Chapter 2.1., Figure S3) and prior to the activation of Cdk1, in which it is involved [74, 160, 161]. Plk1 itself is activated by the mitotic kinase Aurora A, in conjunction with the regulatory protein Bora, by phosphorylation of the residue Thr210 [70, 71]. It was postulated that Plk1 lacking Thr210 phosphorylation inhibits its own activity through folding of its C-terminal substrate binding domain onto the kinase domain [162] and that Bora overrides this autoinhibition of Plk1, making it accessible for phosphorylation by Aurora A [70]. Recently, with SBE13, an inhibitor of Plk1 was described, which blocks Plk1 catalytic activity by ‚freezing' the kinase in its folded, inactive conformation, but does not affect the kinase activity of Thr210-phosphorylated Plk1 [163]. Therefore, by treatment with SBE13, it could be tested, if folded and inactive Plk1 is capable of binding to the parasite. A pool of Plk1 could exist at the parasite surface prior to Plk1 activation, which could be demonstrated by staining with Thr210-specific antibodies. Together, these observations could provide information whether the parasite surface can promote Plk1 activation in a mechanism similar to Bora and thereby promote Cdk1 activation and mitotic entry.

Interestingly, with the entry into M phase, marked by nuclear translocation of cyclin B1 (not shown), Plk1 recruitment to the schizont surface is counteracted by Cdk1 at the onset of mitosis (Chapter 2.1., Figure 3). The sudden inactivation of Cdk1 at the metaphase-anaphase transition, or chemical inhibition of Cdk1, triggers an immediate recruitment of Plk1 to the schizont, followed by prominent parasite-associated central spindle formation. These observations show, that parasite recruitment of Plk1 is timed by host cell factors in a manner that has been described before. Cdk1 phosphorylation of PRC1 at a PBD binding motif prevents its association with Plk1 [77]. Furthermore, Cdk1 inhibits regulators of anaphase and telophase, including PRC1, Mklp1, Mklp2 and ECT2 [77, 164, 165], which are required for central spindle formation and function. One of the main tasks of Cdk1 is thus to prevent activities typical for anaphase and telophase from occurring during early mitosis, such as the bundling activity of PRC1, thereby allowing a flawless and timed progression of M phase. The fact that Cdk1 activity counteracts Plk1 recruitment to the parasite can be interpreted in two ways. Firstly, the presence of Plk1 at the

parasite surface during early mitosis might induce a stabilization of overlapping MTs on the parasite. The proper timing of Plk1 recruitment could therefore prevent a negative effect of the parasite on the metaphase spindle. Secondly, an excessive recruitment of Plk1 during early mitosis could reduce the pool of Plk1 available in the cytoplasm, which might negatively affect its native roles during that time. Such an effect was described for the protein PICH, which was proposed to be involved in spindle assembly checkpoint (SAC) signaling. It was found that PICH depletion inhibited SAC function whereas overexpression of PICH in depleted cells restored SAC function [166]. However, it was shown that, what seemed to be mediated by SAC cell cycle arrest, was in fact due to a downregulation of Plk1 activity [167]. Being the strongest interaction partner of Plk1 during early mitosis, overexpression of PICH sequestered Plk1 and led to a loss of Plk1 function in regulating the SAC. Furthermore, it was proposed for *Drosophila* embryonic cells that the MT-associated protein Map205 binds Polo in interphase and sequesters it to MTs, thereby inhibiting its cellular activities [168]. In this case, release of Polo from Map205 is triggered by Cdk1, making Polo available for its mitotic substrates.

It could thus be argued that sequestration to the parasite surface during early mitosis would be detrimental to host cell Plk1 functions. During anaphase, both, parasite- as well as midzone-associated pools of Plk1 are required for central spindle functionality. Even with a predominant sequestration of cytoplasmic Plk1 to the schizont, the parasite-bound pool of Plk1 could phosphorylate central spindle-targeted components in a distributive fashion, as the central spindle is associated with the parasite surface. This could compensate for a potential deficit of central spindle-bound Plk1.

Plk1 activity is spatio-temporally regulated by an accumulation at specific locations within the cell (reviewed in [49, 57, 68]). This characteristic is also reflected by the presence of a dedicated substrate binding domain, the polo-box domain (PBD), which binds phosphorylated serine and threonine residues [66]. After central spindle formation, Plk1 phosphorylation-primes and binds PRC1 [77] as well as the kinesin Mklp2 [169] and thereby locates to the midzone though a phospho-dependent docking of the PBD [170]. At the central spindle, Plk1 phosphorylates Cyk-4/MgcRacGAP [171], a RhoGAP that is associated with the kinesin Mklp1 to form the centralspindlin complex [172]. Phosphorylation of Cyk-4/MgcRacGAP induces its association with the RhoGEF Ect2 [173]. The formed centralspindlin-Ect2 complex then translocates to the cell cortex via astral as well as midzone MTs where it induces the recruitment and activation of the GTPase RhoA, required for contractile ring formation and onset of division [46, 108, 109].

Using chemical genetics and a Cyk-4-fused Plk1 kinase domain, it was elegantly shown that Plk1 function at the central spindle requires its recruitment to this structure to promote RhoA activation and furrow ingression [171]. It could therefore be that only parasite-associated, but not cytoplasmic Plk1 functions to assemble central spindles on the schizont surface. A way to test this assumption is opened by the discovery of inhibitors of PBD-dependent binding [79, 80]. In *PLK1*-null cells, complementation with an allele expressing the chimeric protein, consisting of the Plk1 kinase domain and Cyk-4/MgcRacGAP, restores Plk1 function during anaphase [171]. The expression of this chimeric protein in parasitized cells and the timed chemical inhibition of PBD-dependent binding at the onset of anaphase

offer opportunities to investigate whether cytoplasmic Plk1 catalytic activity would suffice for central spindle attachment to the parasite in cells that normally progress through cell division.

The binding of Plk1 to its substrates requires the phosphorylated motif S-(pS/pT)-(P/X) [66], preferentially generated by proline-directed Ser/Thr-kinases. Cdk1, besides its inhibitory function on Plk1 binding to PRC1, also primes the interaction of Plk1 with its partners in early mitosis by phosphorylating them. This includes Cdc25C, Bub1, BubR1, PICH and others (reviewed in [67]). Obviously, this does not apply to the parasite binding of Plk1. Apart from Cdk1, Plk1 is known as the only mitotic priming kinase for PBD binding. After Cdk1 activity is downregulated at the onset of anaphase, Plk1 mediates its own interaction with proteins such as Cyk-4/MgcRacGAP, Mklp2 or PRC1 (reviewed in [67]). To date, the *Drosophila* protein MAP205 provides the only example for phosphorylation-independent binding of Plk1 [168]. Parasite recruitment of Plk1, in turn, seems to depend on the presence of the two polo-box domain-1 residues H538 and K540 (Chapter 2.1., Figure 5), which were shown to be required for phosphorylation-primed binding of Plk1 [78, 170]. This raises the question, which kinase, if not Cdk1, is involved in the regulation of Plk1 docking on the schizont surface.

The role of Cdk1 in the regulation of PBD binding is well established, however, no involvement of other proline-directed kinases, such as MAPK or ERK kinases, has been shown to date. We addressed the question, if the parasite surface would stain for pSer/pThr or pSer/pThr-Pro, indicating the involvement of a priming kinase in Plk1 binding, or potentially also the negative regulation of binding through Cdk1. The surface was strongly stained for pThr-Pro during interphase and late telophase, whereas no pThr-Pro or pSer-Pro staining was observed throughout mitosis up until late telophase. Furthermore, P-Ser antibodies did not stain the surface at any cell cycle stage (results not shown). This indicates that a proline-directed Ser/Thr kinase is not directly involved in Plk1 recruitment to the parasite during anaphase and early telophase. Therefore, Cdk1 is also unlikely to prevent Plk1 docking in a mechanism similar to PRC-1, on which it phosphorylates the PBD binding motif and sterically hinders Plk1 docking [77]. Interestingly, antibodies raised against P-Thr weakly labeled the parasite surface following a temporal pattern that resembled that for Plk1 recruitment to the parasite (Figure 3). During interphase, some parasites showed a P-Thr signal, however, it was not tested if these cells are in G2 phase. From prometaphase until metaphase, labeling was absent and reappeared in anaphase. It thus seems, that Plk1 recruitment is regulated by timed Thr phosphorylation of the parasite surface and that Cdk1 does not directly prevent Plk1 binding. This is particularly interesting in light of the fact that most M phase kinases phosphorylate Ser or Thr residues and are regulated in a precise temporal manner.

Taken together, these observations can be interpreted in the following way: Plk1, or another Ser/Thr kinase, phosphorylates a parasite surface protein at a PBD binding motif, which then allows Plk1 docking. This priming phosphorylation could be, directly or indirectly, counteracted by Cdk1, either through inhibitory phosphorylation of the respective kinase, or the activity of a phosphatase during prometaphase and metaphase. Alternatively, a host cell factor, bound to the parasite, could be phosphorylated for Plk1 docking, and the association of this linker with the parasite could be inhibited by Cdk1.

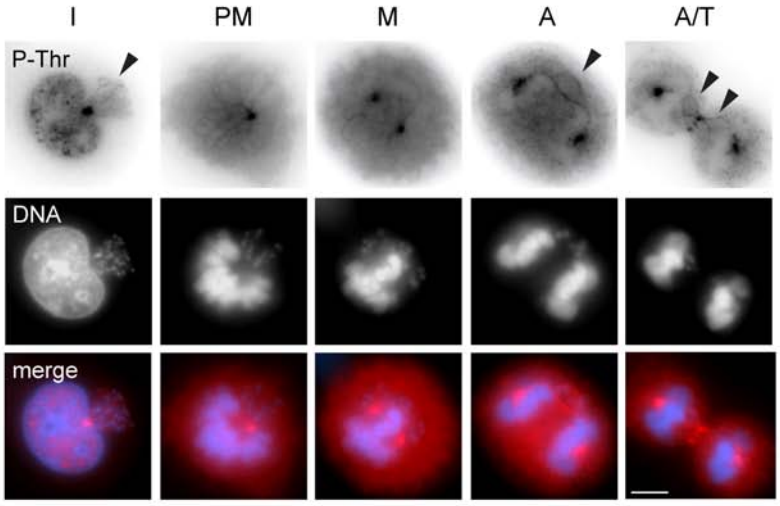

Figure 3. The parasite surface shows Thr phosphorylation during anaphase. *T. annulata*-parasitized cells were analyzed by IFA for Thr phosphorylation on the schizont surface (arrow heads) during different host cells cylce stages. The parasite was visualized by staining of its nuclei (DAPI). I, interphase; PM, prometaphase, M, metaphase; A, anaphase; A/T, anaphase/telophase. Scale bar represents 5 µm.

It could be tested, if chemical inhibition of Cdk1 in prometaphase cells leads to an immediate generation of P-Thr epitopes on the schizont surface. This would support the assumption that Plk1 docking at the parasite surface is in fact regulated by priming through Thr phosphorylation.

Prominent regulators of mitosis are the dual-specificity phosphatases of the Cdc25 family. Mammalian Cdc25B A, B and C act during mitotic entry up until the metaphase-anaphase transition to activate and maintain Cdk1 activity (reviewed in [53, 174, 175]), and Plk1 was shown to support activation of Cdc25 [160]. Once active, Cdk1 maintains Cdc25C activity during early mitosis (reviewed in [174]). Inactivation of Cdc25, in turn, leads to an inactivation of Cdk1, since the phosphatases antagonize the inhibitory phosphorylations of Cdk1 by the Cdk-inactivating kinases Wee1 and Myt-1 (reviewed in [176]). At the metaphase-anaphase transition, Cdc25C is degraded by the anaphase-promoting complex thereby contributing to the downregulation of Cdk1 activity. Early degradation of Cdc25C has been shown to be prevented by the regulatory protein leucine-zipper tumor suppressor 1 (Lzts1) [52], as depletion of Lzts1 inactivated Cdc25 and consequently led to premature progression into anaphase.

BN82685 is one of the most potent Cdc25 inhibitors, which targets all three mammalian Cdc25 phosphatases [175, 177, 178]. Inhibition of Cdc25 impairs G2/M transition and mitotic progression, likely caused by indirect Cdk1 inactivation [176, 178]. Considering the role of Cdc25 in maintaining Cdk1 activity, it was tested if an alternative induction of the metaphase-anaphase transition, other than chemical inhibition of Cdk1, would induce Plk1 recruitment to the schizont. Furthermore, Cdc25 could theoretically function as a phosphatase counteracting the priming phosphorylation which might be required for Plk1 docking on the parasite. Parasitized cells were released from prometaphase arrest in the presence of Cdc25 inhibitor and monitored for Plk1 binding to the schizont. Control cells reached

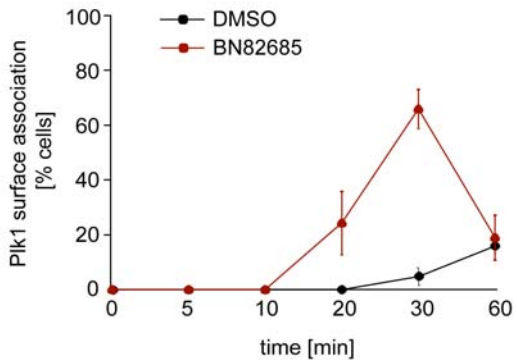

Figure 4. Cdc25 inhibition induces early anaphase and Plk1 recruitment to the schizont surface. Nocodazole-synchronized TaC12 cells (0.1 µg/ml nocodazole for 16 h) were released from prometaphase arrest in the presence of control solvent (DMSO) or 20 µM Cdc25 phosphatase inhibitor BN82685. n=120 cells/ sample; error bars indicate standard deviation.

anaphase between 30 and 60 min of release. Plk1 was recruited to the schizont in 20% of these cells. Cells treated with Cdc25 inhibitor displayed earlier Plk1 recruitment as 60% of these cells reached anaphase already after 20-30 min (Figure 4). Importantly, Plk1 recruitment always appeared at the onset of chromosome separation. This result thus supports the notion that the inactivation of Cdk1 at the metaphase-anaphase transition promotes Plk1 recruitment. However, it cannot be concluded that Cdc25 acts as a phosphatase directed at the priming phosphorylation for Plk1 binding. As Cdc25 inhibition directly affects Cdk1 activity, it is difficult to dissect the role of these two molecules and test their role in Plk1 binding. However, expression of a constitutively active form of Cdk1 (Cdk1-AF, [179]) and Cdc25 inhibition in these cells might allow us to investigate the potential role of Cdc25 independent of Cdk1. Furthermore, it should be tested if co-treatment with Cdc25 inhibitor and proteasomal inhibitor MG132 influences the recruitment of Plk1 to the schizont, as degradation of cyclin B or the Cdc25 activity-promoting Lzts1 are required for Cdk1 shutdown [52, 180].

Besides the Cdc25 phosphatase family, the Ser/Thr-specific phosphatases PP1 and PP2A are important for the progression of M phase and are spatially regulated as holoenzymes (reviewed in [53, 174]). Together, PP1 and PP2A are believed to dephosphorylate most mitotic protein-associated phospho-serines and phospho-threonines. Active throughout mitosis, the enzymes regulate processes ranging from mitotic entry, centrosome splitting, MT stability, Plk1 and Aurora kinase activity or anaphase, to name a few of them (reviewed in [53, 174]). It was thus tested, if inhibition of these phosphatases with okadaic acid [181] provokes the recruitment of Plk1 to the parasite surface.

Prometaphase-synchronized cells, released in the presence of the phosphatase inhibitor, did not show earlier recruitment of Plk1, compared to control cells, whereas Cdk1 inhibition induced an immediate binding of Plk1 to the schizont in all cells (Figure 5A). The effect of phosphatase inhibition was monitored by probing for phosphorylated Ser and Thr residues, which accumulated in the presence of the inhibitor (Figure 5B). Plk1 recruitment always coincided with host cell anaphase and, rather, it appeared that anaphase onset was delayed in okadaic acid-treated cells. Also, Plk1 recruitment to the schizont appeared weaker in these cells, compared to untreated control cells, but parasite positioning on the spindle and central spindle association were normal (not shown).

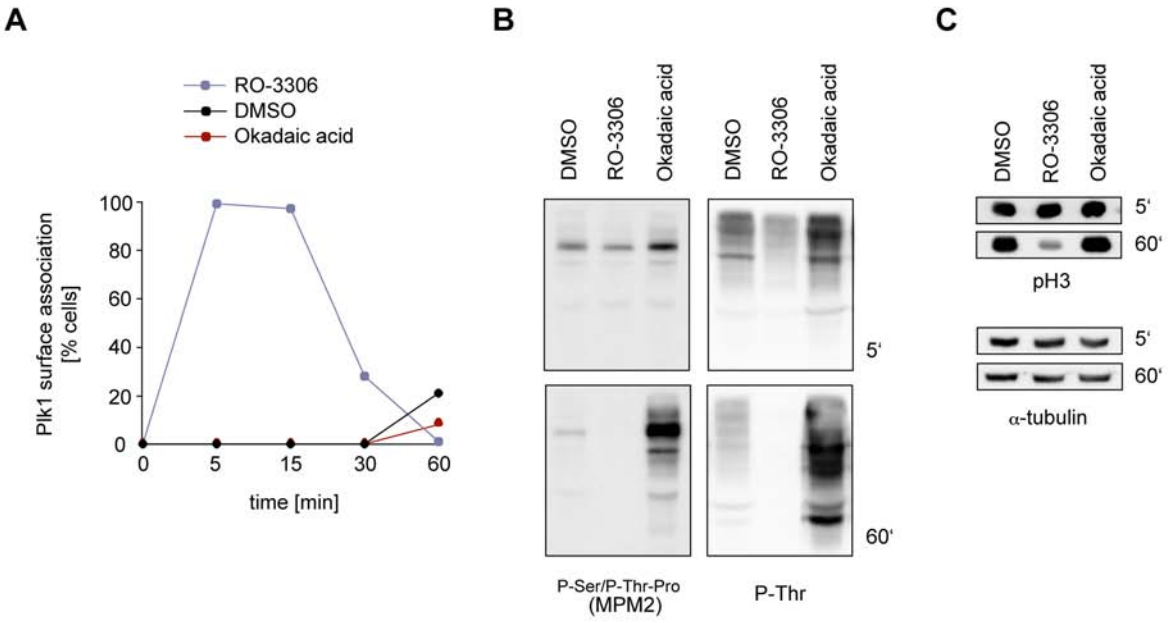

Figure 5. Inhibition of PP1 and PP2A by high doses of okadaic acid does not induce Plk1 recruitment to the schizont surface during early mitosis. (A) TaC12 cells were synchronized in prometaphase by treatment with 0.1 µg/ml nocodazole for 16 h, washed and released in the presence or absence (DMSO) of 1 µM of the PP1/PP2A phosphatase inhibitor okadaic acid. Cell were also released in the presence of 10 µM Cdk1 inhibitor (RO-3306). Cells were harvested at the indicated time points and analyzed for Plk1 association with the parasite by IFA; n=100 cells/sample. (B) Cells form (A) were harvested and whole cell lysates were analyzed by western blot, probed with antibodies specific for epitopes created by proline-directed Ser/Thr kinases (MPM2), such as Cdk1, or anti phospho-threonine (P-Thr). (C) Western blot analysis of lysates from (B), using an phospho-histone H3 antibody to monitor the mitotic state; α-tubulin was monitored as loading control.

Due to the very broad effect of okadaic acid treatment, it is difficult to conclude on a specific role of PP1 or PP2A in the recruitment of Plk1 to the schizont. Although these phosphatases might indeed counteract phosphorylation-primed binding of Plk1 on the parasite, it could also be that the activity of the priming kinase is affected by phosphatase inhibition. Taken together, inhibition of prominent phosphatases regulating early mitosis did not alter the timing of Plk1 recruitment to the schizont. It seems that the re-appearance of Plk1 on the parasite is tightly linked to the onset of anaphase and thus depends on the inactivation of Cdk1. The proline-directed kinase Cdk1, however, is unlikely to phosphorylate the site of Plk1 docking on the schizont, as no P-Thr or P-Ser epitopes were detected at the surface during prometaphase and metaphase. Hence, a temporal regulation of a priming kinase for Plk1 could be assumed.

Apart from Cdk1, Plk1 itself is the only kinase described to prime its phospho-dependent binding. Whereas Cdk1 provides docking sites during prophase and metaphase, Plk1 takes over with the onset of anaphase (reviewed in [49, 67, 68, 182]). The same observations were made with the Plk1 inhibitor BTO-1 (not shown). It was thus first tested if Plk1 catalytic activity is required for its recruitment. At concentrations of 100 nM up to 1 µM of the potent Plk1 inhibitor BI-2536 [91, 92], endogenous Plk1 as well as ectopically expressed wild-type and kinase dead (K82R) Plk1 were still observed to bind the

parasite surface during G2 phase as well as during anaphase (Chapter 2.1., Figure 4, 6, S8). Already at 100 nM, BI-2536 showed the described phenotypes of Plk1 inhibition (Chapter 2.1., Figure S7, S12), including G2/M arrest, loss of spindle bipolarity, lack of Plk1 recruitment to the central spindle, absence of furrow ingression and binucleation (reviewed in [49, 57, 67, 68]), confirming the functionality of the inhibitor.

Cells released from S phase in the presence of 100 nM BI-2536 showed delayed entry into mitosis (not shown) and eventually arrested in prometaphase (Chapter 2.1., Figure 4A, S7A). In these cells, G2 phase recruitment of Plk1 to the parasite occurred, and was increased 3-fold compared to control cells (Chapter 2.1., Figure 4B-D), but eventually ceased as cells reached prometaphase. Likewise, in prometaphase cells, treated with the kinase inhibitor RO-3306 (to induce anaphase) and Plk1 inhibitor, Plk1 accumulated on the parasite (Chapter 2.1., Figure 4D). The abundance of Plk1 on the schizont surface was markedly higher in G2 phase cells which were incubated for 15 h in the presence of Plk1 inhibitor, compared to Cdk1-inhibited cells, which were treated for a short time with Plk1 inhibitor. Similar observations were made in cells in which Plk1 was inhibited upon normal entry into anaphase. Also in this case, Plk1 accumulated at the parasite surface to a higher level than in untreated anaphase cells, but markedly lower than in Plk1-inhibited G2 cells (not shown).

These data suggest that the accumulation of Plk1 on the parasite correlates with the duration of Plk1 inhibitor treatment. As Plk1 regulates the G2/M transition [73, 74] as well as the cytokinetic phase [89, 183, 184], this could be explained by a persisting priming activity for Plk1 binding, allowed by the slow progression through, or arrest of, the cell cycle. Firstly, Plk1 could have time to accumulate on the parasite due to delayed Cdk1 activation during G2/M in Plk1-inhibited cells. Although the priming activity is maintained during prolonged G2 phase, the eventual entry into mitosis with augmenting Cdk1 activity indirectly counteracts Plk1 recruitment. As Cdk1 is inactivated at the metaphase-anaphase transition, a Cdk1-dependent phosphatase activity could decline strongly and/or a priming kinase activity could become reinstated. Secondly, it could be assumed that a Plk1-dependent process of late cytokinesis promotes the downregulation of a priming kinase activity for parasite-binding of Plk1. Little is known about the regulation of late cytokinesis and the precise role of M phase kinases during this period. However, when Plk1 was inhibited at a time point that still allowed furrow ingression, Plk1 activity was still found to be required for the completion of cytokinesis [89]. This observation is supported by studies on the MT bundling protein Cep55, a binding partner and substrate of Plk1, that potentially requires Plk1-dependent phosphorylation for cytokinetic abscission [183, 185]. Cep55 binds Mklp1 and is found at the midbody during anaphase, where it provides a binding platform for the ESCRT complex which is involved in cytokinetic abscission (reviewed in [47]). Another late interaction partner of Plk1 is the protein Nir2, which locates to the cleavage furrow and midbody and requires phosphorylation-primed docking of Plk1 for successful cytokinesis [184].

Further evidence for the requirement of Plk1 in timing cytokinesis comes from the interesting role of Plk1 in activating the mitotic phosphatase Cdc14A. The dual specificity phosphatases Cdc14A and B are regulators of late M phase (reviewed in [53, 174]). Budding yeast Cdc14 is activated at the onset of

anaphase by the protease separase [186], which is involved in sister-chromatid separation by cohesin cleavage. Mammalian Cdc14B locates to the central spindle and midbody where it is involved in the stabilization and bundling of MTs [187]. Cdc14A, in turn, is involved in the inhibition of Cdc25C [188], and consequently Cdk1, and is also found on the midbody where it is, at least in budding yeast, required for mitotic exit [189, 190]. Importantly, mammalian Plk1 has been shown to phosphorylate and thereby activate Cdc14A activity in vitro and in vivo [182, 191]. It could thus be that, during its association with the parasite in anaphase, Plk1 locally upregulates Cdc14A activity on the schizont surface. Cdc14A, in turn, could be counteracting the priming phosphorylation for Plk1 binding. This would result in a self-regulatory mechanism of Plk1 binding on the parasite, in that Plk1 would trigger its own dissociation during telophase.

During anaphase, Cdc14A dephosphorylates and activates the the anaphase-promoting complex (APC) regulator Cdh1, and leads to APC-Cdh1-dependent ubiquitylation of late M phase factors and their proteasomal degradation [192]. One of these APC-Cdh1 targets is Plk1 itself [72, 193], and it is believed that proteasomal degradation of Plk1 is one of the mechanisms to shut down Plk1 activity at the exit from M phase. But how can Plk1 activity required for cytokinesis be safeguarded while Plk1 degradation is proceeding during telophase? Firstly, midbody-localized Plk1 appears to be less affected by proteasomal degradation compared to the cytosolic pool. Secondly, the binding mode of Plk1 at the midbody is stabilized by a positive feedback-loop. Whereas early mitotic binding of Plk1 is not regulated by self-priming, Plk1 generates its own docking sites from anaphase onwards. The recruitment of Plk1 thus provides new docking sites for further Plk1 molecules, thereby creating a positive feed-back loop, which leads to a very stable, self-regulated accumulation of Plk1 (discussed in [194, 195]). Such an autonomous regulation of binding also has its down-side, however, in particular if Plk1 activity should be maintained but specific substrate interactions abrogated. Such a scenario applies to the early Plk1 interaction partner PBIP1, which anchors Plk1 at the centromeres during late G2 phase. To allow Plk1 recruitment to other binding partners, PBIP is proteasomally degraded during prometaphase [76], and it is believed that this is the only mechanism to effectively disrupt a self-primed interaction of Plk1 [194, 195]. Furthermore, Plk1 activity during late G2 phase is low compared to mitosis. The mechanism of self-priming could be particularly useful under such conditions, when Plk1 not yet fully activated or is less abundant.

Thus, a self-primed binding of Plk1 is therefore unlikely to occur at the parasite surface, since its dissociation at the G2/M transition would be difficult to explain, unless the parasite would recruit PBIP for Plk1 binding. However, this is unlikely, as it would presumably affect PBIP function during late G2 phase. Furthermore, as Plk1 activity and protein level decrease during late M phase, it is vital to maintain Plk1 activity at the midbody. A massive recruitment of Plk1 to the parasite during that time would very likely interfere with Plk1 function during cytokinesis. The dissociation of Plk1 from the parasite during telophase therefore requires a less stable interaction than is usually the case for Plk1 self-priming. Apart from the downregulation of non-self-priming kinase activity and the activation of a phosphatase, one could imagine that a maybe more dynamically associated pool of Plk1 at the parasite would be more susceptible for

proteasomal degradation, compared to midbody-localized Plk1. However, general Plk1 levels do not seem to be decreased at times, when it dissociates from the parasite (Chapter 2.1., Figure 2). Also, Plk1 degradation is believed to occur late and at relatively low rates during exit from M phase, as it is sstill required for cytokinesis [193].

If Plk1 does not prime its binding to the schizont, which kinase does? Another important family of mitotic Ser/Thr kinases are Aurora kinases. In mammalian cells, three paralogues, Aurora A, B and C, regulate important aspects of the cell cycle and show distinct localizations and functions. During mitosis, Aurora B plays a dominant role, regulating processes such as chromosome condensation and cohesion, chromatin-directed spindle assembly, the spindle assembly checkpoint, kinetochore biorientation, and cytokinesis (reviewed in [39, 55, 196]). Aurora B is the catalytic subunit of the chromosomal passenger complex (CPC), which it forms together with the proteins INCENP, Survivin and Borealin [197, 198]. At the onset of anaphase, Aurora B translocates with the CPC from the centromeres to the central spindle and to the region of cortical contraction. The localization of Aurora B reflects its functions during late M phase, as depletion of the kinase prevents central spindle formation and cleavage furrow induction [197-199]. The midzone localization of the CPC is maintained by Mklp2 at anaphase onset [148].

Considering it‘s involvement in central spindle formation and cytokinesis, it was tested if Aurora B acts as a priming kinase for Plk1 recruitment to the parasite surface during anaphase. To test this, parasitized cells were synchronized in metaphase, released in the presence or absence of the Aurora B inhibitor ZM447439 [200, 201], and microscopically analyzed for Plk1 recruitment to the parasite (Figure 6). Cells released in the absence of inhibitor reached anaphase after 20 min, marked by abundant Plk1 labeling of the parasite. Aurora B-inhibited cells, in turn, showed weaker Plk1 recruitment that was delayed by 10-20 min, but occurred upon anaphase onset. Indicative of full Aurora B inhibition, cells lacked central spindle formation, spindle elongation as well as the formation of a cleavage furrow (not shown). Many control cells reached telophase between 30 and 60 min of release and consequently lost Plk1 staining at the parasite surface. M phase exit failed in Aurora B-inhibited cells due to the lack of cytokinesis, but Plk1 levels at the parasite surface eventually ceased.

More and more evidence suggests that Aurora kinases phosphorylate Plk1 on Thr210 and thus maintain the enzyme in its active conformation (reviewed in [182]). Aurora A-Bora is responsible for Plk1 activation at the G2/M transition in vertebrate cells [70, 71]. During early mitosis, Bora is proteasomally degraded, which eliminates Aurora A-dependent phosphorylation of Plk1 [71, 202]. However, in the absence of Aurora A and Bora, Plk1 activation is delayed but still occurs [71]. The Aurora A and B paralogues share very high sequence identity and a single amino acid residue change transforms Aurora A into a functional Aurora B [203]. It was therefore proposed that Aurora B might also be involved in promoting Plk1 activity [71, 182]. It is conceivable that inhibition of Aurora B could affect Plk1 Thr210 phosphorylation and thus eliminate Plk1‘s active conformation [162], which could affect the Plk1 docking to the parasite. It is unlikely that reduced Plk1 levels at the parasite are caused by incomplete inhibition of a Aurora B priming activity for Plk1, however, as other Aurora B-mediated processes were fully blocked.

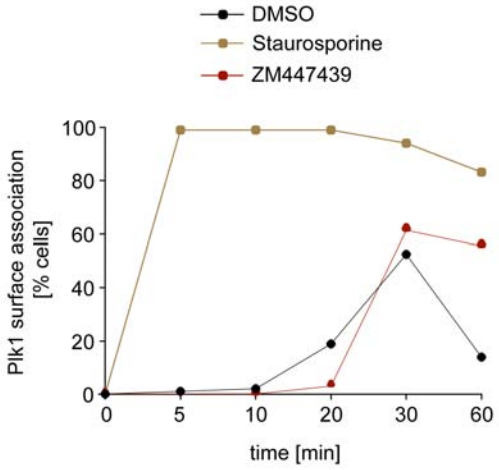

Figure 6. Aurora B inhibition and Staurosporine treatment in cells entering anaphase counteracts Plk1 dissociation from the schizont surface.
TaC12 cells were synchronized in prometaphase by treatment with 0.1 µg/ml nocodazole for 16 h, washed and incubated in the presence of 20 µM MG132 for 2h. The Metaphase-synchronized cells were then washed and released in the presence of control solvent (DMSO), 1 µM Staurosporine or 10 µM Aurora B inhibitor ZM447439. Cells were fixed at the indicated time points and Plk1 recruitment to the parasite surface was monitored and quantified by IFA.

Aurora B inhibition in these cells did not abrogate Plk1 recruitment to the schizont, the broad-scale kinase inhibitor staurosporine was used under identical conditions. Staurosporine is known to block a wide panel of kinases, including Cdk's, and consequently arrests cells at the G1/S- and G2/M-transitions [204, 205]. Furthermore, staurosporine induces premature mitotic exit due to Cdk1 inhibition [206, 207]. Indeed, parasitized cells, treated with staurosporine upon release from metaphase arrest, showed immediate mitotic exit, as cells underwent early anaphase and chromatin decondensation (not shown). Staurosporine treatment prevented the formation of central spindles and cleavage furrow formation, most likely due to inhibition of Aurora B. Under these conditions, Plk1 was recruited to the parasite in all observed cells within 5 min (Figure 6). These cells showed a marked increase in Plk1 at the parasite surface over time, persisting throughout the observation period and the timing and strength of Plk1 recruitment were comparable to conditions, in which cells were released into anaphase in the presence of the Plk1 inhibitor BI-2536 (Chapter 2.1., Figure 4).

Together, the results show that the priming for Plk1 binding is not provided by kinases effectively inhibited by staurosporine, including Plk1 and Aurora B. They support the observation that Plk1 recruitment to the parasite surface is linked to the inactivation of Cdk1 and the onset of anaphase.

Staurosporine is an ATP-competitive inhibitor and despite its broad spectrum of inhibited kinases, it targets only a subset of Ser/Thr-kinases, due to the divergence of catalytic sites of these enzymes [204]. A priming activity by another Ser/Thr kinase can therefore not be ruled out. But which kinase(s) - not targeted by Staurosporine and active during G2 phase as well as late M phase - could provide a Plk1 docking site on the parasite surface?

Interesting candidates for this job are the casein kinases, specifically casein kinase 2 (CK2). The Ser/Thr kinase CK2 has pleiotropic functions and is constitutively active as its catalytic subunits (α,α') are in their processive conformation without the requirement of activating phosphorylations (reviewed in [208, 209]). Lacking post-translational regulation, its persisting kinase activity is kept in check by controlled expression and upregulation of the CK2 protein level has been linked to tumorigenesis through abnormal

pro-survival and anti-apoptotic effects (reviewed in [210]). Interestingly, disregulated expression of CK2 and c-myc have been shown to be sufficient to induce the transformation of lymphocytes and the development of leukemia in transgenic mice [211]. CK2 was also linked to host cell transformation by *Theileria* schizonts, and protein levels of the kinase were found to be upregulated in *T. annulata*-infected cells [212]. Due to a simple consensus motifs for CK2 phosphorylation and for phospho-primed Plk1 docking [213], CK2 could potentially generate a PBD binding site [66]. Furthermore, CK2 displays only a low sensitivity to staurosporine [204]. It is thus possible that CK2 might act as a priming kinase for Plk1 binding on the parasite surface. The availability of a number of CK2 inhibitors (reviewed in [214, 215]) opens possibilities to test if the kinase is required for Plk1 recruitment. This assumption is attractive, as the parasite-induced upregulation of a single host cell kinase would promote several processes that are important for the schizont stage, including a contribution to host cell transformation as well as Plk1-dependent central spindle association.

Besides the requirement of host cell factors for the regulation of the parasite-Plk1 interaction, one could imagine the parasite to actively induce Plk1 docking and central spindle recruitment. However, a direct contribution of the schizont is unlikely for the following reasons: Firstly, no parasite kinases or phosphatases are predicted to be secreted by the schizont or expressed on its surface [12]. The schizont is therefore assumed to achieve host cell transformation through the binding and activation of host cell kinases at its surface, bypassing an interference via secreted enzymes. This is also reflected by the recruitment, and possibly surface-associated activation, of IκB kinases to the schizont [21]. Secondly, the dynamic recruitment of Plk1 is obviously tightly linked to host cell cycle transitions and thus likely to be exclusively timed by host cell regulatory mechanisms. The non-self-priming mechanism of Plk1 binding on the parasite and the lack of Plk1 recruitment during prometaphase and metaphase point towards a strategy of minimal interference with host cell processes (see above), as they might prevent sequestration of Plk1 away from its native substrates.

To further compensate adverse effects of Plk1 recruitment by the schizont, the Plk1 expression level could be upregulated in *Theileria*-parasitized cells. Plk1 is known to be overexpressed in many tumors, including lymphomas, carcinomas and melanomas (reviewed in [65]). Interestingly, the role of Plk1 as an oncoprotein seems to be based only on transcriptional deregulation, as no Plk1 mutations, that promote activity of the kinase, have been found in human tumor cells lines [216]. Transcription of mammalian *PLK1* is stimulated by forkhead (FKH) and MYB transcription factors and peaks during G2/M phase, whereas during G1 phase, *PLK1* is repressed by p53, p21 and the Rb-E2F pathway (reviewed in [57]). Furthermore, Plk1 feeds back on its own expression by activating the FKH transcription factors. Nothing is known on the activity of FKH or MYB transcription factors in *Theileria*-parasitized cells. However, p53 has been recently reported to be sequestered by the schizont surface, preventing it from translocating to the nucleus and inducing apoptosis [217]. It would be worthwhile investigating if Plk1 expression levels differ between parasitized cells and unparasitized cells, cured with the theilericidal drug Buparvaquone. Upregulation of *PLK1* transcription could either be a side effect of host cell transformation or more directly

targeted by the schizont. In both cases, it would be beneficial for the maintenance of parasitemia, as an elevated Plk1 level would directly promote proliferation and help to neutralize potential Plk1 scavenging by the parasite.

Cytokinetic abscission

Cytokinetic abscission occurs at the intercellular bridge adjacent to a dense structure termed ‚midbody', and physically divides the daughter cells after exit from mitosis. Detailed knowledge on how this process occurs is just about to emerge, and three models for the abscission mechanism were proposed (reviewed in [47]). The ‚rupture model' assumes mechanical traction forces to sever the intercellular bridge at a stage of maximal membrane constriction, followed by cellular wound healing. However, conditions under which cells are able to generate high traction forces are not always met, such as in non-motile cells or certain tissues, but cytokinesis nevertheless occurs. The two other models propose a more controlled mechanism of membrane fusion that leads to abscission, independent of strong physical forces. The intercellular channel could thus be either be filled with Golgi- and endocytosis-derived vesicles that are transported along central spindle MTs to the midbody, or the intercellular bridge could constrict and abscission could occur by hemifusion or fission. There is evidence for both of the latter models. Firstly, membrane docking factors such as v- and t-SNARES are being targeted to the midbody [218, 219] and cytokinetic abscission in some cell types can be inhibited by the Golgi-disrupting drug brefeldin A [218, 220]. Vesicles found at the intercellular bridge prior to abscission are also likely to originate from endocytosis [221] and recycling endosomes [222]. Secondly, late stages of cytokinesis display constriction zones adjacent to the midbody [223] and a CEP55-dependent delivery of the endosomal sorting complex required for transport (ESCRT) to the midbody is essential for abscission [224-227]. ESCRT was shown to recruit the MT-severing protein spastin, and is believed to form spiral filaments, which induce membrane curvature and thereby promote membrane fusion or fission [228-231].

Further requirements have to be met for cytokinetic abscission: (i) MT bundles, actin filaments and cellular organelles have to be removed from the site of abscission [47, 232, 233] (ii) the membrane at the midbody has to be polarized into specialized domains, enriched of $PI(4,5)P_2$ and phosphatidyl-ethanolamine (PE) (iii) and the cleavage furrow has to be stably anchored to MTs of the intercellular bridge. The latter is likely mediated by anillin [234, 235], which is delivered to the midbody by the centralspindlin complex [236].

Considering these processes that lead to the physical separation of daughter cells, it is startling how *Theileria*-parasitized cells manage to abscise flawlessly. Although binucleation is observed in cultures of parasitized cells, it is not more frequent than in unparasitized transformed cancer cell lines such as, for example, COS-7. Unfortunately, nothing is known on the abscission of *Theileria* schizonts and it can be assumed that most of the processes described above apply only to the host cell. However, since central spindle MTs play a fundamental role in cytokinetic abscission - through CEP55-ESCRT or anillin-recruitment, furrow stabilization and the delivery of vesicles required for abscission - it seems plausible

that an association of the central spindle with the parasite surface would strictly be required to allow termination of cytokinesis. Besides a positional effect of parasite-central spindle association, the actual relevance might thus lie in limiting the interference with host cell abscission. A very important experiment would therefore be to test if in cells, in which Plk1 is inhibited and thus the parasite-central spindle association disrupted, cytokinetic abscission can occur. Although the potent inhibitor BI-2536 was used for most experiments in this study, it is not suitable for this approach, as its inhibitory effect is irreversible, whereas Plk1 inhibitors such as BTO-1 [159] or TAL [89] can be readily washed out.

Furthermore, it should be verified if the timing of cytokinetic abscission in *Theileria*-infected cells differs from unparasitized cells. Recently, an Aurora B-mediated abscission checkpoint, was discovered in mammalian cells, which is located at the midbody and triggered in the presence of thin chromatin bridges between daughter cells, derived from chromosome segregation errors [232, 237]. As this checkpoint becomes activated during late telophase, at a time when the nuclear envelope has been reformed, it is possible that the presence of the parasite membrane in the intercellular bridge could as well induce a checkpoint arrest. As this chromosome segregation checkpoint depends on prolonged Aurora B activity, a comparison of the timing of abscission in parasitized and unparasitized telophase cells, in the presence or absence of the Aurora B inhibitor ZM447439 [200, 201], could indicate the presence of such a mechanism in *Theileria*-infected cells.

It would also be worth investigating whether host cell components actively constrict the parasite during late telophase, or whether the schizont itself mediates its membrane ingression. A likely candidate molecule is dynamin, a GTPase that is required for membrane scission in endocytotic and Golgi vesicle trafficking, as well as for cytokinesis (reviewed in [238]). Dynamin inhibitors such as dynasore [239] provide tools to test for host cell-mediated constriction of the parasite during late telophase.

The timing of parasite DNA replication

With the formation of central spindles at the parasite surface during anaphase, a potential role for the recruitment of Plk1 to the schizont is proposed. However, what is the biological significance of the parasite-Plk1 interaction during G2? On the one hand, it could be a mere consequence of the mechanism by which Plk1 is directed to the schizont. Assuming a constitutive priming activity is present, that is counteracted during prometaphase and metaphase by phosphatases or an inhibitory kinase, Plk1 could bind the parasite surface as soon as it obtains its active conformation in late G2. This early recruitment could lack any significance but just reflect conditions for Plk1 binding that are met in G2 phase as well as during anaphase. Plk1 docking to its early host cell interaction partner PBIP1 is provided by self-priming in a stabilizing positive feedback loop **[76]**, and might therefore not be affected by sequestration of Plk1 to the schizont. On the other hand, the recruitment of Plk1 to the schizont during G2 phase might well be of functional significance for the parasite.

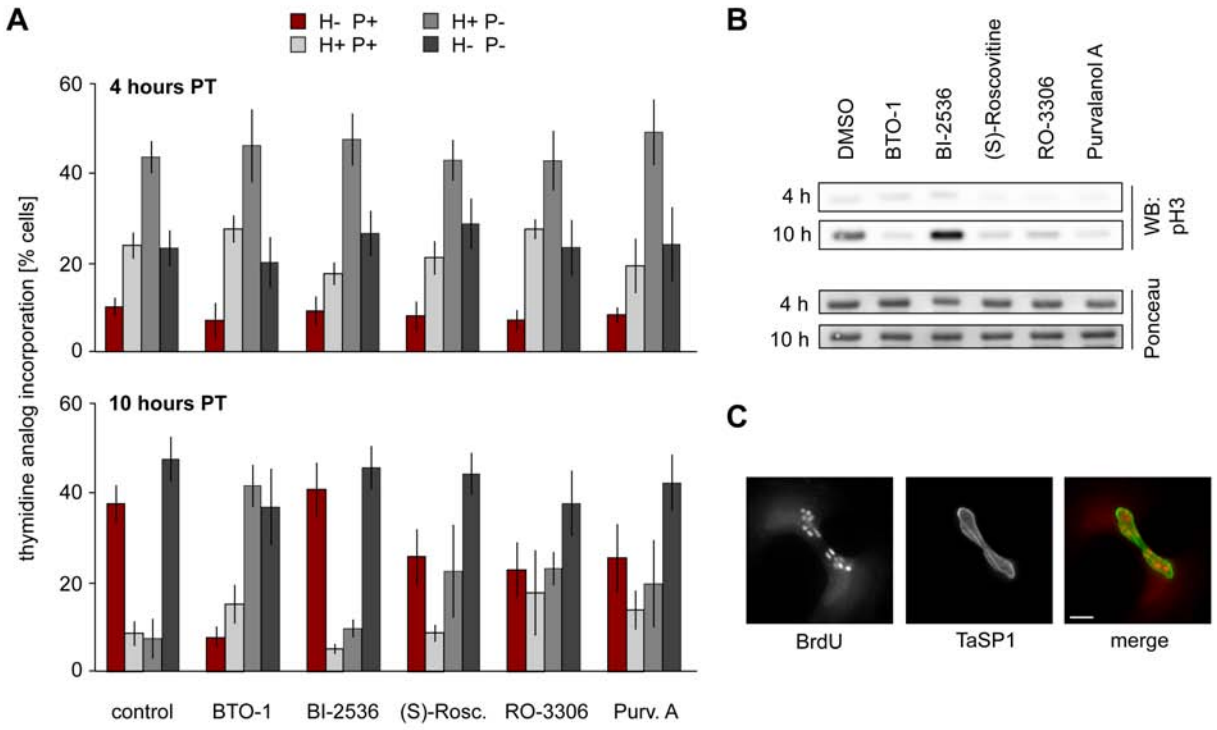

Figure 7. Parasite replication occurs during host cell M phase and is not affected by inhibition of host Plk1. (A) *T. annulata* parasitized cells (TaC12) were synchronized host cell S phase by treatment with 4 mM thymidine for 24 hours and released in the presence of either solvent (DMSO), the Plk1 inhibitors BTO-1 (20 µM) and BI-2536 (100 nM) or the Cdk1 inhibitors (S)-Roscovitine (50 µM), RO-3306 (10 µM) and Purvalanol A (10 µM) for the indicated time points. Cells were incubated with 10 µM of the nucleoside analogue 5-ethynyl-2´-deoxyuridine (EdU) 2 hours prior harvesting and probed for its incorporation into host cell or parasite DNA as indicator for replicational activity. Cells were analyzed and quantified for EdU incorporation by IFA. n=200 cells/sample; error bars indicate standard deviation. H-/+, host cell negative/positive for EdU incorporation; P-/+, parasite negative/positive for EdU incorporation. PT, post thymidine block. (B) At the indicated time points, cells described in (A) were used to prepare whole cell lysate and analyzed by western blot for the presence of histone H3 phosphorylation on Ser10. Histone protein levels were monitored by ponceau staining. (C) A dividing host cell harboring a parasite undergoing DNA replication. Nocodazole-blocked TaC12 cells were treated with the nucleoside analogue 5-bromo-2-deoxyuridine (BrdU) and analyzed by IFM during release from nocodazole arrest. Cells were stained with antibodies against BrdU and TaSP1; scale bar represents 5 µm; picture by

Replication of the *Theileria parva* schizont was reported to occur during early host cell mitosis [240]. It has not yet been shown if this also applies or *T. annulata*-infected cells. Furthermore, as Plk1 promotes the host cell G2/M transition [69, 74, 160, 161], its recruitment to the parasite during G2 phase could provide a timing cue for the initiation of schizont DNA replication. To test this assumption, *T. annulata*-parasitized cells were synchronized in host cell S phase and released to progress into mitosis. Before harvesting, cells were treated with thymidine analogs [241] to monitor their incorporation into host cell and parasite DNA, indicative of replicational activity. The released cells terminated DNA-replication and entered mitosis, marked by histone H3 phsophorylation (Figure 7A, B). Parasites, in turn, started DNA replication by the time host cells entered G2/M phase. Similar results were obtained for host cells arrested in prometaphase by nocodazole treatment; in these cells, only parasites, incorporated thymidine analogs (not shown, result by Gongda Xue). Furthermore, cells released from prometaphase arrest displayed parasite DNA replication during host cell progression through M phase (Figure 7C).

Interestingly, when host cells were released form S phase in the presence of the Plk1 inhibitor BTO-1 [159], parasite DNA replication did not occur, indicating a possible involvement of Plk1 activity in triggering parasite S phase. However, the continued presence of host cells incorporating thymidine analogues over the whole observation period, as well as the absence of Ser10 histone H3 phosphorylation indicated an off-target effect of BTO-1 on host cell S phase progression (Figure 7A, B). This effect shows that preventing the onset of host cell G2/M phase affects the initiation of parasite DNA replication. However, it does not allow to conclude on a role for Plk1 in triggering parasite replication. Treatment with the unrelated Plk1 inhibitor BI-2536 [91, 92], in turn, did not affect the initiation of parasite S phase.

Plk1 inhibition delays Cdk1 activation and thus G2/M transition and cells subsequently arrest in early mitosis due to spindle collapse (reviewed in [49, 57, 68]). BI-2536 treatment led to the expected prometaphase arrest of host cells, marked by accumulating histone phosphorylation, which confirms Plk1 inhibition. As in these cells parasite DNA replication occurred, Plk1 but not Cdk1 catalytic activity can be ruled out as a trigger during G2/M transition. Release of parasitized cells form host cell S phase arrest in the presence of chemical Cdk1 inhibitors did prevent mitotic entry, as histone phosphorylation was mostly absent, and the occurrence of parasite S phase was reduced by about 40% compared to control cells (Figure 7A, B). It is not clear from these results, if residual Cdk1 activity is permissive for parasite DNA replication, or if off-target effects on *Theileria* Cdk's led to this observation. One possibility could be that a factor upstream of Cdk1 contributes to the timing of parasite S phase.

It should be further tested if prevention of the G2/M transition, for example by induction of the G2 DNA damage checkpoint, would affect parasite S phase. The drug doxorubicin chemically induces DNA damage and thereby leads to G2 phase arrest in cells released from S phase synchronization; caffeine, in turn, can be used to override the G2 checkpoint [71]. These tools would allow to investigate how tightly parasite DNA replication is linked to the onset of host cell mitosis.

Taken together, the results presented in this section demonstrate a link between the timing of host cell G2/M phase and *T. annulata* S phase. Although Plk1 is recruited to the schizont surface during G2 phase, its catalytic activity is dispensable for the initiation of parasite DNA replication.

The schizont-expressed GPI-anchored protein gp34

In parallel to the efforts towards unraveling the significance of Plk1 recruitment to the schizont surface, we examined gp34, a GPI-anchored schizont protein that could function as a potential Plk1 binding partner. Gp34 containings a signal peptide (SP) and a GPI anchor signal sequence (GSS), and was found to be conserved in both *T. annulata* and *T. parva* (detailed results are given in chapter 2.2.). The proteins, have a molecular weight of 34 kDa and share 63% identity and 81% similarity at the amino acid level and can thus be considered to be orthologs (Chapter 2.2., Figure 1). *T. parva* gp34 was experimentally characterized as a GPI-anchored protein, expressed at the schizont surface facing the

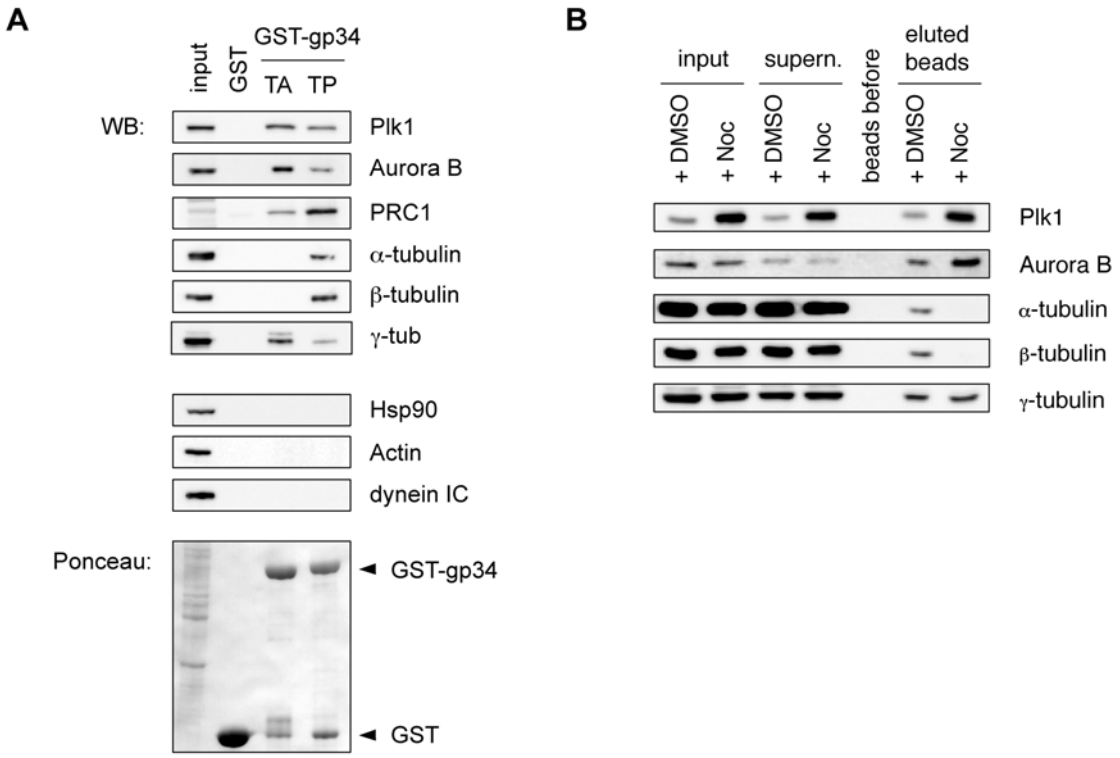

Figure 8. Gp34 brings down host cell central spindle components in GST pull-down assays. (A) Glutathione S-transferase (GST) or GST-fused gp34 from *T. annulata* (TA) and *T. parva* (TP) were subjected to pull-down assays using lysates of Jurkat T cells released from nocodazole arrest (input). Samples were subjected to western blot (WB) analysis; dynein IC, dynein intermediate chain. (B) GST pull-downs were performed in the presence of 3.0 µg/ml nocodazole (NOC) and lysates from nocodazole-synchronized Jurkat T cells (input). DMSO was used as control solvent; supern., supernatant.

host cell cytosol (Chapter 2.2., Figure 2). Ectopic expression of GFP- and epitope-tagged versions of mature *T. parva* gp34 (Tp-gp34), lacking the SP and GSS, led to cytoplasmic localization of the protein in parasitized as well as unparasitized cells. Interestingly, during anaphase, overexpressed TP-gp34 was recruited to the middle region of the central spindle and remained on the midbody during telophase until cytokinetic abscission occurred (Chapter 2.2., Figure 3). Endogenous Tp-gp34 was also found to accumulate at the midbody in *T. parva*-infected T cells, and such an accumulation could not be detected for other molecules such as the surface protein PIM. Surprisingly, overexpressed as well as endogenous Ta-gp34 failed to locate to the central spindle or midbody. However, gp34 from both species induced cytokinetic defects, as cells, overexpressing these proteins, became binucleated, failing either cleavage furrow ingression or cytokinetic abscission (Chapter 2.2., Figure 5A, B, suppl. data). These defects might be provoked by the high levels of cytoplasmically expressed gp34 and indicate a role for the protein in parasite cell division.

When subjected to GST pull-downs using lysates of mitotic mammalian cells, Ta- and Tp-gp34 brought down proteins that locate to the central spindle and midbody, including Plk1, Aurora B, PRC1 and γ-tubulin (Figure 8A). Other proteins, such as Hsp90, actin or dynein, could not be detected in pull-down eluates. The subunits of tubulin dimers, α- and β-tubulin, were only brought down by Tp-gp34. To

determine if Plk1 and Aurora B where brought down in Tp-gp34 pull-downs via MTs, cells were cultivated and assays performed in the presence of the MT-disrupting drug nocodazole (Figure 8B). Drug-treated samples lacked the presence of α- and β-tubulin, indicating an interaction of Tp-gp34 with polymerized tubulin, whereas Plk1, Aurora B and γ-tubulin could be still detected.

The absence of α- and β-tubulin in Ta-gp34 pull-downs is in agreement with the absence of Ta-gp34 from the central spindle and midbody, as determined by IFM. The fact that Plk1 and Aurora B are still present in Ta-gp34 and nocodazole-treated Tp-gp34 pull-down samples, indicates that these proteins might interact with gp34 via a common binding partner, most likely independent of MTs. The kinesin Mklp2 has been shown to interact with both, Plk1 and Aurora B, during anaphase and telophase [148]. It should be verified, if Mklp2 is present in GST pull-downs of gp34; commercial MKlp2 antibodies tested so far, failed to generate a reliable signal. Aurora B constitutes the catalytic subunit of the chromosomal passenger complex, but the other subunits of this complex, including borealin, survivin or INCENP, could not be detected in gp34 pull-downs. Also, Aurora B is not recruited to the parasite surface in *T. annulata* and *T. parva*-infected cells. It is therefore unclear how Aurora B associates with gp34 and if other Aurora B-containing protein complexes might be involved. Likewise, Plk1 is a stoichiometric binding partner of the MT bundling protein PRC1 on central spindles [77] and it could be assumed that both should be present at the parasite surface. However, although Plk1 is prominently recruited by both *T. annulata* and *T. parva* schizonts during anaphase, PRC1 is also not found at the parasite surface.

How can one explain the cytokinetic defects provoked by both orthologues of gp34, if only Tp-gp34 localizes to the midbody? In dividing cells, ectopically expressing Tp-gp34, Aurora B or Plk1 binding to the midbody is not affected, which indicates that the protein does not interfere with these kinases for their midbody recruitment. It could be that gp34 orthologues interact with a yet unidentified cytokinetic factor. To identify a direct interaction partner of gp34, Ta-gp34 was permanently expressed in mammalian cells and subjected to mass spectronomy analysis (results by Kerry Woods, not shown). This assay revealed the protein ELKS to be brought down by gp34, whereas all other components detected in GST pull-downs could bot be confirmed. The possible link between ELKS and gp34 was subsequently shown in co-immunoprecipitations and pull-down assays (results by Kerry Woods, not shown). A potential interaction with ELKS is particularly interesting, since ELKS was shown to associate with MT-associated protein CLASP [242]. CLASP1, is known to interact with PRC1 at the central spindle [149] and depletion of CLASP1 provokes central spindle instability and cytokinetic defects in frogs and flies [156, 158]. Endogenous gp34 could thus sequester ELKS, and with it CLASP1, thereby promoting the formation and stability of central spindle MTs at the parasite surface. It will be interesting to see, if ELKS and CLASP can be detected at the parasite during host cell anaphase and telophase.

Although nothing is known about a requirement of ELKS for cell division, it can be assumed that overexpression of gp34 might impair the function of ELKS and thus of CLASP1, which could explain the impaired cleavage furrow ingression and defective cytokinetic abscission. However, central spindle

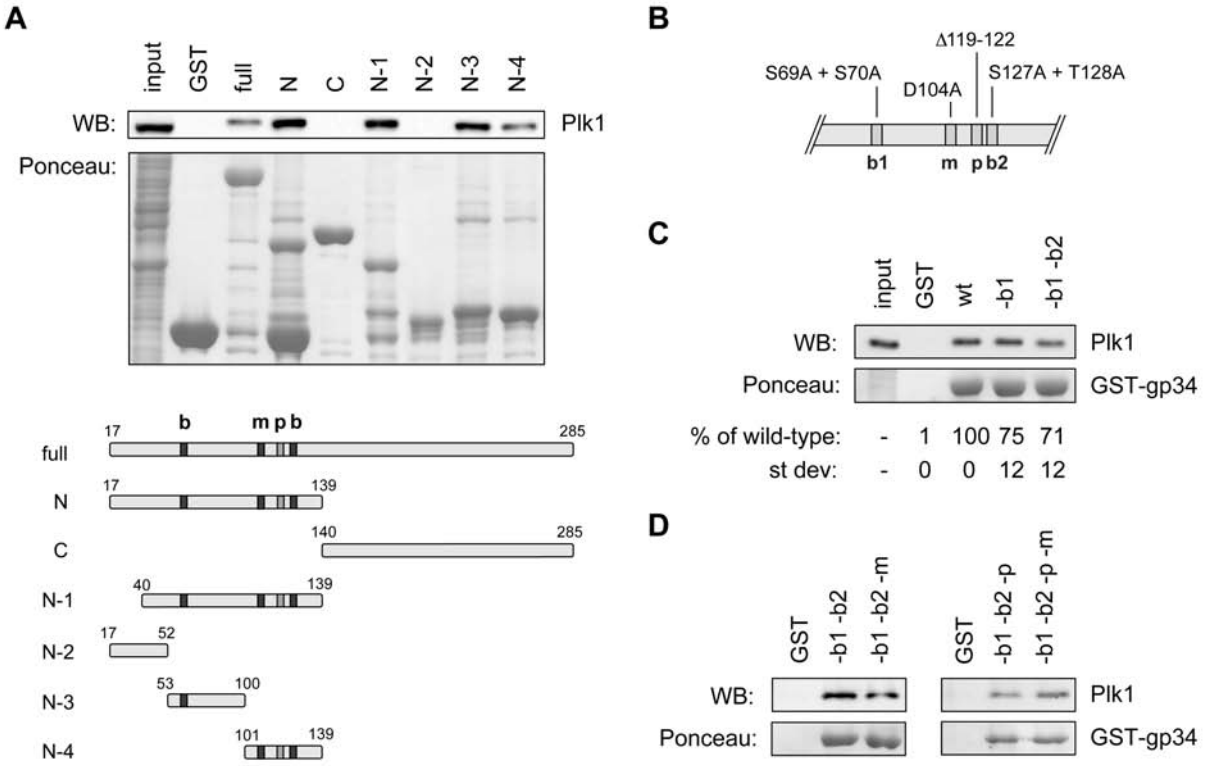

Figure 9. Analysis of the interaction of Tp-gp34 mutants with Plk1. (A) Glutathione S-transferase (GST), GST-fused full-length Tp-gp34 or truncation mutants were subjected to pull-down assays using lysates of Jurkat T cells (input). Samples were subjected to western blot (WB) analysis; N/C, N/C-terminal half; N-1 to N-4, fragments of the N-terminal half; b, PBD binding site; m, mimicking site for PBD binding; p, Plk1 phosphorylation site; numbers indicate amino acid positions. (B) Scheme of Plk1 motifs in Tp-gp34; b1/2, PBD binding sites; m, mimicking site for PBD binding; p, Plk1 phosphorylation site; amino acid substitutions and deletion are indicated. (C) GST pull-downs of GST, wild-type Tp-gp34 (wt) or full-length mature protein lacking PBD binding sites (-b1, -b1-b2). Samples from three repetitions were analyzed by western blot (WB). Chemiluminescent signal strength of Plk1 probings is given relative to wild-type Tp-gp34. st dev; standard deviation. (D) GST pull-downs using full-length mature Tp-gp34 lacking PBD binding sites, the mimicking site for PBD binding and the Plk1 phosphorylation site. b, PBD binding site; m, mimicking site for PBD binding; p, Plk1 phosphorylation site; samples were obtained and analyzed as in (C).

abnormalities were not observed in cells overexpressing gp34. More detailed studies on the interaction of gp34 with ELKS will tell if CLASP1 might play a role.

Gp34 is unlikely to be a direct interaction partner of Plk1

Amino acid sequence analysis of Ta- and Tp-gp34 (Chapter 2.2., Figure 1) showed that both proteins lack an Aurora B phosphorylation site, but contain at least one potential Plk1 polo-box domain (PBD) binding site of the type S-(S/T)-(P/X) [170] as well as a putative PBD binding mimicking site (S-D-P/X). Tp-gp34 furthermore possesses a Plk1 phosphorylation site that matches the consensus sequence X-D/E-X-S/T-ϕ-X [243] (ϕ being any hydrophobic amino acid). It was therefore assumed that gp34 could be an interaction partner for Plk1. In GST pull-downs, Plk1 was brought down by fragments of Tp-gp34

harboring the potential Plk1 binding sites (Figure 9A, B). However, mutagenesis of the predicted PBD binding sites in Tp-gp34 reduced Plk1 in pull-downs by only 25-30% (Figure 9C). Further elimination of a potential mimicking site for PBD binding and the Plk1 phosphorylation site did not affect Plk1 levels in pull-down eluates (Figure 9D). It is thus unlikely that Plk1 directly associates with gp34 via these sites, also, since the finding could not be reproduced in a variety of alternative assays. Co-immunoprecipitations of endogenous or overexpressed proteins, yeast-two-hybrid assays as well as co-fractionation assays of endogenous gp34 and Plk1 failed to confirm the interaction of both proteins (results by Pascal Hermann, not shown). Also, Plk1 was not found to convincingly co-localize with gp34 on the surface of schizonts. Overexpression or microinjection of recombinantly expressed gp34 did not affect Plk1 or PBD recruitment to the parasite surface; targeting of gp34 to the mitochondrial outer membrane via a C-terminal sequence element of the *Vaccinia* virus protein F1L [244] did not lead to mitochondrial recruitment of endogenous or ectopically expressed Plk1; and finally, inhibition of Plk1 prior to and during pull-down assays, using GST-fused Tp-gp34, did not increase the presence of Plk1 in eluates, whereas Plk1 accumulates on the parasite surface in the presence of Plk1 inhibitor, as observed by fluorescence microscopy (results not shown).

Nevertheless, deletion of the Plk1 phosphorylation site in Tp-gp34 prevented its recruitment to the midbody (Chapter 2.2., Figure 4B). Furthermore, constitutively active Plk1 (T210D) weakly phosphorylated Tp-gp34 in vitro, whereas Aurora B or Cdk1 did not (results not shown), and it remains to be tested if deletion or mutagenesis of the Plk1 phosphorylation site in Tp-gp34 affects Plk1-mediated phosphorylation. Thus, if gp34 does not directly interact with Plk1, how is it phosphorylated by the kinase, and is such a phosphorylation significant for Tp-gp34 function? Transfection experiments indicate that the binding of Plk1 to the schizont is mediated by its PBD and not the kinase domain (Chapter 2.1, Figure 5). However, the Plk1 kinase domain was brought down by gp34 in pull-down assays (not shown). This indicates that, at least in vitro, Plk1 can bind gp34 via its kinase domain. Alternatively, on could assume a third protein that interacts with gp34 and also binds the PBD. This would allow Plk1 to phosphorylate gp34 in a distributive manner. Although distributive phosphorylation has not yet been described for Plk1 (discussed in [67]), at least one PBD-binding protein, Cenexin1, does not appear to be phosphorylated by Plk1 [245], which points towards the existence of such a mechanism.

A Tp-gp34 mutant lacking the Plk1 phosphorylation site and hence any midbody recruitment, induced binucleation to the same extent as wild-type Tp-gp34 did (Chapter 2.2., Figure 5C). Also, Ta-gp34 does not contain a corresponding phosphorylation site and it is not recruited to the midbody but provokes cytokinetic defects upon overexpression. This indicates that the interference with host cell cytokinesis is not linked to central spindle/midbody recruitment. Whether failure of cytokinesis in the presence of gp34 indicates the interaction of gp34 with crucial cytokinetic factors, and whether this reflects a role for gp34 in the synchronous cytokinesis of parasite and host cell remains to be confirmed.

4. Conclusions

The work presented in this thesis reflects the dependency of the *Theileria annulata* schizont on host cell cycle events and illustrates the extent to which host-pathogen interactions have evolved. By inducing continuous proliferation and survival of the cells it infects (reviewed in [12]), *Theileria* creates itself a microenvironment that is beneficial for the main purpose of this life cycle stage: the schizont‘s clonal expansion. Only when efficiently replicated, chances increase for survival within the intermediate host and eventually the transmission onto the definitive host, the tick. *Theileria* thus faces the challenging task of persisting in the rapidly dividing bovine host cell. It is startling how the schizont manages to overcome the different hurdles. The parasite positions itself on the host cell mitotic spindle apparatus in a manner that ensures its distribution over the two daughter cells. The temporal and spatial synchronicity of host and parasite cell division leads to the distribution of the schizont over new daughter cells - at the pace and timing determined by the host cell cycle. It appears that the schizont has lost its capacities to actively divide at this stage of the life cycle, as schizont cytokinesis was never observed independent from that of the host cell. This is also reflected by the fact that *Theileria* lacks any conserved factors for cytokinesis, such as Aurora kinases, Plk1, RhoA GTPase and other. Also, *T. annulata* does not possess any kinases or phosphatases predicted to be secreted or expressed at the parasite surface [12]. How is schizont division then accomplished? The parasite very likely follows a strategy that does not include an active manipulation of host cell M phase processes. Considering the vast complexity of mammalian mitotic processes, it would make sense that the parasite co-opts established and highly conserved host cell mechanisms - as they are - by-passing a risky manipulation of host cell division using its own factors.

The results presented in this study are in agreement with this assumption. By recruiting the host cell kinase Plk1 during anaphase, the parasite favors, by an yet unidentified mechanism, the formation of the central spindle on its surface. At the same time, the schizont is bound to and positioned by astral MTs. Both astral and central spindle MTs provide the spatio-temporal information required for cleavage furrow formation. Furthermore, the central spindle MTs recruit the factors required for cytokinetic abscission during late stages of cell division. Thus, by associating with cytokinetic structures of the mitotic apparatus, the schizont precisely positions itself for cell division and does not alter the relative position or impede the normal function of these host cell structures. In essence, the schizont possibly blends into the processes host cell cytokinesis with minimal interference. This is particularly important as any interference with negative consequences could induce host cell apoptosis, and thus also elimination of the parasite. Furthermore, the distribution of the schizont over the forming daughter cells as such is crucial. If the schizont would only be delivered to one daughter cell at each host cell division, the number of parasitized cells would not increase. This would likely affect the chances of the parasite to persist in the host and to be efficiently delivered to feeding ticks. Thus, by linking its division to host cell cytokinesis, the parasite is equally distributed over the daughter cells and the distribution of the schizont ensures transformation of the newly formed cells and their effective clonal expansion.

Also, a dependency of schizont division on host cell cytokinesis helps to keep the parasite cell cycle in tune with that of the host cell. An alternative would be that the parasite decreased in size and increased in number - a strategy observed for large organelles such as the Golgi apparatus, which fragments upon cell division and make its distribution a stochastic event [246, 247]. However, an independent parasite cell division bears the risk of a parasite replication rate that exceeds the capacities of the host cell. Although this appears beneficial for the pathogen, it would eventually force the parasites to leave the shelter of the host cell, and be directly exposed to the host‘s immune system.

It was reported for *T. parva*, that parasite DNA replication is triggered during host cell G2/M phase [240]. Experiments presented in this study indicate that this also applies to *T. annulata* schizonts. This is particularly interesting, as, with the passing of the restriction point at the G0,G1/S transition, each host cell cycle is committed to completion - or deliberate cell death (reviewed in [248]). Furthermore, proteasomal degradation of cell cycle regulators, such as cyclins, makes the cell cycle unidirectional and irreversible (reviewed in [34]). The timing of schizont DNA replication and cytokinetic division to the beginning and end of host cell M phase could support the sequential occurrence of these parasite cell cycle phases. Furthermore, the identification the *Theileria* schizont kinase TaCRK3 [249], which has strong homology to eukaryotic Cdks, suggests the presence of a rudimentary cell cycle that could be ‚exogenously‘ timed by the host cell.

Taken together, the schizont stage of the *T. annulata* provokes host cell proliferation but apparently leaves the orchestration of its own cell division to the host cell. This makes sense, as in continuously dividing cells, growth rate is likely to be the limiting factor that influences the frequency of division (reviewed in [248]). Further support for the cross-talk of the parasite with the host cell division comes from the studies with the schizont surface protein gp34. *T. parva* gp34 localizes the midbody of dividing host cells, whereas overexpression of *T. annulata* or *T. parva* gp34 impairs cytokinesis. Although, at this stage, nothing more is known about the specific function of these proteins, their presence underpins the intricate relationship between host and parasite. Hopefully, this study will stimulate further investigations on this unique example of host-pathogen interactions.

5.1. The IKK Inhibitor BMS-345541 Affects Multiple Mitotic Cell Cycle Transitions

Hana Blazkova, Conrad von Schubert, Keith Mikule, Rebekka Schwab, Nico Angliker, Jacqueline Schmuckli-Maurer, Paula C. Fernandez, Stephen Doxsey, Dirk A. Dobbelaere

Cell Cycle (2007) vol. 6 (20) pp. 2531-40

The IκB kinase (IKK) complex is a conserved upstream regulator of the NF-κB signal transduction cascade. It consists of the Ser/Thr kinases IKK1 and IKK2 and the regulatory subunit NEMO (NF-κB essential modulator). The IKK complex phosphorylates inhibitor of κB (IκB) proteins, inducing their ubiquitylation and degradation, resulting in the release and nuclear translocation of the transcription factor NF-κB. The cascade is activated by a variety of stimuli, including cytokines such as tumor necrosis factor-α or interleukin-1, mitogens, ionizing radiation, toxic metals and pathogens. It is therefore not surprising that activation of NF-κB has been ascribed to a number of regulatory tasks such as inflammatory and immune responses, developmental processes as well as protection against apoptosis. In addition, IκB kinases have been shown to be involved in the regulation of cell proliferation of both normal and tumor cells [250-252]. For example, IKK1 activity directly promotes the G0/G1-S transition by regulating the expression of cyclin D1, its subcellular localization as well as its degradation [253-256]. The kinase also regulates hormone-induced expression of E2F1-responsive genes and thereby entry into S phase [257]. IKK1 has also been shown to modulate the phosphorylation and proteolysis of the FOXO3 transcription factor, which, similar to p53, is involved in stress-induced cell cycle arrest and the initiation of apoptosis .

The publication presented in this section demonstrates multiple effects of the allosteric IKK inhibitor BMS-345541 on the regulation of M phase and thereby expands the impact of IKK activity on proliferation. BMS-345541 treatment of cells synchronously approaching M phase provokes an arrest at the G2/M transition. This is reflected by low Cdk1 activity and persisting high levels of cyclins A and B1 as well as a total lack of histone H3 Ser10 phosphorylation. Also, these cells showed an absence of activating T-loop phosphorylation of the Aurora kinase family members. A BMS-345541-induced S phase arrest could be experimentally excluded.

Cells that were allowed to enter mitosis prior to BMS-345541 administration, showed precocious and premature anaphase upon drug treatment, marked by extensive DNA bridges between separating chromatids and a disorganized central spindle. Consequently, cytokinetic abscission failed resulting in an accumulation of bi-nucleated cells. Compared to control cells, mitotic cells treated with BMS-345541 showed an early degradation of cyclin B1 and securin, indicating an untimed activation of the anaphase-promoting complex (APC/C). Indeed, persisting nocodazole-induced spindle checkpoint activity was overridden by the additional treatment with BMS-345541, as observed by cyclin B1 degradation and histone H3 dephosphorylation. In vitro kinase assays for a panel of important mitotic Ser/Thr kinases indicate that these results are unlikely to be due to off-target effects of BMS-345541. The observed mitotic effects did not seem to be associated with NF-κB function, as transcriptional inhibition did not

affect M phase progression. The differential inhibitory effect of BMS-345542 towards IKK1 and IKK2 furthermore allowed the assumption that either both kinases or primarily IKK1 is involved in mitotic regulation.

Shortly before the acceptance of the study presented in this section, Prajapati et al. demonstrated a role for IKK1 in the regulation of M phase entry [258]. Similar to our observations, siRNA-mediated knock-down of IKK1 resulted in delayed mitotic entry and decreased T-loop phosphorylation of Aurora A on Thr288. The authors link the disturbed G2/M transition upon siIKK1-treatment with an IKK1-dependent activation of Aurora A at the centrosome. In centrosomal preparations, both enzymes where enriched in the same fractions as the centrosomal markers ninein and γ-tubulin, and Aurora A and IKK1 could be co-immunoprecipitated from centrosomal fractions. Furthermore, IKK1 was shown to phosphorylate Aurora A on Thr288 in vitro. The evidence that IκB kinase functions in the regulation of mitosis was further substantiated by the findings of Irelan et al., proposing a role for IKK2 in the regulation of bipolar spindle assembly [259]. According to their results, siRNA-mediated knock-down of IKK2 expression led to an accumulation of cells with 4N DNA content and delayed transition through M phase into G1 phase, which was due to the formation of disorganized multipolar mitotic spindles. Interestingly, the phenotype, reminiscent of Aurora A deregulation, is independent of NF-κB activity but reproduced by IKK1 or NEMO knock-down. In co-immunoprecipitation experiments, the authors consequently identify an interaction of the IKK complex with Aurora A and its regulator TPX2, timed by the opposing actions of importin α/β and Ran-GTP and demonstrate IKK2-dependent phosphorylation of Aurora A in vitro. IKK2-mediated phosphorylation is shown to allow binding of the ubiquitin ligase β-TRCP and the tagging of Aurora A for proteasomal degradation. The role of Aurora A in spindle formation is exerted through the activation of Eg5/KIF11, a kinesin-like protein required for the formation of bipolar spindles, and IKK2 depleted cells display increased activation of the motor protein. The effect of multipolar spindles in IKK2-depleted cells is antagonized by the chemical inhibition of Eg5 at low doses. The authors therefore conclude with the interpretation that IKK2-mediated phosphorylation of Aurora A leads to its proteasomal degradation and thus serves to provide appropriate levels of Aurora A activity to allow proper bipolar spindle formation and maintain spindle integrity.

Taken together, these studies provide first evidence of a potential intersection of IKK and mitotic events. However, the findings are partially conflicting. Prajapati et al. propose a role for the IKK complex, in particular IKK1, in the centrosomal activation of Aurora A. This is interesting in the light that Aurora A has been recently demonstrated to act as an activator of Plk1 [71], which, in turn, is known to promote mitotic entry. Also, both enzymes locate to the centrosomes during G2 phase and recruitment of active Thr210-phosphorylated Plk1 depends on the action of Aurora A. These findings are also reflected in our observation of an impaired G2/M transition in IKK-inhibited cells. Furthermore, our data suggest an involvement of IKK1, rather than IKK2, which again is in line with the observations by Prajapati and colleagues. The work of Irelan et al., on the other hand, clearly indicates an Aurora A-antagonizing role for IKK2, and to a lower extent, for the other complex members IKK1 and NEMO. We did not observe increased Aurora A phosphorylation upon IKK inhibition, but rather a lack of Aurora A, B and C activation

in cells that attempt G2/M transition. Also, the proposed role for IKK2-mediated spindle integrity was not observed by our group. At concentrations of BMS-345542 that block IKK2, cells progressed normally through M phase and the formation of multipolar spindles was not observed at these or higher concentrations of the IKK inhibitor. However, BMS-345542 treated mitotic cells showed disorganized metaphase plates. It remains unclear whether these are the result of defective chromosome disjunction that is observed after BMS-345542 treatment that also blocks IKK1. In addition, full Eg5 activity requires Cdk1-dependent phosphorylation which allows the association of this motor protein with MTs [260] up until metaphase. With the onset of anaphase, Eg5 localizes only in low amounts to MTs [260, 261] and it is assumed that other MAP's such as PRC1 play a more important role for spindle maintenance during that time. It thus seems unlikely that the BMS-345542-induced central spindle defects are related to the proposed indirect impact of IKK2 on Eg5 activity.

In summary, the body of work from our laboratory as well as the findings from other groups demonstrate another aspect in the broad spectrum of functions for the components of the NF-κB pathway. NF-κB signaling is known to be involved in tumorigenesis, however, its roles appear paradoxical and likely depends on the cellular context. For example, in many cancers, NF-κB is unchecked by IκB and transcriptionally upregulates tumor-promoting proinflammatory cytokines [262] or triggers anti-apoptotic processes [263]. On the other hand, the pathway has been associated with the expression of pro-apoptotic genes and anti-proliferative and anti-migratory functions [264, 265]. Whereas most of these processes have been linked to the deregulation of NF-κB-dependent transcription, new insight is emerging that there might be a more direct role of IκB kinase signaling in tumorigenesis. Our work indicates that IKK might have both, oncogenic, as well as tumor-suppressive potential in promoting G2/M transition and spindle checkpoint functioning, respectively. Albeit insinuative, our findings are supported by the study from Prajapati and colleagues, which states a role for IKK1 in the promotion of the cell cycle.

Figure contributions: Figure 3C, Figure 7B, Figure 8.

[Cell Cycle 6:20, 2531-2540, 15 October 2007]; ©2007 Landes Bioscience

Report

The IKK Inhibitor BMS-345541 Affects Multiple Mitotic Cell Cycle Transitions

Hana Blazkova[1]
Conrad von Schubert[1]
Keith Mikule[2,†]
Rebekka Schwab[1,‡]
Nico Angliker[1]
Jacqueline Schmuckli-Maurer[1]
Paula C. Fernandez[1,§]
Stephen Doxsey[2]
Dirk A. Dobbelaere[1,*]

[1]Division of Molecular Pathology; Vetsuisse Faculty; University of Bern; Bern, Switzerland

[2]Department of Molecular Medicine; University of Massachusetts Medical School; Worcester, Massachusetts USA

[†]Current address: Boston Biomedical, Inc.; Norwood, Massachusetts USA

[‡]Current address: Molecular Haematology and Cancer Biology Unit; Institute of Child Health; UCL; London, UK

[§]Current address: Kantonspital Aarau; Aarau, Switzerland

*Correspondence to: Dirk A. Dobbelaere; Division of Molecular Pathology; Vetsuisse Faculty; University of Bern; Länggassstrasse 122; Bern CH-3012 Switzerland; Tel.: +41.31.631.2625; Fax: +41.31.631.2658; Email: dirk.dobbelaere@mopa.unibe.ch

Original manuscript submitted: 05/18/07
Revised manuscript submitted: 07/24/07
Manuscript accepted: 07/30/07

Previously published online as a Cell Cycle E-publication:
http://www.landesbioscience.com/journals/cc/article/4807

KEY WORDS

IKK complex, BMS-345541, cell cycle, mitosis, flow cytometry, immunofluorescence

ACKNOWLEDGEMENTS

James Burke is thanked for supplying BMS-345541 and Patrick Meraldi for helpful discussions. Laurent Meijer is thanked for help with Cdk1 kinase assays. This work was supported by grants GM051994 (NIH), PC030931 (Dept. Defense) and CA82834 (NCI) to Stephen Doxsey; grant DAMD17-03-1-0303 (Dept. Defense) to Keith Mikule and OCS-01414-08-2003 (Oncosuisse), 3100AO-102164 (Swiss National Science Foundation) and 02C52 (Novartis Stiftung) to Dirk A. Dobbelaere.

ABSTRACT

The IκB kinase (IKK) complex controls processes such as inflammation, immune responses, cell survival and the proliferation of both normal and tumor cells. By activating NFκB, the IKK complex contributes to G_1/S transition and first evidence has been presented that IKKα also regulates entry into mitosis. At what stage IKK is required and whether IKK also contributes to progression through mitosis and cytokinesis, however, has not yet been determined. In this study, we use BMS-345541, a potent allosteric small molecule inhibitor of IKK, to inhibit IKK specifically during G_2 and during mitosis. We show that BMS-345541 affects several mitotic cell cycle transitions, including mitotic entry, prometaphase to anaphase progression and cytokinesis. Adding BMS-345541 to the cells released from arrest in S-phase blocked the activation of Aurora A, B and C, Cdk1 activation and histone H3 phosphorylation. Additionally, treatment of the mitotic cells with BMS-345541 resulted in precocious cyclin B1 and securin degradation, defective chromosome separation and improper cytokinesis. BMS-345541 was also found to override the spindle checkpoint in nocodazole-arrested cells. In vitro kinase assays using BMS-345541 indicate that these effects are not primarily due to a direct inhibitory effect of BMS-345541 on mitotic kinases such as Cdk1, Aurora A or B, Plk1 or NEK2. This study points towards a new potential role of IKK in cell cycle progression. Since deregulation of the cell cycle is one of the hallmarks of tumor formation and progression, the newly discovered level of BMS-345541 function could be useful for cell cycle control studies and may provide valuable clues for the design of future therapeutics.

ABBREVIATIONS

APC/C, anaphase promoting complex/cyclosome; BMS-345541, 4(2'-aminoethyl) amino-1,8-dimethylimidazo(1,2-a)quinoxaline; Cdk1, cyclin-dependent kinase 1; DAPI, 4′,6-diamino-2-phenylindole dihydrochloride; DMSO, dimethyl sulfoxide; IKK, IκB kinase; NEMO, NFκB essential modulator; P-H3^{Ser10}, phospho-Ser-10 on histone H3; Plk1, polo-like kinase 1

INTRODUCTION

The nuclear factor NFκB family of eukaryotic transcription factors not only plays an important role in the regulation of inflammatory and immune responses, it also contributes to developmental processes, protection against programmed cell death and cell cycle progression.[1-3] Moreover, it has also been proposed that aberrant regulation of NFκB could also underlie different types of cancer.[4-6] In many cancers and transformed cells, NFκB is persistently activated, protecting developing tumor cells from programmed cell death, thus contributing to tumorigenesis[7] and cancer therapy resistance.[8] A wide range of stimuli, including mitogens or cytokines such as tumor necrosis factor α or interleukin 1, ionizing radiation, toxic metals, parasites and viral or bacterial products, activate NFκB signaling pathway. In unstimulated cells, NFκB resides in the cytoplasm of the cells as an inactive complex with a member of the IκB inhibitory protein family, which mask its nuclear localization signal.[9,10] Signals that activate NFκB converge on IκB kinase (IKK), a multisubunit complex containing two catalytic subunits, termed IKKα (or IKK1) and IKKβ (or IKK2),[11,12] and a regulatory component, IKKγ/NEMO (NFκB essential modulator) that also functions as a scaffolding protein.[13,14] The kinase activity of IKK is essential for the phosphorylation of IκB proteins leading to their subsequent ubiquitination and

degradation, allowing released NFκB to translocate to the nucleus where it activates downstream targets (reviewed in refs. 15 and 16). The spectrum of IKK substrates was recently extended to a number of transcriptional regulators (reviewed in ref. 17). IKK activation can be induced by recruiting the complex to specific cellular sites where activating triggers are delivered, suggesting that the intracellular topology of IKK activation may determine the specificity of the activated pathway as well as its biological outcome.

The cell cycle is a highly regulated process and the progression through the different phases requires the tightly orchestrated expression and activation of several elements, including cyclins, cyclin-dependent kinases (Cdks) and a wealth of other regulatory components (reviewed in ref. 18). Different complexes of cyclin-Cdk appear to drive each phase of the cell cycle, cyclin D-Cdk4/6 and cyclin E-Cdk2 complexes regulate G_1/S progression, cyclin A-Cdk2 complexes mediate S/G_2 transitions and cyclin B-Cdk1 complexes mediate M-phase progression (reviewed in ref. 19). In addition to Cdk1, several other mitotic kinases such as Plk1 (polo-like-kinase), Aurora kinases and NIMA (never in mitosis A) participate in mitosis (reviewed in ref. 20). Cdk1 activation requires the dephosphorylation of Thr-14 and Tyr-15 which occurs when the activity of the phosphatase Cdc25 towards Cdk1 exceeds that of the opposing kinases such as Wee1 and Myt1.[20] The metaphase to anaphase transition is triggered by activation of the anaphase promoting complex or cyclosome (APC/C) which is controlled by the spindle assembly checkpoint, a regulatory system that ensures proper connections exist between kinetochores and spindle microtubules (reviewed in ref. 21). The APC/C functions as a ubiquitin ligase complex that triggers the degradation of specific substrates such as cyclins or securin. The latter functions as an anaphase inhibitor that regulates sister chromatid separation,[22] and its destruction results in activation of the protease separase which separates sister chromatids by cleaving cohesion complexes (reviewed in ref. 23).

Although the role of NFκB in immune response, inflammation and apoptosis has been intensively explored, only limited information is available regarding the involvement of this pathway—or components thereof—in cell cycle regulation. By regulating the transcription of a select number of genes, NFκB has been implicated in the regulation of G_0/G_1-S transition and DNA synthesis (reviewed in ref. 3). There is also evidence that IKK activation regulates the transcription of anti-apoptotic proteins that may promote cell survival during mitotic cell cycle arrest.[24] Furthermore, a genome-wide screen of the *Drosophila* kinome for kinases involved in cell cycle regulation indicated a potential role in mitosis for *nmo* and *ik2*, two genes involved in *Drosophila* NFκB activation.[25] Recently, first evidence was presented for a role of IKK1 in regulating entry into mitosis in mammalian cells.[26] However, a direct involvement of IKK in progression through mitosis has not yet been investigated.

Recently, NFκB and the signaling pathways that regulate its activity have become a focal point for intense drug discovery and development efforts. For instance, the two kinase subunits of the IKK complex are considered to be therapeutic targets for development of anti-inflammatory and anticancer agents.[27,28] Here we used a recently developed drug BMS-345541 (4(2'-aminoethyl)amino-1,8-dimethylimidazo(1,2-a) quinoxaline), that was identified as a highly selective inhibitor of IKK1 and IKK2.[29] Unlike other reported IKK inhibitors, BMS-345541 was found to bind to an unidentified allosteric site of the catalytic subunits, and so behaves as an ATP-non-competitive inhibitor. The high selectivity of BMS-345541 for IKK1 and IKK2 suggests that the allosteric site is unique to the IKKs, although it cannot be excluded that the site may also be present within other kinases not yet tested for selectivity. BMS-345541 does not inhibit IKKε and failed to inhibit a panel of 135 different kinases even at concentrations as high as 100 μM (Burke J, personal communication).

BMS-345541 inhibits NFκB-dependent transcription of pro-inflammatory cytokines both in vitro and in vivo,[29] blocks both joint inflammation and destruction in collagen-induced arthritis[30] and reduces the severity of dextran sulphate sodium-induced colitis[31] or neutrophilic lung inflammation in mice.[32] Moreover, administration of BMS-345541 improved graft survival in a murine model of cardiac graft rejection.[33] Recently, it was also shown that BMS-345541-induced inhibition of IKK activity results in mitochondria-mediated apoptosis of melanoma cells.[34] Here we investigated in detail the effect of BMS-345541 on several cell cycle transition, including mitotic entry, prometaphase to anaphase progression and cytokinesis.

MATERIALS AND METHODS

Cell culture. COS-7 and HeLa cells were maintained in Dulbeccos Modified Eagles medium—DMEM (Gibco) and hTERT-RPE-1 cells in DMEM:F12 (Gibco) both suplemented with 10% heat-inactivated foetal calf serum (AMIMED, Allschwil, CH) and penicillin-streptomycin in a humidified atmosphere of 5% CO_2 at 37°C.

Inhibitor experiments. COS-7, hTERT-RPE-1 or HeLa cells were arrested in early S-phase by a double-thymidine block (18 h culture in 2 mM thymidine, 9 h in the absence and another 18 h in 2 mM thymidine). After removal of the thymidine by washing, cells were cultured in the presence or absence 25 μM BMS-345541 (a kind gift from Dr. James R. Burke, Bristol-Myers Squibb, New York, NY; stock solution 100 mM in DMSO) as indicated. For synchronization in promethaphase, exponentially growing COS-7, hTERT-RPE-1 or HeLa cells were treated with 0.1 μg/ml nocodazole for 16 h. Mitotically rounded cells were collected by mechanical shake-off, washed 3x in PBS and cultured as indicated in the presence or absence of 25 μM BMS-345541 or 1 μg/ml actinomycin D or 5 μM MG132.

Flow cytometry. Treated or untreated COS-7 or hTERT-RPE-1 cells were trypsinized, harvested by centrifugation, washed in ice-cold PBS, fixed in 100% ethanol (cooled to -20°C) for at least 2 h and washed again in PBS. The pellet was resuspended in 100 μl PBS containing 200 μg/ml RNAse A. After incubation at RT for 30 min, 400 μl of propidium iodide solution (0.1% NP-40, 0.2 mg/ml RNAse A, 12.5 μg/ml propidium iodide) was added. Flow-cytometric analysis was carried out using a Becton Dickinson FACScan and data were evaluated using Cell Quest software.

Immunoflourescence microscopy. For immunoflourescence microscopy, cells were seeded onto coverslips; when indicated, slides were coated with 0.1 mg/ml poly-lysine. Cells were first rinsed in PBS and then fixed in 4% paraformaldehyde at RT or 100% methanol at -20°C for at least 5 min. Fixed cells were then permeabilized for 10 min with 0.2% Triton X-100, again washed with PBS and blocked for 30 min in 10% FCS-PBS or 1% BSA-PBS, depending on the primary antibody. Incubation with primary antibodies was for 60 min at RT: rabbit anti-P-H3^{Ser10} (1:200 in 1% BSA-PBS,

Upstate #06-570), mouse anti-Ki67 (1:40 in 1% BSA-PBS, Zymmed #18-0192), mouse anti-α-tubulin A2 (1:5,000 in 10% FCS-PBS, Sigma-Aldrich #T9028), mouse or rabbit anti-γ-tubulin (1:1,000 in 10% FCS-BSA, Sigma-Aldrich #T6557, #T3559), mouse anti-Aurora B (1:200 in 10% FCS-PBS, BD Biosciences #611082) or mouse anti-cyclin B1 (1:50 in 10% FCS-PBS, Pharmingen #554176). Following a PBS wash, the coverslips were incubated with goat anti-rabbit or anti-mouse Alexa Fluor 488 (1:1,500; Molecular Probes #A11034, #A11029) or goat anti-mouse Texas Red (1:800; Molecular Probes #T862) secondary antibodies at RT for 60 min. After a PBS rinse, nuclei were stained with DAPI (1:3,000 in PBS, Molecular Probes #D-21490). Finally, coverslips were mounted using anti-fading mounting reagent (Vectashield) and analyzed using a Nikon Eclipse fluorescence microscope. Images were generated by digital imaging using Openlab 3.1.5. software.

Cell lysates and Western blotting. Collected cells were washed with PBS and lysed directly in standard 1x Lämmli buffer followed by sonication, or in RIPA buffer (50 mM Tris-HCl, pH 7.4, 1% NP-40, 0.25% Na-deoxycholate, 150 mM NaCl, 1 mM EDTA, 1 mM PMSF, 1 mM Na_3VO_4, 1 mM NaF, aprotinin, leupeptin, pepstatin—1mg/ml each) followed by centrifugation at 10,000 x g for 5 min at 4°C. Lysates were subjected to SDS-PAGE and proteins transferred onto membranes. Membranes were blocked with 5% milk in TBS containing 0.05% Tween 20 and probed with the following antibodies: rabbit anti-P-H3^{Ser10} (1:2,000; Upstate #06-570), mouse anti-cyclin A (1:500; Pharmingen #14531A), mouse anti-cyclin B1 (1:500; Pharmingen #554176), mouse anti-securin (1:500; MBL #K0090-3), rabbit anti-phospho-Aurora A (Thr-288), Aurora B (Thr-232), Aurora C (Thr-198) (1:1,000; Cell Signaling #3068), rabbit anti-phospho-Cdk1 (Tyr-15) (1:1,000; Cell Signaling #9111), goat anti-actin (1:500; Santa Cruz #sc-1616), mouse anti-γ-tubulin (1:1,000; Sigma-Aldrich #T6557) or mouse anti-α-tubulin A2 (1:5,000; Sigma-Aldrich #T9028). Antigens were then visualized by chemiluminiscence (Amersham) using an X-ray film (FUJI) or a FUJIFILM LAS-3000 and Aida Image Analyzer software.

Immunoprecipitation and kinase assays. HeLa cells were synchronized by double-thymidine block (2 mM), released for 2 h in the absence of thymidine and then incubated for 5 h in the presence of either 25 μM BMS-345541 or the corresponding concentration of DMSO. Cells were lysed (20 mM Tris-HCl, pH 8.0, 1 mM EDTA, 400 mM NaCl, 0.5% NP-40, 5 mM NaF, 1 mM PMSF, Roche protease inhibitor cocktail, 0.5 mM Na_3VO_4, 20 mM β-Glycerophosphate) and Cdk1/cyclin B1 complexes immunoprecipitated from 500 μg total protein per sample with 1 μg of monoclonal anti-cyclin B1 (Pharmingen) at 4°C o/n. Cdk1 kinase activity was assayed as described by van Vugt et al.[35] and analyzed using a FUJIFILM FLA-3000 and Aida Image Analyzer software.

To monitor the effect of BMS-345541on Cdk1, in vitro kinase assays were carried out using the CycLex Cdc2-cyclin B Kinase Assay Kit (CY-1164, CycLex, Nagano), following the manufacturer's instructions and using 5 mU/reaction human recombinant Cdc2/CyclinB and 125 μM ATP (Cy-E1164). To monitor the effect on Plk1, the Cyclex Polo-like kinase Assay/Inhibitor Screening Kit (CY-1163) was used, utilizing human GST-tagged Plk1 (CY-E1163; 0.5 mU/reaction and 50 μM ATP). Measurements were made by reading absorbance (dual wavelength at 450/540 nm) using a VersaMax (Molecular Devices). HTScan Kinase Assay Kits from Cell Signaling were used to test the effect of BMS-345541on Aurora A (Cat. Nr. 7510; 10 u/reaction, 50 μM ATP), Aurora B (Cat. Nr. 7513; 100 ng/reaction, 100 μM ATP) and NEK2 (Cat. Nr. 7555; 50 ng/reaction, 200 μM ATP), Measurements were made by monitoring fluorescence using a SpectraMax Gemini (Molecular Devices; excitation 340 nm, emission 615 nm, cutoff 590 nm timeresolvement 400-800 μsec, 30 cycles). BMS-345541was tested at concentrations ranging from 0 to 300 μM and the IC_{50} calculated.

RESULTS

BMS-345541 affects cell dycle progression of unsychronized mammalian cells. We first examined whether the IKK inhibitor BMS-345541 affects cell cycle progression in asynchronously growing cells. Unsynchronized hTERT-RPE-1 or COS-7 cells were cultured for different time-periods in the absence or presence of BMS-345541 and analyzed by immunofluorescence microscopy. When cells were incubated with BMS-345541 for 18, 24 or 48 h, no cells with condensed chromosomes could be found. In addition, virtually no positive cells could be detected when cells were stained with antibodies that specifically recognize phospho-Ser-10 on histone H3 (P-H3^{Ser10}), a common marker of mitosis.[36] In contrast, P-H3^{Ser10} could readily be detected in approximately 10 % of DMSO-treated control cells (data not shown). Furthermore, in BMS-345541-treated cultures, increased numbers of multinucleate cells could be observed (Fig. 1A). Additionally, when cells treated with BMS-345541 for 48 h were stained for the proliferation marker Ki67, only few cells were positive compared to control DMSO-treated cells (Fig. 1B), indicating that they had exited the cell cycle.

BMS-345541 blocks entry into mitosis and chromosome segregation. To investigate whether BMS-345541 blocks entry into mitosis, hTERT-RPE-1 or COS-7 cells were first synchronized in S phase by double-thymidine block and then released to complete the cell cycle. Flowcytometric analysis shows the kinetics with which COS-7 cells, upon release from thymidine block, complete S-phase and progress through G_2 to enter mitosis (Fig. 2A). BMS-345541 was added to the culture medium at different time-points after release. As IKK1 and IKK2 differ in their sensitivity to BMS-345541, we selected a concentration of 25 μM at which both IKK subunits are fully inhibited.[29] After a total of 8 h of cell culture, BMS-345541-treated and control cells were fixed, stained with DAPI and anti-γ-tubulin antibody and examined by fluorescence microscopy. By 8 h after release from double-thymidine block, many control cells had entered mitosis (Fig. 2B). In contrast, addition of BMS-345541 to COS-7 cells 2 or 3 h after release prevented entry into mitosis as judged by the absence of mitotic figures (Fig. 2B). In the few cells in which mitosis could be detected, severe defects in chromosome segregation were usually detected (Fig. 2C). This was reflected by the presence of DNA bridges that persisted during anaphase. Such defects were particularly prominent when BMS-345541 was added 4-6 h after release from double-thymidine block. The capacity to block mitotic entry decreased when BMS-345541 was added at later time-points as witnessed by the increased mitotic index (Fig. 2D, 500 cells counted per sample).

Phosphorylation of histone H3 on serine 10 (P-H3^{Ser10}) and cyclin A degradation are good markers for the early stages of mitosis.[37,38] Western blot analysis of COS-7 cells harvested between 8 and 11 h after release from S-phase block showed that histone H3 phosphorylation and cyclin A degradation were inhibited in cells

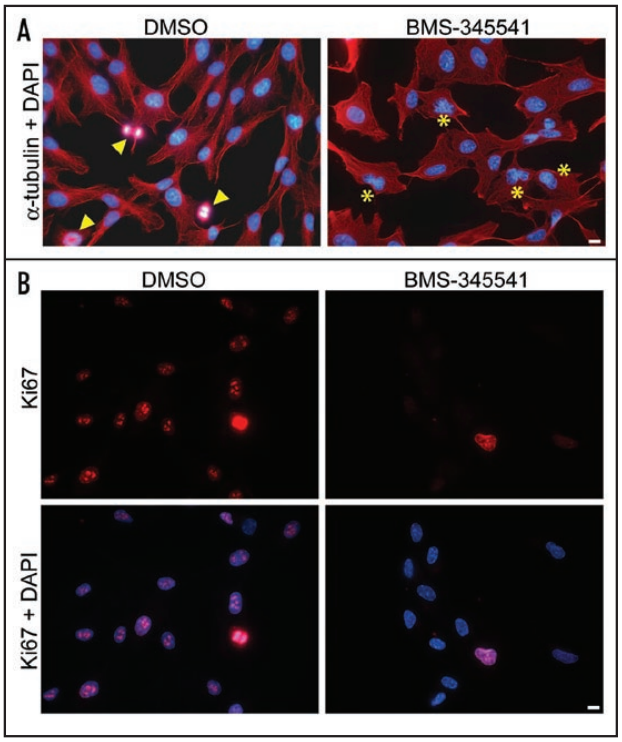

Figure 1. Effects of BMS-345541 on unsynchronized hTERT-RPE-1 cells. (A) 18 h after incubation with DMSO (control) or BMS-345541, cells were fixed and stained with anti-α-tubulin (red) and DAPI (blue). Mitotic figures (arrowheads) can only be found in the control sample; in BMS-345541-treated samples a number of ‚binucleate' cells (asterisks) were observed. (B) Upon treatment with BMS-345541, many cells exit from the cell cycle and become negative for Ki67. Control (DMSO) or BMS-345541-treated cells were stained with anti-Ki67 (red) and DAPI (blue) 48 h after the onset of treatment. The bottom panels show an overlay of Ki67 and DAPI staining. Bars, 10 μm.

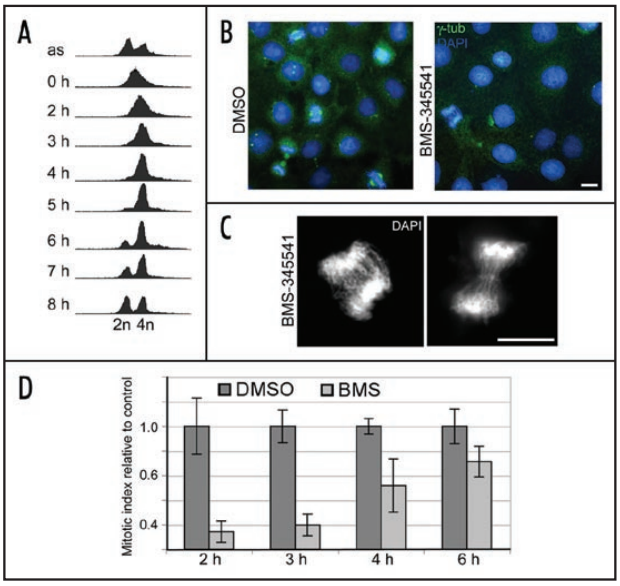

Figure 2. BMS-345541 prevents entry into mitosis. (A) The DNA content of COS-7 cells, arrested in S-phase by double-thymidine block (0 h) and subsequently released to proceed to G_2/M, was monitored by flow-cytometric analysis at the indicated times after release; (as) depicts the cell cycle distribution of asynchronously growing cells. (B) COS-7 cells were treated with either DMSO or BMS-345541 starting 2 h after release from S-phase arrest and cultured for an additional 6 h. Cells were then stained for γ-tubulin (green) and DNA (blue) and analyzed by immunofluorescence microscopy for the presence of mitotic cells. Bar, 10 μm. (C) Mitotic BMS-345541-treated COS-7 cells showing the typical anaphase bridges that accompany chromosome separation defects (the left panel is a higher magnification of the BMS-345541-treated cell undergoing defective mitosis in Fig. 3B); DNA is stained with DAPI. Bar, 10 μm. (D) COS-7 cells were treated with BMS-345541 (BMS) or DMSO, starting 2, 3, 4 or 6 h after release from S-phase arrest; 8 h after release, the number of mitotic cells was determined. The mitotic index for control DMSO-treated cells is set as 1.0. Error bars represent the s.d. for three separate experiments.

exposed to BMS-345541 2 h after release from double-thymidine block (Fig. 3A) confirming that cells did not proceed to mitosis. The gradual decrease in histone H3 Ser-10 phosphorylation in control cells reflects their progression from metaphase to anaphase and telophase, which coincides with histone H3 dephosphorylation. As would be expected, cyclin B1 degradation, initiated as APC/C becomes activated at anaphase,[23] was also inhibited by treatment with BMS-345541. Similar results were obtained with hTERT-RPE-1 cells and HeLa cells (data not shown).

Entry into mitosis is accompanied by the activation of several mitotic kinases including Aurora kinases and the Cdk1/cyclinB complex.[39,40] The activation of Aurora kinases involves de novo phosphorylations, and, in the case of Cdk1 activation, the removal of an inhibitory phosphate group on Tyr-15 by the phosphatase Cdc25B is required.[41] We monitored these events using phospho-specific antibodies that detect activation-specific phosphorylation of Aurora kinases and the state of Cdk1-Tyr-15 phosphorylation. Eight hours after release from double-thymidine block, control cells showed pronounced phosphorylation of the activated Aurora kinases, which gradually decreased as cells proceeded through mitosis. In contrast, phosphorylated Aurora was barely detectable in BMS-345541-treated cells. In control cells, Cdk1 activation was reflected by the gradual dephosphorylation of Tyr-15 (Fig. 3B). BMS-345541 treatment blocked Cdk1 dephosphorylation and in vitro kinase assays performed on immunoprecipitated Cdk1/cyclin B1 complexes showed that this was accompanied by a marked reduction in Cdk1 kinase activity (Fig. 3C). Taken together, these data show that exposure to 25 μM BMS-345541 blocks entry into M-phase.

Effects of BMS-345541 on progression through mitosis. When BMS-345541 was added at later time-points after release from S-phase block, cells that had started mitosis and entered anaphase invariably displayed DNA bridges indicating that, in addition to inhibiting entry, BMS-345541 might also interfere with mitosis per se. We therefore investigated whether BMS-345541 affected mitotic progression of cells that had already entered mitosis. For this purpose, hTERT-RPE-1 or COS-7 cells were first synchronized in prometaphase by nocodazole treatment, collected by mitotic shake-off, washed and subsequently cultured in normal medium in the absence or presence of BMS-345541. Progression through mitosis into G_1 was analyzed by flow-cytometry. Different

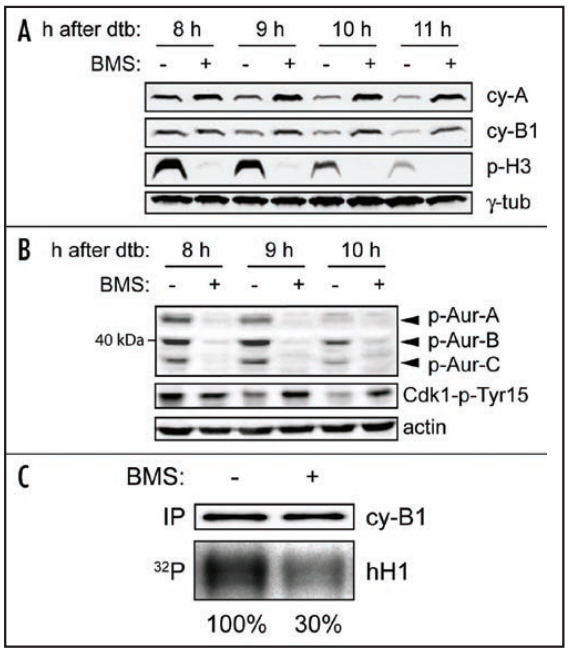

Figure 3. BMS-345541 blocks the degradation of cyclin A and B1 and the activation of mitotic kinases. (A) COS-7 cells were treated with BMS-345541 (BMS) 2 h after release from S-phase arrest and whole cell lysates were prepared at the indicated times after release. Lysates were analyzed by immunoblot using antibodies directed against cyclin A (cy-A), cyclin B1 (cy-B1) or antibodies specific for histone H3 phosphorylated at Ser-10 (p-H3); γ-tubulin functioned as a loading control. (B) Synchronized HeLa cells were treated with BMS-345541 (BMS) starting 2 h after release from double-thymidine block and lysates were analyzed by immunoblot using antibodies specific for phosphorylated Aurora A, B and C (p-Aur) or Cdk1 (p-Tyr15). Actin was monitored as a loading control. (C) Synchronized HeLa cells were cultured for 5 h in the presence or absence of BMS-345541 (BMS) starting 2 h after release from S-phase arrest. In vitro kinase assays were performed on Cdk1/cyclin B immunoprecipitates, using histone H1 (hH1) as a substrate. The top panel (cy-B1) shows a control immunoblot demonstrating that the complexes contain an equal amounts of cyclin B1. The bottom panel (hH1) shows an autoradiograph of the phosphorylated substrate. The numbers represent relative Cdk1 activity measured in BMS-345541-treated cells versus control (100%).

concentrations of BMS-345541 were tested. (Fig. 4A). In untreated control cultures, >30% of the cells completed mitosis and entered G_1 within 2 h of release from nocodazole block. At concentrations of BMS-345541 (≤10 μM) that only block IKK2, no inhibition was observed, and progression from G_2/M to G_1 was first affected at BMS-345541 concentrations that fully block both IKK1 and IKK2. These experiments indicate that IKK1 rather than IKK2, or both IKKs together, participate in regulating mitosis. Since IKK is primarily known as a regulator of NFκB-dependent transcription we also tested whether defects in mitotic progression could result from interference with NFκB transcriptional activity. Although transcription is largely downregulated as cells enter mitosis, selective RNA polymerase II-dependent transcription has been demonstrated.[42] Therefore, we treated nocodazole-synchronized cells with the general transcriptional inhibitor actinomycin D. Upon nocodazole removal, cells progressed through mitosis into G_1 with the same kinetics as did control cells (Fig. 4B), indicating that de novo transcription, including NFκB-dependent transcription, is not required for mitotic progression.

Immunofluorescence analysis revealed that treatment of prometaphase cells with BMS-345541 did not significantly affect mitotic spindle assembly although chromosomes were not as tightly organized on the metaphase plate as in controls. On the other hand, BMS-345541-treated cells failed to enter proper anaphase, corroborating the mitotic defects described above. Chromosomes failed to disjoin in the presence of BMS-345541 (Fig. 5A). Aurora B (AIM-1) immunostaining of control cells released from nocodazole block revealed the pinched furrow staining typical of cells in anaphase and Aurora B was subsequently found localized to the midbodies of cells in telophase. In BMS-345541-treated cells, however, a highly disorganized Aurora B staining pattern could first be observed (50

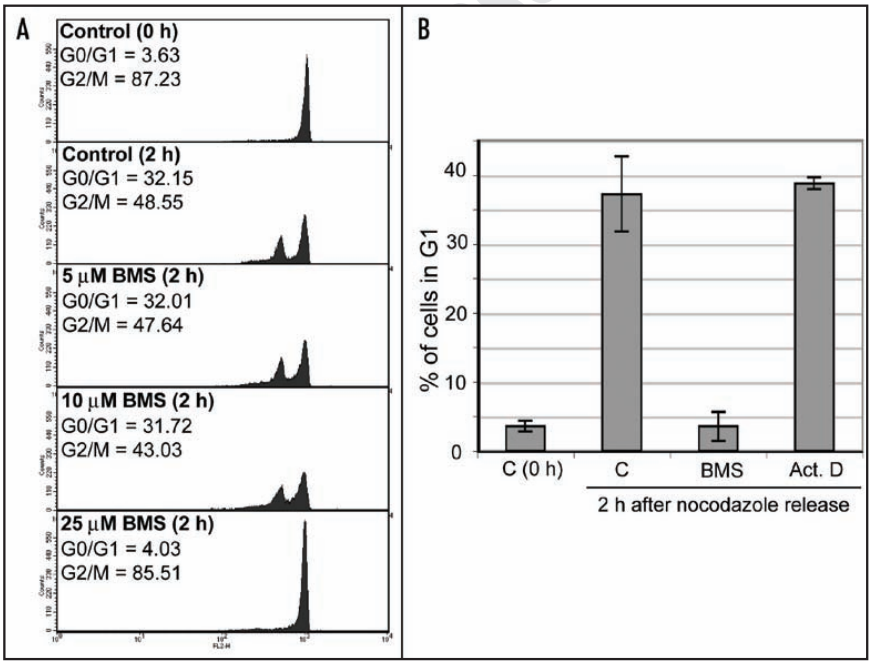

Figure 4. BMS-345541 blocks progression through mitosis. (A) COS-7 cells were synchronized in prometaphase by nocodazole arrest, collected by mitotic shake-off and cultured for 2 h in the absence or presence of 5, 10 or 25 μM BMS-345541 (BMS). The DNA content was measured by flow-cytometry. The percentage of cells in either G_0/G_1 or G_2/M are indicated. (B) COS-7 cells were synchronized in prometaphase by nocodazole arrest (C (0h)), collected by mitotic shake-off and cultured for 2 h in the absence (C) or presence of BMS-345541 (BMS) or actinomycin D (Act. D); progression to G_1 was monitored by flow-cytometry. Error bars indicate s.d.

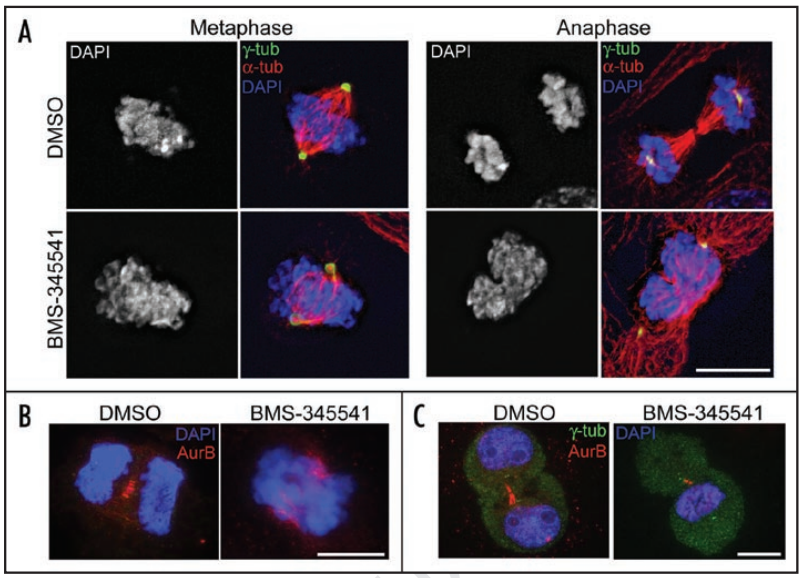

Figure 5. BMS-345541 interferes with chromosome segregation. (A) Nocodazole-synchronized hTERT-RPE-1 cells were exposed to DMSO (control) or BMS-345541 for 30 min before fixation. In BMS-345541-treated cells, metaphase is characterized by irregular spindles with a decreased pole-to-pole distance and less tightly compacted DNA (left panels) and anaphase can progress without chromosome segregation, resulting in a "cut" DNA phenotype (right panels). Cells were stained with anti-γ-tubulin (green), anti-α-tubulin (red) and DAPI (blue). COS-7 cells were collected by mitotic shake-off and cultured in the presence or absence of BMS-345541 for 50 (B) or 100 min (C). Aurora B (red) staining reveals a disorganized central spindle pattern in BMS-345541-treated cells (B). In some cases, defective cytokinesis results in cytoplast generation with all DNA remaining in one of the daughter cells (C); γ-tubulin (green), DNA (blue) was stained with DAPI. Bars, 10 μM.

min after release), which was mostly positioned across condensed chromosomes (Fig. 5B). Intriguingly, a small number of cells formed midbodies and attempted cytokinesis, but, in such cases, only one of the two 'daughter cells' contained DNA (100 min after release) (Fig. 5C). When BMS-345541 was added to nocodazole-synchronized cells at later time-points after release, cells with long persistent DNA bridges (mainly seen in hTERT-RPE-1 cells) and cells that failed cytokinesis altogether to form binucleates appeared (Fig. 6A). Together these cells comprised 71% of the total cell population (Fig. 6B; 1,000 cells counted per sample). Time-lapse imaging showed that cleavage furrow formation and chromosome segregation were initiated normally, but cytokinesis ultimately failed (27 out of 28 vs. 1 out of 13 for controls) (Fig. 6C).

In addition, in cells released from nocodazole block in the presence of BMS-345541, many cells were found to contain four centrioles, compared to control cells, in which the typical set of two centrioles could be observed (Fig. 6D). To quantify this phenomenon, the cells were fixed and stained with DAPI and anti-γ-tubulin 7 h after adding BMS-345541 and the number of centrioles in cells containing only one nucleus was calculated (Fig. 6E, 200 cells counted per sample). These cells in all likelihood represented cells with 4N DNA that failed division and exited mitosis.

BMS-345541 induces precocious anaphase and overrides the spindle checkpoint. To investigate whether IKK inhibition affects the activity of the APC/C, we monitored the degradation of cyclin B1, one of the major APC/C targets. Cells synchronized in prometaphase were incubated for 30 min in the presence or absence of BMS-345541 and analyzed by immunofluorescence using anti-cyclin B1 and anti-γ-tubulin antibodies. Addition of BMS-345541 to nocodazole-synchronized cells did not inhibit cyclin B1 degradation (Fig. 7A), indicating that the APC/C is functional and the spindle assembly checkpoint switched off. Interestingly, immunoblot analysis of both COS-7 cells and hTERT-RPE-1 cells revealed that the degradation of cyclin B1 and securin occurred with faster kinetics in BMS-345541 treated cells than in control cells (Figs. 7B and C).

The spindle checkpoint system ensures accurate chromosome segregation by delaying anaphase initiation until all chromosomes are properly attached to the mitotic spindle. If the spindle checkpoint system is inhibited, securin and cyclin B1 are destroyed prematurely (reviewed in ref. 23). To study if BMS-345541 abrogates spindle checkpoint function, we synchronized hTERT-RPE-1 cells with nocodazole, washed and then cultured them for 0.5 to 6 h in fresh nocodoazole-containing medium in the presence or absence of 25 μM BMS-345541 and proteasome inhibitor MG132 (5 μM) as indicated. At each time-point, cells were lysed and analyzed by immunoblotting for cyclin B1 or fixed and stained for immunofluorescence analysis with anti-P-H3^{Ser10}. Levels of cyclin B1, normally rise in late G_2 and are sustained when spindle checkpoint is activated,[20] (Fig. 8A, Noc). In contrast, when nocodazole-arrested cells were cultured for 3-6 h in the presence of BMS-345541 cyclin B1 levels dropped markedly (Fig. 8A, Noc/BMS). This process was blocked when proteasomal activity was inhibited by MG132. These findings indicate that BMS-345541-treated cells progressed past the spindle checkpoint system resulting in APC/C activation and proteasomal degradation of cyclin B1 by the proteasome. As cells proceed through mitosis the serine 10 residue of histone H3 is dephosphorylated, a process that does not occur when the spindle checkpoint is active.[21] In the presence of BMS-345541, the percentage of P-H3^{Ser10}-positive cells decreased over a period of 6 h (Fig. 8B, 300 cells counted per sample), indicating that spindle checkpoint was overridden, and also this process was blocked by MG132.

Effect of BMS-345541 on the mitotic kinases. NEK2, Plk1, Cdk1, Aurora A and Aurora B, are critical regulators of entry into and progression through mitosis and inhibition of these kinases can provoke phenotypes similar to what we observed using BMS-345541,[43-47] As, in preliminary experiments, we had observed a mild inhibition of Cdk1, we carried out more extensive in vitro kinase assays, to examine whether BMS-345541 was capable of directly blocking the activity of any of these mitotic kinases. A range of different concentrations of BMS-345541 was tested using commercially available in vitro kinase assay kits, and the IC_{50} of BMS-345541 determined for each of the kinases. The following IC50 values were obtained: 320 μM for NEK2, 130 μM for

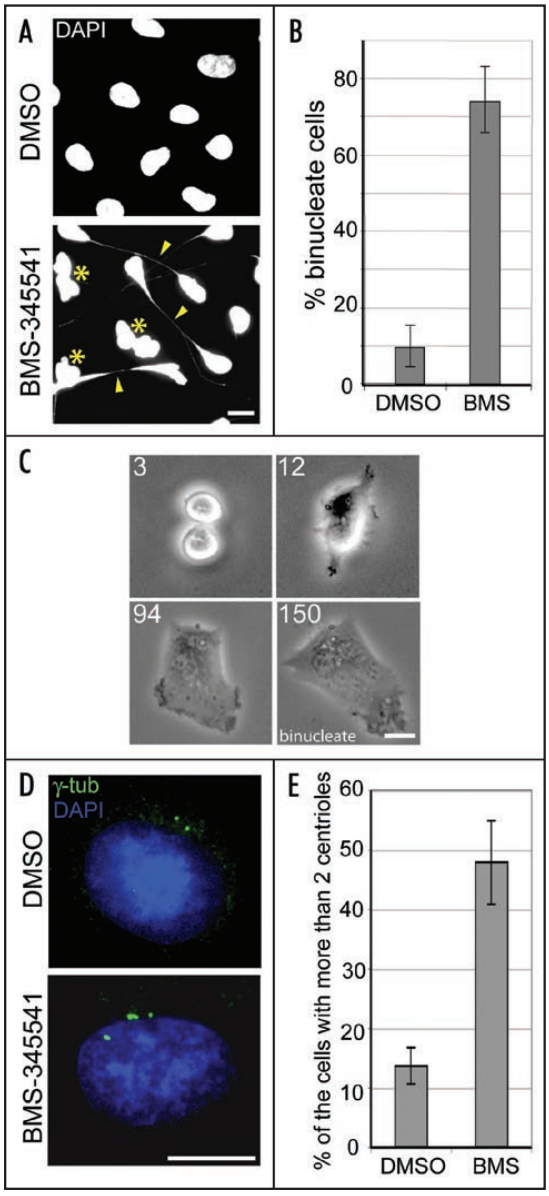

Figure 6. BMS-345541-treatment induces the formation of binucleate cells and cytokinesis defects. (A) Cultures of mitotic hTERT-RPE-1 cells treated with BMS-345541 (BMS) at the time cells approached anaphase/telophase show binucleate cells (asterisks), often showing extended DNA bridges (arrowheads); control cells were treated with DMSO. Bar, 10 μM. (B) Quantification of the number of binucleates (including cells with DNA bridges); data are presented as % binucleate cells; error bars represent s.d.. (C) Still images taken from time-lapse video microscopy, showing cytokinesis failure in nocodazole-synchronized hTERT-RPE1 cells. BMS-345541 was added at 0 min and images were recorded every 3 min; numbers indicate minutes after BMS-345541 addition. (D) COS-7 cells were treated either with DMSO or BMS-345541 (BMS) 60 min after nocodazole release, fixed 7 h later and stained with anti-γ-tubulin (green) and DAPI (blue). DMSO-treated cells contain one pair of centrioles, BMS-345541-treated cells 2 pairs. Bar, 10 μM. (E) Quantification of the number of the cells with more than 2 centrioles; error bars represent s.d.

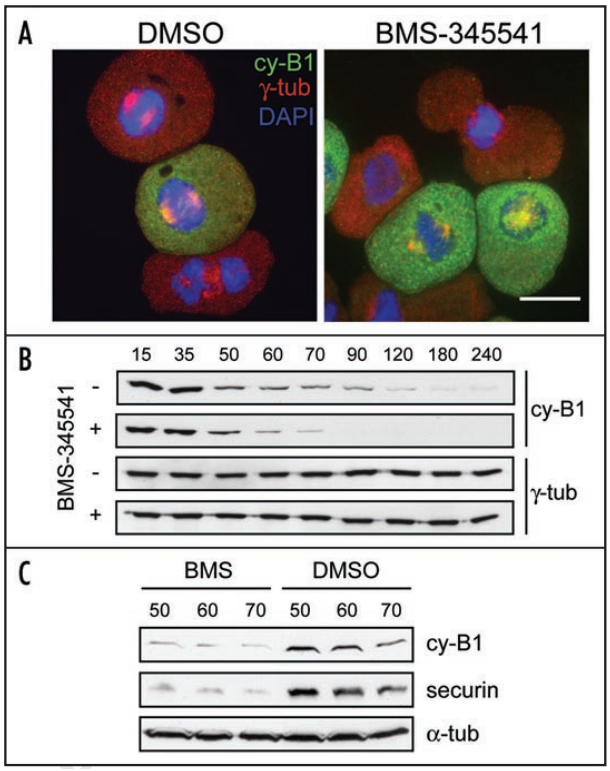

Figure 7. BMS-345541 induces precocious cyclin B1 and securin degradation and impedes chromosome separation. (A) COS-7 mitotic shake-off cells were stained for cyclin B1 (green) and γ-tubulin (red) 30 min after release from nocodazole-arrest; cyclin B1 degradation can be observed in both control (DMSO) and BMS-345541-treated cells. Bar, 10 μM. Immunoblot analysis of total cell lysates prepared from COS-7 (B) or hTERT-RPE-1 cells (C) released from nocodazole-arrest and cultured for the indicated times in the absence (DMSO) or presence of BMS-345541 (BMS). Blots were probed with anti-cyclin B1 (cy-B1) or anti-securin as indicated; γ- or α-tubulin were used as a loading control.

Cdk1, 255 μM for Aurora A and 110 μM for Aurora B. These are all considerably higher than the concentration (25 μM) at which BMS-345541was applied in our experiments and BMS-345541 was void of any inhibitory activity for Plk1 at all concentrations tested. As expected, the Cdk1 inhibitor roscovitine potently blocked Cdk1 activity at the concentration 30 μM and also the broad spectrum inhibitor staurosporine, used as a positive control in NEK2 and Aurora A or B inhibitor assays, strongly blocked kinase activity (not shown).

Taken together, these results show that pharmacologic inhibition of mammalian cells with BMS-34551—depending on when the drug is applied—prevents entry into mitosis, induces precocious anaphase and overrides the spindle checkpoint, impairs chromosome segregation during anaphase or induces cytokinesis defects resulting in multinucleation.

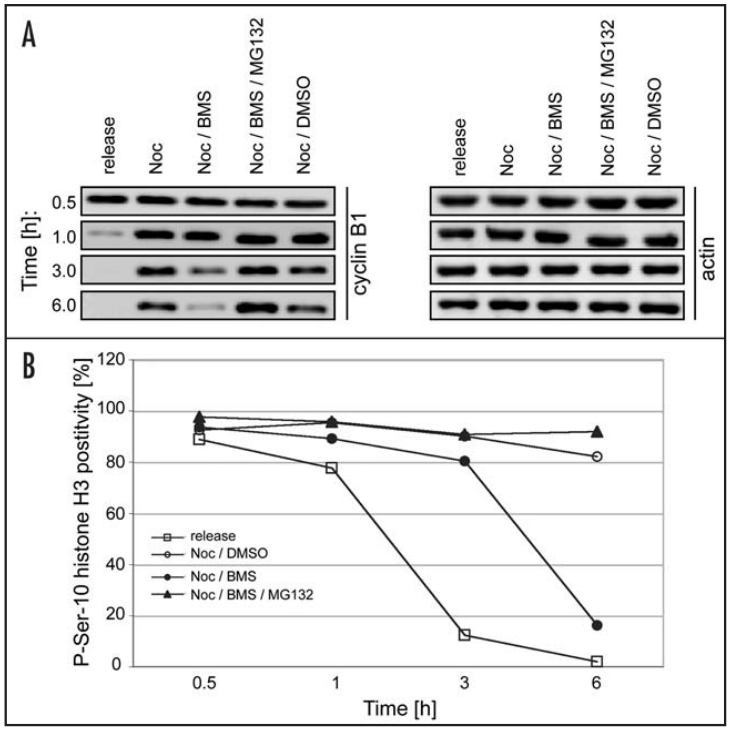

Figure 8. BMS-345541 disrupts spindle checkpoint function. Nocodazole-synchronized hTERT-RPE-1 cells were collected by mitotic shake-off and reseeded into fresh medium containing either nocodazole (Noc) alone or in combination with BMS-345541 (BMS), DMSO or MG132. The cells released from nocodazole block were analyzed in parallel (release). (A) At indicated time-points, cell lysates were prepared and cyclin B1 level of determined by immunoblot analysis. Actin was used as a loading control. (B) In a parallel experiment, a fraction of the cells was fixed and analyzed by immunofluorescence microscopy for P-H3^{Ser10} positivity. Data are expressed as the percentage of cells stained by anti-P-H3^{Ser10}.

DISCUSSION

While investigating the NFκB signaling pathway in different cell types using a new IKK inhibitor BMS-345541, we noticed the absence of mitotic cells in cultures treated with the drug. Partial cell cycle inhibition started at BMS-345541 concentrations between 10 and 15 μM, whereas an almost complete block was seen at concentrations between 20 to 25 μM, pointing towards a regulatory role in mitosis for IKK1 rather than IKK2. This finding is in agreement with that of Prajapati et al who, using siRNA-mediated IKK knock-down, demonstrated that IKK1 participates in regulating M-phase.[26] Not unexpectedly, we found that siRNA-mediated down-regulation of NEMO, the regulatory subunit of IKK, also delayed entry into mitosis of cells released from double-thymidine block (Blazkova H, unpublished observation). Both IKK1 and IKK2 have previously been shown to be involved either directly or indirectly in the regulation of cellular proliferation.[28,48,49] For example, IKK1 has been shown to contribute to the control of proliferation by regulating cyclin D1 expression, its subcellular localization and proteolysis.[50-53] In this context, one explanation for the lack of mitotic cells in the cultures of unsynchronized BMS-345541-treated cells could have been that the drug, by blocking the activation of NFκB, interfered with the transition from G_0/G_1 to S phase, thus preventing cells from proceeding to mitosis. Since NFκB has also been linked to protection against apoptosis, an alternative explanation could have been that BMS-345541 induced apoptosis of cells before they entered mitosis.[34] Even though the number of apoptotic cells increased upon longer exposure to BMS-345541, it does not explain the conspicuous absence of mitosis in cultures exposed to the drug. Since flow-cytometric analysis carried out in our laboratory showed that BMS-345541 does not prevent the completion of S phase upon release from double-thymidine block (H.B., unpublished observation), we hypothesized that BMS-345541 might block entry into mitosis in a more direct manner. A careful analysis of cells synchronized in S-phase and subsequently released to allow G_2 transition and entry into M, confirmed this hypothesis. The mitotic index of cells released from double-thymidine block was significantly reduced when BMS-345541 was added at early time-points after release. These microscopic observations could be confirmed biochemically. Addition of BMS-345541 prevented the phosphorylation of histone H3 on Ser-10 which normally begins in late G_2 and correlates with chromatin condensation during mitosis.[37] Also cyclin A degradation, which occurs around prometaphase, and subsequent degradation of cyclin B1 in early anaphase were blocked.

It has previously been shown that IKK1 phosphorylates Aurora A at Thr-288, a T-loop residue that is important for Aurora A activation and subsequent mitotic entry.[26] Adding of BMS-345541 to the cells synchronized with double-thymidine block resulted in reduced Aurora A phosphorylation on Thr-288. Consistent with the lack of Aurora A activity, we found that Cdk1 Tyr-15 was not dephosphorylated by Cdc25B[54,55] and also showed a corresponding decrease in Cdk1 kinase activity in BMS-345541-treated cells. BMS-345541 also blocked the activation of Aurora B and C. Lack of activity both these kinases probably results from the fact that the cells never entered mitosis. We also found that, once all three aurora kinases were active (in nocodazole-synchronized cell), administration of BMS-345541 failed to block their phosphorylation (H.B., unpublished observation).

BMS-345541, added later after release from double-thymidine block, also had pronounced effects on cells that had already started entry into mitosis. In this case, mitotic cells showed disordered metaphase plates and, during anaphase, chromosome segregation was clearly defective. This was reflected by the presence of extensive DNA strands which also appeared to interfere with proper cytokinesis and final abscission of the daughter cells. The hypothesis that BMS-345541 also inhibits progression through mitosis could be confirmed by investigating cells that had been synchronized in early mitosis (prometaphase) by nocodazole treatment. Flow-cytometric analysis confirmed that BMS-345541 potently blocks the transition from early mitosis into G_1. The fact that progression from prometaphase to G_1 occurred in the presence of the transcriptional inhibitor actinomycin D, but can nevertheless be blocked by BMS-345541, excludes a role of IKK as a transcriptional regulator for this stage of the cell cycle.

In addition, immunofluorescence analysis revealed that mitosis and cytokinesis were severely disturbed when the cells were released from prometaphase block in the presence of BMS-345541. Chromosomes consistently failed to disjoin and remained linked by strands of DNA forming typical anaphase bridges. Cytokinesis defects included disorganized central spindles and daughter cells that either received all detectable chromatin or none. When BMS-345541 was added to cells in late anaphase/telophase, cytokinesis defects became more pronounced and the number of binucleate cells increased. Defects in chromosome segregation could explain the accumulation of cells interconnected by long DNA strands. Cytokinesis defects, on the other hand, can be expected to contribute to multinucleation. Cells showing severe mitotic defects can exit mitosis without completing chromosome segregation of cytokinesis.[56] This could explain the accumulation of mononuclear cells containing four centrioles, rather than the two centrioles, as would be expected after normal mitosis and cytokinesis.

For a cell to proceed to anaphase, the APC/C has to become activated.[22] Activated APC/C ubiquitinates numerous regulatory proteins which are then degraded by the 26S proteasome. One of these target proteins is securin which binds to separase. Upon degradation of securin, separase becomes activated and cleaves cohesin, a protein that keeps the sister chromatids together, allowing sister chromatids to move towards the spindle poles.[23] The defects in sister chromatid segregation observed in drug-treated cells, cannot be explained by a BMS-345541-induced inhibition of the APC/C and block of securin degradation. On the contrary, rather than inhibiting the APC/C, BMS-345541 induced precocious APC/C activation, which was reflected by an overall faster degradation of the APC/C substrates. Western blot analysis of two different cell lines showed that the degradation of cyclin B1 and securin occurred up to 60 minutes earlier in BMS-345541-treated cells compared to control cells. The most plausible explanation is that BMS-345541 overrides the spindle checkpoint (Fig. 8) and that untimely degradation of these important cell cycle proteins is responsible for at least some of the mitotic defects.[56,57]

Even though BMS-345541 has been described as a highly specific IKK inhibitor, it cannot be completely excluded that kinases other than IKK are blocked by this compound. In different tests, BMS-345541 failed to inhibit a battery of 135 different kinases (Burke J, personal communication). The kinases NEK2, Plk1, Cdk1, Aurora A and Aurora B that are critical for initiation and transition through mitosis, however had not yet been tested. As several of the phenotypic changes observed upon treatment with BMS-345541 can also be observed upon interference with these kinases,[58,59] we established the IC_{50} of BMS-345541 for these kinases using in vitro kinase assays. BMS-345541 did not inhibit Plk1 in vitro at all concentrations used, and the IC_{50} for the other kinases was several-fold higher than the concentration of 25 μM used in our experiments. Considering these findings, it is unlikely that the mild inhibition of Cdk1 that we had observed in preliminary experiments could account for the dramatic cell cycle inhibitory effects observed for BMS-345541. Cdk1 becomes activated at G_2/M transition and its activity is terminated with the degradation of cyclin B.[60,61] To block mitotic entry, BMS-345541 had to be administrated within hours after release from S-phase arrest, at a time-point when Cdk1 is not yet activated. This further indicates that Cdk1 is not the principle target and underpins the role for IKK1, as proposed by Prajapati et al.[26] However, it cannot be ruled out, that a partial BMS-345541-mediated inhibition of other kinases contributes to the defects observed during mitosis. Exactly at which point IKK is involved in the regulation of mitosis is not known. The different functions and levels of regulation of Cdk1 are still not fully accounted for at the molecular level and it is plausible that IKK acts upstream or downstream in the Cdk1 activation network.

In conclusion, these data show that treatment with the IKK inhibitor BMS-345541 affects several cell cycle transitions, including entry into mitosis, prometaphase to anaphase progression and cytokinesis accompanied by dramatic defects in chromosome segregation and cellular ploidy. These findings open new perspectives on the physiological role of IKK in cell cycle regulation and on its relationship to disease, in particular cancer.[4-6] The induction of cell cycle arrest and potentially apoptosis by this IKK inhibitor suggests that, in addition to modulating immune and inflamatory responses, drugs that target IKK can also be expected to affect cell proliferation and genomic stability. In view of our unexpected finding, the clinical relevance of BMS-345541-induced cell cycle inhibition also deserves further exploration.

References

1. Karin M, Delhase M. The I kappa B kinase (IKK) and NFκB: Key elements of proinflammatory signalling. Semin Immunol 2000; 12:85-98.
2. Israel A. The IKK complex: An integrator of all signals that activate NFκB? Trends Cell Biol 2000; 10:129-33.
3. Joyce D, Albanese C, Steer J, Fu MF, Bouzahzah B, Pestell RG. NFκB and cell-cycle regulation: The cyclin connection. Cytokine Growth F R 2001; 12:73-90.
4. Balkwill F, Coussens LM. Cancer - An inflammatory link. Nature 2004; 431:405-6.
5. Greten FR, Eckmann L, Greten TF, Park JM, Li ZW, Egan LJ, Kagnoff MF, Karin M. IKKβ links inflammation and tumorigenesis in a mouse model of colitis-associated cancer. Cell 2004; 118:285-96.
6. Pikarsky E, Porat RM, Stein I, Abramovitch R, Amit S, Kasem S, Gutkovich-Pyest E, Urieli-Shoval S, Galun E, Ben-Neriah Y. NFκB functions as a tumour promoter in inflammation-associated cancer. Nature 2004; 431:461-6.
7. Richmond A. NFκB, chemokine gene transcription and tumour growth. Nat Rev Immunol 2002; 2:664-74.
8. Orlowski RZ, Baldwin AS. NFκB as a therapeutic target in cancer. Trends Mol Med 2002; 8:385-9.
9. Whiteside ST, Israel A. IκB proteins: Structure, function and regulation. Semin Cancer Biol 1997; 8:75-82.
10. Huxford T, Huang DB, Malek S, Ghosh G. The crystal structure of the IκBα/ NFκB complex reveals mechanisms of NFκB inactivation. Cell 1998; 95:759-70.
11. Mercurio F, Zhu HY, Murray BW, Shevchenko A, Bennett BL, Li JW, Young DB, Barbosa M, Mann M. IKK-1 and IKK-2: Cytokine-activated IκB kinases essential for NFκB activation. Science 1997; 278:860-6.
12. Zandi E, Rothwarf DM, Delhase M, Hayakawa M, Karin M. The IκB kinase complex (IKK) contains two kinase subunits, IKKα and IKKβ, necessary for IκB phosphorylation and NFκB activation. Cell 1997; 91:243-52.
13. Rothwarf DM, Zandi E, Natoli G, Karin M. IKK-γ is an essential regulatory subunit of the IκB kinase complex. Nature 1998; 395:297-300.
14. Yamaoka S, Courtois G, Bessia C, Whiteside ST, Weil R, Agou F, Kirk HE, Kay RJ, Israel A. Complementation cloning of NEMO, a component of the IκB kinase complex essential for NFκB activation. Cell 1998; 93:1231-40.
15. Hayden MS, Ghosh S. Signaling to NFκB. Gene Dev 2004; 18:2195-224.
16. Hacker M, Karin M. Regulation and function of IKK and IKK-related kinases. Science's STKE 2006; 357:1-19.
17. Perkins ND. Integrating cell-signalling pathways with NFκB and IKK function. Nat Rev Mol Cell Bio 2007; 8:49-62.
18. Nurse P. A long twentieth century of the cell cycle and beyond. Cell 2000; 100:71-8.
19. Malumbres M, Barbacid M. Mammalian cyclin-dependent kinases. Trends Biochem Sci 2005; 30:630-41.
20. Nigg EA. Mitotic kinases as regulators of cell division and its checkpoints. Nat Rev Mol Cell Bio 2001; 2:21-32.
21. Kops GJPL, Weaver BAA, Cleveland DW. On the road to cancer: Aneuploidy and the mitotic checkpoint. Nat Rev Cancer 2005; 5:773-85.
22. Hagting A, den Elzen N, Vodermaier HC, Waizenegger IC, Peters JM, Pines J. Human securin proteolysis is controlled by the spindle checkpoint and reveals when the APC/C switches from activation by Cdc20 to Cdh1. J Cell Biol 2002; 157:1125-37.
23. Peters JM. The anaphase-promoting complex: Proteolysis in mitosis and beyond. Mol Cell 2002; 9:931-43.

24. Mistry P, Deacon K, Mistry S, Blank J, Patel R. NFκB promotes survival during mitotic cell cycle arrest. J Biol Chem 2004; 279:1482-90.
25. Bettencourt-Dias M, Giet R, Sinka R, Mazumdar A, Lock WG, Balloux F, Zafiropoulos PJ, Yamaguchi S, Winter S, Carthew RW, Cooper M, Jones D, Frenz L, Glover DM. Genome-wide survey of protein kinases required for cell cycle progression. Nature 2004; 432:980-7.
26. Prajapati S, Tu Z, Yamamoto Y, Gaynor RB. IKK-α regulates the mitotic phase of the cell cycle by modulating Aurora A phosphorylation. Cell Cycle 2006; 5:2371-80.
27. Karin M, Yamamoto Y, Wang QM. The IKK NFκB system: A treasure trove for drug development. Nat Rev Drug Discov 2004; 3:17-26.
28. Karin M, Greten FR. NFκB: Linking inflammation and immunity to cancer development and progression. Nat Rev Immunol 2005; 5:749-59.
29. Burke JR, Pattoli MA, Gregor KR, Brassil PJ, MacMaster JF, McIntyre KW, Yang XX, Iotzova VS, Clarke W, Strnad J, Qiu YP, Zusi FC. BMS-345541 is a highly selective inhibitor of IκB kinase that binds at an allosteric site of the enzyme and blocks NFκB-dependent transcription in mice. J Biol Chem 2003; 278:1450-6.
30. McIntyre KW, Shuster DJ, Gillooly KM, Dambach DM, Pattoli MA, Lu P, Zhou XD, Qiu YP, Zusi FC, Burke JR. A highly selective inhibitor of IκB kinase, BMS-345541, blocks both joint inflammation and destruction in collagen-induced arthritis in mice. Arthritis Rheum 2003; 48:2652-9.
31. MacMaster JF, Dambach DM, Lee DB, Berry KK, Qiu Y, Zusi FC, Burke JR. An inhibitor of IκB kinase, BMS-345541, blocks endothelial cell adhesion molecule expression and reduces the severity of dextran sulfate sodium-induced colitis in mice. Inflamm Res 2003; 52:508-11.
32. Everhart MB, Wei H, Sherrill TP, Arutiunov M, Polosukhin VV, Burke JR, Sadikot RT, Christman JW, Yull FE, Blackwell TS. Duration and intensity of NFκB activity determine the severity of endotoxin-induced acute lung injury. J Immunol 2006; 176:4995-5005.
33. Townsend RM, Postelnek J, Susulic V, McIntyre KW, Shuster DJ, Qiu YP, Zusi FC, Burke JR. A highly selective inhibitor of IκB kinase, BMS-345541, augments graft survival mediated by suboptimal immunosuppression in a murine model of cardiac graft rejection. Transplantation 2004; 77:1090-4.
34. Yang JM, Amiri KI, Burke JR, Schmid JA, Richmond A. BMS-345541 targets inhibitor of κB kinase and induces apoptosis in melanoma: Involvement of nuclear factor κB and mitochondria pathways. Clin Cancer Res 2006; 12:950-60.
35. van Vugt MATM, Smits VAJ, Klompmaker R, Medema RH. Inhibition of polo-like kinase-1 by DNA damage occurs in an ATM- or ATR-dependent fashion. J Biol Chem 2001; 276:41656-60.
36. Wei Y, Yu LL, Bowen J, Gorovsky MA, Allis CD. Phosphorylation of histone H3 is required for proper chromosome condensation and segregation. Cell 1999; 97:99-109.
37. Hendzel MJ, Wei Y, Mancini MA, VanHooser A, Ranalli T, Brinkley BR, BazettJones DP, Allis CD. Mitosis-specific phosphorylation of histone H3 initiates primarily within pericentromeric heterochromatin during G_2 and spreads in an ordered fashion coincident with mitotic chromosome condensation. Chromosoma 1997; 106:348-60.
38. Pines J, Hunter T. Human cyclin-a is adenovirus e1a-associated protein-p60 and behaves differently from cyclin-B. Nature 1990; 346:760-3.
39. Ferrari S. Protein kinases controlling the onset of mitosis. Cell Mol Life Sci 2006; 63:781-95.
40. Li JJ, Li SA. Mitotic kinases: The key to duplication, segregation, and cytokinesis errors, chromosomal instability, and oncogenesis. Pharmacol Therapeut 2006; 111:974-84.
41. Izumi T, Maller JL. Elimination of cdc2 phosphorylation sites in the cdc25 phosphatase blocks initiation of m-phase. Mol Biol Cell 1993; 4:1337-50.
42. Sciortino S, Gurtner A, Manni I, Fontemaggi G, Dey A, Sacchi A, Ozato K, Piaggio G. The *cyclin B1* gene is actively transcribed during mitosis in HeLa cells. Embo Rep 2001; 2:1018-23.
43. Vassilev LT, Tovar C, Chen SQ, Knezevic D, Zhao XL, Sun HM, Heimbrook DC, Chen L. Selective small-molecule inhibitor reveals critical mitotic functions of human CDK1. P Natl Acad Sci USA 2006; 103:10660-5.
44. Meijer L, Borgne A, Mulner O, Chong JPJ, Blow JJ, Inagaki N, Inagaki M, Delcros JG, Moulinoux JP. Biochemical and cellular effects of roscovitine, a potent and selective inhibitor of the cyclin-dependent kinases cdc2, cdk2 and cdk5. Eur J Biochem 1997; 243:527-36.
45. Lansing TJ, McConnell RT, Duckett DR, Spehar GM, Knick VB, Hassler DF, Noro N, Furuta M, Emmitte KA, Gilmer TM, Mook RA, Cheung M. In vitro biological activity of a novel small-molecule inhibitor of polo-like kinase 1. Mol Cancer Ther 2007; 6:450-9.
46. Eckerdt F, Strebhardt K. Polo-like kinase 1: Target and regulator of anaphase-promoting complex/cyclosome-dependent proteolysis. Cancer Res 2006; 66:6895-8.
47. D'Angiolella V, Mari C, Nocera D, Rametti L, Grieco D. The spindle checkpoint requires cyclin-dependent kinase activity. Gene Dev 2003; 17:2520-5.
48. Greten FR, Karin M. The IKK/ NFκB activation pathway - A target for prevention and treatment of cancer. Cancer Lett 2004; 206:193-9.
49. Park KJ, Krishnan V, O'Malley BW, Yamamoto Y, Gaynor RB. Formation of an IKK-α-dependent transcription complex is required for estrogen receptor-mediated gene activation. Mol Cell 2005; 18:71-82.
50. Cao YX, Bonizzi G, Seagroves TN, Greten FR, Johnson R, Schmidt EV, Karin M. IKK alpha provides an essential link between RANK signaling and cyclin D1 expression during mammary gland development. Cell 2001; 107:763-75.
51. Albanese C, Wu KM, D'Amico M, Jarrett C, Joyce D, Hughes J, Hulit J, Sakamaki T, Fu MF, Ben-Ze'ev A, Bromberg JF, Lamberti C, Verma U, Gaynor RB, Byers SW, Pestell RG. IKKα regulates mitogenic signaling through transcriptional induction of cyclin D1 via Tcf. Mol Biol Cell 2003; 14:585-99.
52. Hinz M, Krappmann D, Eichten A, Heder A, Scheidereit C, Strauss M. NFκB function in growth control: Regulation of cyclin D1 expression and G_0G_1-to-S-Phase transition. Mol Cell Biol 1999; 19:2690-8.
53. Kwak YT, Li R, Becerra CR, Tripathy D, Frenkel EP, Verma UN. IκB kinase a regulates subcellular distribution and turnover of cyclin D1 by phosphorylation. J Biol Chem 2005; 280:38888-33945.
54. Dutertre S, Cazales M, Quaranta M, Froment C, Trabut V, Dozier C, Mirey G, Bouche JP, Theis-Febvre N, Schmitt E, Monsarrat B, Prigent C, Ducommun B. Phosphorylation of CDC25B by Aurora-A at the centrosome contributes to the G_2-M transition. J Cell Sci 2004; 117:2523-31.
55. Kramer A, Lukas J, Bartek J. Checking out the centrosome. Cell Cycle 2004; 3:1390-3.
56. Michel L, Diaz-Rodriguez E, Narayan G, Hernando E, Murty VVVS, Benezra R. Complete loss of the tumor suppressor MAD2 causes premature cyclin B degradation and mitotic failure in human somatic cells. P Natl Acad Sci USA 2004; 101:4459-64.
57. Canman JC, Salmon ED, Fang GW. Inducing precocious anaphase in cultured mammalian cells. Cell Motil Cytoskel 2002; 52:61-5.
58. Murray AW. Recycling the cell cycle: Cyclins revisited. Cell 2004; 116:221-34.
59. Barr FA, Sillje HHW, Nigg EA. Polo-like kinases and the orchestration of cell division. Nat Rev Mol Cell Bio 2004; 5:429-40.
60. Nurse P. Universal control mechanism regulating onset of m-phase. Nature 1990; 344:503-8.
61. Coleman TR, Dunphy WG. Cdc2 regulatory factors. Curr Opin Cell Biol 1994; 6:877-82.

5.2. Rapid Cytopathic Effects of *Clostridium perfringens* Beta-Toxin on Porcine Endothelial Cells

Corinne Gurtner, Francesca Popescu, Marianne Wyder, Esther Sutter, Friederike Zeeh, Joachim Frey, Conrad von Schubert, and Horst Posthaus

Infection and Immunity (2010) vol. 78 pp. 2966-2973

Figure contributions: time-lapse recordings of the cytopathic effect of *C. perfringens* type C β-toxin (CPB) on primary porcine aortic endothelial cells and porcine fibroblasts (included as supplementary data).

INFECTION AND IMMUNITY, July 2010, p. 2966–2973 Vol. 78, No. 7
0019-9567/10/$12.00 doi:10.1128/IAI.01284-09

Rapid Cytopathic Effects of *Clostridium perfringens* Beta-Toxin on Porcine Endothelial Cells▽†

Corinne Gurtner,[1] Francesca Popescu,[1] Marianne Wyder,[1] Esther Sutter,[1] Friederike Zeeh,[2] Joachim Frey,[3] Conrad von Schubert,[4] and Horst Posthaus[1]*

Institute of Animal Pathology,[1] Porcine Clinic,[2] Institute of Veterinary Bacteriology,[3] and Division of Molecular Pathobiology,[4] Vetsuisse Faculty, University of Bern, 3001 Bern, Switzerland

Received 17 November 2009/Returned for modification 19 December 2009/Accepted 10 April 2010

***Clostridium perfringens* type C isolates cause fatal, segmental necro-hemorrhagic enteritis in animals and humans. Typically, acute intestinal lesions result from extensive mucosal necrosis and hemorrhage in the proximal jejunum. These lesions are frequently accompanied by microvascular thrombosis in affected intestinal segments. In previous studies we demonstrated that there is endothelial localization of *C. perfringens* type C β-toxin (CPB) in acute lesions of necrotizing enteritis. This led us to hypothesize that CPB contributes to vascular necrosis by directly damaging endothelial cells. By performing additional immunohistochemical studies using spontaneously diseased piglets, we confirmed that CPB binds to the endothelial lining of vessels showing early signs of thrombosis. To investigate whether CPB can disrupt the endothelium, we exposed primary porcine aortic endothelial cells to *C. perfringens* type C culture supernatants and recombinant CPB. Both treatments rapidly induced disruption of the actin cytoskeleton, cell border retraction, and cell shrinkage, leading to destruction of the endothelial monolayer *in vitro*. These effects were followed by cell death. Cytopathic and cytotoxic effects were inhibited by neutralization of CPB. Taken together, our results suggest that CPB-induced disruption of endothelial cells may contribute to the pathogenesis of *C. perfringens* type C enteritis.**

The anaerobic, spore-forming bacterium *Clostridium perfringens* is an important Gram-positive pathogen of humans and animals (18, 42). It causes diverse gastrointestinal diseases, such as food poisoning, enterotoxemia, and enteritis, as well as wound infections and septicemias (37). The virulence of different *C. perfringens* strains is related to the production of a large array of exotoxins (34). *C. perfringens* type C isolates are defined by production of two major toxins, α-toxin (CPA) and β-toxin (CPB). In addition, type C isolates may secrete other toxins, such as β2-toxin (CPB2), perfringolysin (PFO), enterotoxin (CPE), and TpeL (2, 34, 36) *C. perfringens* type C strains cause severe, acute, necrotizing enteritis in livestock and humans (18, 42). Outbreaks of human type C enteritis were recorded after the Second World War in Germany (20), but this disease has been reported only sporadically in developed countries (25, 27, 39, 51). A similar disease has been diagnosed more frequently in parts of Southeast Asia (7, 17, 26), particularly in the highlands of Papua New Guinea (23), where it was a frequent cause of childhood mortality until vaccination programs were initiated (24). *C. perfringens* type C causes enteritis more frequently in animals, such as calves, sheep, goats, and particularly pigs (42, 43). Typically, neonatal piglets are affected from the first day of life until they are approximately 3 weeks old. The peracute to acute type of the disease affects piglets within the first few days postpartum (12, 14, 43). Macroscopic lesions at necropsy are pathognomonic, with deep, segmental mucosal necrosis and massive hemorrhage in the small intestine. In most cases the lesions are confined to the proximal jejunum; however, they can extend into the distal small intestine and the colon. This suggests that lesions are initiated in the upper small intestine and can spread rapidly throughout the intestine. In addition to these marked necrohemorrhagic lesions, thrombosis of small vessels in the lamina propria and submucosa is a consistent finding (12, 14). A more protracted clinical course of type C enteritis is seen mainly in piglets that die when they are 1 to 3 weeks old (12, 14, 43). The pathological lesion is a segmental to diffuse fibrino-necrotizing enteritis. Histopathologically, such cases are characterized by demarcation of the deeply necrotic mucosa by marked infiltration of neutrophilic granulocytes. Similar acute and subacute forms of type C enteritis also occur in humans (6, 18, 21). In humans, however, subacute lesions are more often described as multifocal patchy necrosis of the small intestine. Again, mucosal and submucosal vascular thrombosis is a frequent finding, especially in acute lesions (20, 21).

Besides the clear epidemiological evidence for the importance of CPB in type C enteritis (41, 42), recent experimental studies using a rabbit intestinal loop model and a mouse infection model clearly demonstrated that CPB is the essential virulence factor of type C strains (38, 47, 49). In rabbit ileal loops, application of purified CPB and infection with *C. perfringens* type C strains caused villous tip necrosis, which indicated that there was initial intestinal epithelial damage. Vascular thrombosis in mucosal and submucosal vessels was also observed in this model. In general, the vascular damage observed in naturally occurring and experimentally induced type

* Corresponding author. Mailing address: Institute of Animal Pathology, Vetsuisse Faculty, University of Bern, P.O. Box 8466, 3001 Bern, Switzerland. Phone: 41-(0)31-6312399. Fax: 41-(0)31-6312635. E-mail: horst.posthaus@itpa.unibe.ch.

† Supplemental material for this article may be found at http://iai.asm.org/.

▽ Published ahead of print on 19 April 2010.

6. Curriculum vitae

Personal information

Born	November 12, 1979
Nationality	German
Marital status	unmarried
Position held	PhD student Graduate School for Cellular and Biomedical Science, University of Bern
Work address	Molecular Pathobiology DCR-VPH, University of Bern Länggassstrasse 122 3012 Bern, Switzerland +41 (0)31 631 2408 conrad.vonschubert@mopa.unibe.ch
Home address	Altenbergstrasse 38 3013 Bern, Switzerland +41 (0)78 842 1457

Education

2006-2010	PhD student	Graduate School for Cellular and Biomedical Science, University of Bern
2004-2006	Master of science	Cell biology, University of Bern
2001-2004	Undergraduate studies	Biology, University of Bern
1999-2001	Undergraduate studies	Biology, Technical University of Munich, Germany
until 1999	High school	German School Geneva, Switzerland

Research experience

2006-2010	Graduate studies in the laboratory of Prof. Dirk A.E. Dobbelaere, University of Bern
2004-2006	Undergraduate studies in the laboratory of Prof. Dirk A.E. Dobbelaere, University of Bern

Collaborations

2009-2010	Dr Horst Posthaus, Marianne Wyder, Corinne Gurtner, University of Bern; experimental setup and performance of live imaging; cytopathic effects of Clostridium perfringens beta-toxin on porcine and human endothelial cells.
	Prof. Dr. Erich A. Nigg, Max-Planck Institute for Biochemistry; Biozentrum, University of Basel

Oral presentations

2009	Institute of Cell Biology, University of Bern: „Propagation of *Theileria* schizonts - hitching a ride to division“
2007	4th Happycomplexan Symposium, Imperial College, London; UK: „Aspects of *Theileria*-induced host cell transformation: hitching a ride to division“
	Molecular Parasitology Meeting, Marine Biological Laboratory, Woods Hole, USA: „Identification of a *Theileria* surface protein potentially involved in cytokinesis“
	American Society of Tropical Medicine and Hygiene, 56th annual meeting, Philadelphia, USA: „Identification of a *Theileria* surface protein potentially involved in cytokinesis“
	COST action 857, Geneva, Switzerland: „Identification of a *Theileria* surface protein potentially involved in cytokinesis“

Poster presentations

2010	EMBO meeting „Microtubules: Structure, Regulation and Fuctions“, EMBL Heidelberg
2009	32nd annual meeting of the German Society for Cell Biology, University of Konstanz
2008-2010	Annual PhD symposium, Graduate School for Cellular and Biomedical Science, University of Bern

Courses / scientific retreats

2006-2010	PhD program provided by the Graduate School for Cellular and Biomedical Science, University of Bern
2007	PhD students retreat „Apicomplexan biology in the post-genomic era“, provided by the European Cooperation in Science and Technology, Geneva
	Light Microscopy and Imaging course provided by the Swiss Committee for Molecular Biology, University of Geneva

Teaching experience

2009	Seminar in signal transduction
2007-2009	Bench-side training of students at pre-doctoral level, 1 month/year
2006-2009	Tutor at the imaging facility of the Vetsuisse Campus, University of Bern

Awards

2007	Oral presentation award at the Molecular Parasitology Meeting, Marine Biological Laboratory, Woods Hole, USA; awarded by the American Society of Tropical Medicine and Hygiene

References

Prof. Dr. Dirk A.E. Dobbelaere
DCR-VPH, Molecular Pathobiology, Länggassstrasse 122
3012 Bern, Switzerland
+41 31 631 2625
dirk.dobbelaere@mopa.unibe.ch

Prof. Dr. Beat Suter
Institute of Cell Biology, University of Bern, Baltzerstrasse 4
3012 Bern, Switzerland
+41 31 631 4715
beat.suter@izb.unibe.ch

Prof. Dr. Andrew Hemphill
Institute of Parasitology, University of Bern, Länggassstrasse 122
3012 Bern, Switzerland
+41 31 631 2384
andrew.hemphill@ipa.unibe.ch

Languages

- German (mother tongue)
- English (fluent, C2)
- French (fluent, B2)

Non-scientific work experience

2003	International Conservation Union (IUCN), Gland, Switzerland.
	Implementation and evaluation of a survey on the incorporation of carbon sequestration and climate change adaptation measures into IUCN field projects; 2 month internship during semester break
2002	International Organization for Migration (IOM), German Forced Labour Compensation Programme, Geneva, Switzerland.
	Evaluation and classification of worldwide requests concerning the financial compensation for National Socialist injustice, maintenance and updating of archives; 3 month employment during semester break

7. Publications

2010 von Schubert, C., Xue, G., Schmuckli-Maurer, J., Nigg, E.A., Dobbelaere, D. A.
The transforming parasite Theileria co-opts host cell mitotic and central spindles to persist in continuously dividing cells.
PLoS Biology, in press

Xue, G.*, von Schubert, C.*, Hermann, P., Peyer, M., Schmuckli-Maurer, J., Bütikofer, P., Langsley, G., Dobbelaere, D.A.
Characterisation of gp34, a GPI-anchored protein expressed by schizonts of Theileria parva and T. annulata.
Molecular & Biochemical Parasitology (2010) vol. 172 (2) pp.113-120
* shared first-authorship

Gurtner, C., Popescu, F., Wyder, M.; Sutter, E., Zeeh, F., von Schubert, C., Frey, J., Posthaus, H.
Rapid Cytopathic Effects of C. perfringens Beta-Toxin on Porcine Endothelial Cells.
Infection and Immunity (2010) vol. 78 (7) pp. 2966-2973

2007 Blazkova, H., von Schubert, C., Keith Mikule, K., Rebekka Schwab, R. Angliker, N., Schmuckli- Maurer, J., Paula C. Fernandez, P., C., Doxsey, S. and Dobbelaere, D. A.
The IKK inhibitor BMS-345541 affects multiple mitotic cell cycle transitions.
Cell Cycle (2007) vol. 6 (20) pp. 2531-40

8. Acknowledgements

I would like to express my dearest gratitude to all people who made this Ph.D. thesis possible. Above all, I deeply thank my parents and my sister for their love and permanent support throughout the ups and downs of my quest as a PhD student. A big and warm ‚thank you' also goes to my two grand mothers, who encouraged me whenever they could.

Of course, all this would have never happened without the trust and faith I received from Dirk Dobbelaere. I am very grateful for receiving the opportunity to work on several projects in his group and for being granted such a lot of freedom in the lab. I always appreciated his creative and passionate spirit that often led to heated, but eventually very fruitful discussions. I was also thrilled by the numerous meetings I could attend, which taught me what science was all about.

Also, very special thanks go Jacqueline Schmuckli for being a fantastic supervisor during my master's thesis and lab psychologist during my PhD.

I thank all the dear people with whom I shared projects: Hana Blazkova, Jacqueline Schmuckli, Gongda Xue, Pascal Hermann, Martin Baumgartner, Kerry Woods, Andrew Hemphill, Regina Maushagen and Martina Peyer. It was a pleasure to team up with them.

The same applies to the other members of the lab who, over the years, contributed to the warm and enjoyable atmosphere in the group, including Iana Parvanova, Carlo Casanova, Marc Witschi, Stefanie Schmied, Sarah Affentranger, Romina Theiler, Olga Wiens, Min Ma and Adrian Segiser. Stephan Grimm is especially thanked for his technical assistance and constant good mood.

I would also like to thank Horst Posthaus, Marianne Wyder and Corinne Gurtner for offering me the collaboration in documenting the cytopathic effects of the *C. perfringens* β-toxin.

Prof. Beat Suter and Prof. Andrew Hemphill are thanked for their committed role as a co-referee and mentor, respectively. I also acknowledge the organization of the PhD program by the Graduate School for Cellular and Biomedial Science, notably Marlene Wolf, Gabrielle Favre and the expert committee for their efforts.

I gratefully acknowledge the financial support that came from grants to Prof. Dirk Dobbelaere: Swiss National Science Foundation (3100A0-116653), The Wellcome Animal Health Initiative (GR075820MA), Integrated Consortium on Ticks and Tick-borne Diseases ICTTD (510561).

9. References

1. Dobrowolski, J.M. and L.D. Sibley, *Toxoplasma invasion of mammalian cells is powered by the actin cytoskeleton of the parasite.* Cell, 1996. **84**(6): p. 933-9.
2. Meissner, M., D. Schluter, and D. Soldati, *Role of Toxoplasma gondii myosin A in powering parasite gliding and host cell invasion.* Science, 2002. **298**(5594): p. 837-40.
3. Dobbelaere, D.A.E., S.Z. Shapiro, and P. Webster, *Identification of a surface antigen on Theileria parva sporozoites by monoclonal antibody.* Proc. Natl. Acad. Sci. U S A, 1985. **82**(6): p. 1771-1775.
4. Nene, V., et al., *Characterisation of the gene encoding a candidate vaccine antigen of Theileria parva sporozoites.* Mol Biochem Parasitol, 1992. **51**(1): p. 17-27.
5. Hall, R., et al., *Mimicry of elastin repetitive motifs by Theileria annulata sporozoite surface antigen.* Mol Biochem Parasitol, 1992. **53**(1-2): p. 105-112.
6. Shaw, M.K., L.G. Tilney, and A.J. Musoke, *The entry of Theileria parva sporozoites into bovine lymphocytes: evidence for MHC class I involvement.* J. Cell. Biol., 1991. **113**(1): p. 87-101.
7. Shaw, M.K., et al., *MHC class I molecules are an essential cell surface component involved in Theileria parva sporozoite binding to bovine lymphocytes.* J. Cell Sci., 1995. **108**(Pt 4): p. 1587-1596.
8. Syfrig, J., et al., *Proteolytic cleavage of surface proteins enhances susceptibility of lymphocytes to invasion by Theileria parva sporozoites.* Eur. J. Cell Biol., 1998. **76**(2): p. 125-132.
9. Dobbelaere, D.A., et al., *Theileria parva: expression of a sporozoite surface coat antigen.* Exp. Parasitol., 1985. **60**(1): p. 90-100.
10. Webster, P., D.A. Dobbelaere, and D.W. Fawcett, *The entry of sporozoites of Theileria parva into bovine lymphocytes in vitro. Immunoelectron microscopic observations.* Eur J Cell Biol, 1985. **36** (2): p. 157-162.
11. Shaw, M.K., *Cell invasion by Theileria sporozoites.* Trends Parasitol, 2003. **19**(1): p. 2-6.
12. Shiels, B., et al., *Alteration of host cell phenotype by Theileria annulata and Theileria parva: mining for manipulators in the parasite genomes.* Int J Parasitol, 2006. **36**(1): p. 9-21.
13. Baumgartner, M., et al., *Constitutive PI3-K activity is essential for proliferation, but not survival, of Theileria parva-transformed B cells.* Cell Microbiol, 2000. **2**(4): p. 329-39.
14. Heussler, V.T., et al., *The Akt/PKB pathway is constitutively activated in Theileria- transformed leucocytes, but does not directly control constitutive NF- kappaB activation.* Cell Microbiol, 2001. **3**(8): p. 537-550.
15. Dobbelaere, D.A. and P. Kuenzi, *The strategies of the Theileria parasite: a new twist in host-pathogen interactions.* Curr Opin Immunol, 2004. **16**(4): p. 524-30.
16. Adamson, R., et al., *Loss of matrix metalloproteinase 9 activity in Theileria annulata- attenuated cells is at the transcriptional level and is associated with differentially expressed AP-1 species.* Mol Biochem Parasitol, 2000. **106**(1): p. 51-61.
17. Kuenzi, P., P. Schneider, and D.A. Dobbelaere, *Theileria parva-transformed T cells show enhanced resistance to Fas/Fas ligand-induced apoptosis.* J Immunol, 2003. **171**(3): p. 1224-31.
18. Ricci, M.S., et al., *Reduction of TRAIL-induced Mcl-1 and cIAP2 by c-Myc or sorafenib sensitizes resistant human cancer cells to TRAIL-induced death.* Cancer Cell, 2007. **12**(1): p. 66-80.
19. Ricci, M.S., et al., *Direct repression of FLIP expression by c-myc is a major determinant of TRAIL sensitivity.* Mol Cell Biol, 2004. **24**(19): p. 8541-55.
20. Dessauge, F., et al., *c-Myc activation by Theileria parasites promotes survival of infected B-lymphocytes.* Oncogene, 2005. **24**(6): p. 1075-83.
21. Heussler, V.T., et al., *Hijacking of host cell IKK signalosomes by the transforming parasite Theileria.* Science, 2002. **298**(5595): p. 1033-6.
22. Dyer, M., et al., *Theileria annulata: alterations in phosphoprotein and protein kinase activity profiles of infected leukocytes of the bovine host, Bos taurus.* Exp. Parasitol., 1992. **74**(2): p. 216-227.
23. ole MoiYoi, O.K., et al., *Evidence for the induction of casein kinase II in bovine lymphocytes transformed by the intracellular protozoan parasite Theileria parva.* Embo J, 1993. **12**(4): p. 1621-1631.

24. Pain, A., et al., *Genome of the host-cell transforming parasite Theileria annulata compared with T. parva.* Science, 2005. **309**(5731): p. 131-3.
25. Gardner, M.J., et al., *Genome sequence of Theileria parva, a bovine pathogen that transforms lymphocytes.* Science, 2005. **309**(5731): p. 134-7.
26. Swan, D.G., et al., *Evidence for localisation of a Theileria parasite AT hook DNA-binding protein to the nucleus of immortalised bovine host cells.* Mol Biochem Parasitol, 1999. **101**(1-2): p. 117-129.
27. Schmuckli-Maurer, J., et al., *Expression analysis of the Theileria parva subtelomere-encoded variable secreted protein gene family.* PLoS One, 2009. **4**(3): p. e4839.
28. Irvin, A.D. and W.I. Morrison, *Immunopathology, immunology and immunoprophylaxis of Theileria infection*. Immune responses in parasite infection: immunology, immunopathology and immunoprophylaxis, ed. E.J.L. Soulsby. Vol. 3. 1987, Boca Ratan, Florida: CRC Press. 223-274.
29. Shiels, B., et al., *Disruption of synchrony between parasite growth and host cell division is a determinant of differentiation to the merozoite in Theileria annulata.* J Cell Sci, 1992. **101**(Pt 1): p. 99-107.
30. Schmuckli-Maurer, J., B. Shiels, and D.A. Dobbelaere, *Stochastic induction of Theileria annulata merogony in vitro by chloramphenicol.* Int J Parasitol, 2008.
31. Hulliger, L., C.G. Brown, and J.K. Wilde, *Transition of developmental stages of Theileria parva in vitro at high temperature.* Nature, 1966. **211**(46): p. 328-329.
32. Shaw, M.K. and L.G. Tilney, *How individual cells develop from a syncytium: merogony in Theileria parva (Apicomplexa).* J Cell Sci, 1992. **101**(Pt 1): p. 109-123.
33. Hulliger, L., et al., *Mode of Multiplication of Theileria in Cultures of Bovine Lymphocytic Cells.* Nature, 1964. **203**: p. 728-30.
34. Nigg, E.A., *Mitotic kinases as regulators of cell division and its checkpoints.* Nat Rev Mol Cell Biol, 2001. **2**(1): p. 21-32.
35. Heald, R., et al., *Self-organization of microtubules into bipolar spindles around artificial chromosomes in Xenopus egg extracts.* Nature, 1996. **382**(6590): p. 420-5.
36. Sharp, D.J., et al., *The bipolar kinesin, KLP61F, cross-links microtubules within interpolar microtubule bundles of Drosophila embryonic mitotic spindles.* J Cell Biol, 1999. **144**(1): p. 125-38.
37. Musacchio, A. and E.D. Salmon, *The spindle-assembly checkpoint in space and time.* Nat Rev Mol Cell Biol, 2007. **8**(5): p. 379-93.
38. Morales-Mulia, S. and J.M. Scholey, *Spindle pole organization in Drosophila S2 cells by dynein, abnormal spindle protein (Asp), and KLP10A.* Mol Biol Cell, 2005. **16**(7): p. 3176-86.
39. Glotzer, M., *The 3Ms of central spindle assembly: microtubules, motors and MAPs.* Nat Rev Mol Cell Biol, 2009. **10**(1): p. 9-20.
40. Barr, F.A. and U. Gruneberg, *Cytokinesis: placing and making the final cut.* Cell, 2007. **131**(5): p. 847-60.
41. Mishima, M., S. Kaitna, and M. Glotzer, *Central spindle assembly and cytokinesis require a kinesin-like protein/RhoGAP complex with microtubule bundling activity.* Dev Cell, 2002. **2**(1): p. 41-54.
42. Wheatley, S.P., et al., *Phosphorylation by aurora-B negatively regulates survivin function during mitosis.* Cell Cycle, 2007. **6**(10): p. 1220-30.
43. Williams, B.C., et al., *The Drosophila kinesin-like protein KLP3A is a midbody component required for central spindle assembly and initiation of cytokinesis.* J Cell Biol, 1995. **129**(3): p. 709-23.
44. Piekny, A., M. Werner, and M. Glotzer, *Cytokinesis: welcome to the Rho zone.* Trends Cell Biol, 2005. **15**(12): p. 651-8.
45. Glotzer, M., *The molecular requirements for cytokinesis.* Science, 2005. **307**(5716): p. 1735-9.
46. Yuce, O., A. Piekny, and M. Glotzer, *An ECT2-centralspindlin complex regulates the localization and function of RhoA.* J Cell Biol, 2005. **170**(4): p. 571-82.
47. Steigemann, P. and D.W. Gerlich, *Cytokinetic abscission: cellular dynamics at the midbody.* Trends Cell Biol, 2009. **19**(11): p. 606-16.
48. Sen, S., *Aneuploidy and cancer.* Curr Opin Oncol, 2000. **12**(1): p. 82-8.
49. Barr, F.A., H.H. Sillje, and E.A. Nigg, *Polo-like kinases and the orchestration of cell division.* Nat Rev Mol Cell Biol, 2004. **5**(6): p. 429-40.

50. Timofeev, O., et al., *Cdc25 phosphatases are required for timely assembly of CDK1-cyclin B at the G2/M transition.* J Biol Chem, 2010. **285**(22): p. 16978-90.
51. Peters, J.M., *The anaphase promoting complex/cyclosome: a machine designed to destroy.* Nat Rev Mol Cell Biol, 2006. **7**(9): p. 644-56.
52. Vecchione, A., et al., *Fez1/Lzts1 absence impairs Cdk1/Cdc25C interaction during mitosis and predisposes mice to cancer development.* Cancer Cell, 2007. **11**(3): p. 275-89.
53. Bollen, M., D.W. Gerlich, and B. Lesage, *Mitotic phosphatases: from entry guards to exit guides.* Trends Cell Biol, 2009. **19**(10): p. 531-41.
54. Salaun, P., Y. Rannou, and C. Prigent, *Cdk1, Plks, Auroras, and Neks: the mitotic bodyguards.* Adv Exp Med Biol, 2008. **617**: p. 41-56.
55. Carmena, M. and W.C. Earnshaw, *The cellular geography of aurora kinases.* Nat Rev Mol Cell Biol, 2003. **4**(11): p. 842-54.
56. van de Weerdt, B.C. and R.H. Medema, *Polo-like kinases: a team in control of the division.* Cell Cycle, 2006. **5**(8): p. 853-64.
57. Archambault, V. and D.M. Glover, *Polo-like kinases: conservation and divergence in their functions and regulation.* Nat Rev Mol Cell Biol, 2009. **10**(4): p. 265-275.
58. Zimmerman, W.C. and R.L. Erikson, *Polo-like kinase 3 is required for entry into S phase.* Proc Natl Acad Sci U S A, 2007. **104**(6): p. 1847-52.
59. Myer, D.L., M. Bahassi el, and P.J. Stambrook, *The Plk3-Cdc25 circuit.* Oncogene, 2005. **24**(2): p. 299-305.
60. Bahassi el, M., et al., *Mammalian Polo-like kinase 3 (Plk3) is a multifunctional protein involved in stress response pathways.* Oncogene, 2002. **21**(43): p. 6633-40.
61. Matthew, E.M., et al., *Replication stress, defective S-phase checkpoint and increased death in Plk2-deficient human cancer cells.* Cell Cycle, 2007. **6**(20): p. 2571-8.
62. Matthew, E.M., et al., *The p53 target Plk2 interacts with TSC proteins impacting mTOR signaling, tumor growth and chemosensitivity under hypoxic conditions.* Cell Cycle, 2009. **8**(24).
63. Bettencourt-Dias, M. and D.M. Glover, *Centrosome biogenesis and function: centrosomics brings new understanding.* Nat Rev Mol Cell Biol, 2007. **8**(6): p. 451-63.
64. Swallow, C.J., et al., *Sak/Plk4 and mitotic fidelity.* Oncogene, 2005. **24**(2): p. 306-12.
65. Winkles, J.A. and G.F. Alberts, *Differential regulation of polo-like kinase 1, 2, 3, and 4 gene expression in mammalian cells and tissues.* Oncogene, 2005. **24**(2): p. 260-6.
66. Elia, A.E., L.C. Cantley, and M.B. Yaffe, *Proteomic screen finds pSer/pThr-binding domain localizing Plk1 to mitotic substrates.* Science, 2003. **299**(5610): p. 1228-31.
67. Park, J.E., et al., *Polo-box domain: a versatile mediator of polo-like kinase function.* Cell Mol Life Sci, 2010.
68. Petronczki, M., P. Lenart, and J.M. Peters, *Polo on the Rise-from Mitotic Entry to Cytokinesis with Plk1.* Dev Cell, 2008. **14**(5): p. 646-59.
69. Takaki, T., et al., *Polo-like kinase 1 reaches beyond mitosis--cytokinesis, DNA damage response, and development.* Curr Opin Cell Biol, 2008. **20**(6): p. 650-60.
70. Seki, A., et al., *Bora and the kinase Aurora a cooperatively activate the kinase Plk1 and control mitotic entry.* Science, 2008. **320**(5883): p. 1655-8.
71. Macurek, L., et al., *Polo-like kinase-1 is activated by aurora A to promote checkpoint recovery.* Nature, 2008. **455**(7209): p. 119-23.
72. Lindon, C. and J. Pines, *Ordered proteolysis in anaphase inactivates Plk1 to contribute to proper mitotic exit in human cells.* J Cell Biol, 2004. **164**(2): p. 233-41.
73. Qian, Y.W., et al., *Activated polo-like kinase Plx1 is required at multiple points during mitosis in Xenopus laevis.* Mol Cell Biol, 1998. **18**(7): p. 4262-71.
74. Sumara, I., et al., *Roles of polo-like kinase 1 in the assembly of functional mitotic spindles.* Curr Biol, 2004. **14**(19): p. 1712-22.
75. Bassermann, F., et al., *The Cdc14B-Cdh1-Plk1 axis controls the G2 DNA-damage-response checkpoint.* Cell, 2008. **134**(2): p. 256-67.
76. Kang, Y.H., et al., *Self-regulated Plk1 recruitment to kinetochores by the Plk1-PBIP1 interaction is critical for proper chromosome segregation.* Mol Cell, 2006. **24**(3): p. 409-22.
77. Neef, R., et al., *Choice of Plk1 docking partners during mitosis and cytokinesis is controlled by the activation state of Cdk1.* Nat Cell Biol, 2007. **9**(4): p. 436-44.
78. Hanisch, A., et al., *Different Plk1 functions show distinct dependencies on Polo-Box domain-mediated targeting.* Mol Biol Cell, 2006. **17**(1): p. 448-59.

79. Watanabe, N., et al., *Deficiency in chromosome congression by the inhibition of Plk1 polo box domain-dependent recognition.* J Biol Chem, 2009. **284**(4): p. 2344-53.
80. Reindl, W., et al., *Inhibition of polo-like kinase 1 by blocking polo-box domain-dependent protein-protein interactions.* Chem Biol, 2008. **15**(5): p. 459-66.
81. Fawcett, D., A. Musoke, and W. Voigt, *Interaction of sporozoites of Theileria parva with bovine lymphocytes in vitro. I. Early events after invasion.* Tissue Cell, 1984. **16**(6): p. 873-884.
82. Musisi, F.L., et al., *The fine structural relationship between Theileria schizonts and infected bovine lymphoblasts from cultures.* Z Parasitenkd, 1981. **65**(1): p. 31-41.
83. Shaw, M.K., *Theileria parva: sporozoite entry into bovine lymphocytes is not dependent on the parasite cytoskeleton.* Exp Parasitol, 1999. **92**(1): p. 24-31.
84. Kline-Smith, S.L. and C.E. Walczak, *Mitotic spindle assembly and chromosome segregation: refocusing on microtubule dynamics.* Mol Cell, 2004. **15**(3): p. 317-27.
85. De Brabander, M., et al., *Taxol induces the assembly of free microtubules in living cells and blocks the organizing capacity of the centrosomes and kinetochores.* Proc Natl Acad Sci U S A, 1981. **78**(9): p. 5608-612.
86. Lane, H.A. and E.A. Nigg, *Antibody microinjection reveals an essential role for human polo-like kinase 1 (Plk1) in the functional maturation of mitotic centrosomes.* J Cell Biol, 1996. **135**(6 Pt 2): p. 1701-13.
87. Casenghi, M., et al., *Polo-like kinase 1 regulates Nlp, a centrosome protein involved in microtubule nucleation.* Dev Cell, 2003. **5**(1): p. 113-25.
88. Oshimori, N., M. Ohsugi, and T. Yamamoto, *The Plk1 target Kizuna stabilizes mitotic centrosomes to ensure spindle bipolarity.* Nat Cell Biol, 2006. **8**(10): p. 1095-101.
89. Santamaria, A., et al., *Use of the novel Plk1 inhibitor ZK-thiazolidinone to elucidate functions of Plk1 in early and late stages of mitosis.* Mol Biol Cell, 2007. **18**(10): p. 4024-36.
90. van Vugt, M.A., et al., *Polo-like kinase-1 is required for bipolar spindle formation but is dispensable for anaphase promoting complex/Cdc20 activation and initiation of cytokinesis.* J Biol Chem, 2004. **279**(35): p. 36841-54.
91. Lenart, P., et al., *The small-molecule inhibitor BI 2536 reveals novel insights into mitotic roles of polo-like kinase 1.* Curr Biol, 2007. **17**(4): p. 304-15.
92. Steegmaier, M., et al., *BI 2536, a potent and selective inhibitor of polo-like kinase 1, inhibits tumor growth in vivo.* Curr Biol, 2007. **17**(4): p. 316-22.
93. Khodjakov, A., et al., *Minus-end capture of preformed kinetochore fibers contributes to spindle morphogenesis.* J Cell Biol, 2003. **160**(5): p. 671-83.
94. Forer, A., *Local Reduction of Spindle Fiber Birefringence in Living Nephrotoma Suturalis (Loew) Spermatocytes Induced by Ultraviolet Microbeam Irradiation.* J Cell Biol, 1965. **25**: p. SUPPL: 95-117.
95. Mitchison, T.J., *Polewards microtubule flux in the mitotic spindle: evidence from photoactivation of fluorescence.* J Cell Biol, 1989. **109**(2): p. 637-52.
96. Seitzer, U., et al., *Schizonts of Theileria annulata interact with the microtubuli network of their host cell via the membrane protein TaSP.* Parasitol Res, 2010. **106**(5): p. 1085-102.
97. Ganem, N.J., K. Upton, and D.A. Compton, *Efficient mitosis in human cells lacking poleward microtubule flux.* Curr Biol, 2005. **15**(20): p. 1827-32.
98. Piehl, M. and L. Cassimeris, *Organization and dynamics of growing microtubule plus ends during early mitosis.* Mol Biol Cell, 2003. **14**(3): p. 916-25.
99. Burkhardt, J.K., et al., *Overexpression of the dynamitin (p50) subunit of the dynactin complex disrupts dynein-dependent maintenance of membrane organelle distribution.* J Cell Biol, 1997. **139**(2): p. 469-84.
100. Varma, D., et al., *Direct role of dynein motor in stable kinetochore-microtubule attachment, orientation, and alignment.* J Cell Biol, 2008. **182**(6): p. 1045-54.
101. Sharp, D.J., G.C. Rogers, and J.M. Scholey, *Cytoplasmic dynein is required for poleward chromosome movement during mitosis in Drosophila embryos.* Nat Cell Biol, 2000. **2**(12): p. 922-30.
102. Alsop, G.B. and D. Zhang, *Microtubules are the only structural constituent of the spindle apparatus required for induction of cell cleavage.* J Cell Biol, 2003. **162**(3): p. 383-90.
103. Canman, J.C., et al., *Determining the position of the cell division plane.* Nature, 2003. **424**(6952): p. 1074-8.

104. Foe, V.E. and G. von Dassow, *Stable and dynamic microtubules coordinately shape the myosin activation zone during cytokinetic furrow formation.* J Cell Biol, 2008. **183**(3): p. 457-70.
105. Odell, G.M. and V.E. Foe, *An agent-based model contrasts opposite effects of dynamic and stable microtubules on cleavage furrow positioning.* J Cell Biol, 2008. **183**(3): p. 471-83.
106. Werner, M., E. Munro, and M. Glotzer, *Astral signals spatially bias cortical myosin recruitment to break symmetry and promote cytokinesis.* Curr Biol, 2007. **17**(15): p. 1286-97.
107. Bement, W.M., H.A. Benink, and G. von Dassow, *A microtubule-dependent zone of active RhoA during cleavage plane specification.* J Cell Biol, 2005. **170**(1): p. 91-101.
108. Nishimura, Y. and S. Yonemura, *Centralspindlin regulates ECT2 and RhoA accumulation at the equatorial cortex during cytokinesis.* J Cell Sci, 2006. **119**(Pt 1): p. 104-14.
109. Kamijo, K., et al., *Dissecting the role of Rho-mediated signaling in contractile ring formation.* Mol Biol Cell, 2006. **17**(1): p. 43-55.
110. Shannon, K.B., et al., *Taxol-stabilized microtubules can position the cytokinetic furrow in mammalian cells.* Mol Biol Cell, 2005. **16**(9): p. 4423-36.
111. Motegi, F., et al., *Two phases of astral microtubule activity during cytokinesis in C. elegans embryos.* Dev Cell, 2006. **10**(4): p. 509-20.
112. Wadsworth, P., *Cytokinesis: Rho marks the spot.* Curr Biol, 2005. **15**(21): p. R871-4.
113. Canman, J.C., D.B. Hoffman, and E.D. Salmon, *The role of pre- and post-anaphase microtubules in the cytokinesis phase of the cell cycle.* Curr Biol, 2000. **10**(10): p. 611-4.
114. Pletjushkina, O.J., et al., *Induction of cortical oscillations in spreading cells by depolymerization of microtubules.* Cell Motil Cytoskeleton, 2001. **48**(4): p. 235-44.
115. Paluch, E., et al., *Cortical actomyosin breakage triggers shape oscillations in cells and cell fragments.* Biophys J, 2005. **89**(1): p. 724-33.
116. Murthy, K. and P. Wadsworth, *Dual role for microtubules in regulating cortical contractility during cytokinesis.* J Cell Sci, 2008. **121**(Pt 14): p. 2350-9.
117. von Dassow, G., et al., *Action at a distance during cytokinesis.* J Cell Biol, 2009. **187**(6): p. 831-45.
118. Straight, A.F., et al., *Dissecting temporal and spatial control of cytokinesis with a myosin II Inhibitor.* Science, 2003. **299**(5613): p. 1743-7.
119. Mollinari, C., et al., *Ablation of PRC1 by small interfering RNA demonstrates that cytokinetic abscission requires a central spindle bundle in mammalian cells, whereas completion of furrowing does not.* Mol Biol Cell, 2005. **16**(3): p. 1043-55.
120. Vassilev, L.T., et al., *Selective small-molecule inhibitor reveals critical mitotic functions of human CDK1.* Proc Natl Acad Sci USA, 2006. **103**(28): p. 10660-5.
121. Cassimeris, L. and C. Spittle, *Regulation of microtubule-associated proteins.* Int Rev Cytol, 2001. **210**: p. 163-226.
122. Andersen, S.S., *Spindle assembly and the art of regulating microtubule dynamics by MAPs and Stathmin/Op18.* Trends Cell Biol, 2000. **10**(7): p. 261-7.
123. Kinoshita, K., B. Habermann, and A.A. Hyman, *XMAP215: a key component of the dynamic microtubule cytoskeleton.* Trends Cell Biol, 2002. **12**(6): p. 267-73.
124. Moritz, M., et al., *Microtubule nucleation by gamma-tubulin-containing rings in the centrosome.* Nature, 1995. **378**(6557): p. 638-40.
125. Di Fiore, B., M. Ciciarello, and P. Lavia, *Mitotic functions of the Ran GTPase network: the importance of being in the right place at the right time.* Cell Cycle, 2004. **3**(3): p. 305-13.
126. Kalab, P., K. Weis, and R. Heald, *Visualization of a Ran-GTP gradient in interphase and mitotic Xenopus egg extracts.* Science, 2002. **295**(5564): p. 2452-6.
127. Torosantucci, L., et al., *Localized RanGTP accumulation promotes microtubule nucleation at kinetochores in somatic mammalian cells.* Mol Biol Cell, 2008. **19**(5): p. 1873-82.
128. Peters, U., et al., *Probing cell-division phenotype space and Polo-like kinase function using small molecules.* Nat Chem Biol, 2006. **2**(11): p. 618-26.
129. Jourdain, L., et al., *Stathmin: a tubulin-sequestering protein which forms a ternary T2S complex with two tubulin molecules.* Biochemistry, 1997. **36**(36): p. 10817-21.
130. Niethammer, P., P. Bastiaens, and E. Karsenti, *Stathmin-tubulin interaction gradients in motile and mitotic cells.* Science, 2004. **303**(5665): p. 1862-6.
131. Budde, P.P., et al., *Regulation of Op18 during spindle assembly in Xenopus egg extracts.* J Cell Biol, 2001. **153**(1): p. 149-58.

132. Lee, J., et al., *Centrobin/NIP2 is a microtubule stabilizer whose activity is enhanced by PLK1 phosphorylation during mitosis.* J Biol Chem, 2010. **285**(33): p. 25476-84.
133. Cassimeris, L. and J. Morabito, *TOGp, the human homolog of XMAP215/Dis1, is required for centrosome integrity, spindle pole organization, and bipolar spindle assembly.* Mol Biol Cell, 2004. **15**(4): p. 1580-90.
134. Holmfeldt, P., S. Stenmark, and M. Gullberg, *Differential functional interplay of TOGp/XMAP215 and the Kinl kinesin MCAK during interphase and mitosis.* EMBO J, 2004. **23**(3): p. 627-37.
135. Gergely, F., V.M. Draviam, and J.W. Raff, *The ch-TOG/XMAP215 protein is essential for spindle pole organization in human somatic cells.* Genes Dev, 2003. **17**(3): p. 336-41.
136. Schroer, T.A., *Microtubules don and doff their caps: dynamic attachments at plus and minus ends.* Curr Opin Cell Biol, 2001. **13**(1): p. 92-6.
137. Tirnauer, J.S., et al., *EB1-microtubule interactions in Xenopus egg extracts: role of EB1 in microtubule stabilization and mechanisms of targeting to microtubules.* Mol Biol Cell, 2002. **13** (10): p. 3614-26.
138. Hammond, J.W., D. Cai, and K.J. Verhey, *Tubulin modifications and their cellular functions.* Curr Opin Cell Biol, 2008. **20**(1): p. 71-6.
139. Peris, L., et al., *Tubulin tyrosination is a major factor affecting the recruitment of CAP-Gly proteins at microtubule plus ends.* J Cell Biol, 2006. **174**(6): p. 839-49.
140. Gundersen, G.G. and J.C. Bulinski, *Distribution of tyrosinated and nontyrosinated alpha-tubulin during mitosis.* J Cell Biol, 1986. **102**(3): p. 1118-26.
141. Busson, S., et al., *Dynein and dynactin are localized to astral microtubules and at cortical sites in mitotic epithelial cells.* Curr Biol, 1998. **8**(9): p. 541-4.
142. O'Connell, C.B. and Y.L. Wang, *Mammalian spindle orientation and position respond to changes in cell shape in a dynein-dependent fashion.* Mol Biol Cell, 2000. **11**(5): p. 1765-74.
143. Verhey, K.J. and J. Gaertig, *The tubulin code.* Cell Cycle, 2007. **6**(17): p. 2152-60.
144. Westermann, S. and K. Weber, *Post-translational modifications regulate microtubule function.* Nat Rev Mol Cell Biol, 2003. **4**(12): p. 938-47.
145. Mollinari, C., et al., *PRC1 is a microtubule binding and bundling protein essential to maintain the mitotic spindle midzone.* J Cell Biol, 2002. **157**(7): p. 1175-86.
146. Gruneberg, U., et al., *KIF14 and citron kinase act together to promote efficient cytokinesis.* J Cell Biol, 2006. **172**(3): p. 363-72.
147. Kurasawa, Y., et al., *Essential roles of KIF4 and its binding partner PRC1 in organized central spindle midzone formation.* EMBO J, 2004. **23**(16): p. 3237-48.
148. Gruneberg, U., et al., *Relocation of Aurora B from centromeres to the central spindle at the metaphase to anaphase transition requires MKlp2.* J Cell Biol, 2004. **166**(2): p. 167-72.
149. Liu, J., et al., *PRC1 cooperates with CLASP1 to organize central spindle plasticity in mitosis.* J Biol Chem, 2009. **284**(34): p. 23059-71.
150. Zhu, C. and W. Jiang, *Cell cycle-dependent translocation of PRC1 on the spindle by Kif4 is essential for midzone formation and cytokinesis.* Proc Natl Acad Sci U S A, 2005. **102**(2): p. 343-8.
151. Akhmanova, A., et al., *Clasps are CLIP-115 and -170 associating proteins involved in the regional regulation of microtubule dynamics in motile fibroblasts.* Cell, 2001. **104**(6): p. 923-35.
152. Mimori-Kiyosue, Y., et al., *CLASP1 and CLASP2 bind to EB1 and regulate microtubule plus-end dynamics at the cell cortex.* J Cell Biol, 2005. **168**(1): p. 141-53.
153. Yin, H., et al., *Stu1p is physically associated with beta-tubulin and is required for structural integrity of the mitotic spindle.* Mol Biol Cell, 2002. **13**(6): p. 1881-92.
154. Gonczy, P., et al., *Functional genomic analysis of cell division in C. elegans using RNAi of genes on chromosome III.* Nature, 2000. **408**(6810): p. 331-6.
155. Maiato, H., et al., *MAST/Orbit has a role in microtubule-kinetochore attachment and is essential for chromosome alignment and maintenance of spindle bipolarity.* J Cell Biol, 2002. **157**(5): p. 749-60.
156. Hannak, E. and R. Heald, *Xorbit/CLASP links dynamic microtubules to chromosomes in the Xenopus meiotic spindle.* J Cell Biol, 2006. **172**(1): p. 19-25.
157. Mimori-Kiyosue, Y., et al., *Mammalian CLASPs are required for mitotic spindle organization and kinetochore alignment.* Genes Cells, 2006. **11**(8): p. 845-57.

158. Inoue, Y.H., et al., *Mutations in orbit/mast reveal that the central spindle is comprised of two microtubule populations, those that initiate cleavage and those that propagate furrow ingression.* J Cell Biol, 2004. **166**(1): p. 49-60.
159. Brennan, I.M., et al., *Polo-like kinase controls vertebrate spindle elongation and cytokinesis.* PLoS ONE, 2007. **2**(5): p. e409.
160. Kumagai, A. and W.G. Dunphy, *Purification and molecular cloning of Plx1, a Cdc25-regulatory kinase from Xenopus egg extracts.* Science, 1996. **273**(5280): p. 1377-80.
161. Inoue, D. and N. Sagata, *The Polo-like kinase Plx1 interacts with and inhibits Myt1 after fertilization of Xenopus eggs.* EMBO J, 2005. **24**(5): p. 1057-67.
162. Jang, Y.J., et al., *Functional studies on the role of the C-terminal domain of mammalian polo-like kinase.* Proc Natl Acad Sci U S A, 2002. **99**(4): p. 1984-9.
163. Keppner, S., et al., *Biological impact of freezing Plk1 in its inactive conformation in cancer cells.* Cell Cycle, 2010. **9**(4): p. 761-73.
164. Hummer, S. and T.U. Mayer, *Cdk1 negatively regulates midzone localization of the mitotic kinesin Mklp2 and the chromosomal passenger complex.* Curr Biol, 2009. **19**(7): p. 607-12.
165. Mishima, M., et al., *Cell cycle regulation of central spindle assembly.* Nature, 2004. **430**(7002): p. 908-13.
166. Baumann, C., et al., *PICH, a centromere-associated SNF2 family ATPase, is regulated by Plk1 and required for the spindle checkpoint.* Cell, 2007. **128**(1): p. 101-14.
167. Hubner, N.C., et al., *Re-examination of siRNA specificity questions role of PICH and Tao1 in the spindle checkpoint and identifies Mad2 as a sensitive target for small RNAs.* Chromosoma, 2010. **119**(2): p. 149-65.
168. Archambault, V., et al., *Sequestration of Polo kinase to microtubules by phosphopriming-independent binding to Map205 is relieved by phosphorylation at a CDK site in mitosis.* Genes Dev, 2008. **22**(19): p. 2707-20.
169. Neef, R., et al., *Phosphorylation of mitotic kinesin-like protein 2 by polo-like kinase 1 is required for cytokinesis.* J Cell Biol, 2003. **162**(5): p. 863-75.
170. Elia, A.E., et al., *The molecular basis for phosphodependent substrate targeting and regulation of Plks by the Polo-box domain.* Cell, 2003. **115**(1): p. 83-95.
171. Burkard, M.E., et al., *Plk1 self-organization and priming phosphorylation of HsCYK-4 at the spindle midzone regulate the onset of division in human cells.* PLoS Biol, 2009. **7**(5): p. e1000111.
172. Pavicic-Kaltenbrunner, V., M. Mishima, and M. Glotzer, *Cooperative assembly of CYK-4/MgcRacGAP and ZEN-4/MKLP1 to form the centralspindlin complex.* Mol Biol Cell, 2007. **18**(12): p. 4992-5003.
173. Wolfe, B.A., et al., *Polo-like kinase 1 directs assembly of the HsCyk-4 RhoGAP/Ect2 RhoGEF complex to initiate cleavage furrow formation.* PLoS Biol, 2009. **7**(5): p. e1000110.
174. Trinkle-Mulcahy, L. and A.I. Lamond, *Mitotic phosphatases: no longer silent partners.* Curr Opin Cell Biol, 2006. **18**(6): p. 623-31.
175. Boutros, R., C. Dozier, and B. Ducommun, *The when and wheres of CDC25 phosphatases.* Curr Opin Cell Biol, 2006. **18**(2): p. 185-91.
176. Boutros, R., V. Lobjois, and B. Ducommun, *CDC25 phosphatases in cancer cells: key players? Good targets?* Nat Rev Cancer, 2007. **7**(7): p. 495-507.
177. Brezak, M.C., et al., *Inhibition of human tumor cell growth in vivo by an orally bioavailable inhibitor of CDC25 phosphatases.* Mol Cancer Ther, 2005. **4**(9): p. 1378-87.
178. Cazales, M., et al., *Pharmacologic inhibition of CDC25 phosphatases impairs interphase microtubule dynamics and mitotic spindle assembly.* Mol Cancer Ther, 2007. **6**(1): p. 318-25.
179. Katsuno, Y., et al., *Cyclin A-Cdk1 regulates the origin firing program in mammalian cells.* Proc Natl Acad Sci U S A, 2009. **106**(9): p. 3184-9.
180. Tsichlis, P.N., M. Hatziapostolou, and P.W. Hinds, *Timing is everything: regulation of Cdk1 and aneuploidy.* Dev Cell, 2007. **12**(4): p. 477-9.
181. Honkanen, R.E., et al., *Characterization of natural toxins with inhibitory activity against serine/threonine protein phosphatases.* Toxicon, 1994. **32**(3): p. 339-50.
182. Yuan, K., Y. Huang, and X. Yao, *Illumination of mitotic orchestra during cell division: A polo view.* Cell Signal, 2010.
183. Fabbro, M., et al., *Cdk1/Erk2- and Plk1-dependent phosphorylation of a centrosome protein, Cep55, is required for its recruitment to midbody and cytokinesis.* Dev Cell, 2005. **9**(4): p. 477-88.

184. Litvak, V., et al., *Mitotic phosphorylation of the peripheral Golgi protein Nir2 by Cdk1 provides a docking mechanism for Plk1 and affects cytokinesis completion.* Mol Cell, 2004. **14**(3): p. 319-30.
185. Zhao, W.M., A. Seki, and G. Fang, *Cep55, a microtubule-bundling protein, associates with centralspindlin to control the midbody integrity and cell abscission during cytokinesis.* Mol Biol Cell, 2006. **17**(9): p. 3881-96.
186. Stegmeier, F., R. Visintin, and A. Amon, *Separase, polo kinase, the kinetochore protein Slk19, and Spo12 function in a network that controls Cdc14 localization during early anaphase.* Cell, 2002. **108**(2): p. 207-20.
187. Cho, H.P., et al., *The dual-specificity phosphatase CDC14B bundles and stabilizes microtubules.* Mol Cell Biol, 2005. **25**(11): p. 4541-51.
188. Krasinska, L., et al., *Regulation of multiple cell cycle events by Cdc14 homologues in vertebrates.* Exp Cell Res, 2007. **313**(6): p. 1225-39.
189. Stegmeier, F. and A. Amon, *Closing mitosis: the functions of the Cdc14 phosphatase and its regulation.* Annu Rev Genet, 2004. **38**: p. 203-32.
190. Mailand, N., et al., *Deregulated human Cdc14A phosphatase disrupts centrosome separation and chromosome segregation.* Nat Cell Biol, 2002. **4**(4): p. 317-22.
191. Pereira, G. and E. Schiebel, *Separase regulates INCENP-Aurora B anaphase spindle function through Cdc14.* Science, 2003. **302**(5653): p. 2120-4.
192. van Leuken, R., et al., *Polo-like kinase-1 controls Aurora A destruction by activating APC/C-Cdh1.* PLoS One, 2009. **4**(4): p. e5282.
193. Rape, M., S.K. Reddy, and M.W. Kirschner, *The processivity of multiubiquitination by the APC determines the order of substrate degradation.* Cell, 2006. **124**(1): p. 89-103.
194. Lee, K.S., et al., *Mechanisms of mammalian polo-like kinase 1 (Plk1) localization: self- versus non-self-priming.* Cell Cycle, 2008. **7**(2): p. 141-5.
195. Rape, M., *Cell cycle: on-time delivery of Plk1 during cytokinesis.* Curr Biol, 2007. **17**(13): p. R506-8.
196. Taylor, S. and J.M. Peters, *Polo and Aurora kinases: lessons derived from chemical biology.* Curr Opin Cell Biol, 2008. **20**(1): p. 77-84.
197. Vader, G., R.H. Medema, and S.M. Lens, *The chromosomal passenger complex: guiding Aurora-B through mitosis.* J Cell Biol, 2006. **173**(6): p. 833-7.
198. Vagnarelli, P. and W.C. Earnshaw, *Chromosomal passengers: the four-dimensional regulation of mitotic events.* Chromosoma, 2004. **113**(5): p. 211-22.
199. Kaitna, S., et al., *Incenp and an aurora-like kinase form a complex essential for chromosome segregation and efficient completion of cytokinesis.* Curr Biol, 2000. **10**(19): p. 1172-81.
200. Ditchfield, C., et al., *Aurora B couples chromosome alignment with anaphase by targeting BubR1, Mad2, and Cenp-E to kinetochores.* J Cell Biol, 2003. **161**(2): p. 267-80.
201. Girdler, F., et al., *Validating Aurora B as an anti-cancer drug target.* J Cell Sci, 2006. **119**(Pt 17): p. 3664-75.
202. Seki, A., et al., *Plk1- and beta-TrCP-dependent degradation of Bora controls mitotic progression.* J Cell Biol, 2008. **181**(1): p. 65-78.
203. Hans, F., et al., *Molecular distinctions between Aurora A and B: a single residue change transforms Aurora A into correctly localized and functional Aurora B.* Mol Biol Cell, 2009. **20**(15): p. 3491-502.
204. Meggio, F., et al., *Different susceptibility of protein kinases to staurosporine inhibition. Kinetic studies and molecular bases for the resistance of protein kinase CK2.* Eur J Biochem, 1995. **234** (1): p. 317-22.
205. Gadbois, D.M., et al., *Staurosporine is a potent inhibitor of p34cdc2 and p34cdc2-like kinases.* Biochem Biophys Res Commun, 1992. **184**(1): p. 80-5.
206. Hall, L.L., et al., *A brief staurosporine treatment of mitotic cells triggers premature exit from mitosis and polyploid cell formation.* Cancer Res, 1996. **56**(15): p. 3551-9.
207. Th'ng, J.P., et al., *Inhibition of histone phosphorylation by staurosporine leads to chromosome decondensation.* J Biol Chem, 1994. **269**(13): p. 9568-73.
208. Pinna, L.A., *Protein kinase CK2: a challenge to canons.* J Cell Sci, 2002. **115**(Pt 20): p. 3873-8.
209. Litchfield, D.W., *Protein kinase CK2: structure, regulation and role in cellular decisions of life and death.* Biochem J, 2003. **369**(Pt 1): p. 1-15.
210. Ruzzene, M. and L.A. Pinna, *Addiction to protein kinase CK2: a common denominator of diverse cancer cells?* Biochim Biophys Acta, 2010. **1804**(3): p. 499-504.

211. Seldin, D.C. and P. Leder, *Casein kinase II alpha transgene-induced murine lymphoma: relation to theileriosis in cattle.* Science, 1995. **267**(5199): p. 894-7.
212. Shayan, P. and J.S. Ahmed, *Theileria-mediated constitutive expression of the casein kinase II-alpha subunit in bovine lymphoblastoid cells.* Parasitol. Res., 1997. **83**(6): p. 526-532.
213. Marin, O., et al., *The consensus sequences for cdc2 kinase and for casein kinase-2 are mutually incompatible. A study with peptides derived from the beta-subunit of casein kinase-2.* FEBS Lett, 1992. **301**(1): p. 111-4.
214. Prudent, R. and C. Cochet, *New protein kinase CK2 inhibitors: jumping out of the catalytic box.* Chem Biol, 2009. **16**(2): p. 112-20.
215. Duncan, J.S., et al., *An unbiased evaluation of CK2 inhibitors by chemoproteomics: characterization of inhibitor effects on CK2 and identification of novel inhibitor targets.* Mol Cell Proteomics, 2008. **7**(6): p. 1077-88.
216. Simizu, S. and H. Osada, *Mutations in the Plk gene lead to instability of Plk protein in human tumour cell lines.* Nat Cell Biol, 2000. **2**(11): p. 852-4.
217. Haller, D., et al., *Cytoplasmic sequestration of p53 promotes survival in leukocytes transformed by Theileria.* Oncogene, 2010. **29**(21): p. 3079-86.
218. Gromley, A., et al., *Centriolin anchoring of exocyst and SNARE complexes at the midbody is required for secretory-vesicle-mediated abscission.* Cell, 2005. **123**(1): p. 75-87.
219. Low, S.H., et al., *Syntaxin 2 and endobrevin are required for the terminal step of cytokinesis in mammalian cells.* Dev Cell, 2003. **4**(5): p. 753-9.
220. Skop, A.R., et al., *Completion of cytokinesis in C. elegans requires a brefeldin A-sensitive membrane accumulation at the cleavage furrow apex.* Curr Biol, 2001. **11**(10): p. 735-46.
221. Montagnac, G., A. Echard, and P. Chavrier, *Endocytic traffic in animal cell cytokinesis.* Curr Opin Cell Biol, 2008. **20**(4): p. 454-61.
222. Boucrot, E. and T. Kirchhausen, *Endosomal recycling controls plasma membrane area during mitosis.* Proc Natl Acad Sci U S A, 2007. **104**(19): p. 7939-44.
223. Mullins, J.M. and J.J. Biesele, *Terminal phase of cytokinesis in D-98s cells.* J Cell Biol, 1977. **73** (3): p. 672-84.
224. Carlton, J.G. and J. Martin-Serrano, *Parallels between cytokinesis and retroviral budding: a role for the ESCRT machinery.* Science, 2007. **316**(5833): p. 1908-12.
225. Carlton, J.G., M. Agromayor, and J. Martin-Serrano, *Differential requirements for Alix and ESCRT-III in cytokinesis and HIV-1 release.* Proc Natl Acad Sci U S A, 2008. **105**(30): p. 10541-6.
226. Morita, E., et al., *Human ESCRT and ALIX proteins interact with proteins of the midbody and function in cytokinesis.* EMBO J, 2007. **26**(19): p. 4215-27.
227. Lee, H.H., et al., *Midbody targeting of the ESCRT machinery by a noncanonical coiled coil in CEP55.* Science, 2008. **322**(5901): p. 576-80.
228. Lata, S., et al., *Helical structures of ESCRT-III are disassembled by VPS4.* Science, 2008. **321** (5894): p. 1354-7.
229. Hanson, P.I., et al., *Plasma membrane deformation by circular arrays of ESCRT-III protein filaments.* J Cell Biol, 2008. **180**(2): p. 389-402.
230. Wollert, T., et al., *Membrane scission by the ESCRT-III complex.* Nature, 2009. **458**(7235): p. 172-7.
231. Yang, D., et al., *Structural basis for midbody targeting of spastin by the ESCRT-III protein CHMP1B.* Nat Struct Mol Biol, 2008. **15**(12): p. 1278-86.
232. Steigemann, P., et al., *Aurora B-mediated abscission checkpoint protects against tetraploidization.* Cell, 2009. **136**(3): p. 473-84.
233. Piel, M., et al., *Centrosome-dependent exit of cytokinesis in animal cells.* Science, 2001. **291** (5508): p. 1550-3.
234. Hickson, G.R. and P.H. O'Farrell, *Anillin: a pivotal organizer of the cytokinetic machinery.* Biochem Soc Trans, 2008. **36**(Pt 3): p. 439-41.
235. Piekny, A.J. and M. Glotzer, *Anillin is a scaffold protein that links RhoA, actin, and myosin during cytokinesis.* Curr Biol, 2008. **18**(1): p. 30-6.
236. D'Avino, P.P., et al., *Interaction between Anillin and RacGAP50C connects the actomyosin contractile ring with spindle microtubules at the cell division site.* J Cell Sci, 2008. **121**(Pt 8): p. 1151-8.
237. Steigemann, P. and D.W. Gerlich, *An evolutionary conserved checkpoint controls abscission timing.* Cell Cycle, 2009. **8**(12): p. 1814-5.

238. Konopka, C.A., et al., *Dynamin and cytokinesis.* Traffic, 2006. **7**(3): p. 239-47.
239. Macia, E., et al., *Dynasore, a cell-permeable inhibitor of dynamin.* Dev Cell, 2006. **10**(6): p. 839-50.
240. Irvin, A.D., J.G. Ocama, and P.R. Spooner, *Cycle of bovine lymphoblastoid cells parasitised by Theileria parva.* Res. Vet. Sci., 1982. **33**(3): p. 298-304.
241. Salic, A. and T.J. Mitchison, *A chemical method for fast and sensitive detection of DNA synthesis in vivo.* Proc Natl Acad Sci U S A, 2008. **105**(7): p. 2415-20.
242. Lansbergen, G., et al., *CLASPs attach microtubule plus ends to the cell cortex through a complex with LL5beta.* Dev Cell, 2006. **11**(1): p. 21-32.
243. Nakajima, H., et al., *Identification of a consensus motif for Plk (Polo-like kinase) phosphorylation reveals Myt1 as a Plk1 substrate.* J Biol Chem, 2003. **278**(28): p. 25277-80.
244. Stewart, T.L., S.T. Wasilenko, and M. Barry, *Vaccinia virus F1L protein is a tail-anchored protein that functions at the mitochondria to inhibit apoptosis.* J Virol, 2005. **79**(2): p. 1084-98.
245. Soung, N.K., et al., *Plk1-dependent and -independent roles of an ODF2 splice variant, hCenexin1, at the centrosome of somatic cells.* Dev Cell, 2009. **16**(4): p. 539-50.
246. Colanzi, A., C. Suetterlin, and V. Malhotra, *Cell-cycle-specific Golgi fragmentation: how and why?* Curr Opin Cell Biol, 2003. **15**(4): p. 462-7.
247. Lowe, M., N. Nakamura, and G. Warren, *Golgi division and membrane traffic.* Trends Cell Biol, 1998. **8**(1): p. 40-4.
248. Jorgensen, P. and M. Tyers, *How cells coordinate growth and division.* Curr Biol, 2004. **14**(23): p. R1014-27.
249. Kinnaird, J., et al., *TaCRK3 encodes a novel Theileria annulata protein kinase with motifs characteristic of the family of eukaryotic cyclin dependent kinases: a comparative analysis of its expression with TaCRK2 during the parasite life cycle.* Gene, 2001. **279**(2): p. 127-35.
250. Karin, M. and F.R. Greten, *NF-kappaB: linking inflammation and immunity to cancer development and progression.* Nat Rev Immunol, 2005. **5**(10): p. 749-59.
251. Greten, F.R. and M. Karin, *The IKK/NF-kappaB activation pathway-a target for prevention and treatment of cancer.* Cancer Lett, 2004. **206**(2): p. 193-9.
252. Park, K.J., et al., *Formation of an IKKalpha-dependent transcription complex is required for estrogen receptor-mediated gene activation.* Mol Cell, 2005. **18**(1): p. 71-82.
253. Cao, Y., et al., *IKKalpha provides an essential link between RANK signaling and cyclin D1 expression during mammary gland development.* Cell, 2001. **107**(6): p. 763-75.
254. Albanese, C., et al., *IKKalpha regulates mitogenic signaling through transcriptional induction of cyclin D1 via Tcf.* Mol Biol Cell, 2003. **14**(2): p. 585-99.
255. Hinz, M., et al., *NF-kappaB function in growth control: regulation of cyclin D1 expression and G0/G1-to-S-phase transition.* Mol Cell Biol, 1999. **19**(4): p. 2690-8.
256. Kwak, Y.T., et al., *IkappaB kinase alpha regulates subcellular distribution and turnover of cyclin D1 by phosphorylation.* J Biol Chem, 2005. **280**(40): p. 33945-52.
257. Tu, Z., et al., *IKK alpha regulates estrogen-induced cell cycle progression by modulating E2F1 expression.* J Biol Chem, 2006. **281**(10): p. 6699-706.
258. Prajapati, S., et al., *IKKalpha regulates the mitotic phase of the cell cycle by modulating Aurora A phosphorylation.* Cell Cycle, 2006. **5**(20): p. 2371-80.
259. Irelan, J.T., et al., *A role for IkappaB kinase 2 in bipolar spindle assembly.* Proc Natl Acad Sci U S A, 2007. **104**(43): p. 16940-5.
260. Cahu, J., et al., *Phosphorylation by Cdk1 increases the binding of Eg5 to microtubules in vitro and in Xenopus egg extract spindles.* PLoS One, 2008. **3**(12): p. e3936.
261. Blangy, A., et al., *Phosphorylation by p34cdc2 regulates spindle association of human Eg5, a kinesin-related motor essential for bipolar spindle formation in vivo.* Cell, 1995. **83**(7): p. 1159-69.
262. Li, Q., S. Withoff, and I.M. Verma, *Inflammation-associated cancer: NF-kappaB is the lynchpin.* Trends Immunol, 2005. **26**(6): p. 318-25.
263. Greten, F.R., et al., *IKKbeta links inflammation and tumorigenesis in a mouse model of colitis-associated cancer.* Cell, 2004. **118**(3): p. 285-96.
264. Chen, F., et al., *Loss of Ikkbeta promotes migration and proliferation of mouse embryo fibroblast cells.* J Biol Chem, 2006. **281**(48): p. 37142-9.
265. Dajee, M., et al., *NF-kappaB blockade and oncogenic Ras trigger invasive human epidermal neoplasia.* Nature, 2003. **421**(6923): p. 639-43.

10. Declaration of originality

Last name, first name: von Schubert, Conrad

Matriculation number: 01-137-835

I hereby declare that this thesis represents my original work and that I have used no other sources except as noted by citations.
All data, tables, figures and text citations which have been reproduced from any other source, including the internet, have been explicitly acknowledged as such.
I am aware that in case of non-compliance, the Senate is entitled to divest me of the doctorate degree awarded to me on the basis of the present thesis, in accordance with the “Statut der Universität Bern (Universitätsstatut; UniSt)”, Art. 20, of 17 December 1997.

Bern, 06.09.2010